Development and preclinical assessment of old and new vaccine candidates against *Mycobacterium abscessus*

A thesis submitted by

Sherridan Warner

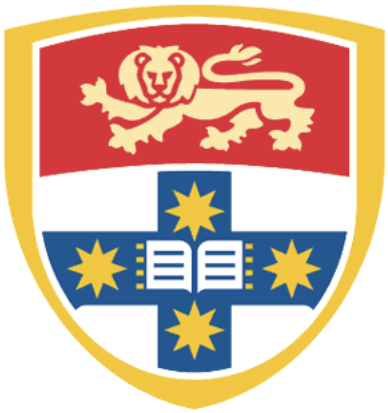

In fulfillment of the requirements for the degree of

Doctor of Philosophy

Faculty of Medicine and Health

The University of Sydney

2023

Statement of Originality

The work outlined in this thesis has been performed within the Faculty of Medicine and Health at the Charles Perkins Centre, University of Sydney, and at the Centenary Institute of Cancer Medicine and Cell Biology. This thesis was carried out under the supervision of Professor James A Triccas, Doctor Claudio Counoupas, and Professor Carl Feng.

I hereby declare that to the best of my knowledge, the content of this thesis is my own work, and this thesis has not been submitted as part of another degree.

I declare that the intellectual content of this thesis is also my own. Any additional support that I received in the development of this thesis is acknowledged below.

Work performed by Dr Andrea Bustamante

Isolation and Whole Genome Sequencing of *M. abscessus* strains used in this thesis, as described in Table 3.1.

Work performed by Anneliese Blaxland, Janine Verstraete, Mark Zampoli, Dominic A Fitzgerald and Paul D Robinson

Collection, acquisition and analysis of clinical epidemiological data described in Chapter 4 (Table 4.1, 4.2).

Work performed by Australian Nuclear Science and Technology Organisation, Sydney Australia

Gamma-irradiation of *M. abscessus* as outlined in Chapter 2 (Section 2.2.3).

Signed:……
Sherridan Warner
Date: 28.02.2023

Authorship Attribution Statement

This thesis does not, to the best of my knowledge, contain previously published material unless otherwise referenced.

Chapter 4: Part of this Chapter forms a manuscript submitted to Journal of Cystic Fibrosis, entitled:

Sherridan Warner, Anneliese Blaxland, Claudio Counoupas, Janine Verstraete, Mark Zampoli, Ben Marais, Dominic A. Fitzgerald, Paul D. Robinson, James A Triccas. (2023). Clinical and experimental determination of protection afforded by BCG vaccination against infection with non-tuberculous mycobacteria. (Submitted manuscript).

My contribution to this manuscript was planning, performing and analysing all animal and *in vitro* studies, as well as the writing of the introduction, results and discussion of these studies. Excerpts from this manuscript have been included in this thesis with permission of all contributors, who are explicitly acknowledged in the foreword to Chapter 4.

Signed:……
Sherridan Warner
Date: 28.02.2023

As supervisor for the candidature upon which this thesis is based, I can confirm that the above statements are correct.

Signed:……
James A Triccas
Date: 27.02.2023

Acknowledgements

They say it takes a village to raise a child. And this child, my thesis, was raised by an incredible village of people. Although this thesis has been a labour of love, it has also been extremely challenging. Without the support system of my colleagues, friends and loving family, I would not have been able to complete it. Whenever I doubted my ability or could not see the light at the end of the tunnel, they were there to give me the strength I needed to push through. So I dedicate this thesis to all those who have stood by me during this period of my life. It has been a long, hard road to get to the end, but I am so thankful of the journey we made.

Firstly, I must thank my supervisor, Professor Jamie Triccas. From the first lecture I had in undergraduate Infectious Diseases, I was inspired and determined to pursue research in mycobacterial disease under your supervision. Thank you for making this project possible. You have been more supportive of me than I ever could deserve; your patience, understanding and encouragement to pursue medicine as well as research has been invaluable. Thank you for always being so accommodating, and for your patience with long experiments that sometimes didn't go to plan (even if it was my fault). I am truly grateful to have been mentored by you throughout the last seven years.

To Dr Claudio Counoupas, my Cloody, thank you for being you. You have been a lifesaver throughout this process. I cannot even begin to describe the gratitude I have for your unwavering support, your patience with my avoidance of analysing data, for making time for my experiments, for helping me run Flow when I was trying to juggle two degrees. Your excitement about my results helped me to be excited about them, and to persevere. On top of your help in the lab, thank you for being a truly beautiful person, for our coffatos, for making me laugh, and for being there in times of need. I am blessed to have had you throughout these years, and I am a better person for it.

Thank you to Professor Carl Feng, my co-supervisor, for always challenging my results, for pushing me to think outside the box. Professor Warwick Britton, your wisdom and passion has been inspiring. To the other people who made this project come to life, thank you. To Dr Paul Robinson, I am grateful for your passion for this project, for always offering support and ideas, and excitement about our findings. To Dr Ben Marais, thank you for your expertise

in this field, and your passion for paediatric infectious diseases is something I will always cherish, and aspire to maintain as I move through my career.

To my angels, Kia and Erica, thank you for your friendship and support throughout the years. Kia, you have been the best desk buddy I could ever ask for, and for always being up for a centrifuge dance party or singalong in the lab. Erica, thank you for always being around for a giggle when times were tough. I will cherish our group chat and your unwavering support forever. To all the other members of the Tricky lab, past and present, thank you for your friendship and help with experiments, whether it was through making reagents, making sure the lab was stocked, or offering a helping hand when things got too much.

To my Lunch Club, your friendship became a reason to look forward to coming in every day. I am incredibly grateful for each and every one of you and cannot describe how thankful I am to have met you, and that our friendships have blossomed into what they are today. Annie Tasker, your bubbly energy and infectious smile was always able to cheer me up on a hard day. Rebecca Kasalo, thank you for our affogato runs, dumpling runs, all the spontaneous food and beverage runs. I will never forget the times you helped me in a crisis by offering me comfort food. Gabi Gregoriou, I have never met someone who could make me laugh like you do. Harry Black, thank you for being you, for your dark humour and being such a great friend. To Stuart Cook, thank you for encouraging me to pursue my dreams when they felt impossible to achieve, and for always being around for a laugh. Taylor Cootes, thank you for being such a supportive friend, for always offering solutions to problems, for going out of your way to help me, and for being a fabulous listener when I just needed to vent frustrations about failed experiments. Thank you for always checking in on me, and in these last few weeks, for your help in editing, which I am forever grateful for. I am truly blessed to have had you by my side throughout these years. Nayan Bhattacharyya, you are the friendship soulmate I never knew I needed. Thank you for your unwavering support both in the lab and out. Thank you for staying late when I had long experiments just so I had company, for indulging my Uber Eats addiction, for our plate-pouring parties, our lab techno dance parties, and for helping troubleshoot anything I didn't understand. I do not think I would have finished this thesis if it wasn't for your belief in me, your support of me, and knowing that you were there if I needed you.

To all my supportive friends outside the lab, thank you for being there for me. To my school friends – Ashleigh, Maddie, Kate, Nicole, Hayley, Leila, Alex, Flynn, Sarah and Steph –

thank you for being around for a walk, a coffee, a movie night, when I needed a break from the world of science. Thank you for listening to me vent, even if you didn't understand what I was venting about, and for offering support and advice. Mem, you have been my biggest supporter since day one, and have always had an uncanny ability to pull me out of my wallowing about hard work, to find solutions to all my silly little conundrums, and keeping me on track. Thank you for being an incredible best friend. To my Med friends, thank you for making the last three years easier. Daniel, Juliet, Keenan, and James, I especially must thank you for always offering to help with study while I tried to balance the writing of this thesis, and for checking in with me to make sure I was okay. Daniel, thank you for always keeping me company in the study while I wrote, even just to throw paper planes at me to make me laugh. To Emily and Jacob, thank you for being my favourite housemates and always suggesting a good camping or surf trip to reset. To my dearest Claire, thank you. From the bottom of my heart, thank you for being an incredibly supportive friend over the last few years. From sending me silly animal videos to cheer me up, to sending me pep talks when I wanted to give up, and for our pizza and Messina nights when I needed a break. Your help has meant more than words can describe.

Finally, to my family, The Griswalds; thank you for your unwavering belief in me. To my mum, Lisa, thank you for being my inspiration as such a hardworking, determined, passionate woman. Thank you for going out of your way to make sure I had everything I needed to pursue my dreams. I wouldn't be the person I am today without your unconditional love. To my dad, Steve, thank you for always checking in on me, for offering your help in any way you could, even if you didn't know how. Knowing you were there made this process easier. To my siblings: Brianna, thank you for always supporting me. Knowing how proud you were of me made me strive to be better. Thank you for letting me sit silently in your room when I needed a break, and thank you for bringing me my favourite donut as I'm writing this. Kieren, thank you for always asking how I was going, even if you didn't understand what I was doing, and for giving me hi-fives when I ticked something off my list. To my adopted siblings, Nathan and Emma, thank you for your support over the years. Nathan, thank you for always keeping the peace. Emma, thank you for telling me I was doing a good job. And to Riley, thank you for being the perfect furry companion along the way.

Publications

1. **Warner, S. E.**, Blaxland, A., Counoupas, C., Verstraete, J., Zampoli, M., Marais, B., Fitzgerald, D. A., Robinson, P. D., & Triccas, J. A. (2023). Clinical and experimental determination of protection afforded by BCG vaccination against infection with non-tuberculous mycobacteria. (Submitted manuscript).
2. Kam, J. Y., Hortle, E., Krogman, E., **Warner, S. E**., Wright, K., Luo, K., Cheng, T., Manuneedhi Cholan, P., Kikuchi, K., & Triccas, J. A. (2022). Rough and smooth variants of *Mycobacterium abscessus* are differentially controlled by host immunity during chronic infection of adult zebrafish. *Nature Communications*, *13*(1), 1-11.

Abstract

Mycobacterium abscessus is a respiratory pathogen of growing concern within individuals with compromised respiratory systems, such as in Cystic Fibrosis (CF) and Chronic Pulmonary Obstructive Disease (COPD). It is associated with accelerated lung function decline and in some cases, respiratory failure. Treatment requires multiple antibiotics which can be futile, due to both intrinsic and acquired antibiotic resistance mechanisms. Further, little is known about the immunological correlates of protection against *M. abscessus*. While urgently needed, there is currently no licensed vaccine to prevent *M. abscessus* infection.

There has been a lack of consensus on the most appropriate animal model in which to study host-pathogen interactions of *M. abscessus*. Many models use immuno-deficient strains, which may not be useful in studying complex immunological mechanisms contributing to protection against *M. abscessus*. In this thesis, a pulmonary infection model in C57BL/6 mice was developed using intranasal delivery of clinical *M. abscessus* isolates. Detailed assessment of the pulmonary cell subsets responding to *M. abscessus* infection identified interstitial macrophages (IMs) as the key correlate of protective immunity. IMs were the major producers of iNOS in the lung, and their presence correlated with Th1 responses and bacterial clearance. This process was dependent on tumour necrosis factor (TNF), as TNF-deficient mice displayed poor recruitment of IMs, limited iNOS production in the lung and reduced Th1 immunity. Thus this study highlights the complex interplay between TNF, IMs and iNOS, how they work together to mediate early innate responses and how they function to induce adaptive immunity. These results also provide targets for host-directed therapies where pathogen-directed therapies may fail.

The next component of this thesis sought to determine how Bacille Calmette-Guérin (BCG) vaccination may impact infection with non-tuberculous mycobacteria (NTM), using the murine model of *M. abscessus* infection described in Chapter 3 and observational data across CF clinics. BCG vaccination induced Th1 effector responses in the mouse lung with intermediate levels of protection against pulmonary *M. abscessus* infection. However, BCG vaccination induced multifunctional antigen-specific CD4+ T cells circulating in the blood and was highly protective against dissemination of bacteria to the spleen. Prior infection with *M. abscessus* afforded the highest level of protection against *M. abscessus* challenge in the lung, and immunity was characterised by a greater frequency of pulmonary cytokine-

secreting $CD4^+$ T cells compared to BCG vaccination. To explore whether these findings had clinical relevance, observational data across two CF clinics in Australia and South Africa was examined, where BCG vaccination policy differs. The overall rates of NTM sampling during a three-year period were equivalent between the two CF cohorts, however rates of NTM colonisation were significantly lower in the BCG-vaccinated cohort (South Africa), which was most apparent for *M. abscessus*. This study provides evidence that BCG vaccination can reduce *M. abscessus* colonisation in individuals with CF, which corelates with the ability of BCG to induce multifunctional $CD4^+$ T cells recognising *M. abscessus* in a murine model. Further research is needed to determine the optimal strategies for limiting NTM infections in individuals with CF.

The final objective of this thesis was to explore whole-cell inactivated vaccination as a strategy to control *M. abscessus* infection. Three formulations of whole-cell inactivated *M. abscessus* were investigated; γ-irradiated (γ-*Mabs*), heat-killed (HK- *Mabs*) and paraformaldehyde-inactivated (PFA-*Mabs*). While all inactivated vaccine were confirmed to be non-viable, only γ-*Mabs* showed metabolic activity comparable to live *M. abscessus* controls and stimulated release of a broad array of cytokines/chemokines by macrophages *in vitro.* Vaccination of C57BL/6 mice mice with γ-*Mabs* or HK-*Mabs* conferred significant protection against pulmonary *M. abscessus* infection, which correlated with the influx of iNOS-producing IMs and the recruitment of Th1 $CD4^+$ T cells to the lungs. Vaccine approaches that were unable to afford significant protective efficacy (i.e. PFA- *Mabs*) were poor stimulators of iNOS-producing IMs and Th1 cell recruitment, identifying these immune parameters as key correlates of protection against infection. Addition of the Advax polysaccharide adjuvant to γ-*Mabs* enhanced the immunogenicity of the vaccine but also resulted in greater inflammation in the lungs and the site of vaccination. These results identify immune correlates of vaccine-induced protection against *M. abscessus,* but also highlight the requirement to balance vaccine efficacy with safety.

List of Figures

List of Tables

Abbreviations

ADC	Albumin-Dextrose-Catalase
AB-free	Antibiotic Free
ACK	Ammonium-Chloride-Potassium
AF700	AlexaFluor 700
AM	Alveolar Macrophage
ANOVA	Analysis of Variance
ANTSO	Australia's Nuclear Science and Technology Organisation
APC	Antigen Presenting Cell
ATS	American Thoracic Society
BCG	Bacillus Calmette-Guérin
BMI	Body Mass Index
BSA	Bovine Serum Albumin
CBA	Cytokine Bead Array
CCL	C-C Motif Chemokine Ligand
CCR	Chemokine Receptor
CD	Cluster of Differentiation
CF	Cystic Fibrosis
CFTR	Cystic Fibrosis Transmembrane Conductance Regulator
CFU	Colony-forming Unit
CHW	The Children’s Hospital at Westmead
CM	Central Memory-like
CNS	Central Nervous System
COPD	Chronic Obstructive Pulmonary Disease
cRPMI	Complete Roswell Park Memorial Institute
CTL	Cytotoxic T Lymphocyte
CXCL	Chemokine Ligand
DC	Dendritic Cell
DC-SIGN	Dendritic Cell-Specific Intracellular Adhesion Molecule-3- Grabbing Non-integrin
dLN	Draining Lymph Nodes
Dpi	Days post-infection

EDTA	Ethylene Diamine Tetra Acetic Acid
ELISA	Enzyme-Linked Immunosorbent Assay
FACS	Fluorescence Activated Cell Sorting
FCS	Foetal Calf Serum
FEV1	Forced Expiratory Volume in 1 Second
FITC	Fluorescein Isothiocyanate
G-CSF	Granulocyte Colony-Stimulating Factor
GPL	Glycopeptidolipids
GM-CSF	Granulocyte-Macrophage Colony-Stimulating Factor
HIV	Human Immunodeficiency Virus
HK-Mabs	Heat-Killed *M. abscessus*
hpi	Hours Post-Infection
i.n.	Intranasal
i.v.	Intravenous
iBALT	Inducible Bronchus-Associated Lymphoid Tissue
IDSA	Infectious Diseases Society of America
IFN-γ	Interferon-Gamma
IL	Interleukin
IM	Interstitial Macrophage
iNOS	Inducible Nitric Oxide Synthase
KLRG-1	Killer Cell Lectin-like Receptor Subfamily G Member 1
LB	Luria Bertani
M. abscessus	*Mycobacterium abscessus*
MHCII	Major Histocompatibility Complex Class II
mLN	Mediastinal Lymph Nodes
NAD	Nicotinamide Adenine Dinucleotide
NADPH	Nicotinamide Adenine Dinucleotide Phosphate
NET	Neutrophilic Extracellular Trap
NFκB	Nuclear Factor Kappa B
NK	Natural Killer
NO	Nitric Oxide
NTM	Non-Tuberculosis Mycobacteria
OADC	Oleic Acid-Albumin-Dextrose-Catalase
PAMPs	Pathogen-Associated Molecular Pattern Molecules

PBMC	Peripheral Mononuclear Blood Cells
PBS	Phosphate-Buffered Saline
PE	Phycoerythin
PerCP	Peridinin Chlorophyll Protein
PFA	Paraformaldehyde
PFA-*Mabs*	Paraformaldehyde-Inactivated *M. abscessus*
PLC	Phospholipase C
PMBC	Peripheral Blood Mononuclear Cell
PRR	Pattern Recognition Receptor
R	Rough
RCWMCH	Red Cross War Memorial Children's Hospital
RGM	Rapid Growing Mycobacteria
RORγT	Retinoid-Related Orphan gT
ROS	Reactive Oxygen Species
RT	Room Temperature
S	Smooth
s.c.	Subcutaneous
SCID	Severe Combined Immunodeficient
SGM	Slow Growing Mycobacteria
SSTI	Skin and Soft Tissue Infections
TB	Tuberculosis
Tbet	T-box expressed in T cells
TCM	T Central Memory Cells
TDM	Trehalose Dimycolate
TDW	Triple Distilled Water
TEM	T Effector Memory Cells
Th	T-helper
TLR	Toll-Like Receptor
TNF	Tumour Necrosis Factor
TNFKO	Tumour Necrosis Factor Knock Out
TRM	Tissue- Resident Memory T Cells
tSNE	t-Distributed Stochastic Neighbour Embedding
UV	Ultra Violet
WCV	Whole-Cell Vaccines

WGS	Whole-Genome Sequencing
WT	Wild-Type
ZF	Zebrafish
γ-Mabs	γ-Irradiated *M. abscessus*

Table of Contents

Chapter 1: General Introduction

1.1. *Mycobacterium spp*. is a significant global health problem

Mycobacterium spp. is a large, diverse genus comprising of over one hundred species. Mycobacteria are found ubiquitously in soil and water and possess a characteristic mycolic acid-rich cellular envelope (Brennan & Nikaido, 1995). This waxy, hydrophobic layer surrounding the cell is thicker, less permeable, and biochemically unique compared to Gram-positive and Gram-negative bacteria. Mycobacteria tend to be protected from desiccation and resistant to common antimicrobials and environmental stressors (Nguyen & Thompson, 2006). Although most mycobacteria are non-pathogenic, many can cause severe disease in humans, and thus the mycobacterial genus remains a considerable clinical concern. The two most significant human mycobacterial pathogens are *Mycobacterium tuberculosis,* the causative agent of tuberculosis, and *Mycobacterium leprae*, the causative agent of leprosy. While these pathogens are the most well-known mycobacterial pathogens, there has been a significant emergence of non-tuberculosis mycobacterial (NTM) infections in humans, particularly in the immunocompromised population (Dahl et al., 2022). These include, but are not limited to, *Mycobacterium abscessus, Mycobacterium avium,* and *Mycobacterium kansaii* (Johnson & Odell, 2014).

Mycobacteria can be divided into two categories based on their replication on solid media: rapid-growing mycobacteria and slow-growing mycobacteria (RGM and SGM, respectively). RGM are visible on solid agar between three to five days after inoculation, whereas SGM are defined as mycobacteria that take seven days or more to form visible colonies on agar (Kim et al., 2013). Clinically relevant RGM include *M. abscessus* and *Mycobacterium fortuitum*, while *M. tuberculosis* and *M. leprae* are the most common SGM infections in humans.

1.2. *Mycobacterium abscessus* is an emerging clinical pathogen

M. abscessus is a rapid-growing NTM that is of increasing clinical concern. It is a saprophytic mycobacteria, considered to be ubiquitously found in soil and water (Sabin et al., 2017). It was first isolated from a knee abscess in 1952 by Moore and Freichs, and classified as an entirely new species of mycobacteria, named for its potential to cause subcutaneous abscesses (Moore & Frerichs, 1953). At the time, *M. abscessus* was regarded as a minimally virulent, self-limiting, cutaneous infection. Since then, its clinical relevance has exponentially

increased with implication in pulmonary infections, particularly in vulnerable populations, such as Cystic Fibrosis (CF) patients and the elderly (Johansen et al., 2020).

Historically, *M. abscessus* was considered to be a strictly opportunistic pathogen, infecting patients from contaminated soil and water sources. However transmission between patients – both within CF centres and globally – has been demonstrated. Bryant et al. (2013) used whole-genome sequencing (WGS) of 168 clinical isolates of *M. abscessus* to phylogenetically map the global distribution of subspecies, identifying distinct clusters spread throughout the world, clearly implicating common-source infection and potential patient-patient transmission (Bryant et al., 2016; Ruis et al., 2021). A recent long-term follow-up study of patients with NTM disease demonstrated that infection with *M. abscessus* was associated with poorer outcome and higher rates of mortality compared to any other NTM infection (Jhun et al., 2020).

1.2.1. Classification of *M. abscessus* subspecies

The classification and taxonomy of the *M. abscessus* complex has been an area of rapid evolution and contention since its isolation. Originally designated a subspecies of *M. chelonae*, it was recognised as an independent species, *M. abscessus*, in 1992 (Lopeman et al., 2019). In 2006, with the identification of two closely related species, *M. bolettii* and *M. massiliense*, the *Mycobacterium abscessus* complex was proposed, and divided into three subspecies (Tortoli et al., 2016). Since then, there has been much discussion in the literature regarding this classification. Recently, Gupta and colleagues proposed an amendment to the classification of Mycobacterial genera, in which *M. abscessus* belongs to a distinct clade, the *Mycobacteroides* gen. nov. *Abscessus-Chelonae* (Gupta et al., 2018). The *Abscessus-Chelonae* clade, regarded to have the earliest branching lineage, is highly genetically cohesive and distinct from other clades. However, as a relatively new proposal, this nomenclature has not yet been widely adopted.

The three subspecies of *M. abscessus* do possess some differences, particularly their resistance to currently available antibiotics. *M. abscessus* subsp. *abscessus* is the most common subtype isolated from infections (Sabin et al., 2017). Sequencing reveals the presence of *erm*, an inducible macrolide resistance gene, and is a distinguishing factor of this subspecies. The presence of a single aminoglycoside resistance gene renders *M. abscessus* subsp. *abscessus* more susceptible to resistance against amikacin and streptomycin (Rubio et al., 2015). *M. abscessus* subsp. *bolettii* is the least commonly

identified *M. abscessus* subspecies. It displays a similar resistance profile to that of *M. abscessus* subsp. *abscessus*. However, a kanamycin resistance encoding plasmid compounds the antibiotic resistance, making it particularly difficult to treat (Rubio et al., 2015). The final and most recently identified subspecies of *M. abscessus* is *M. abscessus* subsp. *massiliense*. Since its discovery in 2004, *M. abscessus* subsp. *massiliense* has been shown to be distributed globally. Clinical presentations of this subspecies are often more virulent due to the possession of distinct virulence factors. However, most clinical isolates of *M. abscessus* subsp. *massiliense* lack the *erm* resistance gene, allowing better treatment options (Sassi & Drancourt, 2014).

While the subspecies of *M. abscessus* have now been well-characterised, classification of *M. abscessus* clinical isolates remains challenging in many cases. Co-infections with other pathogenic and commensal organisms allows for the horizontal transfer of genetic material. These co-infections prevent precise subspecies identification using a single gene or method (Boeck et al., 2022; Mougari et al., 2016). Genomic analysis has revealed that *M. abscessus* can be separated into clusters with distinct virulence traits and clinical outcomes, suggesting the isolate selection is critically important for the analysis of *M. abscessus* virulence (Bryant et al., 2021).

1.2.2. Epidemiology and clinical presentations of *M. abscessus* infections

M. abscessus infections are diverse, but most commonly manifest as respiratory, skin, or soft-tissue infections. Most *M. abscessus* infections occur in immunocompromised patients or those with underlying pathologies such as CF or Chronic Obstructive Pulmonary Disease (COPD). However, infections can also occur in immunocompetent patients; for example, skin and soft-tissue infections may occur in patients following surgical procedures with contaminated equipment or instruments.

The global distribution and epidemiology of *M. abscessus* is diverse and can be challenging to attain due to complexities in the classification and identification of subspecies. However, there is no doubt that it has been steadily increasing over the past 20 years, partly due to improved diagnostic tools and species classification. In general, the incidence rate of NTM infections in industrialised countries is approximately 1-1.8 cases per 100 000, with *M. abscessus* accounting for 3-13% of all NTM disease (Honda et al., 2018).

The acquisition and transmission of *M. abscessus* is poorly understood. Historically, *M. abscessus* was considered a purely environmentally acquired, opportunistic pathogen due to its ubiquitous presence in soil, water, and plumbing (De Groote et al., 2006; Falkinham, 2011; Feazel et al., 2009). However, studies have yet to prove a strong causation link between the exposure to biofilms and *M. abscessus* niches in the household and acquisition of *M. abscessus* infection. Interestingly, a genetic link between *M. abscessus* isolated from pulmonary infections and contaminated water sources has been shown (Thomson et al., 2013). However, it was not determined whether contamination of the water source caused the pulmonary infection, or vice versa.

With the availability of WGS and other genetic studies, insight into potential patient transmission has arisen in the field of *M. abscessus* research. Examining the genetic diversity of pulmonary isolates of *M. abscessus* both within CF centres and across trans-continental CF centres have identified clusters of isolates that appear to have originated from a single source; thus, the potential for indirect patient transmission exists (Bryant et al., 2013; Bryant et al., 2016). Further, these studies highlighted that isolates could be grouped into "dominant clones" spread across continents (Ruis et al., 2021). These findings suggest that instead of existing environmentally as an opportunistic pathogen, *M. abscessus* has evolved into a true pathogen adapted to the human host. At the time of writing, studies are yet to show direct transmission of *M. abscessus* between patients, however it is postulated that accelerated pathogenic adaptation is possible once direct transmission occurs, as seen for *M. tuberculosis* (Bryant et al., 2021).

Respiratory *M. abscessus* infection

M. abscessus is the most predominant RGM causing respiratory infection; it is estimated that *M. abscessus* is the causative agent of up to 80% of all respiratory infections caused by RGM (Griffith et al., 2007). The symptoms of *M. abscessus* respiratory infections can be diverse and non-specific. However, most patients will have a persistent cough, following a slow yet progressive course, inevitably leading to respiratory decline and reduced quality of life (Griffith et al., 2007). On the other hand, serious, fulminant infections can occur, causing rapid pulmonary function decline and acute respiratory failure (Lee et al., 2015). Diagnosis of pulmonary *M. abscessus* can be difficult according to the American Thoracic Society/Infectious Diseases Society of America (ATS/IDSA). Diagnosing *M. abscessus* pulmonary infection requires both clinical and microbiological criteria to be met. This includes the presentation of clinical symptoms, positive culture from a minimum of 2

separate sputum samples, and evidence of pulmonary lesions per typical NTM infections as determined by radiography (Griffith et al., 2007). The implications of *M. abscessus* infections in CF patients will be discussed in more detail in Section 1.4.

Skin and soft-tissue *M. abscessus* infections

Extra-pulmonary *M. abscessus* infections are mostly skin and soft-tissue infections (SSTIs); these can range in severity from localised skin infections to deep tissue infections. Symptoms associated with SSTIs from *M. abscessus* can include abscesses, tender cutaneous nodules, and erythematous papules/pustules (Kothavade et al., 2013). *M. abscessus* SSTIs can be acquired either directly through contact with environmental *M. abscessus* (that is, contaminated soil or water, usually through an open wound) or by dissemination of primary disease at another body site (Kothavade et al., 2013). Forty-five percent of all extra-pulmonary *M. abscessus* infections are caused by post-operative infections (Chadha et al., 1998).

Other *M. abscessus* presentations

M. abscessus can also cause Central Nervous System (CNS) infections, particularly following neurosurgical procedures and intracranial catheters and patients with underlying otological pathologies (M. R. Lee et al., 2012). Contaminations of catheters can cause disseminated *M. abscessus* infections and bacteraemia. Disseminated *M. abscessus* infection is also associated with immunocompromised patients, such as those with cancer or Human Immunodeficiency Virus (HIV) (El Helou et al., 2013). Other extra-pulmonary *M. abscessus* infections include ocular infections, such as keratitis, endophthalmitis, and scleritis (Moorthy et al., 2012).

Considering respiratory infections are the most common and the most severe manifestations of *M. abscessus* infection, these will be the focus in the remainder of this thesis.

1.2.3. *M. abscessus* is a significant clinical problem in Cystic Fibrosis patients

M. abscessus has emerged in recent years as a significant pathogen, particularly within the CF community. CF is an autosomal recessive disorder involving mutations in the Cystic fibrosis transmembrane conductance regulator (CFTR) gene (Riordan et al., 1989). It is the most common congenital life-limiting disorder affecting Caucasians and carries significant morbidity (Guo et al., 2022). Currently, it is estimated that the prevalence in North Americans

is 30,000 (Elborn, 2016), with respiratory failure and infection being the most common cause of mortality (Cantin et al., 2015).

The CFTR protein is predominantly expressed on the apical surface of epithelial cells and functions to regulate chloride ion transport across luminal surfaces (Riordan et al., 1989). Defective or absent CFTR results in mucus accumulation in the airways, pancreatic insufficiency, gastrointestinal complications, and infertility in males due to vas deferens impairment (Elborn, 2016). The lack of mucociliary clearance in the airways provides a rich micro-environment for colonisation and persistent infection with bacteria, particularly *Pseudomonas aeruginosa, Staphylococcus aureus,* and *Burkholderia cenocepacia* (Cantin et al., 2015). Treatment of concurrent infections such as *S. aureus* and *P. aeruginosa* with broad-spectrum antibiotics further predispose CF patients to acquire *M. abscessus* infection due to its multidrug resistance (Catherinot et al., 2013). Concurrent infections with other pathogenic bacteria have also allowed for the evolution of *M. abscessus* over time into a more virulent species through horizontal gene transfer, with the acquisition of genes such as *mtgC* and *plc*, which have been implicated in intracellular survival capabilities (Maloney & Valvano, 2006; Mathee et al., 2008; Ripoll et al., 2009).

The prevalence of *M. abscessus* infections in CF patients has been steadily rising over the last two decades and has presented a significant clinical problem for this population. Indeed, it has been projected that between 10-20% of CF patients will develop an NTM infection within their lifetime, with most of these being *M. abscessus* as the causative agent (Roux et al., 2009). The observed global rise in *M. abscessus* cases may reflect improved diagnostics and classification of the species, yet it is still significantly underestimated in many countries. This may be attributed to the lack of mandatory reporting guidelines, false-negative cultures, and interference of concomitant bacterial colonisers, such as *P. aeruginosa*, during isolation (Mougari et al., 2016). Between 2016 and 2020, the proportion of NTM-positive sputum cultures in Australian CF patients aged 18-30 years old increased from 2.1% to 5.2% (Australian Cystic Fibrosis Data Registry, 2021). The prevalence is even higher in USA and European CF centres, with a period prevalence of *M. abscessus* culture positivity of 8% and 3.4-5.8%, respectively (Ademhan Tural et al., 2021; Adjemian et al., 2018). Further, the proportion of infections caused by *M. abscessus* among all NTM infections has risen and is now the most commonly isolated RGM in CF patients (Honda et al., 2018; Mougari et al., 2016) (Table 1.1).

Table 1.1: Proportions of cases caused by *M. abscessus* of all respiratory NTM infections in CF patients by country*

Country	Proportions of cases caused by *M. abscessus* of all respiratory NTM infections in CF patients
United Kingdom	56%
France	52%
USA	45%
China	13.3%

**Adapted from Mougari et al.* (2016).

M. abscessus infection can be particularly devastating in CF patients as it is correlated with a progressive decline in lung function. Some risk factors in CF patients have been identified, including age over 40, low body mass index (BMI), poor spirometry results, concurrent infections with *P. aeruginosa* and/or *Stenotrophomonas maltophilia,* and with that, use of antibiotics by inhalation (Viviani et al., 2016). *M. abscessus* is intrinsically resistant to many antibiotics currently available. In many cases, it may prove impossible to treat. In some centres, *M. abscessus* infection may be a contraindication for a lung transplant, a last-line treatment for many CF patients, and hence may be the cause of death in some CF patients. However, this remains controversial (Chandrashekaran et al., 2017) and more recently it has been observed that it is no longer a contraindication for a lung transplant, though serious post-operative complications are likely to occur (Benwill & Wallace, 2014). Thus, new tools are required to effectively treat and prevent *M. abscessus* infections in susceptible populations, such as CF patients.

1.2.4. *M. abscessus* can have a smooth or rough morphotype, which may depend on its environment

M. abscessus is further diversified by having either a smooth (S-) or rough (R-) morphotype, which can determine the fate of the organism within the host upon infection. S- and R-morphotypes are classified based on the expression of glycopeptidolipids (GPLs). GPLs are expressed on many of mycobacterial species' surface and serve various functions, including motility, biofilm formation, host-cell interactions, and survival within macrophages (Roux et al., 2016). The presence (S-variants) or absence (R-variants) of these surface GPLs have many pathophysiological and immunological consequences and can determine the outcome of infection with *M. abscessus*. S-*M. abscessus* variants display abundant GPL expression and are consequently non-cording, motile, and can form biofilms (Roux et al., 2016).

Conversely, R-*M. abscessus* strains lack GPLs, yet possess the propensity to form cords – long, dense groups of bacilli – but are non-motile and do not tend to form biofilms (Medjahed & Reyrat, 2009).

It is well-established that S and R variants have distinct fates within the host. S-*M. abscessus* have the propensity to form biofilms: communities of micro-organisms that can colonise an environmental surface, biomaterial, or, indeed, the lung alveoli, particularly in patients with established lung disease such as CF or bronchiectasis. Within biofilms, bacteria are embedded within a complex matrix of extracellular DNA, glycopeptides, and other protein and lipid molecules (Esteban & García-Coca, 2017). The high GPL expression of the S variant facilitates this kind of colonisation. In addition, the high GPL content of the S-*M. abscessus* cell wall has been shown to "mask" other immunogenic peptides – such as trehalose dimycolate (TDM), a key regulator in the cording phenotype and virulence that is associated with *M. abscessus* infection – resulting in reduced macrophage activation and apoptosis. Roux and colleagues demonstrated that S-*M. abscessus*, despite being readily phagocytosed by macrophages *in vitro*, prevents phagosome acidification and maturation, thereby failing to trigger macrophage apoptosis (Roux et al., 2016). Consequently, S-*M. abscessus* variants have limited potential to spread amongst macrophages, ultimately limiting their virulence within a host (Howard et al., 2006; Kam et al., 2022).

The R-*M. abscessus* phenotype, on the other hand, is considered to be more detrimental to macrophage survival. The lack of surface GPLs results in more potent Toll-Like Receptor-2 (TLR2) agonism by *M. abscessus*, driving potent tumour necrosis factor (TNF) expression, and subsequent inflammatory responses (Davidson et al., 2011). In addition to driving strong macrophage recruitment via TLR2 signalling, when phagocytosed, R-*M. abscessus* is more apoptotic than S variants (Roux et al., 2016). As a result, high numbers of bacteria are released from macrophages, where they rapidly replicate into large, extracellular cords. These large aggregates are then unable to be phagocytosed; instead, they form abscesses, resulting in tissue damage and, ultimately, tissue death (Bernut et al., 2014). Furthermore, Howard and colleagues (2006) demonstrated that R variants cause a more invasive pulmonary infection in mice. Hence, the R variant of *M. abscessus* is significantly more virulent and correlated with more severe disease. In particular, colonisation of CF patient lungs with R-*M. abscessus* results in severe, progressive decline in lung function, ultimately causing respiratory failure (Jönsson et al., 2007).

The ability of *M. abscessus* clinical isolates to transition from S to R variants has been referred to as a "double-edged sword" (Gutiérrez et al., 2018); it efficiently transitions between a colonising, environmental micro-organism to an invasive human pathogen. Little is known about this process, including what triggers it and the precise mechanism by which it occurs. Nessar and colleagues (2011) demonstrated that the deletion of the *mmpL4b* gene – a membrane protein crucial for GPL expression – results in the S- to R-*M. abscessus* transition. This was characterised by the loss of sliding motility and biofilm formation, but the acquisition of virulence and an invasive phenotype (Nessar et al., 2011). Further, differences in immunopathogenesis have been shown (Kam et al., 2022). The dichotomy between S- and R-variants of *M. abscessus* must be carefully considered in experimental approaches to the immune response to *M. abscessus* infection *in vitro.* It may be useful to elucidate particular immune responses to *M. abscessus* in vaccine design by extension.

1.3. *M. abscessus* is notoriously difficult to treat, and new tools are required to manage infection in CF patients

1.3.1. Current treatment guidelines for *M. abscessus* infection in CF patients

M. abscessus is renowned for its difficulty to treat, so much so that it is still regarded as a "chronic, incurable disease," given its resistance to almost all anti-tuberculous treatments as well as broader spectrum antimicrobials (Johansen et al., 2020). Given its pathogenicity and likelihood to cause rapid respiratory decline, treatment is urged in patients experiencing the criteria outlined in Table 1.2. Like most mycobacterial infections, treatment of *M. abscessus* requires an intensive phase followed by a continuation phase. The current guidelines suggest that the intensive phase be a 3-12 week course of a macrolide and parenteral amikacin, and tigecycline, imipenem or cefoxitin. The subsequent continuation phase should extend for at least 12 months following conversion of culture (sputum, bronchoalveolar lavage or bronchial washing) and consist of oral macrolide and inhaled amikacin, with 2-3 of the following: minocycline, clofazimine, moxifloxacin, linezolid (oral) (Floto et al., 2016). Surgical resection of infected tissue may be considered in some cases, albeit with variable success (Jarand et al., 2011).

While these are the currently recommended and accepted treatment guidelines, no randomised controlled trials assessing these regimens have been performed. Much of the evidence comes from retrospective studies of non-CF patient cohorts (Waters et al., 2016). This is further compounded by the observation that *in vitro* susceptibility for *M. abscessus*

does not correlate well with clinical response (Griffith et al., 2007). As such, our current methods of predicting the efficacy of *M. abscessus* treatment regimens are not much better than "trial and error."

Table 1.2: Criteria suggesting that treatment of *M. abscessus* infection should be considered in paediatric CF patients*.

(i)	Deterioration in lung function and/or symptoms, despite treatment of comorbidities (diabetes, allergic bronchopulmonary aspergillosis) and concurrent infections
(ii)	At least two sputum cultures that are positive for *M. abscessus*
(iii)	Radiological evidence of NTM pulmonary disease (inflammatory nodules, "tree-in-bud opacities," cavities)

**Adapted from Andrew et al. (Andrew et al., 2019)*

1.3.2. Current antimicrobials for *M. abscessus* infection are costly and pose significant safety threats to the patient

As detailed in the section above, the currently advised treatment regimens for *M. abscessus* are lengthy and arduous. This carries significant implications for both the patient and the healthcare system. Notably, high rates of antibiotic toxicity and intolerability have been reported. A retrospective study in South Korea revealed that 51% of patients treated with cefoxitin developed leukopenia, 15% had drug-induced hepatotoxicity, and 6% experienced thrombocytopenia (Jeon et al., 2009). In addition, gastrointestinal symptoms (anorexia, nausea, diarrhoea) were observed in 22% of patients. A North American study reported 74 side effects – namely nausea, vomiting, and skin changes – in 62% of patients attributed to amikacin and tigecycline treatment (Novosad et al., 2016). Another important safety consideration in treating *M. abscessus* is hearing loss, which occurs at a rate of up to 7% of patients treated with clarithromycin (Coulston & Balaratnam, 2005; Heffernan et al., 2018).

1.3.3. *M. abscessus* possesses both intrinsic and acquired resistance mechanisms, which make it a difficult pathogen to treat

In addition to safety considerations, current *M. abscessus* treatment options confer high rates of treatment failure. The average treatment success rates for *M. abscessus* have been estimated to be 45.6%, varying with subspecies (Choi et al., 2018; W. J. Koh et al., 2017; Kwak et al., 2019). This can be attributed to the possession of resistance mechanisms, both intrinsic and acquired.

Intrinsic resistance can be attributed to many mechanisms: impermeability of the cell envelope, expression of efflux pumps that inhibit the accumulation of sufficient drug concentrations within bacterial cells, expression of enzymes that modify and/or degrade drugs or drug targets, and reducing or destroying the antimicrobial's affinity for drug targets within the bacteria (Nessar et al., 2012; Ripoll et al., 2009). These innate mechanisms have resulted in *M. abscessus* being resistant to almost all β-lactams, tetracyclines, aminoglycosides, and macrolides. A more detailed overview of resistance mechanisms identified in *M. abscessus* isolates can be found in Degiacomi et al. (2019).

The rise in acquired resistance factors further compounds the difficulty in treating *M. abscessus*. It has been hypothesised that horizontal transfer of resistance genes occurs in patients due to the numerous and diverse range of bacteria that may colonise the lung of CF patients simultaneously, as well as inappropriate and/or prolonged exposure to antibiotics (Nessar et al., 2012). One of the primary mechanisms by which this may occur is the mutation of target genes. Perhaps one of the most clinically significant acquired drug resistance mechanisms is that of acquired macrolide resistance, which occurs due to mutation in the *erm*(41) gene, rendering the clinical isolate entirely resistant to macrolides, one of the most essential antibiotic classes required for successful NTM treatment. Interestingly, this confers a high positive predictive value for treatment failure, not only for macrolide treatment but also for amikacin (Griffith, 2019).

1.3.4. Novel compounds in the clinical pipeline for the treatment of *M. abscessus* infections

Despite the limited efficacy of currently available antimicrobials for *M. abscessus* infection, little progress has been made in developing novel compounds to combat this pathogen. These include repurposed antimicrobials, such as oral clofazimine and inhaled amikacin, as well as rifabutin, tigecycline and bedaquiline (Victoria et al., 2021). Novel compounds such as delamanid, pretomanid and, PIPD1, as well as new beta-lactamase inhibitors, avibactam, relebactam and vaborbactam, have shown promise in pre-clinical models (Meir & Barkan, 2020). However these antimicrobials have not yet shown significant efficacy in patients infected with *M. abscessus*, and more work is needed to harness their therapeutic potential.

Perhaps one of the most exciting prospects in novel *M. abscessus* therapeutics is phage therapy. A case of completely drug-resistant strain and progressive *M. abscessus* infection in a fifteen-year-old was treated with a cocktail of three bacteriophages, with no adverse

effects and resulted in complete clearance of *M. abscessus* infection (Dedrick et al., 2019). This represents an exciting prospect for the future of *M. abscessus* treatment, however, it is highly involved due to its patient- and strain-specific nature (Dedrick et al., 2022; Meir & Barkan, 2020).

Many new drugs in the pipeline are bacteriostatic instead of bactericidal, leading to poor therapeutic outcomes (Maurer et al., 2014). Perhaps, given its propensity for acquired or inducible resistance, more efforts should be made in developing strategies to prevent infection in the first place, rather than treating them after colonisation.

1.4. Immune response to mycobacterial pathogens

Due to the increasing prevalence and difficulty in treating *M. abscessus*, improved knowledge of immunity to infection is critical for the development of effective immunotherapies such as vaccines. Pulmonary disease is believed to begin with inhalation of *M. abscessus* aerosols, followed by phagocytosis of mycobacteria by macrophages. A complex cascade of events results in inflammation and cellular recruitment, eventuating in the formation of granulomas, the hallmark of mycobacterial infection (Johansen et al., 2020). Granulomas are aggregates of cells, predominantly macrophages, T cells, and B cells, that physically contain the infection to prevent bacterial dissemination (Bernut et al., 2016). However, the propensity of *M. abscessus* to transition from smooth to rough variant during intracellular infection, allows uncontrolled replication of the bacteria into large extracellular cords, disrupting the tight granulomatous structure and causing disseminated infection (Johansen et al., 2020; Kam et al., 2022).

1.4.1. Innate immune response to *M. abscessus* infection

Macrophages

It is well-known that macrophages are the primary host cell for mycobacteria and are essential in controlling infection. Once phagocytosed by the macrophage, *M. abscessus* is subject to many fates: it may undergo phagolysosomal destruction, serve as a dormant reservoir of infection, or propagate and disseminate infection by intracellular replication (Awuh & Flo, 2017). *M. abscessus* antigens trigger signalling through pattern recognition receptors (PRRs) such as TLR-2 and Dectin-1, a C-type lectin-like pattern recognition receptor, causing active phagocytosis of the bacilli (Shin et al., 2008). *M. abscessus*

activates the NLRP3 inflammasome by spleen tyrosine kinase (Syk)-dependent signalling which then contributes to the microbicidal capacity of the macrophage (H. M. Lee et al., 2012).

Despite the potent antimicrobial capacity of the macrophage, *M. abscessus* has evolved to resist phagosome maturation, allowing it to survive intracellularly (Oberley-Deegan et al., 2010). In particular, the R-variant is able to inhibit phagolysosomal fusion, and replicate within vacuoles (Kim et al., 2017). As the bacilli continue to replicate, the macrophage is no longer able to contain the infection, allowing it to spread extracellularly. *M. abscessus* continues to replicate into extracellular cords which are too large to be phagocytosed, facilitating the spread and propagation of infection (Bernut et al., 2014).

Phagocytosis of *M. abscessus* by macrophages triggers the recruitment of other inflammatory cells to control infection. TLR-2 signalling in macrophages triggers transcriptional activation of pro-inflammatory genes; in particular, TNF, Interleukin-1 (IL-1β), IL-6, IL-12, nitric oxide (NO), reactive oxygen species (ROS) and other chemokines (Wang et al., 2019). Infection of *tlr2*$^{-/-}$ mice with *M. abscessus* resulted in the loss of several crucial events that allow for bacterial clearance: there was a lack of interferon-gamma (IFN-γ), TNF, and IL-12p70 production, no early migration of neutrophils, monocytes or dendritic cells (DCs), as well as an absence of important adaptive immune responses such as early CD4^{+} and CD8^{+} T cell migration, as well as memory and effector T cell expansion (Kim et al., 2015). Macrophages infected with *M. abscessus* had significantly increased expression of IFN-I, which strongly correlated with increased TNF production and intracellular killing (Ruangkiattikul et al., 2019). In this study, it was shown that signalling through the TLR2-TLR4-MyD88-TRIF-IRF3 axis upregulates type I interferon expression, which subsequently drives the expression of inducible nitric oxide synthase (iNOS). iNOS is the enzyme required for the production of NO, a potent antimicrobial agent employed by macrophages (Flynn & Chan, 2001). An overview of the virulence mechanisms involved in *M. abscessus* resistance of phagosome maturation can be found in Ferrell et al. (2022).

There is thought to be two main macrophage subsets in the lung – alveolar macrophages (AMs) and interstitial macrophages (IMs). AMs are embryologically derived from foetal liver, and self-renew in the lung during steady state (Guilliams et al., 2013). IMs, on the other hand, are considered to be monocyte-derived and replenished by chemokine receptor-2 (CCR2) dependent circulating monocytes (Gibbings & Jakubzick, 2018; Liegeois et al.,

2018). Historically, AMs have been considered to be the predominant subset essential in mycobacterial infection clearance, whereas IMs are often overlooked as a transient myeloid subset in the processes of differentiating into AMs (Liegeois et al., 2018). However, IMs may indeed play an active role in infection. IMs possess high phagocytic capacity and express Major Histocompatibility Complex Class II (MHCII) at high levels, suggesting their propensity for professional antigen presentation to DCs in order to engage the adaptive immune response to infection (Bedoret et al., 2009; Gibbings et al., 2017). They have also been shown to produce IL-1, IL-6, and TNF, important pro-inflammatory cytokines in the context of controlling infection (Hoppstädter et al., 2010). Invariably, IMs have been shown to express high levels of CX3CR1 and CD14, which can be used to identify them from other myeloid subsets (Gibbings et al., 2017). Interestingly, detailed transcriptomic analysis of IMs isolated from murine lungs has revealed three distinct IM subsets, expressing varying levels of pro-inflammatory cytokines, chemokine ligands, MHCII, CD11c, CD206, and Lyve-1 (Gibbings et al., 2017). However, the functional significance of these subsets remains to be elucidated.

A role for IMs particularly in the context of mycobacterial infection has been described. Srivastava and colleagues (2014) revealed that IMs are recruited to the lung during *M. tuberculosis* infection. Another pivotal study in this field was conducted by Huang and colleagues, which showed that AMs are more permissible to *M. tuberculosis* infection, providing a nutrient-rich environment for bacilli to replicate intracellularly (Huang et al., 2018). Conversely, IMs were shown to restrict mycobacterial growth and intracellular survival, by restricting the nutrients available for bacterial metabolism. Further, depletion of AMs reduced *M. tuberculosis* bacterial load in the lungs, while depletion of IMs significantly increases the bacterial load (Huang et al., 2018). Interestingly, dissemination from and activation of AMs and IMs has been shown to be dependent upon mycobacterial virulence; while intranasal BCG was contained to and subsequently promoted activation of AMs, virulent *M. tuberculosis* strains more readily disseminated to IMs (Mata et al., 2021). These studies highlight IMs as an important – albeit often neglected – immune cell subset that may be crucial to the control of mycobacterial infection more broadly.

Neutrophils

Neutrophils are phagocytic cells with a diverse repertoire of antimicrobial defences. During the steady state, neutrophils are rarely found in peripheral tissues. Rather, they are rapidly recruited in response to infection and inflammation (Pohl et al., 2020). Bernut and colleagues

(2016) demonstrated that TNF/IL-8 signalling in macrophages is essential for neutrophil recruitment after *M. abscessus* infection in a zebrafish model. Importantly, they also demonstrated that neutrophils have an essential role in the formation of structured granulomas to contain *M. abscessus* infection. Impaired TNF signalling resulted in defective IL-8 production, subsequently leading to poor neutrophil migration and a lack of granuloma formation (Bernut et al., 2016).

Once recruited, the control of *M. abscessus* infection requires both intracellular and extracellular mechanisms employed by neutrophils. Intracellular strategies include the production of ROS, a potent antimicrobial causing oxidative damage to the bacteria (Malcolm et al., 2018). Neutrophils are able to kill *M. abscessus* within one hour of *in vitro* infection, highlighting their potent microbicidal capacity (Malcolm et al., 2018). Interestingly, the mechanism by which this occurs differs between S and R variants. S variants are susceptible to both intracellular and extracellular killing, while R variants are resistant to intracellular killing strategies employed by neutrophils; in fact, R- *M. abscessus* variants promote neutrophil necrosis, an evolutionary advantage of the bacteria to propagate infection (Malcolm et al., 2013).

The major extracellular mechanism of neutrophil defence is the formation of neutrophilic extracellular traps (NETs). NETs are composed of extracellular enzymes such as elastase and myeloperoxidase that immobilise extracellular bacteria and other foreign particles allowing them to be cleared by the immune system (Malcolm et al., 2018). When NET formation is disrupted, *M. abscessus* bacterial load significantly increases, thus highlighting their importance in the early response to *M. abscessus* infection. Interestingly, neutrophils have a reduced capacity to internalise *M. abscessus* compared to *S. aureus*, a 'conventional' extracellular bacterial pathogen (Malcolm et al., 2013). This may be partially explained by the propensity for *M. abscessus* to inhibit neutrophil activation, thereby promoting its survival and by extension, its ability to adapt to environmental stressors. Notably, CFTR deficiency – as is the case in CF patients – impairs intracellular growth restriction capacity in neutrophils as well as neutrophil recruitment, due to defective NADPH oxidase-dependent pathway (Bernut et al., 2019). This may contribute to CF patients being susceptible to severe pulmonary *M. abscessus* infection. Thus, while neutrophils are classically an important immune subset for the early control of infection, they are not sufficient to limit *M. abscessus* infection.

Dendritic cells

It is widely accepted that DCs are the most significant stimulators of naïve T cells. Immature DCs are present in large numbers in the lung at the onset of inflammation, highly specialised for antigen uptake and processing (Guilliams et al., 2013). DCs may encounter whole mycobacteria or mycobacterial antigens via stimulation of an array of PRRs, such as complement receptors, mannose receptors, TLRs and Dendritic Cell-Specific Intracellular adhesion molecule-3-Grabbing Non-integrin (DC-SIGN) (Herrmann & Lagrange, 2005). Tailleux et al. (2003) proposed DC-SIGN to be the predominant receptor involved in mycobacterial antigen internalisation by human DCs. In the context of *M. tuberculosis* infection, antigen uptake results in DC maturation and increased CCR7 expression, allowing for migration to draining lymph nodes (Riol-Blanco et al., 2005). Indeed, DC migration from the primary site of infection to the draining lymph nodes (dLN) is the most important means by which naïve T cells are primed, hence "kick-starting" the adaptive immune response to mycobacterial infection (Lee et al., 2014).

While the role of DCs in *M. tuberculosis* infection has been widely studied, little is known about the specific interactions between host DCs and *M. abscessus* infection. Indeed, *M. abscessus* has been shown to stimulate TLR-4 and through MAPK signalling to drive DC maturation. This induces $CD4^+$ and $CD8^+$ T cell differentiation, a crucial step in the adaptive immune response to *M. abscessus* infection (Lee et al., 2014). In particular, this pathway strongly promotes T-helper type 1 (Th1) cell differentiation. However, more insight is needed into the role of DCs in *M. abscessus* infection and, more specifically, the recruitment of T cell subsets, in order to better design vaccines and understand the immune correlates of protection against *M. abscessus* infection.

1.4.2. Adaptive immune response to *M. abscessus* infection

The adaptive immune response, namely $CD4^+$ T cells, $CD8^+$ T cells, B cells, as well as non-conventional subsets, is crucial for clearing intracellular bacterial infections and generating memory cells. Severe Combined Immunodeficient (SCID) mice infected with *M. abscessus* had significantly higher bacterial burdens, and progressive disease up to 40 days post-infection (dpi) (Obregón-Henao et al., 2015). In addition, nude mice, which have significantly reduced T cell populations due to a defective thymus, also had significantly worse disease outcomes when infected with *M. abscessus* infection (Bernut et al., 2017). Thus, there is a clear role for the adaptive immune response in controlling *M. abscessus* infection.

CD4$^+$ T cells

CD4$^+$ T cells have been identified as the key cellular mediators of adaptive immunity to mycobacterial infection. This is evidenced in mice with CD4$^+$ depletion, which show markedly increased severity of mycobacterial infection (Caruso et al., 1999). Effective protection against *Mycobacterium bovis* is achieved when CD4-deficient mice were reconstituted with antigen-specific CD4$^+$ T cells from vaccinated controls, further highlighting the importance of CD4$^+$ T cells in mycobacterial infection (Feng & Britton, 2000). In humans, patients with HIV, and thus a depletion in CD4$^+$ T cells, have increased susceptibility to non-tuberculous mycobacterial infections (Cai et al., 2017).

Th1 CD4$^+$ T cells

Th1 cells appear to be the most important CD4$^+$ T cell subset in controlling mycobacterial infection and are the most widely characterised. Th1 differentiation is driven predominantly by IL-12 secretion by DCs and macrophages (Lee et al., 2016). IL-12 secretion results in upregulation of the master transcription factor T-box expressed in T cells (Tbet), which allows for differentiation into the Th1 phenotype (Johnson et al., 2018). This includes the production of IFN-γ, the key mediator of Th1 function, as well as chemokine receptors such as CXCR3 causing Th1 cells to migrate to the site of infection (Gagliani & Huber, 2017). Once at the site of infection, Th1 cells produce IFN-γ, TNF and IL-2, contributing to granuloma formation (Flynn & Chan, 2001; Johansen et al., 2020). Indeed, polyfunctional CD4$^+$ T cells – that is, IFN-γ^+TNF$^+$IL-2$^+$ CD4$^+$ T cells – have been correlated with protection in mice and humans. When examining the circulating T cell profiles of humans infected with NTM compared to healthy controls, Shu et al. (2019) found that patients with more severe disease had attenuated polyfunctional T cells, whereas patients with less severe disease had strong polyfunctional T cell responses. This suggests a role for these cells in control of disease progression. Finally, beige mice – a mouse strain in which Th2 cell responses are predominant – infected with *M. abscessus* were also more susceptible to disease, further reinforcing the notion that Th1 cell responses are required for adequate immune control of *M. abscessus* infection (Bernut et al., 2017).

Th17 CD4$^+$ T cells

More recently, Th17 cells have been shown to be important in combatting mycobacterial infections, although their precise role is subject to contention. Th17 differentiation requires

IL-6 and IL-1 production through activation of STAT3 upon antigen presentation to naïve T cells by antigen presenting cells (APCs) (Ouyang et al., 2008). Activation of the key transcription factor retinoid-related orphan (ROR)γT drives expression of effector cytokines; IL-17A, IL-17F, IL-21 and IL-22. Th17 cells are able to rapidly proliferate and undergo apoptosis at the site of infection, provide an instantaneous response to inflammation, stimulate B cells to undergo isotype switching, and act on epithelial cells to drive the immune response to infection at mucosal sites (Rathore & Wang, 2016). When stimulated with IL-17 or IL-22, epithelial cells produce granulocyte colony-stimulating factor (G-CSF) and granulocyte-macrophage colony-stimulating factor (GM-CSF), as well as chemokines CXCL1 and CXCL8 to facilitate neutrophil recruitment (Ouyang et al., 2008). This enables neutrophils to engulf and kill pathogens through antimicrobial defences discussed previously. Interestingly, Albanesi and colleagues (1999) showed that the synergism between Th1 cytokines, such as IFN-γ and Th17 lymphocytes, is required for adequate immune responses.

Th17 cells have been shown to play a crucial role in mediating mycobacterial infection. In a study in paediatric idiopathic pulmonary NTM patients, disease was correlated with reduced Th17 responses, while IL-12/IFN-γ signalling appeared intact (thought to be associated with disseminated NTM infection) (Wu et al., 2019). Another study in children with NTM disease showed that patients had attenuated Th1/Th17 differentiation capacity and expressed reduced IFN-γ and IL-17 after stimulation when compared to healthy controls (Claeys et al., 2019). In this way, while Th1 responses may prevent dissemination of NTM disease, Th17 responses are crucial for controlling mucosal immunity.

Though Th17 responses are important for controlling mycobacterial infection, caution must be taken in assigning them a protective role. Th17 cells and subsequent IL-17 and IL-22 production is associated with inflammation which, if not balanced, may be pathogenic. For example, Th17 responses can be detrimental in CF patients which experience chronic pulmonary neutrophil influx (Dubin et al., 2007).

<u>$CD8^+$ T cells</u>

$CD8^+$ T cells, including cytotoxic T lymphocytes (CTLs), are also important mediators in mycobacterial immunity. $CD8^+$ T cells produce high levels of IFN-γ in response to *M. tuberculosis* infection (Flynn et al., 2011). Granulysin-dependent killing of extracellular *M.*

tuberculosis by CTLs has also been shown, as well as Fas ligand-induced apoptosis of infected macrophages (Blomgran & Ernst, 2011; Oddo et al., 1998). Further, mycobacterial antigens produce antigen-specific $CD8^+$ T cell responses in mice, however these are unable to confer protection against *M. tuberculosis* challenge (Lindenstrøm et al., 2014). Thus while $CD8^+$ T cells have some role in mediating mycobacterial immunity, it is unlikely that their contribution is greater than that of $CD4^+$ T cells.

The role of $CD8^+$ T cells in *M. abscessus* infection remains unclear. Intravenous (i.v.) infection of C57BL/6 mice showed both $CD4^+$ and $CD8^+$ T cell recruitment into granulomas. However, the proportion of $CD8^+$ T cells was notably reduced compared to $CD4^+$ T cells (Rottman et al., 2007). Further, when studying circulating T cells in NTM infections, $CD8^+$ T cell levels were similar between NTM-infected subjects and healthy controls (Lim et al., 2010). Therefore, more in-depth analysis is required to further elucidate the role of $CD8^+$ T cells in *M. abscessus* infection and immunity.

<u>B cells</u>

The contribution of B cells to mycobacterial immunity has long been a point of contention. B cells possess the capacity for antigen presentation, antibody production and cytokine secretion, thereby acting on behalf of both innate and adaptive immune responses (Chan et al., 2014). In Tuberculosis (TB) patients, high serum levels of antibodies are correlated with protection against dissemination (Costello et al., 1992). B cells have also been implicated in granuloma formation and containment of infection in mice (Maglione et al., 2007). However, B cell depletion studies have yielded variable results, creating ambiguity in the exact role of B cells in mycobacterial infection. Some studies report an increase in susceptibility to mycobacterial infection (Maglione et al., 2007), while others show a reduction in severity (Turner et al., 2001), or no change (Phuah et al., 2016).

There is also variable evidence for the role of B cells in *M. abscessus* infection. In a high-dose i.v. model of infection, $\mu MT^{-/-}$ mice – that is, mice deficient in B cells – had 100-fold higher bacterial burden in the spleen compared to wild-type (WT) mice, suggesting a protective role of B cells in *M. abscessus* infection (Rottman et al., 2007). This is supported by observations that beige mice, with a predominantly Th2/humoral-mediated immune response, were more susceptible to infection than WT mice (Rottman et al., 2007). However, the exact role of B cells in these studies may be difficult to discern, given the high dose and route of infection, leading to an overwhelming systemic response. Thus more research is

needed in a lower-dose, pulmonary infection model of *M. abscessus* to more accurately identify the contribution of B cells and other cell types in disease.

Interestingly, there appears to be a dichotomy in the role of B cells between S- and R- *M. abscessus* variants. The GPL-rich content of S variants are potent B cell antigens, and thus infections with smooth variants tend to be more humoral mediated. On the other hand, R- *M. abscessus* infection produces a Th1-skewed immune response (Rottman et al., 2007). Thus, B cells may play a minor role in the early containment of S morphotype infection, but have a minimal role compared to Th1 cells in the context of R- *M. abscessus* infection.

1.4.3. Important soluble mediators in *M. abscessus* infection

While the cells described above are crucial in mounting the immune response to *M. abscessus* infection, it is the soluble mediators they produce that are the effectors in this process. The key mediators that have been identified are IFN-γ, TNF and NO.

Interferon gamma (IFN-γ)

IFN-γ production by $CD4^+$ T cells is a potent stimulator of macrophage effector functions and hence an important mediator in antimycobacterial responses. IFN-γ promotes NO production by inducing iNOS transcription, which improves the ability of macrophages to clear intracellular pathogens (Thirunavukkarasu et al., 2017). IFN-γ also stimulates transcription of genes involved in important immunological defences such as antigen processing and presentation, apoptosis, and Th1 development (Dorman & Holland, 2000). Several studies have demonstrated the importance of IFN-γ, such that deficency in IFN-γ or its receptor signalling is detrimental to the host. *Ifngr1*$^{-/-}$ mice infected with *M. abscessus* had significantly increased bacterial burden as well as persistent, progressive disease (Rottman et al., 2007). Deficiencies in IL-12/IFN-γ signalling axis also resulted in severe disseminated *M. abscessus* disease (Casanova & Abel, 2002).

Interestingly, while IFN-γ is clearly essential in fighting mycobacterial infection, the magnitude of IFN-γ response by $CD4^+$ T cells does not strongly correlate with mycobacterial immunity (Counoupas et al., 2020; Kaufmann, 2013). This suggests that the immune response to mycobacteria is complex, and it may be the interplay between a multitude of mediators that induces protection against mycobacterial infection.

Tumour necrosis factor (TNF)

TNF is also an essential effector cytokine in the control of mycobacterial infection. It is produced early in infection by macrophages, as well as being one of the hallmark effector cytokines produced by Th1 cells (Mehta et al., 2018; Parameswaran & Patial, 2010). TNF, like IFN-γ, is a potent inducer of iNOS expression and therefore killing of mycobacteria (Bekker et al., 2001). TNF also induces chemokine expression to foster lymphocyte migration to the site of infection and is crucial in maintaining granuloma formation (Ehlers & Schaible, 2012; Roach et al., 2001). Finally, TNF activates naïve and effector T cells to promote differentiation and proliferation. Interestingly, TNF also has the propensity to induce apoptosis of "over-active" effector T cells, mediating the magnitude of the T cell response (Mehta et al., 2018). Thus, TNF can have both potent inflammatory or anti-inflammatory effects.

The effect of TNF signalling in the context of *M. abscessus* infection has been widely studied. In a zebrafish model, Bernut and colleagues (2016) showed that defective TNFR signalling resulted in complete abrogation of granuloma formation and increased burden of disease. In mice, TNF deficiency (TNFKO mice) in the context of i.v. *M. abscessus* infection leads to severe disease, with all animals succumbing to infection within 20 days (Bernut et al., 2017). Further, TNF has been shown to be critical in preventing disseminated *M. abscessus* infection in C57BL/6 mice (Jeon et al., 2009). The protective role of TNF in *M. abscessus* infection is further supported by observations in humans that patients undergoing anti-TNF therapy for inflammatory conditions are more susceptible to NTM infections (Brode et al., 2015).

Inducible nitric oxide synthase (iNOS)

iNOS is an enzyme that produces large quantities of NO when activated and has potent antimicrobial activity. iNOS expression is induced in macrophages by TNF and IFN-γ during inflammation (Strijdom et al., 2009). The potent antimicrobial activity of NO in the context of mycobacterial infection has been widely studied. When infected with *M. tuberculosis*, iNOS deficient mice are extremely susceptible to disease (MacMicking et al., 1997). In the context of *M. abscessus* infection, Bernut (2017) demonstrated that iNOS deficient mice were unable to clear infection.

NO can also act as a secondary messenger, regulating many intracellular signalling systems thereby altering the outcome of cellular functions. For example, Bailey and colleagues (2019) recently demonstrated that NO can reprogram metabolic processes in macrophages to modulate their cytokine and chemokine expression profile. Interestingly, NO is able to suppress inflammasome-dependent IL-1 production to limit excessive inflammation in the context of infection (Mishra et al., 2013). Evidence has also suggested that NO can act in an anti-inflammatory way by stabilising HIF-1α, a transcription factor that regulates some inflammatory cytokines during *M. tuberculosis* infection (Braverman & Stanley, 2017). Given the diversity and importance of iNOS and the subsequent actions of NO during infection, it would be of interest to further elucidate its role specifically in the context of *M. abscessus* infection.

1.4.4. Animal models of *M. abscessus* infection

While some advances have been made in understanding the immune response to *M. abscessus* infection, a large body of research remains to be elucidated in this field. In-depth analysis of the complex interplay between *M. abscessus* and the host immune system requires robust animal models that accurately represents the major facets of human pulmonary *M. abscessus* infection. At the time of writing, there is no consensus in the field on the best animal model of *M. abscessus* infection; zebrafish, mice and guinea pig models have all been used to examine *M. abscessus* biology, infectivity and immunity.

Zebrafish models

Zebrafish (ZF, *Danio rerio*) have gained interest in the last two decades for a multitude of scientific studies, particularly when studying host-pathogen interactions. ZF embryos are transparent, meaning non-invasive imaging of host-pathogen interactions are readily accessible, especially using fluorescent genes and probes (Davis et al., 2002). Further, ZF are cost-efficient and easy to maintain in the laboratory. In the context of *M. abscessus* infection, ZF have been pivotal in our knowledge of the dichotomy between S and R variants, early macrophage and neutrophil responses to infection, and the process of granuloma formation (Bernut et al., 2015; Bernut et al., 2014). However, ZF models have some disadvantages. ZF embryos do not have an adaptive immune system; this develops later, when ZF are no longer transparent and therefore not as useful for real-time imaging (Novoa & Figueras, 2012). Therefore, they are more suited to studying the acute response to inflammation as opposed to chronic infections. However, recent work by Kam *et al.* outlined

the potential use of adult zebrafish for modelling chronic infection, particularly for investigating the role of T cell subsets in the immune response to *M. abscessus* (Kam et al., 2022). None-the-less, anatomical differences such as gills instead of lungs, renders the ZF model an inaccurate representation of true *M. abscessus* infection, which tends to be a chronic pulmonary disease.

Murine models

Mice (*Mus musculus*) have also been used to investigate the host immune response to *M. abscessus* infection, in part due to their relative accessibility, abundance of tools for evaluation, and low cost. Indeed, most literature regarding the adaptive immune response to *M. abscessus* infection has been derived from murine studies. Immunocompetent strains, such as C57BL/6, typically clear *M. abscessus* infection rapidly; in a low-dose aerosol model in C57BL/6 mice there was lack of sustained infection (Ordway et al., 2008). In these same mice, however, high-dose aerosol infection persists with early recruitment of IFN-γ^+ $CD4^+$ T cells (Ordway et al., 2008).

CH3eB/FeJ – or "Kramnik" – mice have also been explored as a potential model for persistent *M. abscessus* infection. Historically, this strain has been used in *M. tuberculosis* studies to assess granuloma pathology, as infection of these animals produces lesions more similar to those found in humans, as opposed to the 'traditional' C57BL/6 mouse model (Driver et al., 2012; Kramnik et al., 2000). Indeed, it has also been used to study other NTM infections such as *M. avium* (Verma et al., 2019). During *M. abscessus* infection, Kramnik mice were able to clear infection, although bacteria persisted for up to 40 days, longer than typically seen in C57BL/6 mice (Obregón-Henao et al., 2015). In addition, the majority of studies have used the ATCC 19977 type strain, which may not fully recapture the infection paramters observed with diverse clinical isolates.

Immunocompromised mouse models establish persistent and progressive infection. SCID mice show significant persistence of bacterial burden, which demonstrates the importance of adaptive immunity in controlling *M. abscessus* infection (Rottman et al., 2007). Deletions in other components of the immune system, such as IFN-γ, GM-CSF and MyD88, also result in *M. abscessus* persistence for up to 40 days in mice (Obregón-Henao et al., 2015; Rottman et al., 2007). Beige mice, which have a Th2-skewed immune response, are also more susceptible to *M. abscessus* infection, highlighting the importance of Th1 immunity in its clearance (Bernut et al., 2017). While these models may be useful in preclinical evaluation

of antimicrobials, lack of crucial components of the immune system limits the in-depth analysis of the interaction of bacterial infection with the host immune response.

The route of infection of *M. abscessus* also plays a role in the severity of disease. While some studies employ an aerosol route (Ordway et al., 2008), others have used intravenous infection to establish a significantly higher and more persistent bacterial load (Obregón-Henao et al., 2015). While intravenous inoculation induces a persistent, high bacterial burden, *M. abscessus* infection tends to localise to the liver and spleen, as opposed to the lungs when inoculated via a mucosal route (Ordway et al., 2008). This may produce discrepancies in the infection model, as the microenvironment of solid organs such as the liver and spleen can vary greatly from mucosal sites, such as the lung.

More recently, a chronic pulmonary infection model has been proposed using agar beads embedded with *M. abscessus* using intratracheal inoculation (Riva et al., 2020). Indeed, infection persisted up to two months in the lungs, with granulomatous infiltration. Within the lung lesions, neutrophils, lymphocytes and foam cells were identified. However, intratracheal infection with agar beads can be laborious and invasive, requiring significantly more anaesthesia and placing the animals under undue stress, compared to less invasive methods such as aerosol or intranasal infection. Further, some studies have suggested that intratracheal instillation produces more inter-subject variability compared to intranasal techniques (Khadangi et al., 2021). Interestingly, another study reported that intratracheal inoculation with *M. abscessus* resulted in high mortality rates (Le Moigne, Roux, et al., 2020).

Guinea pig models

Guinea pigs (*Cavia porcellus*) have been explored as an *in vivo* model of *M. abscessus* infection. While guinea pigs are an excellent model of granuloma formation, the persistence of aerosol *M. abscessus* infection is only marginally greater in guinea pigs when compared to murine models of infection (Ordway et al., 2008). Due to the maintenance cost, animal size, and avaliability of suitable reagents, guinea pigs are not considered to be an appropriate model for *M. abscessus* studies.

1.5. Vaccination strategies against mycobacterial pathogens

1.5.1. BCG: an old vaccine repurposed for *M. abscessus* infection?

The Bacillus Calmette-Guérin (BCG) vaccine is a live-attenuated strain of *M. bovis,* and is currently the only available vaccine against *M. tuberculosis*. While the immune response to BCG vaccination is well-characterised, its efficacy is contentious; protection induced by BCG vaccination against *M. tuberculosis* ranges from 0-80% (Colditz et al., 1995). Vaccination with BCG induces neutrophil, macrophage and DC migrations to the site of inoculation, whereby DCs then migrate to the lymph nodes to activate $CD4^+$ T cells of Th1 phenotype (Moliva et al., 2017). The activated $CD4^+$ T cells produce IFN-γ, TNF, and IL-2, which is believed to correlate with protective efficacy of BCG (Moliva et al., 2017).

BCG also appears to have cross-protective properties. Many studies have observed that BCG-vaccinated children had lower mortality rates than unvaccinated children. These studies were recently reviewed in-depth (Covián et al., 2019). It has been proposed that BCG induces “trained immunity”, which is defined by Netea and colleagues (2011) as an increase in the non-specific immune response to secondary infections, either of the same microbial origin or different. This is mediated by the innate immune response, namely monocytes, macrophages and NK cells, independent of adaptive immune responses (Netea et al., 2011). This unique phenomenon, combined with its excellent safety profile and approval for human use, makes BCG vaccine an attractive candidate for a range of immunotherapies, both infectious and non-infectious. Indeed, it has been shown that BCG vaccination induced non-specific protection against pathogens such as *Staphylococcus aureus* and *Candida albicans*, which was mediated by circulating monocytes and NK cells producing pro-inflammatory cytokines such as IL-2 (Johanneke Kleinnijenhuis and Jessica Quintin and Frank Preijers and Leo, 2014). More recently, BCG has been proposed to have protective effects against SARS-CoV2 infection (Gonzalez-Perez et al., 2021). Interestingly, BCG has also been explored as an immunotherapy for autoimmune diseases such as multiple sclerosis and Type-1 Diabetes Mellitus, as well as some malignancies, for its immunomodulatory effect (Covián et al., 2019).

The cross-reactive effects of BCG as cited above therefore warrant its investigation to combat the rise in NTM infections in recent decades. Epidemiological data has suggested that BCG vaccination is associated with reduced prevalence of *M. avium* infections in some countries (Švandová, 1994). Further, patients with latent TB infection have lower risk of

acquiring NTM disease (Horsburgh et al., 1996). Most recently, it was found that BCG vaccination induces *M. ulcerans*-specific immune responses, characterised by high levels of polyfunctional $CD4^+$ T cells (Pittet et al., 2021). This suggests some level of cross-reactivity between BCG and NTMs. In this way, it would be of interest to employ similar vaccination strategies that have been applied to *M. tuberculosis* to the field of *M. abscessus* research.

A recent study was undertaken to explore the cross-reactivity of BCG against *M. abscessus* infection. BCG-specific T cells were able to inhibit intracellular growth of *M. abscessus* in an *in vitro* co-culture experiment (Abate et al., 2019). Using paired pre- and post-BCG vaccination peripheral blood mononuclear cells (PBMCs), Abate and colleagues also demonstrated that BCG is able to elicit an *M. abscessus*-specific T cell response in humans, characterised by IFN-γ expression and proliferation. However, a major caveat to this study is that the *in vivo* protective efficacy of BCG against *M. abscessus* was not ascertained. As such, this study demonstrates a limited read-out of the immunogenicity of BCG against *M. abscessus*. More detailed *in vivo* analysis of this interaction remains to be elucidated.

1.5.2. *M. abscessus* vaccine research

Despite the growing concern in *M. abscessus* prevalence, there is unfortunately very little research in vaccine development, compared to the large investment in new vaccines for other infectious diseases such as COVID-19 and *M. tuberculosis.* Reverse vaccinology techniques to identify key antigens that may be useful targets for vaccination (Le Moigne, Gaillard, et al., 2016). An *in silico* hierarchical approach to identifying key immunogenic genes and proteins in *M. abscessus* has been explored, which may serve as a useful database to identify vaccine targets (Shanmugham & Pan, 2013). Phospholipase C (PLC) was identified as one such candidate using genomic analysis comparing *M. abscessus* to other non-pathogenic RGMs (Ripoll et al., 2009). Using a prime-boost immunisation protocol, ΔF08 mice (CF mouse model) or their WT littermates (FVP) were immunised with a plasmid encoding for the *M. abscessus* PLC. While vaccination induced a strong IgG antibody response, aerosol challenge only induced a small protective effect in CF mice, and no protection in WT counterparts (Le Moigne et al., 2015). A similar effect was also observed in mice vaccinated subcutaneously with purified PLC protein. This study did not include any data on cell-mediated immune response to these vaccines, thus limiting the identification of correlates of immune protection.

Another vaccine strategy employed by this group involved the MtgC gene, which plays a key role in survival within macrophages, particularly in the absence of Mg^{2+} (Alix & Blanc-Potard, 2007). MtgC is highly expressed during *M. abscessus* infection and represents a good vaccine candidate (Belon et al., 2015). MtgC DNA immunisation in ΔF08 mice resulted in significant protection against *M. abscessus* challenge, however there was no difference compared to vector-only vaccination in WT mice (Le Moigne, Belon, et al., 2016). Again, no data regarding the cell-mediated response to infection was included in this study.

Finally, a TLR2-activating fraction purified from *M. abscessus* has also been used as an immunisation strategy. As discussed previously, TLR2 is important in the initiation of the immune response to many pathogens, including *M. abscessus*. TLR2 agonists are able to promote the activation and recruitment of adaptive immune components and are often used as adjuvants (Higgins & Mills, 2010). In this study TLR2eF, an *M. abscessus* fraction, was previously identified to be a TLR2 agonist. Mice were subsequently challenged with aerosol or intravenous *M. abscessus* of S phenotype conferred no protection against aerosol *M. abscessus* infection in mice, however, there was some protection against i.v. infection. While these results do not provide strong evidence for its utility as a vaccine candidate, they do demonstrate variability between data gained from differing routes of infection. This in turn highlights the need for a standardised and robust infection model that can be used for vaccine studies.

Whole cell vaccines

Live attenuated vaccines are complete mycobacterial vaccines that have been weakened, by either deletion of virulence genes or passaging, to be less pathogenic (Gonzalo-Asensio et al., 2017). These are an attractive vaccine candidate as they more closely mimic infection without causing significant immunopathology (Vetter et al., 2018). BCG is a live-attenuated vaccine, which as mentioned previously, induces a strong and prolonged immune response. Recombinant BCG strategies have been explored in recent years to induce more TB-specific protection to varying degrees of success (Reviewed in (Kaufmann, 2020)). For example, MTBVAC, currently in recruitment for Phase III clinical trials, is a *M. tuberculosis* clinical isolate that has been attenuated by deletion of the phoP and fadD26 genes (Arbues et al., 2013). NHP studies showed that immunisation with MTBVAC was protective against aerosol *M. tuberculosis* challenge, and induced strong cytokine signatures which have been correlated with protection against TB clinically (White et al., 2021). A recent review of

advances in whole-cell TB vaccines can be found in Bouzeyen and Javid (2022). A major concern about live-attenuated vaccines is their safety and the potential for reversion to pathogenic strains. In the case of MTBVAC, preliminary safety studies showed that it was able to be administered safely in SCID mice, and regarded to have more attenuation of virulence than BCG (Pérez et al., 2020).

Other vaccine strategies

While most previously assessed *M. abscessus* vaccines are subunit vaccines, other methods of vaccine production that have been used for disease prevention and may be useful in developing *M. abscessus* vaccines. Whole cell vaccines are those that involve vaccination with complete mycobacteria. They are an attractive strategy for vaccine design in that they contain a more diverse antigenic profile than subunit vaccines, which more closely mimics active infection (Schrager et al., 2020). The presence of lipids, glycolipids and other metabolites on the mycobacterial cell wall is thought to recruit more diverse components of the immune system, thus contributing to a more robust response and stronger induction of protective immunity (Busch et al., 2016; Spencer et al., 2008; Van Rhijn & Moody, 2015). Whole cell vaccines can be further divided into two categories; live attenuated vaccines, and inactivated/killed vaccines. For the purposes of this thesis, a focus will be on inactivation methods for whole-cell vaccines.

Inactivation has been explored as a solution to possible safety concerns of live attenuated vaccines. Inactivated whole cell vaccines still possess a diverse antigenic profile and induce a diverse immune response, without the possibility of reversion to virulence and infection (Schrager et al., 2020). However, these vaccines are considered to be less immunogenic than live vaccines, and may require multiple doses (Vetter et al., 2018). Chemical inactivation, such as using formal or paraformaldehyde (PFA), are also commonly used inactivation methods. This method is used for inactivation of viral infections, including influenza and Poliovirus (Bruxvoort et al., 2019; Okayasu et al., 2016). These vaccines have been highly efficacious. However, there have been some safety concerns regarding the inactivation chemical, which are toxic if not washed out of the vaccine completely (Fertey et al., 2016). Interestingly, a study of a Japanese Encephalitis vaccine revealed that formalin inactivation can alter the antigenic and immunogenic profile of the vaccine (Fan et al., 2015). For *M. tuberculosis* there are several inactivated whole cell vaccines in the clinical pipeline. Vaccae™ vaccine, a heat-killed version of *M. vaccae*, has been shown to be efficacious in

humans, and is now licensed for use as an adjuvant therapy for TB. The most recent analysis demonstrating that *M. vaccae* combined with conventional TB drugs can reduce treatment length and limit clinical manifestation of TB (Bourinbaiar et al., 2020). Phase III clinical trials have demonstrated safety and efficacy of Vaccae™, however at the time of writing this thesis, results of this trial are not yet available (ClinicalTrials.gov: NCT01979900).

Gamma-irradiation (γ-irradiation) of viruses and bacteria have been explored as vaccine candidates. This method involves subjecting the target to high frequency electromagnetic rays, or "gamma rays", and is widely used to sterilise foods and some pharmaceuticals (Sommers & Rajkowski, 2011). γ-irradiation, unlike heat-killing and formalin inactivation, is able to preferentially inactivate DNA and other nucleic acid components of the cell, leaving the surface antigens intact for immune recognition (Seo, 2015). While γ-irradiation restricts replication, the metabolic machinery of the bacteria remains intact. This allows the bacteria to remain metabolically active which permits prolonged secretion of metabolites (i.e. antigens). γ-irradiation has been widely explored as a tool for influenza vaccine development, and more recently, SARS-CoV2 (Sabbaghi et al., 2019) (Mullbacher et al., 2020). Indeed, it has also been applied to bacterial vaccinology; a γ-irradiated *S. pneumoniae* vaccine has been evaluated. Intranasal immunisation with this vaccine induced potent antibody responses and conferred significant protection when compared to heat-killed or formalin-inactivated *S. pneumoniae* (Jwa et al., 2018). Interestingly, immunisation with γ-irradiated *S. pneumoniae* induced potent mucosal IL-17 responses, which has been correlated previously with protection for this pathogen (Babb et al., 2016). Another striking γ-irradiated vaccine in clinical development is the Sanaria®PfSPZ Vaccine, an irradiated sporozoite formulation that has shown significant protection against malaria. When administered with malaria chemoprophylaxis, irradiated sporozoites confer significant protection against malaria infection through potent CD*+ T cell responses (Sissoko et al., 2022). Therefore, γ-irradiation is an attractive strategy for vaccine development for pathogens where exiting vaccine technology has not proved effective.

1.6. Present study

While *M. abscessus* has become an important pathogen within the context of susceptible populations, the complexity of the host immune response to *M. abscessus* infection is poorly understood. Without detailed understanding of the host-pathogen interplay, it is difficult to implement host-directed therapies and design effective vaccines to prevent infection and/or

disease. A major contributor to the dearth of effective treatments is the lack of consensus regarding a suitable animal model in which these phenomena can be studied. As such, this thesis aims to:

- Establish a pulmonary *in vivo* mouse model in order to identify immune cell subsets that are important in the host response to infection, using clinically relevant *M. abscessus* isolates;
- Define the protective effect of *M. bovis* Bacillus Calmette-Guérin (BCG) vaccine on *M. abscessus* infection; and
- Identify novel vaccine candidates for the prevention of pulmonary *M. abscessus* infection using inactivation techniques.

Chapter 2: Materials and Methods

2.1. Materials

2.1.1. List of reagents

Reagents used in this study are detailed in Table 2.1.

2.1.2. Tissue culture media

- *Complete Roswell Park Memorial Institute (cRPMI) media*: sterile RPMI 1640 (Life Technologies, Thermo Fisher Scientific) was supplemented with 10% (v/v) heat-inactivated foetal calf serum (FCS, 56˚C for 30 minutes) (Sigma-Aldrich), 0.5mM 2-β-mercaptoethanol (Sigma), 100 U mL^{-1} penicillin (Sigma-Aldrich) and 0.1% (v/v) streptomycin (Sigma-Aldrich).
- *RPMI with DNase/Collagenase*: RPMI 1640 was supplemented with 0.1 mg mL^{-1} DNase I (Worthington, Freehold, USA) and 10 U mL^{-1} Collagenase Type IV (Worthington).
- *Wash media*: RPMI 1640 was supplemented with 2% (v/v) FCS.
- *Antibiotic-free media*: RPMI 1640 was supplemented with 10% FCS and 0.5mM 2-β-mercaptoethanol.

2.1.3. Bacterial culture media

- *Complete 7H9 broth:* 0.47% (w/v) Middlebrook 7H9 powder (Difco, Detroit, USA) was dissolved in triple distilled water (TDW), and autoclaved for 10 minutes at 110˚C. Broth was then supplemented with 0.2% (v/v) filter-sterilised glycerol (Thermo Fisher Scientific), 0.02% filter-sterilised Tween20 (Sigma), and ADC (Table 2.1). 7H9 broth was kept sterile and stored at 4˚C.
- *Complete 7H10 agar*: 2.1% (w/v) Middlebrook 7H10 (Difco) agar was dissolved in TDW and autoclaved 110˚C for 10 minutes. This was supplemented with 0.2% (v/v) filter-sterilised glycerol and oleic acid-albumin-dextrose-catalase (OADC) (Table 2.1). Agar was immediately poured into petri dishes and stored in foil at 4˚C.
- *Sauton Media:* the following ingredients were dissolved in TDW and buffered to pH 7.2-7.4 with sodium hydroxide: 0.40% (w/v) L-Aspargin; 0.10% (w/v) magnesium sulphate, $7H_2O$; 0.07% (w/v) dipotassium hydrogen phopspate, $3H_2O$; 0.20% (w/v) citric acid; 0.0005% (w/v) ferric ammonium citrate; 0.50% (w/v) sodium pyruvate;

0.02% (v/v) glycerol. The medium was autoclaved at 110˚C for 10 mins and stored sterile at 4˚C.

- *Luria Bertani (LB) agar*: 1% (w/v) LB broth powder (Difco) was dissolved in TDW with 1.5% (w/v) bacteriological agar and autoclaved at 110˚C for 10 mins, poured into petri dishes and stored at 4˚C.

Table 2.1: General reagents used in this study.

Reagent	Manufacturer	Storage
Ammonium-chloride-potassium (ACK) Lysis Buffer	Thermo Fisher Scientific (MA, USA)	Room Temperature (RT)
Advax-CpG adjuvant	Provided by Professor Nikolai Petrovsky, School of Medicine, Flinders University (Adelaide, Australia)	4˚C
Albumin-dextrose-catalase (ADC): 5% (w/v) BSA, 2% (w/v) dextrose, 0.003% (w/v) catalase, dissolved in TDW and filter-sterilised.	BSA: Moregate Biotech, Australia) Dextrose: Sigma Catalase: Sigma NaCl: Sigma	4˚C, in 50 mL aliquots
Fluorescence activated cell sorting (FACS) buffer: 4% FCS, 5 mM ethylene diamine tetra acetic acid (EDTA) in phosphate-buffered saline (PBS); filter sterilised	N/A	4˚C
Foetal calf serum (FCS, heat-treated at 56˚C for 30 mins)	Scientifix Life (Victoria, Australia)	4˚C, in 50 mL aliquots
Neutral-buffered formalin (10% v/v)	Fronine (Sydney, Australia)	RT
Oleic acid-albumin-dextrose-catalase (OADC): 5% (w/v) Bovine serum albumin (BSA) + 2% (w/v) dextrose + 0.004% (w/v) catalase + 0.05% (w/v) oleic acid + 0.85% (w/v) NaCl dissolved in TDW and filter-sterilised	BSA: Moregate Biotech, Australia) Dextrose: Sigma Catalase: Sigma Oleic acid: Sigma NaCl: Sigma	4˚C, in 50 mL aliquots, away from light
PBS/Heparin: 20 U mL^{-1} Heparin in sterile PBS	Fisions Pharmaceuticals (Sydney, Australia)	4˚C
Phosphate-buffered saline (PBS): 0.14 M NaCl, 2.7 mM KCl), 0.1 M phosphate buffer, pH 7.4	Astral Scientific (Sydney, Australia)	RT
Trypsin-EDTA 0.5% (v/v)	Gibco (Gaithersburg, MD, USA)	4˚C
Tween20	Sigma (St Louis, MO, USA)	RT

2.2. Bacterial culture

2.2.1. General mycobacterial culture

Mycobacterium abscessus strains used in this study were kindly provided by Professor Vitali Sintchenko, Centre for Infectious Diseases and Microbiology, Westmead Hospital (See Table 3.1 for details). *Mycobacterium bovis* BCG Pasteur strain (ATCC35734) was also used in this study.

All bacterial experiments were conducted using aseptic technique in Class II Biosafety cabinets in a PC2 laboratory. *M. abscessus* and BCG were grown in complete 7H9 media in a rolling incubator at 37˚C and maintained at log growth phase (OD_{600} 0.5-1.0), which was measured by spectrophotometry. For bacterial enumeration, mycobacteria were inoculated by serial dilution onto 7H10 agar quad plates. *M. abscessus* plates were incubated for 5 days, and BCG incubated for three weeks at 37˚C before being counted and expressed as colony forming units per millilitre (CFU/mL).

Stocks of *M. abscessus* and BCG were made by culturing bacteria to OD_{600} 0.8. Cultures were then centrifuged at 4800g for 10 mins at room temperature (RT), the supernatant was removed and the pellet resuspended in 25% (v/v) sterile glycerol in PBS. Stocks were stored in 1 mL aliquots in Eppendorf tubes at -80˚C. The concentration of bacterial stocks was enumerated approximately one week after stocks were made. Bacteria were thawed and prepared as described in 2.2.3 and then immediately enumerated onto 7H10 agar.

2.2.2. Preparation of mycobacteria for infection

Stocks of *M. abscessus* of known concentration were thawed quickly, centrifuged at 4800g for 10 mins and the pellet resuspended in 1 mL of sterile PBS. Cells were sonicated using the SonoPlus Ultrasonic Homogeniser (Bandelin, Berlin, Germany) for 30 seconds at 30% amplitude, and cooled on ice. The suspension was further diluted to the desired concentration for infection (CFU/mL) using antibiotic-free cRPMI for *in vitro* infection, or sterile PBS for *in vivo* infection. The final suspension was passed through a 26-gauge syringe 10 times to further disperse any clumps before infection.

BCG was cultured to log phase, centrifuged at 4800g for 10 mins and the supernatant discarded. The pellet was resuspended in sterile PBS and centrifuged again at 100g for 10 mins to pellet any clumps. The supernatant was retained and sonicated at 30% amplitude

for 30 seconds. The OD_{600} was obtained and the sample was diluted in PBS to the desired concentration for vaccination. Immediately prior to vaccinated, BCG was passed through a syringe to further disperse any remaining aggregates.

2.2.3. Preparation of whole cell inactivated *M. abscessus* vaccines

M. abscessus Strain 7 (MA07) was cultured to log phase in 7H9 media to log phase in a rolling incubator at 37˚C for 48-72 hours. Bacteria were centrifuged at 4800g for 10 mins and the pellet was resuspended in one-tenth 10% (v/v) sterile glycerol in PBS. The suspension was sonicated at 30% amplitude for 30 seconds, passed through a 26G syringe to remove any bacterial aggregates and then processed as below, depending on the inactivation method. An aliquot of this mixture was stored immediately at -80˚C and later used to estimate the concentration of bacteria as CFU/mL.

Heat-killed *M. abscessus*

The *M. abscessus* suspension was heat inactivated in a water bath at 80˚C for 30 mins and then rested on ice for 30 mins. One mL aliquots were made and stored at -80˚C until required. One aliquot was kept for validation of heat-killing as outlined in 2.2.3.5.

Paraformaldehyde-inactivated *M. abscessus*

M. abscessus suspension was pelleted by centrifuging at 4800g for 10 mins and the supernatant discarded. The pellet was resuspended in one mL 4% (v/v) paraformaldehyde and covered in foil. Bacteria were incubated at 4˚C in the dark with gentle agitation for 30 mins. The fixed bacteria were then washed 3 times by centrifugation with 10% (v/v) glycerol in PBS, aliquoted into 1mL Eppendorf tubes and stored at -80˚C. One aliquot was kept for validation of PFA-inactivation as outlined in 2.2.3.5.

Gamma-irradiated *M. abscessus*

M. abscessus Strain 7 was aliquoted into 1.5 mL cryovials and placed inside 15 mL Falcon tubes for double concealment. Samples were transported on ice to Australia's Nuclear Science and Technology Organisation (ANTSO) where they were irradiated with 20kGy at 4˚C for 8 hours. Samples were stored at -80˚C as soon as possible with one vial being kept for validation of γ-irradiation.

Validation of inactivation methods

To ensure effectiveness of inactivation methods, samples was inoculated onto 7H10 agar plates and LB agar plates and incubator for up to 14 days to assess for any mycobacterial viability or contamination, respectively. The sample was also cultured in 7H9 broth and OD_{600} monitored up to 14 days for growth. Metabolic activity as assessed as outlined in 2.4.5.

2.2.4. Culture Filtrate Protein

Culture filtrate proteins were harvested by Dr Claudio Counoupas. Briefly, MA07 was cultured to log phase in Sauton medium to a final volume of 100mL. The culture was then centrifuged at 4800g for 10 mins. The supernatant was collected and passed through a size exclusion column (10kDa). The concentration of the culture filtrate was confirmed using NanoDrop.

2.3. Mammalian cell culture

RAW264.7 cells (ATCC TIB-71) were obtained from liquid nitrogen storage, thawed and centrifuged at 300g for 10 mins. The pellet was resuspended in cRPMI and cultured at 37˚C 5% CO_2 in ventilated tissue culture flasks (Corning) to 80% confluence. Passaging confluent cells involved removing culture media and incubating with 0.1% (v/v) Trypsin-EDTA in PBS for 10 mins at 37˚C in 5% CO_2 with intermittent agitation. The resulting suspension was inactivated with cRPMI and centrifuged at 300g for 5 mins. The pellet was resuspended in fresh cRPMI and a cell count performed in 0.1% Trypan Blue and a haemocytometer. To continue culturing, the cell suspension was diluted and transferred to a larger tissue culture flask.

2.4. *In vitro* experiments

2.4.1. Growth curve of *M. abscessus* strains

For assessment of *M. abscessus* clinical isolates in culture, sixteen clinical isolates (Table 3.1) were cultured in duplicate in 7H9 media to log phase. OD_{600} was measured and bacteria were diluted in 7H9 media to OD_{600} 0.05. Samples were incubated in a rolling incubator at 37˚C for 48 hours, with the OD_{600} taken every 4-8 hours.

2.4.2. Intracellular survival of *M. abscessus* clinical isolates

RAW264.7 cells were grown to confluence and seeded into a 96-well flat-bottom tissue culture plate at a concentration of 10^6 cells/mL (10^5 cells per well) and incubated at 37˚C in 5% CO_2 overnight to allow them to adhere. On the day of infection, cells were washed three times with warm antibiotic-free cRPMI. Cells were then infected in triplicate with one of the sixteen *M. abscessus* clinical isolates at MOI 10. The inoculating dose of each *M. abscessus* strain was evaluated by enumeration on 7H10 agar. Plates were incubated for 2 hours at 37˚C in 5% CO_2 to allow *M. abscessus* infection of cells, and subsequently washed three times with warm wash media to remove extracellular bacteria. Cells were then either immediately lysed with sterile TDW and bacterial count enumerated on 7H10 agar, or incubated for a further 48 hours with antibiotic-free media, then lysed and enumerated. Supernatants were collected at both 2 hours post-infection (hpi) and 48hpi. Uptake was calculated as the percentage of bacteria in cells 2 hours after infection compared to the inoculating dose. Persistence within macrophages was calculated by the change in CFU after 48 hours normalised to the CFU at 2hpi. This assay was adapted from Bryant et al. (2016).

2.4.3. Cytokine Bead Array

Supernatants collected from infected RAW264.7 cells were analysed using BD Cytometric Bead Array Kit (BD Biosciences) to assess the inflammatory profile of each *M. abscessus* clinical isolate. A standard curve from 2500 pg/mL to 2.44 pg/mL was made using serial two-fold dilutions of each cytokine being measured. Cytokines measured included GM-CSF, TNF and interleukin 6 (IL-6). Cytokine bead array (CBA) was performed according to the manufacturer's instructions.

CBA was also performed on lung homogenates and serum from *in vivo* experiments (See 2.5). Cytokines measured in this assay included chemokine ligand 1 (CXCL1), G-CSF, IFN-γ, IL-1β, IL-6, interleukin 10 (IL-10), interleukin 12p40 (IL-12p40) and TNF.

Samples were analysed using the BD LSR Fortessa X-20 and 500 events were acquired per sample as per the manufacturer's instructions. Cytokine production was calculated using BD FCAP array software and expressed as pg/mL.

2.4.4. Griess Assay

The Griess assay is a colorimetric assay that has been used extensively to measure the production of nitrite. In its aqueous form, NO auto-oxidises to nitrite, which is much more stable than NO, and therefore the Griess assay can be used as a proxy measure of NO concentration (Tsikas, 2007). A standard curve of sodium nitrite ranging from 100 µM to 1.5 µM was made in duplicate using serial 2-fold dilution in cRPMI. Supernatants from infected cells or lung homogenates from infected mice were aliquoted into a 96-well plate, and Griess reagent added [0.1% (w/v) Napthyllethylene diamine dihydrochloride, 1% (w/v) sulphanilamide, 0.03% (v/v) phosphoric acid] and incubated at RT for 10 mins. Fluorescence was measured at 590nm using the Infinite M1000 Pro plate reader (Tecan, Männedorf, Switzerland), and the standard curve subsequently used to calculate the NO production in samples expressed in µM.

2.4.5. Resazurin assay

The resazurin assay is a colorimetric assay which relies on the reduction of nicotinamide adenine dinucleotide phosphate (NADPH) to nicotinamide adenine dinucleotide (NAD), during active metabolism, which allows resazurin to be reduced to resorufin, causing a colour change that can be detected as fluorescence at 590nm (Mueller et al., 2013). Heat-killed, PFA-inactivated and γ-irradiated samples were incubated with 0.05% (v/v) resazurin (Sigma-Aldrich) in a flat-bottom 96-well plate at 37˚C overnight. Live *M. abscessus* and 10% (v/v) sterile glycerol in PBS were used as positive and negative controls, respectively. Absorbance was subsequently measured at 590 nm using the Infinite M1000 Pro plate reader. Metabolic activity of each inactivation method was expressed as the percentage of absorbance relative to live bacteria.

2.5. *In vivo* experiments

2.5.1. Experimental animals used for infection and vaccine experiments

Six to eight week-old female C57BL/6 mice were used for most experiments, purchased from Australian BioResources (ABR, Sydney, Australia). Female C3HeB/FeJ and *Tnf*$^{-/-}$ mice were sourced from within the Centenary Institute. All animals were maintained under specific pathogen-free conditions in the Animal Facility at the Centenary Institute, and all animal work was conducted in certified PC2 laboratories. All experiments performed involving

animals were done so with approval from the Sydney Local Health District Animal Welfare Committee, protocol 2018/018.

2.5.2. Vaccination of mice

Mice were anaesthetized with isoflurane (Veterinary Companies of Australia, Kings Park, Australia) and vaccinated subcutaneously at the base of tail with 5 x 10^5 CFU BCG once in 200 µL PBS. Some mice were vaccinated subcutaneously 10^6 CFU of PFA-inactivated, heat-killed or γ-irradiated *M. abscessus* Strain 7 in 200µL PBS, or with 20mg Advax-CpG (three times, two weeks apart). Mice were rested for six to twelve weeks before challenge with *M. abscessus*, depending on the experiment.

2.5.3. Intranasal infection of mice with *M. abscessus*

Prior to intranasal inoculation, mice were anaesthetized with Ketamine (80mg/kg)/Xylazine (10mg/kg) in 150 µL PBS via intraperitoneal injection. Anaesthesia was reversed after infection with intraperitoneal injection of 1 mg/kg AntiSedan (Zoetis, USA). Whilst anaesthetized and during recovery, mice were maintained on a heat pad at 37˚C to maintain body temperature.

Once anaesthetized, mice were infected with 10^6 CFU *M. abscessus* in 25 µL PBS via the intranasal route. The infectious dose was verified by plating on 7H10 media lung homogenates collected one hour after inoculation. At various time-points, mice were euthanased, the lungs and spleen collected, homogenised in TDW using the Rotor Stator Homogeniser (Sigma, St Louis, USA), the bacterial burden enumerated on 7H10 plates and expressed as Log_{10}CFU.

2.5.4. Preparation of single cell suspensions

Lung

Lungs of culled mice were perfused with sterile PBS by injection into right ventricle of the heart until they turned white, then excised and placed in RPMI with DNA/Collagenase. The lungs were dissociated using a gentleMACS OctoDissociator, then incubated in a waterbath at 37˚C for 30 minutes. Lungs were further homogenised using the gentleMACs before being passed through a 40µm cell strainer. Cells were washed twice with wash media by centrifugation to remove excess digestive enzymes. The pellet was resuspended in 1mL

ACK lysis buffer for 60 seconds to remove any remaining erythrocytes, wash media added and cells washed a further two times by centrifugation. The final pellet was suspended in 1mL AB-free cRPMI, and a cell count was performed on the single cell suspension using Trypan Blue, in order to adjust the cell concentration for future assays.

Spleen and lymph nodes

Spleens and mediastinal lymph nodes (mLNs) were removed from euthanased mice, placed into 2 mL RPMI, passed through a 40μM cell strainer and erythrocytes removed using ACK lysis buffer as in 2.5.4.2. The recovered cells were resuspended in 2 mL antibiotic-free cRPMI and a cell count performed.

Peripheral blood

While restrained, the lateral tail vein of mice was punctured with a scalpel to collect approximately 200 μL blood into a tube containing 2mL heparin (20 U mL^{-1}) in PBS. The blood solution was then slowly pipetted onto 3mL of Histopaque 1083 (Sigma) without mixing and centrifuged at RT at 300g for 30 mins. The peripheral blood mononuclear cells formed a ring at the interface between aqueous and histopaque layers, which was carefully collected and washed twice in cRPMI. The final pellet was then resuspended in 1 mL ACK lysis buffer for 1 minute to lyse erythrocytes. Ten mL of cRPMI was added immediately to stop the reaction, cells were washed again, and a cell count performed as described for lung single cell suspensions.

2.6. Immunological assays

2.6.1. Flow cytometry

Surface staining

Single cell suspensions were prepared as described in 2.5.4, aliquoted into round-bottom 96-well plates and pelleted by centrifugation at 300g for 4 mins at 4˚C. Cells were then stained with the following antibody panels: myeloid cells (Table 2.2) or T cells (Table 2.3). The supernatant was removed and the cells were stained in 50 μL of surface stain antibody cocktail. Plates were incubated in the dark at 4˚C shaking for 30 mins. Cells were then washed in 200 μL FACS buffer by centrifugation three times, then fixed in 70 μL Cytofix (BD

Biosciences) in the dark for 20 mins at 4˚C. Fixed cells were washed in CytoPerm (BD Biosciences) before intracellular staining.

Intracellular staining

Fixed cells were stained with 50 µL of intracellular antibody cocktail in CytoPerm for 45 minutes at RT (Table 2.2, 2.3, 2.4). Cells were then washed with CytoPerm three times and stored at 4˚C in 10% neutral buffered formalin until flow cytometry acquisition.

Restimulation assay

Single cell suspensions were prepared as described in 2.5.4 and aliquoted into a round-bottom 96-well plate in antibiotic free (AB-free) cRPMI. Cells were stimulated with 50 µg/mL *M. abscessus* whole cell lysate in AB-free cRPMI overnight at 37˚C. Protein Inhibitor Cocktail (manufacturer) was added at 1 in 500 and incubated at 37˚C for 5 hours. Cells were washed 3 times in FACS wash, and the pellet resuspended in the restimulation panel surface stain cocktail as detailed in 2.6.1.1 (See Table 2.5 for antibodies used). Cells were fixed in Cytofix, and stained for intracellular cytokines and transcription factors as detailed in 2.6.1.2.

Table 2.2: Monoclonal antibodies used for myeloid flow cytometry panel.

Marker	Clone	Fluorochrome*	Dilution	Manufacturer
CD103	2.00E+07	BV786	1 in 200	BioLegend
CD11b	M1/70	APC-Cy7	1 in 200	BD Biosciences
CD11c	N418	AF700	1 in 200	BD Pharmingen
CD24	M1/69	BUV737	1 in 200	BD Biosciences
CD3e	145-2C11	PECF594	1 in 200	BD Horizon
CD45	104	BV510	1 in 200	BD Biosciences
CD64	X54-5/7.1	PE/Cy7	1 in 200	BioLegend
FcRIII/II (CD16/32)	2.4G2	NA	1 in 200	BD Pharmingen
Live/Dead		UV450	1 in 300	
Ly6C	HK1.4	PerCP/Cy5.5	1 in 200	Invitrogen
Ly6G	1A8	BUV395	1 in 200	BD Horizon
MHCII	M5/114.15.2	BV421	1 in 200	BD Horizon
NOS2	CXNFT	FITC	1 in 200	Invitrogen
SiglecF	E50-2440	PE	1 in 200	BD Pharmingen

*AF700 – AlexaFluor 700; APC – allochycocyanin; Cy5.5 – cyanine 5.5; Cy7 – cyanine 7; FITC – fluorescein isothiocyanate; PE – phycoerythin; PerCP – peridinin chlorophyll protein; UV – ultra violet.

Table 2.3: Monoclonal antibodies used for T cell flow cytometry panel.

Marker	Clone	Fluorochrome*	Dilution	Manufacturer
B220	PA3-6B2	PerCP/Cy5.5	1 in 200	BD Pharmingen
CD4	RM4-5	AF700	1 in 200	BD Pharmingen
CD44	IM7	PE/Cy7	1 in 300	BD Pharmingen
CD62L	MEL-14	PE	1 in 300	BioLegend
CD8a	53-6.7	APC-Cy7	1 in 200	BD Pharmingen
FcRIII/II	2.4G2	NA	1 in 200	BD Pharmingen
KLRG-1	2F1/KLRG1	FITC	1 in 300	BioLegend
Live/Dead		UV450	1 in 300	
RorγT	Q31-378	PECF594	1 in 200	BD Horizon
Tbet	4B10	APC	1 in 200	BioLegend

*AF700 – AlexaFluor 700; APC – allochycocyanin; Cy5.5 – cyanine 5.5; Cy7 – cyanine 7; FITC – fluorescein isothiocyanate; PE – phycoerythin; PerCP – peridinin chlorophyll protein; UV – ultra violet.

Table 2.4: Monoclonal antibodies used for intracellular cytokine flow cytometry panel.

Marker	Clone	Fluorochrome*	Dilution	Manufacturer
CD4	RM4-5	AF700	1 in 200	BD Pharmingen
CD44	IM7	FITC	1 in 300	BD Pharmingen
CD8a	53-6.7	APC-Cy7	1 in 200	BD Pharmingen
FcRIII/II	2.4G2	NA	1 in 200	BD Pharmingen
IFNγ	XMG1.2	PE/Cy7	1 in 300	BD Pharmingen
IL-17	TC11-18H10	Pacific Blue	1 in 200	BD Horizon
IL-2	JES6-5H4	PE	1 in 200	Miltenyi Biotec
Live/Dead		UV450	1 in 300	
TNF	MP6-XT22	PerCP/Cy5.5	1 in 200	BD Pharmingen

*AF700 – AlexaFluor 700; APC – allochycocyanin; Cy5.5 – cyanine 5.5; Cy7 – cyanine 7; FITC – fluorescein isothiocyanate; PE – phycoerythin; PerCP – peridinin chlorophyll protein; UV – ultra violet.

Flow cytometry acquisition and analysis

Sample analysis was conducted with the LSR-Fortessa Flow Cytometer (BD Biosciences) using the BD FACSDiva software. Before acquisition, compensation controls were generated using microbeads (BD Biosciences) stained with single fluorophores to compensate for any fluorescence overlap between samples. All samples were resuspended and filtered before running, then collected at less than 9000 events per second to ensure a single cell suspension was maintained.

General gating strategies used for flow cytometric analysis

FlowJo was used to analyse cell subsets acquired by flow cytometry. The general gating strategy applied to all samples is detailed in Figure 2.1. Briefly, a size gate was used to select lymphocytes, followed by forward and side scatter gate to exclude doublets. The remaining cells were gated on Live/Dead staining, with negative cells being gated as "live". For myeloid cells, the gating strategy was modified from (Misharin et al., 2013) (Figure 2.2). For adaptive immune cells, the gating strategy employed is shown in Figure 2.3. Further analysis was conducted based on surface and/or intracellular markers of interest.

2.6.2. ELISA

Indirect enzyme-linked immunosorbent assay (ELISA) was used to detect the presence of IgG antibodies in the serum of vaccinated mice post-*M. abscessus* challenge. Substrates and buffers used in this assay are detailed in Table 2.X. Corning 96 Well Clear PVC Assay Microplates (Sigma-Aldrich) were coated with 1µg/mL *M. abscessus* culture filtrate proteins (See 2.2.4) and incubated overnight at RT. Plates were then blocked with 3%(v/v) BSA in PBS for 2 hours at RT, and then washed 4 times with 0.01% Tween + 0.1% BSA in PBS. Serum samples were serially diluted in 1% BSA in PBS and then added to coated plates for 1 hr at RT. After washing, primary antibody was added (Goat Anti-Mouse IgG2c heavy chain (Biotin) (Abcam), 1:10,000) for 1 hr at RT. Plates were washed again before the incubation with Streptavidin-Horse Radish Peroxidase at 1:30,000 (Abcam) for 30 mins at RT. Following washing, antibody binding was visualised by addition of addition of substrate (0.1 mg/mL 3,3',5,5'-Tetramethylbenzidine (Sigma-Aldrich)) and hydrogen peroxide in 0.5 M phosphate citrate buffer (Sigma-Aldrich) for 5-10 mins in the dark or until complete colour change was observed. 10-20µL of 0.2M H_2SO_4 was used to stop the reaction. Absorbance was read at 450nm using M1000 pro plate reader (Tecan, Mannedorf, Switzerland), and serum antibody titres were then ascertained by fitting to a sigmoidal curve using GraphPad Prism 9 (GraphPad, CA, USA).

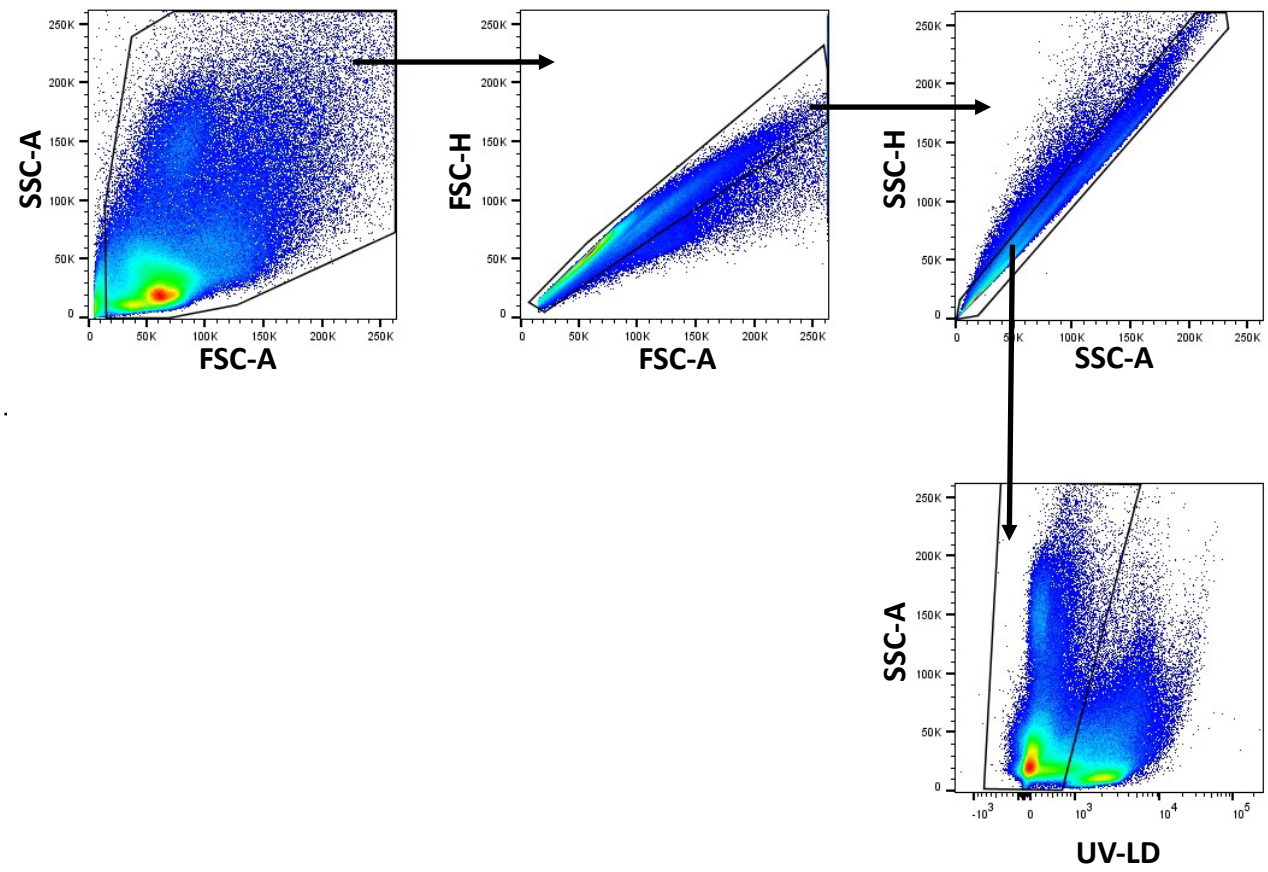

Figure 2.1. Gating strategy to identify murine immune cells. Cells isolated from the lungs, spleen or blood were stained according to 2.6.1 and then identified based on forward scatter (FSC) and side-scatter (SSC) profiles. Dead cells were excluded using UV-Live Dead staining. Further characterisation of cells by either myeloid or T cell markers was then performed as per Figure 3.2 or Figure 3.3.

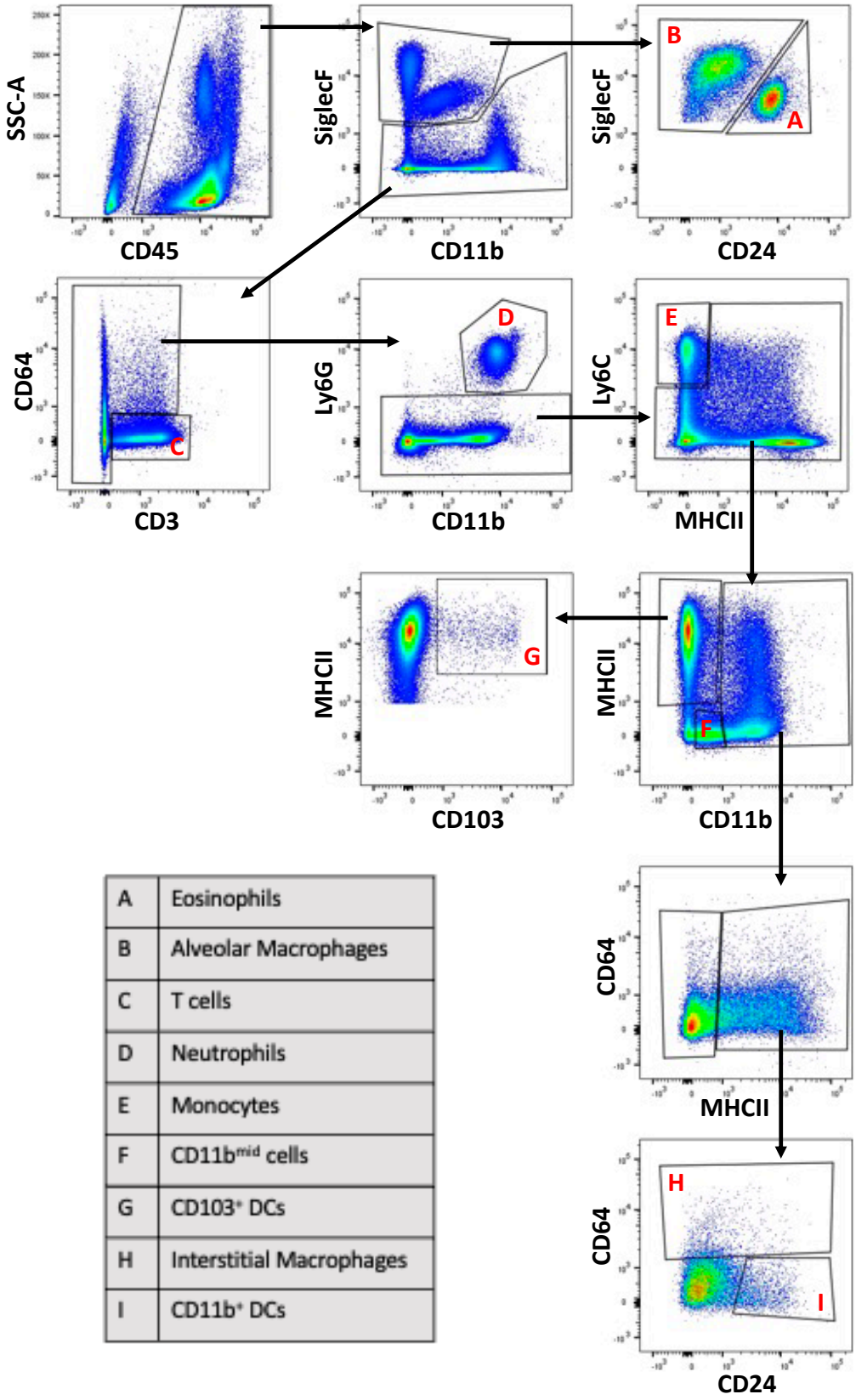

A	Eosinophils
B	Alveolar Macrophages
C	T cells
D	Neutrophils
E	Monocytes
F	CD11b^{mid} cells
G	CD103^{+} DCs
H	Interstitial Macrophages
I	CD11b^{+} DCs

Figure 2.2. Gating stratgey used to identify myeloid cell subsets by flow cytometry. Immune cells were gated on based on Figure 2.1. Adapted from Misharin et al. (2013).

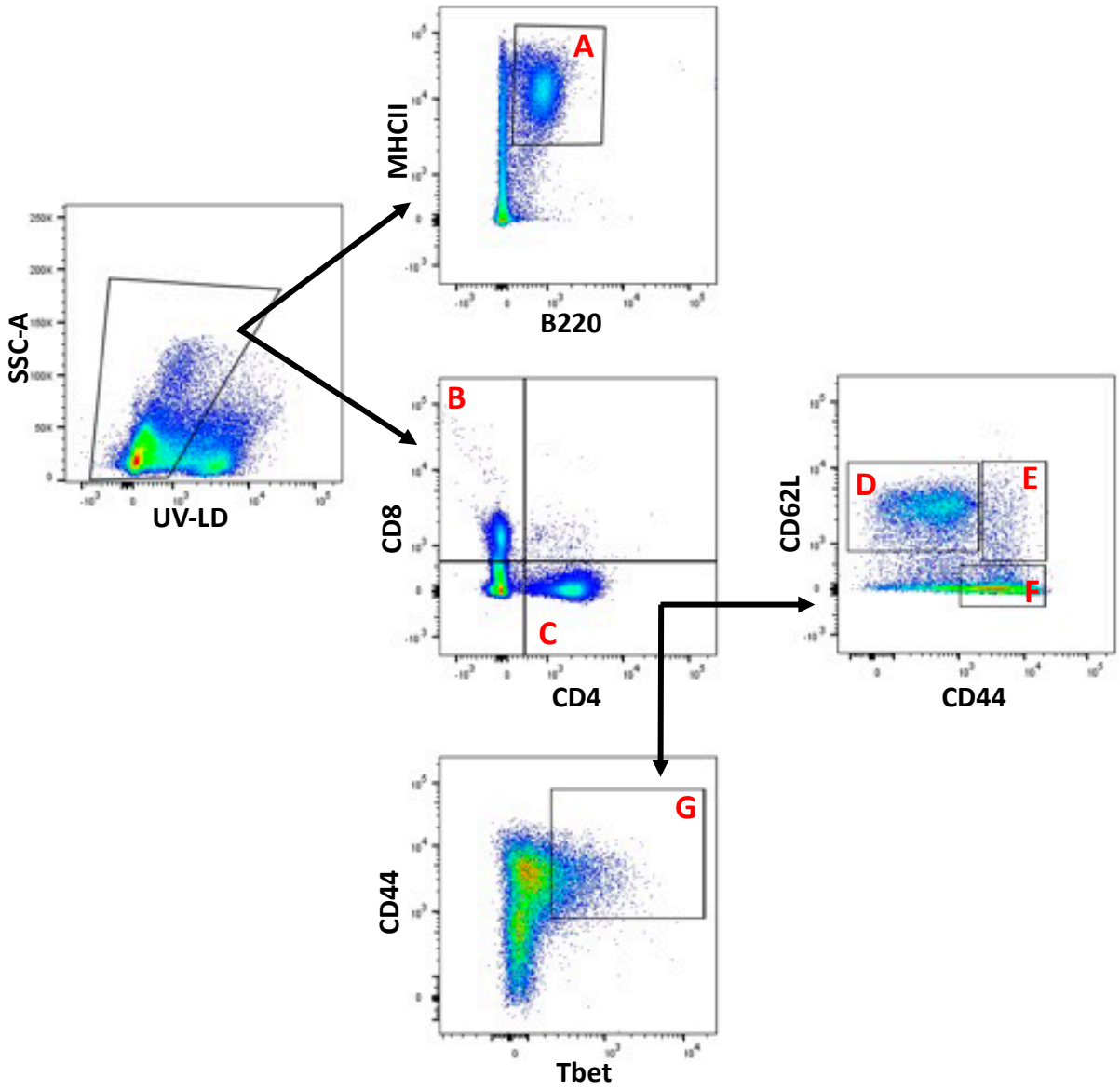

A	B cells
B	CD8⁺ T cells
C	CD4⁺ T cells
D	Naïve CD4⁺ T cells
E	Central Memory CD4⁺ T cells
F	Effector Memory CD4⁺ T cells
G	Tbet⁺ CD4⁺ T cells

Figure 2.3. Identification of adaptive immune cells by flow cytometry.

2.7. Comparison of *M. abscessus* infection across two CF clinics

This work was conducted by Anneliese Blaxland, Janine Verstraete, and Mark Zampoli, who have kindly permitted its inclusion in this thesis. Across a three year period (2017-2019), the medical records of all patients attending CF clinics at The Children's Hospital at Westmead (CHW, Sydney, Australia) and Red Cross War Memorial Children's Hospital (RCWMCH, Cape Town, South Africa) were examined. Ethics approval was granted by the ethics committee at each site (2019/ETH13741). Both CF clinics have NTM specific screening strategies in place to detect and identify NTM infection based on annual surveillance on sputum samples. The following data was collected from the medical record: Demographic data (age, anthropometry), class of CF-causing mutations, baseline lung function (forced expiratory volume in 1 second (FEV_1), defined as the highest value in the calendar year, %predicted), BCG vaccination status and microbiology (NTM*, Pseudomonas aeruginosa, Staphylococcus aureus, Aspergillus spp. and Mycobacterium tuberculosis)*. Infection was defined as one of two categories: intermittent, defined as any laboratory isolation during the year, and colonisation, defined as >3 isolates/year or >50% of samples if >4 samples/year. Parametric data is described as mean (SD) and compared using independent t-tests. Proportions were compared using chi-square tests.

2.8. Statistical analysis

All statistical analysis was conducted using Prism 9 for MacOS (version 9, GraphPad, CA, USA). The significance of protective efficacy and immunological assays were calculated using one-way or two-way analysis of variance (ANOVA). When statistical significance was assessing multiple sets of data, the Dunnet *post-hoc* test of significance was applied. The threshold for significance was defined as a p-value <0.05.

Chapter 3: A murine model of pulmonary *Mycobacterium abscessus* infection to assess immune correlates of protection

3.1. Introduction

In the last two decades, *Mycobacterium abscessus* has emerged as a pathogen of increasing concern within Cystic Fibrosis (CF) patients. While initially considered to be a minimally virulent and self-limiting infection, *M. abscessus* has evolved to be an important respiratory pathogen in CF patients and other vulnerable populations (Bryant et al., 2016). As a pathogen, *M. abscessus* causes progressive lung function decline and reduced quality of life (Griffith et al., 2007). Indeed, in more serious cases, *M. abscessus* infection can cause acute respiratory failure and can be fatal (Jhun et al., 2020). It is estimated that up to 20% of all non-tuberculous mycobacteria (NTM) infections in CF patients are caused by *M. abscessus*, which is predicted to continue to rise (Martiniano et al., 2019).

Although *M. abscessus* is potentially fatal infection in vulnerable individuals, treatment is problematic. *M. abscessus* has an extensive drug resistance profile, possessing both intrinsically and acquired resistance genes that make it almost impossible to treat in some cases (Degiacomi et al., 2019). Further, the extensive treatment regime under the current guidelines confers high rates of adverse effects and treatment failure (Choi et al., 2018). As such, further research into the host immune response to *M. abscessus* is required to develop therapies that are better able to treat infection than existing antibiotics.

Currently, little is known about pulmonary *M. abscessus* infection compared to other more studied mycobacterial infections such as those caused by *M. tuberculosis* or *M. avium*. One explanation for this is a lack of consensus regarding an *in vivo* infection model. Zebrafish models are commonly utilised due to their low cost and ability to perform real-time imaging to assess host-pathogen interplay; however, zebrafish embryos do not possess an adaptive immune system, thus neglecting to identify aspects of memory formation that are essential in vaccine development (Novoa & Figueras, 2012). Recent studies have attempted to address this using adult zebrafish however, this model does not completely capture the true *in vivo* environment (Kam et al., 2022). Animal models including mice and guinea pigs have been explored. However, in these models there is no consensus regarding the route of infection, mouse strain, and degrees of persistence of *M. abscessus* that would allow for determination of immunity that best represents the clinical situation (Nicola et al., 2022).

Over the last decade some key advances have been made in understanding the immune response to *M. abscessus* infection. It is clear that neutrophils and macrophages are

important in early infection from zebrafish studies (Bernut et al., 2015; Bernut et al., 2016). Further, it has been established that a T-helper type 1 (Th1) cell response is important in clearing *M. abscessus* infection (Bernut et al., 2017), while T regulatory populations are important in limiting pulmonary inflammation (Nava et al., 2022). Interestingly, recent studies have acknowledged that smooth (S) and rough (R) morphotypes may differentially interact with the immune system (Kam et al., 2022). However, the current literature is lacking detailed analysis of the precise immune cell populations and complex host-pathogen interplay required to control pathogen persistence within the host during *M. abscessus* infection.

The current study aimed to establish a pulmonary infection model to explore in detail the host-pathogen responses to *M. abscessus* infection and further identify possible immune correlates of protection that could be utilised for vaccine design. Sixteen clinical isolates of *M. abscessus* from CF patients were screened for their persistence, virulence, and potential immunogenicity *in vitro*, with the most promising strains selected for *in vivo* characterisation in mice.

3.2. Results

3.2.1 Assessment of the growth, persistence and inflammatory capacity of *M. abscessus* strains *in vitro*

To identify *M. abscessus* clinical isolates that are suitable for use in mice, sixteen strains from various *M. abscessus* subspecies of both S and R morphotypes were evaluated *in vitro* (Table 3.1). However, MA05 was not able to be cultivated and hence removed from investigations. Firstly, the growth rates of these strains were examined in culture. This was assessed by measuring the OD_{600} of the cultures every 4 hours over a 52 hour time period. MA03, MA09, MA14 and MA16 demonstrated the most rapid growth rate, reaching a final OD_{600} reading of 2.820, 2.628, 2.772, and 2.754, respectively (Figure 3.1). MA01 and MA15 appeared to be more slow-growing, reaching a final OD_{600} of 1.076 and 1.070 at the final time point, respectively. Overall, *M. abscessus massiliense* strains (MA03, MA06, MA08, MA16) appeared to be more rapid-growing than *M. abscessus* subsp. *abscessus* strains, however there was larger variability in the growth rates of strains classified as *M. abscessus* subsp. *abscessus* (Figure 3.1). There was no clear distinction between the growth rates of S and R morphotypes of *M. abscessus*.

Once the growth rate of *M. abscessus* strains was established in culture, it was next determined whether *M. abscessus* isolates displayed differential invasive and persisting capacities in host cells. To investigate this, the murine macrophage cell line, RAW264.7, was infected with a multiplicity of infection (MOI) of 10:1, and bacterial load at 2 and 48 hours post-infection (hpi) enumerated. The invasive capacity of bacteria was expressed as the percentage of bacterial load at 2hpi relative to the infectious dose. Overall, R strains typically displayed a high percentage of uptake after 2 hours compared to S strains (Figure 3.2A). In particular, MA07, MA09, MA10, MA13 and MA15 had the greatest uptake at 2hpi; which were 3.27%, 4.10%, 4.11%, 4.69%, and 5.77% of total bacteria, respectively. Of the S morphotype, MA01, MA02 and MA08 demonstrated the greatest invasive capacity, with the mean percentage of uptake at 2hpi being 5.56%, 4.68% and 4.53%, respectively. To assess the persistence of each strain in macrophages, the fold-change in bacterial load from 2hpi to 48hpi was calculated. Of note, MA08 and MA16 (S variants) and MA09 (R variant) had a reduction in bacterial load over 48 hours, whereas all other strains showed varying degrees of persistence in macrophages (Figure 3.2B). MA03 and MA07 displayed the greatest degree of persistence, with a fold-change of 5.29 and 4.79, respectively.

Interestingly, MA03 also displayed the poorest uptake in macrophages (0.071%) (Figure 3.2A).

Table 3.1: Strains of M. abscessus assessed with morphotype and subspecies, isolated from Cystic Fibrosis (CF) or non-CF patients. Clinical isolates were kindly provided by Professor Vitali Sintchenko (Centre for Infectious Diseases and Microbiology, Westmead Institute). Subspecies was determined using whole genome sequencing (WGS), which was performed by Andrea Bustamante (NSW Health Pathology).

Strain	Smooth/Rough Phenotype	WGS Subspecies Result	Clade	WGS Number
MA01	Smooth	*M. abscessus abscessus*	1	16-3027-0041
MA02	Smooth	Unknown	N/A	17-3027-0026
MA03	Smooth	*M. abscessus massiliense*	N/A	16-3027-0045
MA04	Smooth	*M. abscessus abscessus*	2	17-3027-0029
MA06	Smooth	*M. abscessus massiliense*	N/A	16-3027-0047
MA07	Rough	*M. abscessus abscessus*	1	16-3027-0043
MA08	Smooth	*M. abscessus massiliense*	N/A	16-3027-0044
MA09	Rough	*M. abscessus abscessus*	3	16-3027-0040
MA10	Rough	*M. abscessus abscessus*	1	17-3027-0021
MA11	Rough	*M. abscessus abscessus*	3	17-3027-0002
MA12	Rough	*M. abscessus abscessus*	3	17-3027-0025
MA13	Rough	*M. abscessus abscessus*	N/A	17-3027-0023
MA14	Smooth	*M. abscessus massiliense*	N/A	17-3027-0027
MA15	Rough	*M. abscessus abscessus*	4	17-3027-0022
MA16	Smooth	*M. abscessus massiliense*	N/A	16-3027-0027

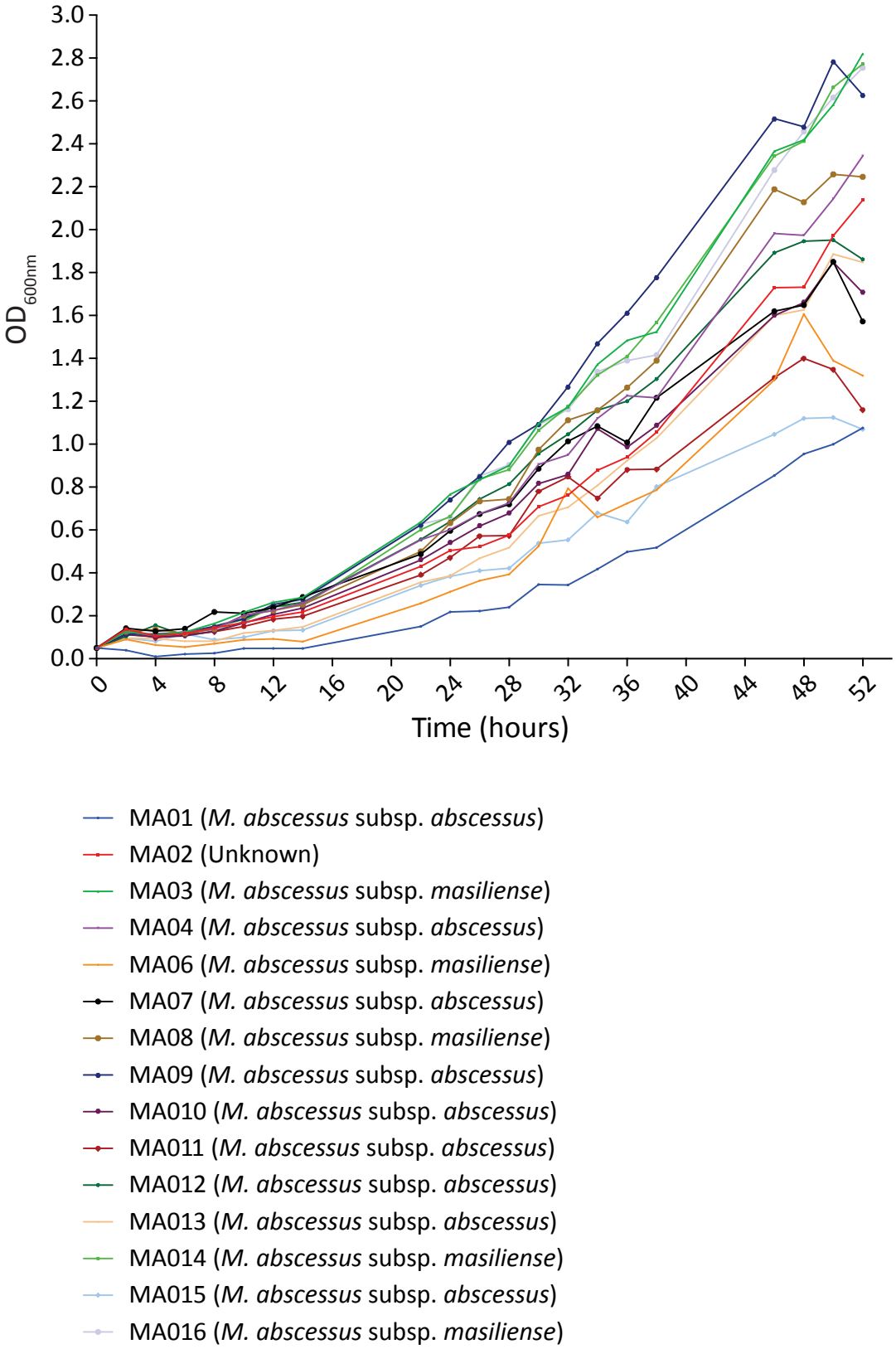

Figure 3.1. Growth curve of *M. abscessus* clinical isolates in vitro. Fifteen clinical isolates of *M. abscessus* were cultured to Log-phase and then diluted to OD_{600} 0.05. Isolates were then incubated at 37˚C and 5% CO_2 for 52 hours. The growth of isolates was estimated by taking OD_{600} readings in triplicate every 4 hours. Data shown is mean OD_{600} of each *M. abscessus* clinical isolate over 52 hours. Data is representative of three independent experiments.

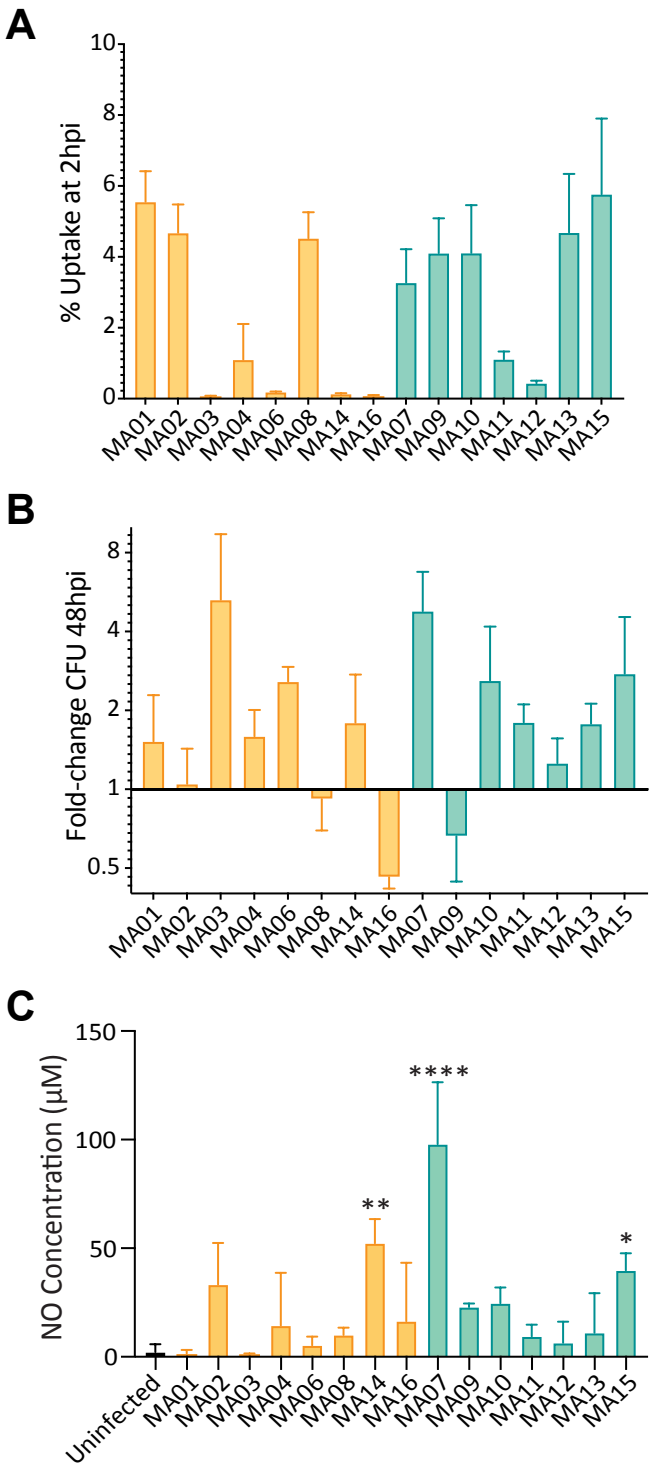

Figure 3.2. Capacity of *M. abscessus* clinical isolates to invade host macrophages and persist in vitro. RAW264.7 cells were infected with one of fifteen *M. abscessus* clinical isolates (Yellow bars = Smooth; Green = Rough) at a MOI of 10:1 and incubated for 2 hours. Cells were washed and replenished with fresh media and incubated for a further 48 hours. Samples were lysed at 2hpi and 48hpi and enumerated on 7H10 agar plates. **(A)** Percentage of *M. abscessus* enumerated in macrophages after 2 hours of infection relative to the infectious dose. **(B)** Fold-change in *M. abscessus* enumerated in macrophages after 48 hours of infection normalised to intracellular bacterial concentration after 2 hours of infection. **(C)** After 48 hours of incubation with *M. abscessus strains*, the production of NO by macrophages was assessed by performing a Griess assay on RAW264.7 supernatants. Data is representative of four independent experiments and is displayed as mean ± SD. Significance of difference between infected and uninfected cells in **(C)** were calculated by one-way ANOVA (*P<0.05, **P<0.01, ****P<0.0001).

All other strains displayed moderate degrees of persistence, with fold-changes in the range of 1.23-2.56 (Figure 3.2B). Again, there was no observable pattern in invasive or persistence capacity in terms of *M. abscessus* subspecies.

Nitric oxide (NO) is a potent antimicrobial produced by macrophages in response to mycobacterial infection. As such, the capacity of *M. abscessus* clinical isolates to invoke a potent NO response in macrophages was explored by Greis Assay. NO production in RAW264.7 cells infected with MA07 was higher than any other *M. abscessus* isolate (Figure 3.2C). There was also significant NO production in macrophages infected with MA14 and MA15. There was no observable difference in NO response between S and R morphotype, nor between *M. abscessus* subspecies.

The next series of experiments assessed the capacity of *M. abscessus* clinical isolates to induce an inflammatory response in RAW264.7 cells. The supernatants of infected cells were collected and cytokine bead array (CBA) was performed to examine cytokine production by infected cells. The cytokines examined included GM-CSF, important in the differentiation and recruitment of myeloid cells during infection, such as dendritic cells (DCs) and macrophages (Hamilton, 2020); TNF, involved in a multitude of functions including iNOS expression and lymphocytic recruitment (Ehlers & Schaible, 2012); and IL-6, which has a broad effects in inflammation, and haematopoiesis. (Tanaka et al., 2014). IL-1β and IL-12p70 were also examined, however sample readouts were below the limit of detection (data not shown). Overall, macrophages infected with R morphotypes produced greater magnitudes of cytokines. There was significant production of GM-CSF in macrophages infected with strains MA02, MA07, MA10 and MA15 relative to uninfected macrophages (Figure 3.3A). MA07 and MA10-infected macrophages displayed the highest levels of IL-6 production (Figure 3.3B). There was also significant IL-6 detected in macrophages infected with MA02, MA14 and MA15 compared to uninfected cells. Finally, TNF production was induced by all macrophages infected with *M. abscessus* to some degree. Strains that reached statistical significance relative to uninfected controls included MA02, MA14, MA07, MA09, MA09, MA10, MA11 and MA15 (Figure 3.3C).

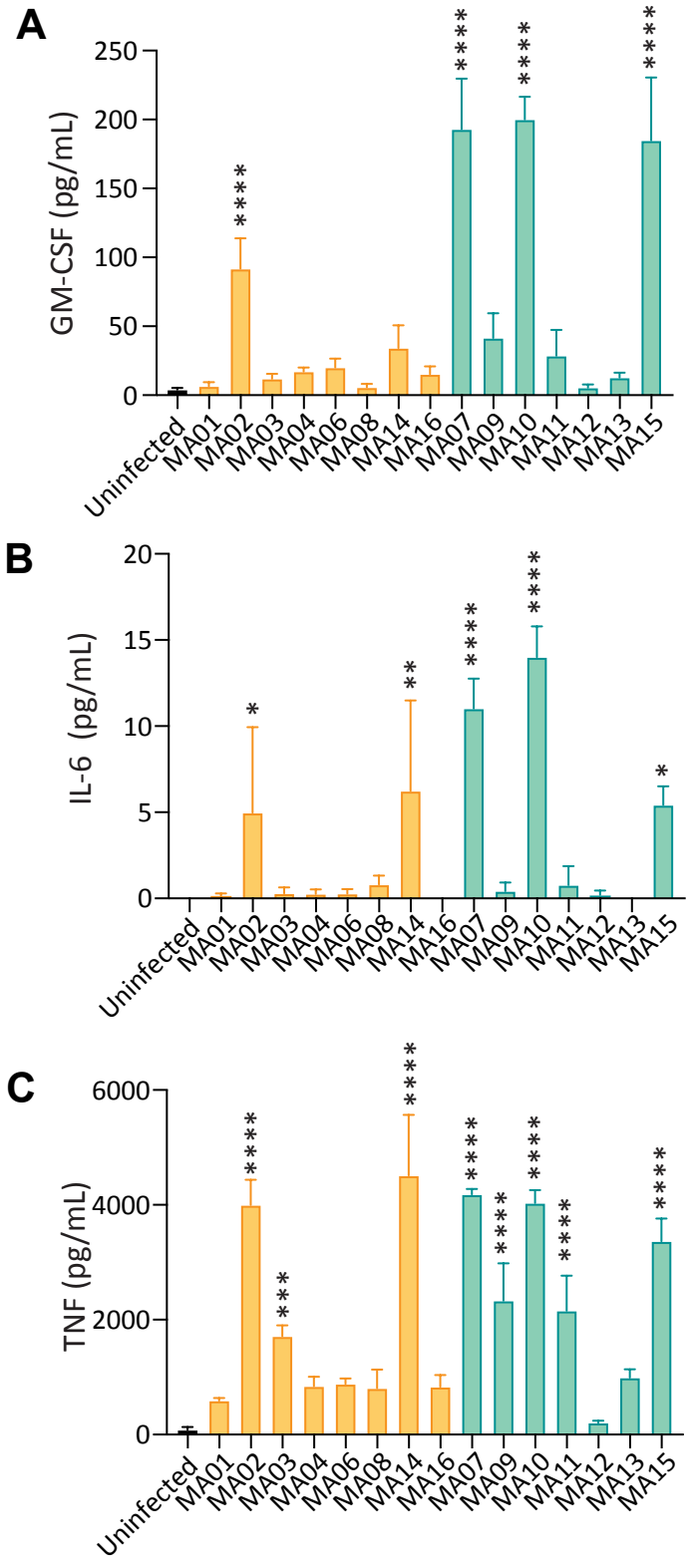

Figure 3.3. Cytokine response induced in macrophages infected with *M. abscessus* clinical isolates *in vitro*. RAW264.7 cells were infected with one of fifteen clinical isolates (Yellow bars = Smooth; Green bars = Rough) of *M. abscessus* infected at an MOI 10:1 for 2 hours or left uninfected. Cells were washed and replenished with fresh media and incubated for a further 48 hours. Supernatants were collected after 48 hours for cytokine analysis by cytokine bead array. Concentration of **(A)** GM-CSF, **(B)** IL-6 and **(C)** TNF production by RAW264.7 cells 48hpi in pg/mL. Data is shown as mean concentration ± SD in pg/mL and is representative of two independent experiments. Significance of difference between infected and uninfected cells in were calculated by one-way ANOVA (*P<0.05, **P<0.01, ***P<0.001, ****P<0.0001).

In conclusion, there were five strains that stood out as potential candidates for *in vivo* model of infection; MA02, MA07, MA10, MA14 and MA15. While MA02 had high uptake by macrophages and high levels of cytokine production *in vitro*, MA02 not appear to persist within macrophages to a significant extent, nor did it elicit a strong NO response. Further, the subspecies and clade details of MA02 is unknown, and therefore was not selected for *in vivo* assessment (Table 2.2). MA07 showed moderate growth in culture, high uptake and persistence in macrophages, high cytokine responses, and significant NO production. MA10 demonstrated moderate to high replication capacity in culture, moderate uptake and persistence in macrophages, low NO production, and high cytokine production. MA14 showed rapid replication capacity, low uptake in macrophages, moderate NO production, and moderate to high cytokine production. MA15 had one of the lowest growth rates extracellularly, but high uptake and persistence in macrophages, and significant NO production. In addition, MA15 was a potent stimulator of cytokine production in macrophages. Thus, to provide a cross section of strains representing different clades and morphotypes, MA07 (clade 1, R morphotype) MA11 (clade 3, R morphotype), MA14 (clade unknown, S morphotype) and MA15 (clade 4, R morphotype) were selected for further analysis.

3.2.2 *M. abscessus* clinical isolates induced comparable bacterial burden and cellular responses in C57BL/6 mice infected via intranasal route

The next series of experiments investigated whether there was any difference in persistence and immunogenicity of the selected strains in a pulmonary infection model. C57BL/6 mice were infected intranasally (i.n.) with 10^6 CFU of *M. abscessus*, and bacterial load, as well as T cell populations, were assessed at day 1, 7, 14 and 21 days post-infection (dpi) in the lung and spleen. In both organs, there was no significant difference between strains in the growth over the time period examined, although there did appear to be greater initial colonisation at day 1 with strains MA11 and MA15 in the lung (Figure 3.4A). The bacterial load in the lung peaked at 1dpi and gradually cleared over the 21 day period. In the spleen, bacterial load peaked 7dpi however, only small numbers of bacteria were recovered (Figure 3.4B). Therefore, the *M. abscessus* strains assessed were able to colonise the lung and were gradually cleared over time, with limited dissemination to the spleen.

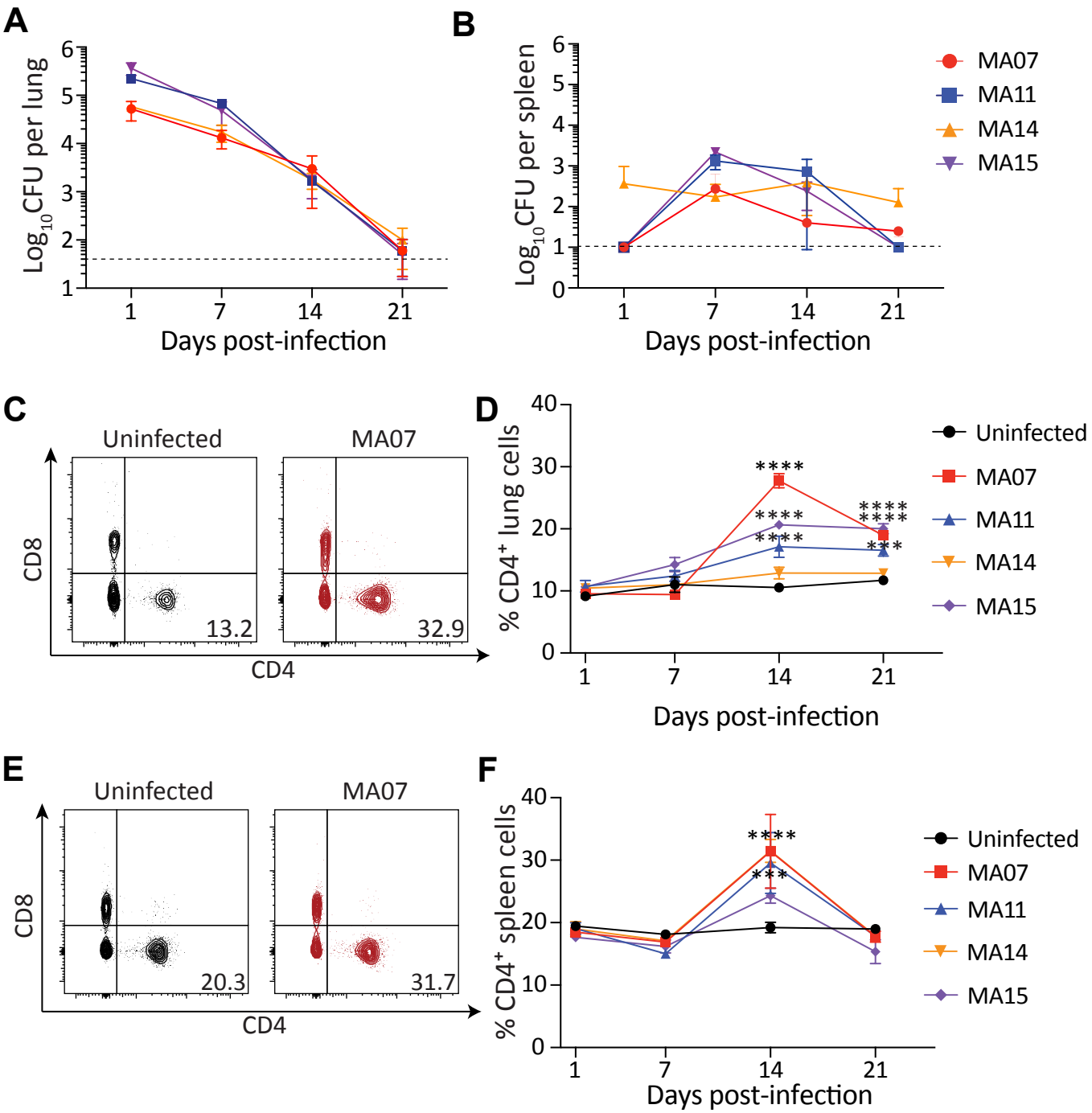

Figure 3.4. Persistence and immunogenicity of selected *M. abscessus* strains in mice. C57BL/6 mice (n=3) were infected with 10^6 CFU *M. abscessus* MA07, MA11, MA14 or MA15 via intranasal route. The lungs and spleens were collected at day 1, 7, 14 and 21 post-infection for bacterial enumeration and flow cytometric analysis. Bacterial load in the lung **(A)** and **(B)** spleen is represented as Log_{10} CFU per organ. **(C)** Representative FACS plots of uninfected and MA07-infected groups at day 7 post-infection and **(D)** Mean percentage ± SEM of $CD4^+$ T cells in the lung over time. **(E)** Representative FACS plots of uninfected and MA07-infected groups at day 7 post-infection and **(F)** Mean percentage ± SEM of $CD4^+$ T cells in the spleen over time. Significance of difference between infected and uninfected groups in **(C-E)** were calculated by two-way ANOVA (***P<0.001, ****P<0.0001). Dashed line = limit of detection of CFU. Data is representative of one individual experiment.

The proportion of T cell populations in the lung over the course of infection were analysed. $CD4^+$ T cells peaked at 14dpi for all four strains, with MA07 having a noticeably stronger response (Figure 3.4C-D). MA07, MA11 and MA15 demonstrated a significant increase in $CD4^+$ T cell responses compared to uninfected control at this timepoint ($P<0.0001$). The accumulation of $CD4^+$ T cells in the lung of mice infected with MA07, MA11, and MA15 remained significantly higher than uninfected controls at 21dpi ($P<0.0001$, $P=0.0008$, $P<0.0001$, respectively). MA14 did not produce a significant $CD4^+$ T cell response. Similar to the pulmonary response, $CD4^+$ T cell responses in the spleen peaked at 14dpi across the four clinical isolates (Figure 3.4E-F). MA07, MA11 and MA14 displayed a significant increase in $CD4^+$ T cell accumulation compared to uninfected controls at 14dpi ($P<0.0001$, $P=0.0002$, $P<0.0001$, respectively). Infection with MA15 did not induce a statistically significant $CD4^+$ T cell response in the spleen compared to uninfected mice.

While infection kinetics of the four clinical isolates were comparable, MA07 demonstrated a significantly stronger immunogenic profile on initial screening; that is, the $CD4^+$ T cell responses in the lung and spleen post-infection were markedly increased compared to uninfected controls, as well as being greater than other clinical isolates. For this reason, MA07 was selected as the most appropriate strain to use in future studies to further elucidate the immune response to pulmonary *M. abscessus* infection.

3.2.3 Pulmonary *M. abscessus* infection persists for 21 days in the lung in C57BL/6 mice

The kinetics of pulmonary *M. abscessus* infection was next examined in more detail using MA07 as the representative strain for these experiments. CFU from the lung and spleen were enumerated at timepoints up to 21dpi after i.n. infection with MA07. As evident in Figure 3.5A, pulmonary *M. abscessus* infection peaked on the first day following infection, replicating approximately 15-fold in the first 24 hours. *M. abscessus* bacterial numbers declined from this peak at 24 hours, with a drop of approximately 4 log at 21dpi, however bacterial loads were still detectable in the lung at this timepoint. *M. abscessus* bacterial load peaked in the spleen at 5dpi; however, dissemination to the spleen was limited, with numbers peaking at approximately 10^3 CFU (Figure 3.5B). By 21dpi, most animals had cleared *M. abscessus* from this site. Previous literature has suggested that C3HeB/FeJ (Kramnik) mice offer a more persistent *M. abscessus* infection model (Driver et al., 2012). Thus, we investigated if persistence of the MA07 strain was impacted in Kramnik mice.

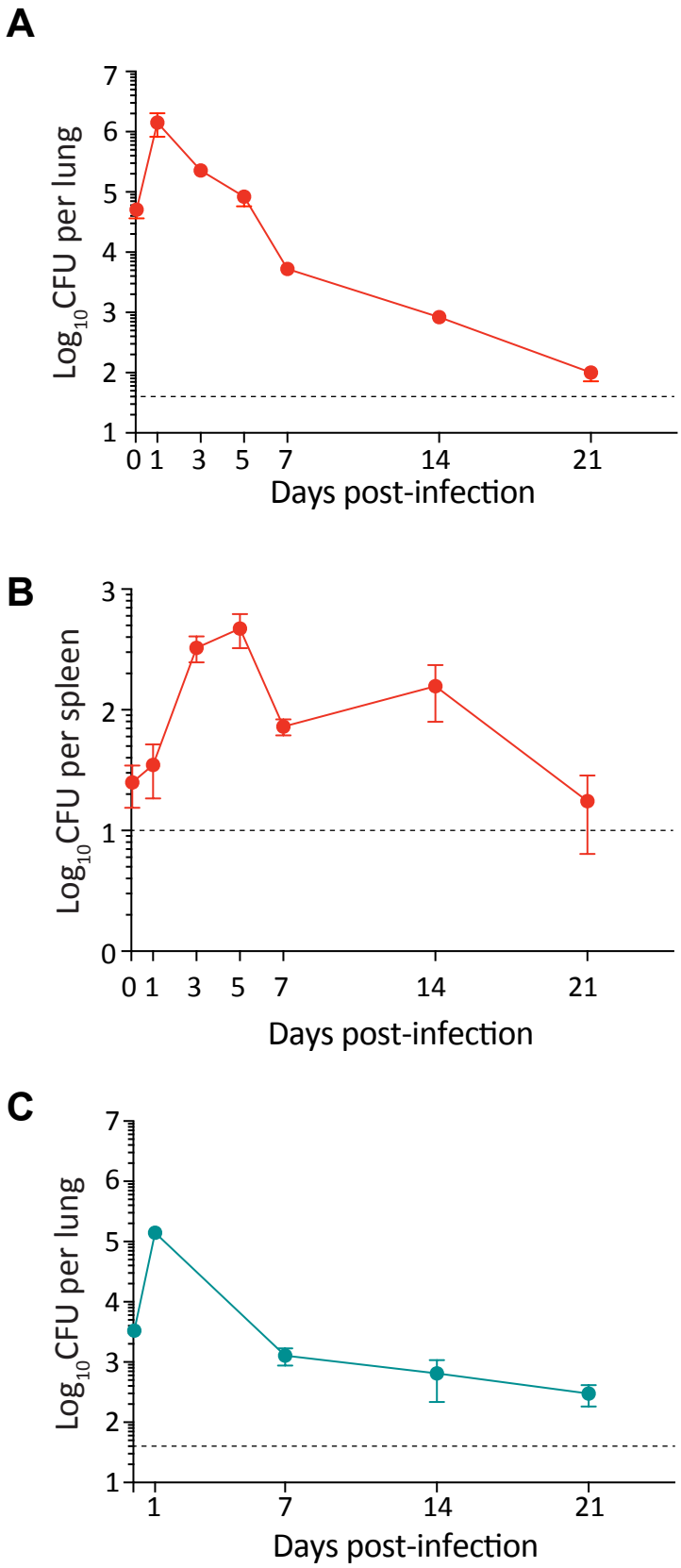

Figure 3.5. Kinetics of *M. abscessus* infection in the C57BL/6 and C3HeB/FeJ mice following intranasal challenge. C57BL/6 mice (n=3, A-B) or Ch3HeB/FeJ (C) were infected with 10^6 CFU *M. abscessus* MA07 via intranasal route. Bacterial load in the **(A)** lung and **(B)** spleen of C57/BL6, or lungs of C3HeB/FeJ **(C)** mice were enumerated at 6 hours, day 1, 3, 5, 7, 14 and 21 following infection. Data is expressed as mean Log_{10}CFU per organ ± SEM. Dashed line = limit of detection for CFU.

Bacterial burdens in the lung for Kramnik mice infected with *M. abscessus* did not appear to persist any longer than in C57BL/6 mice (Figure 3.5C). Further, no dissemination to the spleen of Kramnik-infected mice was detected (data not shown). Hence, C57BL/6 mice were used for all future experiments to establish a pulmonary *M. abscessus* infection.

3.2.4 Marked recruitment of interstitial macrophages to the lung in response to pulmonary *M. abscessus* infection

Pulmonary cellular infiltration was comparable between infected and uninfected mice from days 1-7 post-infection (Figure 3.6). There were significantly more cellular infiltrates in the lungs of infected mice at 14 and 21dpi ($P=0.0296$, $P<0.0001$, respectively). Various myeloid populations were then analysed via flow cytometry to identify cell subsets that may be involved the immune control of infection: alveolar macrophages (AMs), interstitial macrophages (IMs), neutrophils, eosinophils, monocytes, $CD11b^+$ dendritic cells (DCs) and $CD103^+$ DCs, as outlined by the gating strategy in Figure 2.2. Due to logistical constraints, specific natural killer (NK) cell markers were not included, and so $CD11b^{mid}$ cells were analysed as a surrogate for NK cells {Cong, 2019 #1305}. Representative FACS plots of these populations are shown in Figure 3.7. At 24hpi, neutrophils were the predominant myeloid cell subset identified in the lungs of infected mice and present at significantly higher proportions than uninfected mice; by day 3 the proportion of neutrophils in infected mice was comparable to uninfected controls (Figure 3.8A). $CD11b^+$ DCs peaked at day 3 and returned to baseline at day 5, with no significant differences found across time-points (Figure 3.8B). $CD103^+$ DCs peaked later, at day 14, where there were significantly higher proportions in infected mice compared to uninfected controls (Figure 3.8C). Interestingly, the kinetics of AM changes in the lung were mostly comparable between infected and uninfected mice across all timepoints; indeed, at day 7 there were significantly higher proportions of AMs in uninfected controls compared to infected mice (Figure 3.8D). Similarly, *M. abscessus*-infected mice showed reduced proportions of eosinophils at days 1 and 7 post-infection compared to naïve controls (Figure 3.8E). Monocytes demonstrated peak accumulation at day 5, before dropping below uninfected controls at day 7 (Figure 3.8F). $CD11b^{mid}$ cells peaked at days 5 to 7; at this point there were significantly higher numbers in infected mice compared to uninfected controls (Figure 3.8G). $CD11b^{mid}$ cells were comparable between groups by day 14. Finally, the most salient finding in this experiment was the observation that *M. abscessus*-infected mice had significantly higher proportions of IMs at day 3, day 5,

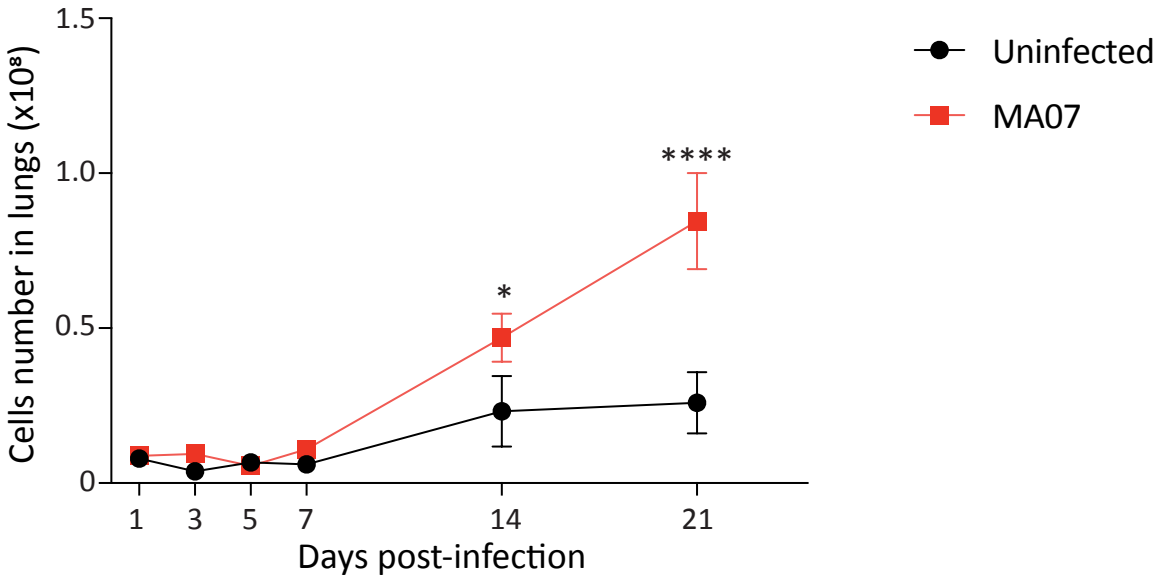

Figure 3.6. Kinetics of inflammatory cell infiltration into the lung following intranasal *M. abscessus* infection. C57BL/6 mice (n=3) were infected with 10^6 CFU M. abscessus MA07 via intranasal route. Total cell number in the lung was enumerated at 6 hours, and day 1, 3, 5, 7, 14 and 21 following infection. Each value represents mean percentage of total lung cells ± SEM of n=3 per group. *P<0.05, ****P<0.0001, two-way ANOVA.

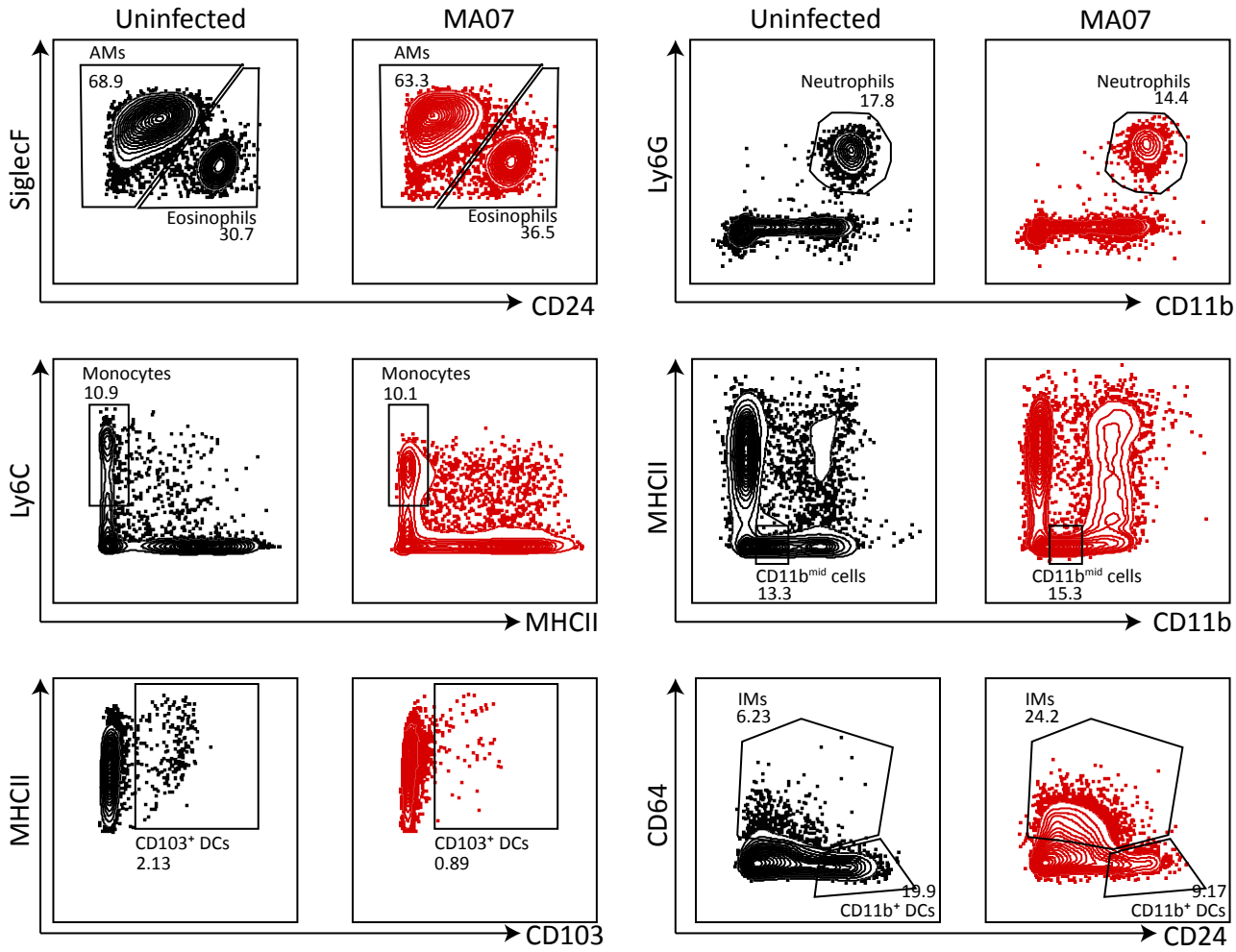

Figure 3.7. Representative FACS plots for myeloid subsets assessed during *M. abscessus* infection. C57BL/6 mice (n=4) were infected with 10^6 CFU *M. abscessus* MA07 via intranasal route or left uninfected. Lungs were collected at 6 hours, day 1, 3, 5, 7, 14 and 21 following infection and proportions of innate immune cells were identified using flow cytometry. FACS plots are shown for day 7 post-infection.

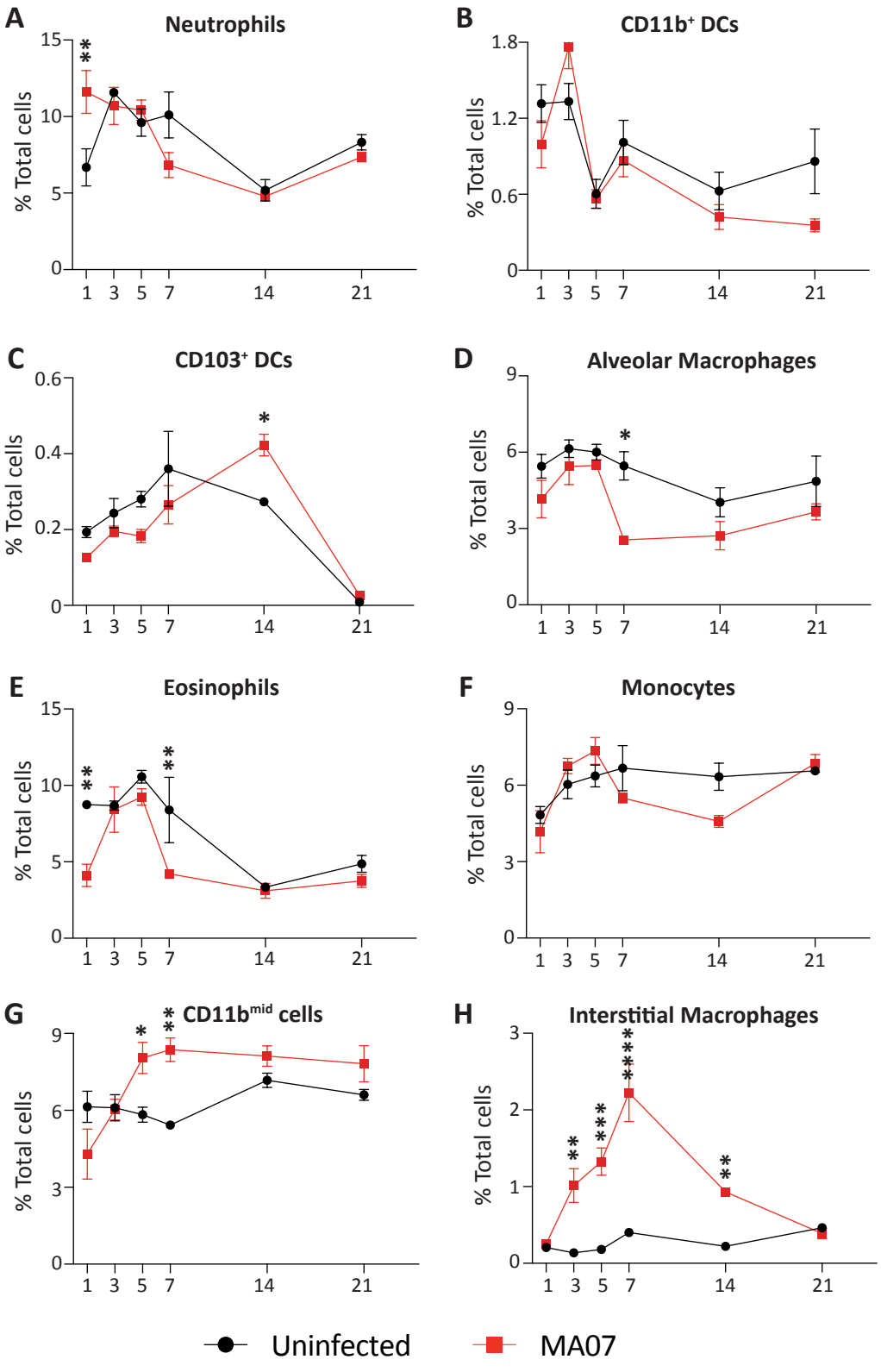

Figure 3.8. Kinetics of myeloid cell accumulation in the lung over the course of intranasal *M. abscessus* infection. C57BL/6 mice (n=4) were infected with 10^6 CFU *M. abscessus* MA07 via intranasal route or left uninfected. Lungs were collected at 6 hours, day 1, 3, 5, 7, 14 and 21 following infection and proportions of innate immune cells were identified using flow cytometry. For **(A-H)** each value represents mean percentage of total lung cells ± SEM of n=3-4 per group. *P<0.05, **P<0.01, ***P<0.001, ****P<0.0001, two-way ANOVA. Data is representative of two individual experiments.

day 7 and day 14 post-infection compared to uninfected mice, with a noticeable peak at day 7 (Figure 3.8H). Considering the importance of iNOS in the control of bacterial infections (Braverman & Stanley, 2017), the kinetics of iNOS production relative to bacterial clearance and immune cell accumulation was investigated by flow cytometry. Total iNOS production peaked at day 7 post-infection with *M. abscessus* and was significantly higher in infected mice compared to uninfected controls across time-points between days 3 and 14 (Figure 3.9A-B). Once it was established that iNOS appeared to be involved in the clearance of *M. abscessus* infection, it was next determined which cell subsets were responsible for its production. Figure 3.8C demonstrates the percentage of iNOS production by cell subset. It is evident that in *M. abscessus* MA07-infected mice, IMs are the major contributors to iNOS production.

In conclusion, i.n. infection with *M. abscessus* MA07 induced the accumulation of a variety of myeloid cell subsets in the lung, however the most noticeable change occurred in IMs. IMs demonstrated the greatest production of iNOS. Additionally, the high levels of iNOS production in infected mice correlated with bacterial clearance.

3.2.5 Pulmonary *M. abscessus* infection induces a robust T-helper type 1 cell response in C57BL/6 mice

To examine the adaptive immune response to intranasally-delivered *M. abscessus* MA07, flow cytometric analysis of T and B cell populations was performed. Overall, $CD4^+$ T cells were the predominant adaptive immune cell type identified in the lung following *M. abscessus* infection (Figure 3.10A). These cells were significantly increased in numbers than uninfected controls at day 7 and 14 ($P=0.033$, $P<0.0001$, respectively), with the peak of the $CD4^+$ T cell response at 14 dpi. There was no significant difference in $CD8^+$ T cell and B cell numbers between infected and uninfected groups across all time-points examined (Figure 3.10B-C).

It is well-established that Th1 responses are crucial in the control of mycobacterial infections (Shu, Wu, et al., 2019), while Th17 cells have been shown to be critical in the control of *M. tuberculosis* using a mucosal vaccination model (Counoupas et al., 2020). To examine the phenotype of responding $CD4^+$ T cells in the lung, the expression of two master regulators of transcription was analysed; Tbet, the regulator of Th1 differentiation, and RorγT, the regulator of Th17 cell differentiation (Mousset et al., 2019). C57BL/6 mice were infected with 10^6 CFU of *M. abscessus* MA07 and the lungs were harvested for flow cytometric analysis

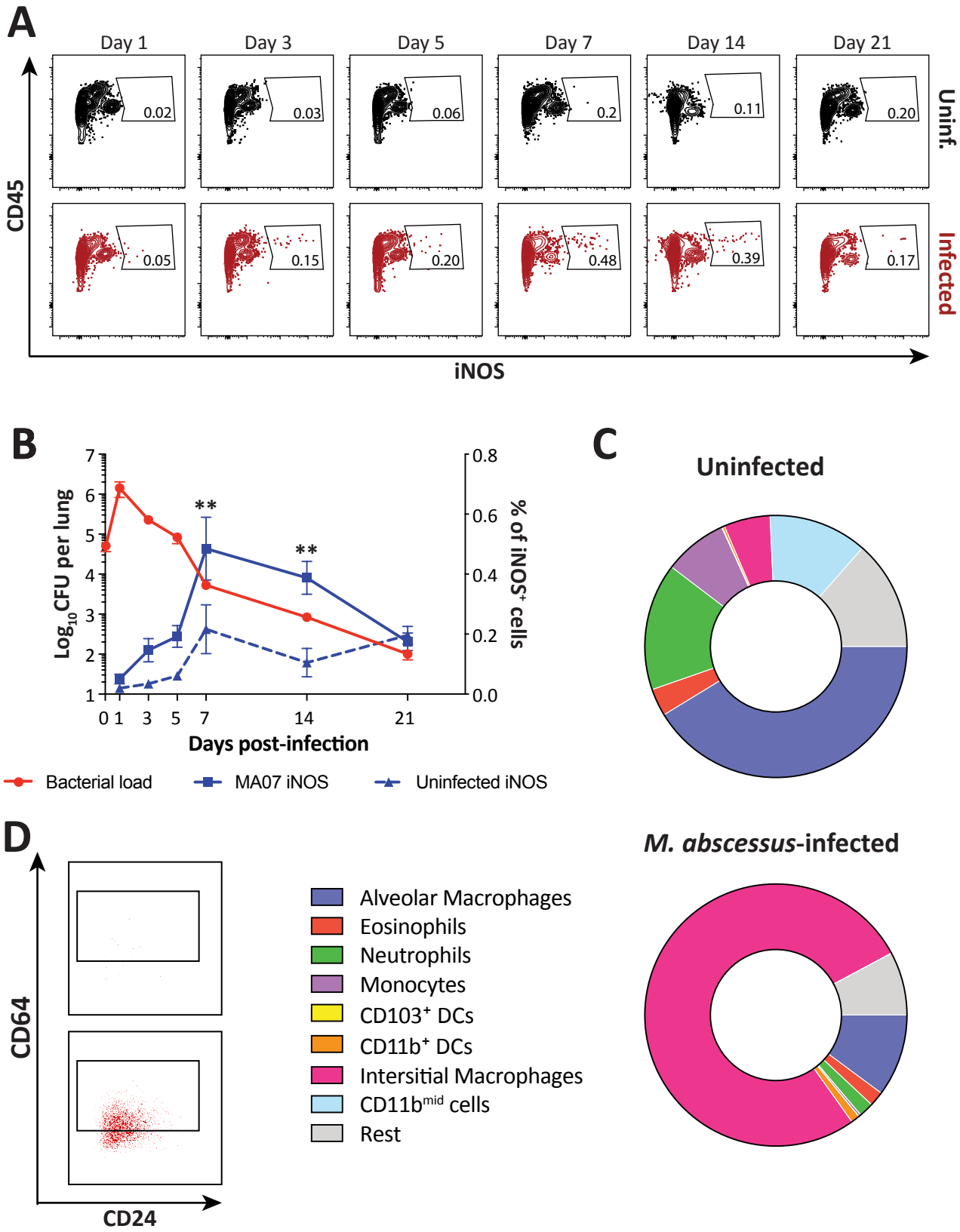

Figure 3.9. iNOS production by myeloid cells in the lung following *M. abscessus* infection. C57BL/6 mice were infected with 10^6 CFU *M. abscessus* MA07 via intranasal route (n=4) or left uninfected (n=3). Lungs were collected at 6 hours, day 1, 3, 5, 7, 14 and 21 following infection and proportions of innate immune cells were identified using flow cytometry. **(A)** Representative FACS plots of percentage of total iNOS-producing $CD45^+$ cells in the lung over time. **(B)** Percentage of $iNOS^+$ cell over time compared to bacterial load. **(C)** Proportional distribution of iNOS expression identified in lung innate immune cells by flow cytometry following *M. abscessus* infection at day 7 post-infection. **(D)** Representative FACS plots of $iNOS^+$ IMs. **P<0.01, two-way ANOVA.

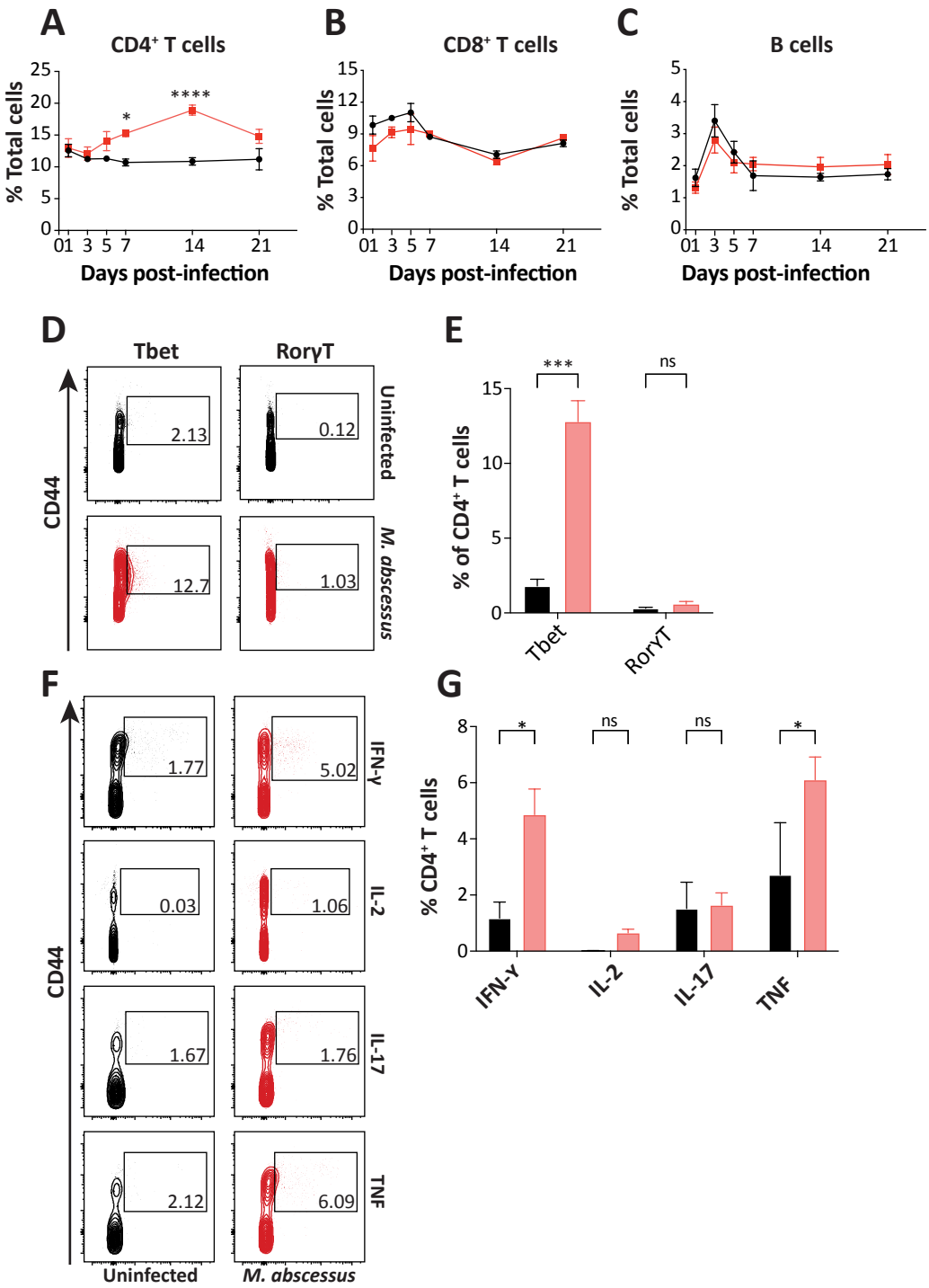

Figure 3.10. Adaptive immune response to intranasal *M. abscessus* challenge. C57BL/6 mice were infected with 10^6 CFU *M. abscessus* MA07 via intranasal route (n=4) or left uninfected (n=3). Lungs were collected at 6 hours, day 1, 3, 5, 7, 14 and 21 following infection and proportions of innate immune cells were identified using flow cytometry. **(A-C)** Shows proportions of CD4⁺ T cells, CD8⁺ T cells and B cells over 21 days in infected (red) and uninfected (black) mice. **(D)** Representative FACS plots of Tbet and RorγT-positive CD4⁺ T cells in the lung at 14 days post-infection. **(E)** Summary data of differences in Tbet and RorγT expression in CD4⁺ T cells between *M. abscessus*-infected (red) and uninfected (black) mice at 14dpi. **(F)** Representative FACS plots and **(G)** summary data of *M. abscessus*-specific CD4⁺ T cells in the lung producing IFN-γ, IL-2, IL-17 and TNF in naïve mice (black) or 14 days following *M. abscessus* infection (red). Data shown in A-C, E, G shows mean ± SEM for n=3-4 and is representative of two independent experiments. Significance of difference between groups was calculated by two-way ANOVA (A-C) or one-way ANOVA (E, G) (*P<0.05, ***P<0.001, ****P<0.0001).

over 21 days. At the peak of the $CD4^+$ T cell response (14dpi), there was significantly higher levels of Tbet expression in *M. abscessus*-infected mice compared to naïve controls (Figure 3.10D-E; P<0.0001). However, there was no significant difference in RorγT expression between infected and uninfected mice (Figure 3.10D-E). Next, to determine the functional capacity of $CD4^+$ T cells, cytokine production by $CD4^+$ T cells in the lungs 14 days after infection was examined following restimulation with 10^5 CFU *M. abscessus*. $CD4^+$ T cells expressing TNF were the most represented cell type identified, with responses significantly higher in *M. abscessus*-infected mice compared to uninfected controls (P=0.039, Figure 3.10F-G). This was followed by IFN-γ-producing $CD4^+$ T cells, which were significantly higher in proportion in *M. abscessus*-infected mice (P=0.022). Both IL-2 or IL-17-expressing $CD4^+$ T cells were comparable between infected and uninfected mice. In conclusion, intranasal *M. abscessus* infection in C57BL/6 mice induces a strong $CD4^+$ T cell response in the lungs, which was characterised by IFN-γ and TNF-expressing $CD4^+$ T cells (Th1 type) and peaked 14 days after infection.

3.2.6 *M. abscessus* MA07 infection leads to a potent pro-inflammatory cytokine profile in the lung

To examine the inflammatory milieu of the lung microenvironment following *M. abscessus* infection, chemokine and cytokine activity was measured in the lung over the course of infection. G-CSF, CXCL1, IL-6 peaked 6 hours after infection and rapidly returned to the limit of detection by 24 hours post-infection (Figure 3.11A-C; P<0.0001, P=0.061; P=0.0206, respectively). Production of TNF had a biphasic pattern, peaking at both 24 hours after infection and day 14 in *M. abscessus*-infected mice (Figure 3.11D). IFN-γ expression increased in *M. abscessus*-infected mice at day 3 and remained elevated until day 14, before returning to baseline at day 21 (Figure 3.11E). IL-10 was undetectable until 14 days after infection and remained elevated at day 21 in infected mice (Figure 3.11F). Taken together, these data suggest that intranasal *M. abscessus* infection invokes varied cytokine and chemokine activity at different times throughout the infectious time-course, characterised by TNF and IFN-γ production and appearance of IL-10 at late timepoints.

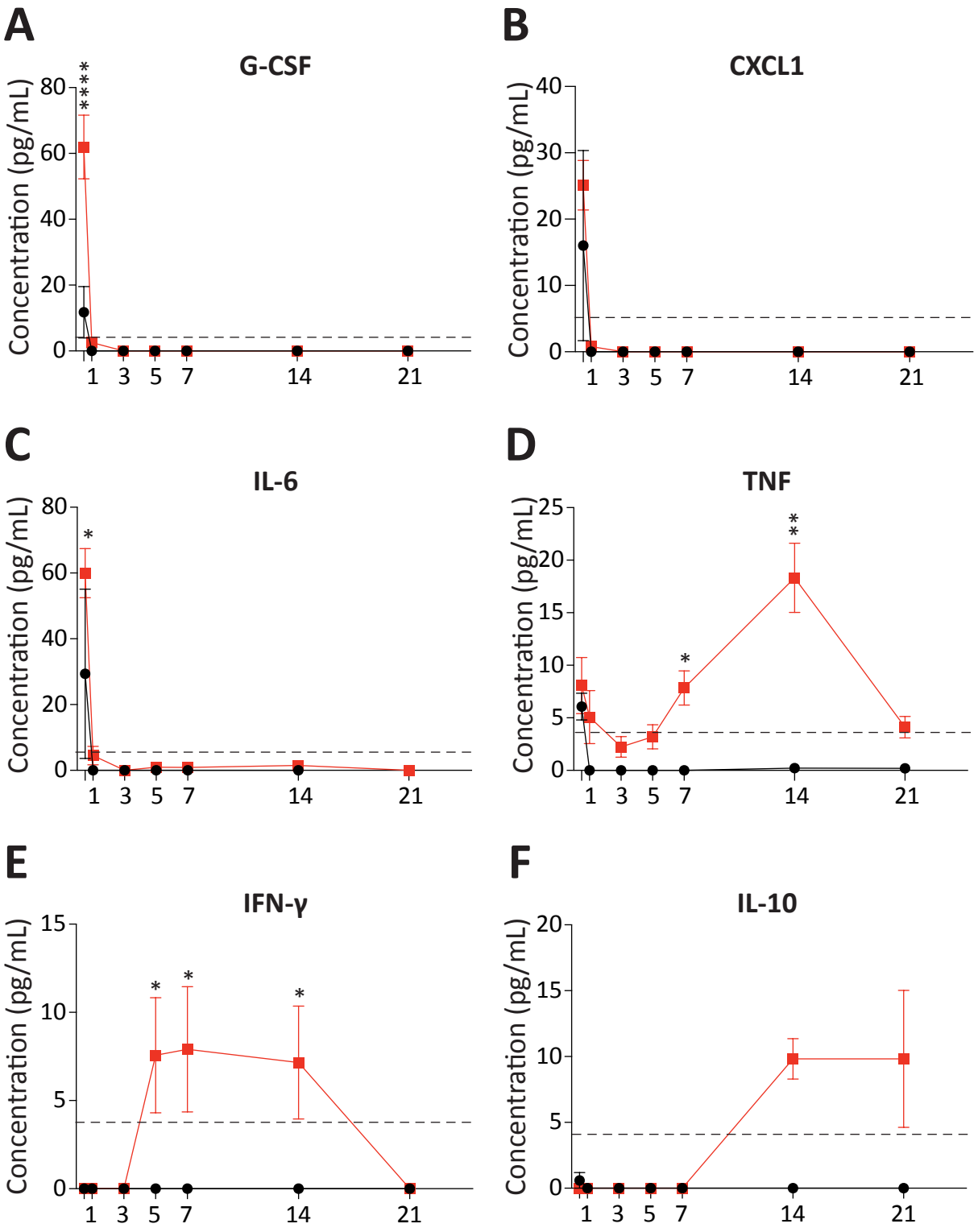

Figure 3.11. Cytokines and chemokines produced in the lung following *M. abscessus* infection. C57BL/6 mice were infected with 10^6 CFU *M. abscessus* MA07 via intranasal route (n=4) or left uninfected (n=3). Lungs were collected at 6 hours, day 1, 3, 5, 7, 14 and 21 following infection and lung homogenate supernatant was analysed for cytokine and chemokine production by cytokine bead array. A-F shows the mean concentration of cytokine/chemokine ± SEM in the lung at each time-point. Significance of difference between groups was conducted using two-way ANOVA (*P<0.05, **P<0.01, ****P<0.0001). Dashed line represents limit of detection for each cytokine.

3.2.7 TNF is required for interstitial macrophage accumulation and iNOS production in the lung following *M. abscessus* infection

Considering the accumulation of TNF-expressing $CD4^+$ T cells and the high level of TNF in lung homogenates in *M. abscessus*-infected mice, the next series of experiments endeavoured to investigate how control of *M. abscessus* infection was impacted in the absence of TNF, using a $tnf^{-/-}$ mouse model (Saunders et al., 2004). Compared to wildtype (WT) mice, $tnf^{-/}$ (TNFKO) mice demonstrated an impaired ability to clear *M. abscessus* infection; indeed, *M. abscessus* persisted to 42 days post-infection in $tnf^{-/-}$ mice, though this did not reach statistical significance (Figure 3.12A). Further, there was significantly higher bacterial burden in the spleen of $tnf^{-/-}$ mice compared to WT mice infected with *M. abscessus*, although the rate of clearance from the spleen was similar from day 7 onwards. (Figure 3.12B).

Given that previous data indicated that IMs are important iNOS-producers in the lungs of *M. abscessus* mice (Section 3.2.5), we investigated their accumulation in the lung in the absence of TNF. In the absence of TNF, iNOS expression was almost completely abolished across all timepoints (Figure 3.12C-D). T-distributed stochastic neighbour embedding (tSNE) analysis was employed to display differences in cell subsets at day 14 post-infection. While most myeloid cell subsets remain unchanged, in the absence of TNF there was a marked absence of the IM population (Figure 3.12E). This translated to a reduced accumulation of IMs in the lungs of $tnf^{-/-}$ mice compared to WT following *M. abscessus* infection (Figure 3.12F). When TNF was not present, iNOS expression in IMs was markedly downregulated compared to all other cell types, which showed a marginal compensatory upregulation of iNOS expression (Figure 3.12G). There was also marked down-regulation of MHCII expression across all myeloid cell subsets in the absence of TNF. Taken together, these data suggest that TNF is crucial in the clearance and containment of *M. abscessus* infection in mice, which correlates with the requirement of TNF for the accumulation of IMs in the lungs and iNOS expression.

3.2.8 TNF is important in Th1 differentiation and prevents T cell exhaustion

TNF is known as an important effector cytokine of $CD4^+$ T cells in mycobacterial infection. As such, the role of TNF in the adaptive immune cell response to intranasal *M. abscessus* infection was investigated. There were significantly higher proportions of $CD4^+$ T cells in infected mice in the absence of TNF, persisting to day 42 post-infection (Figure 3.13A-B).

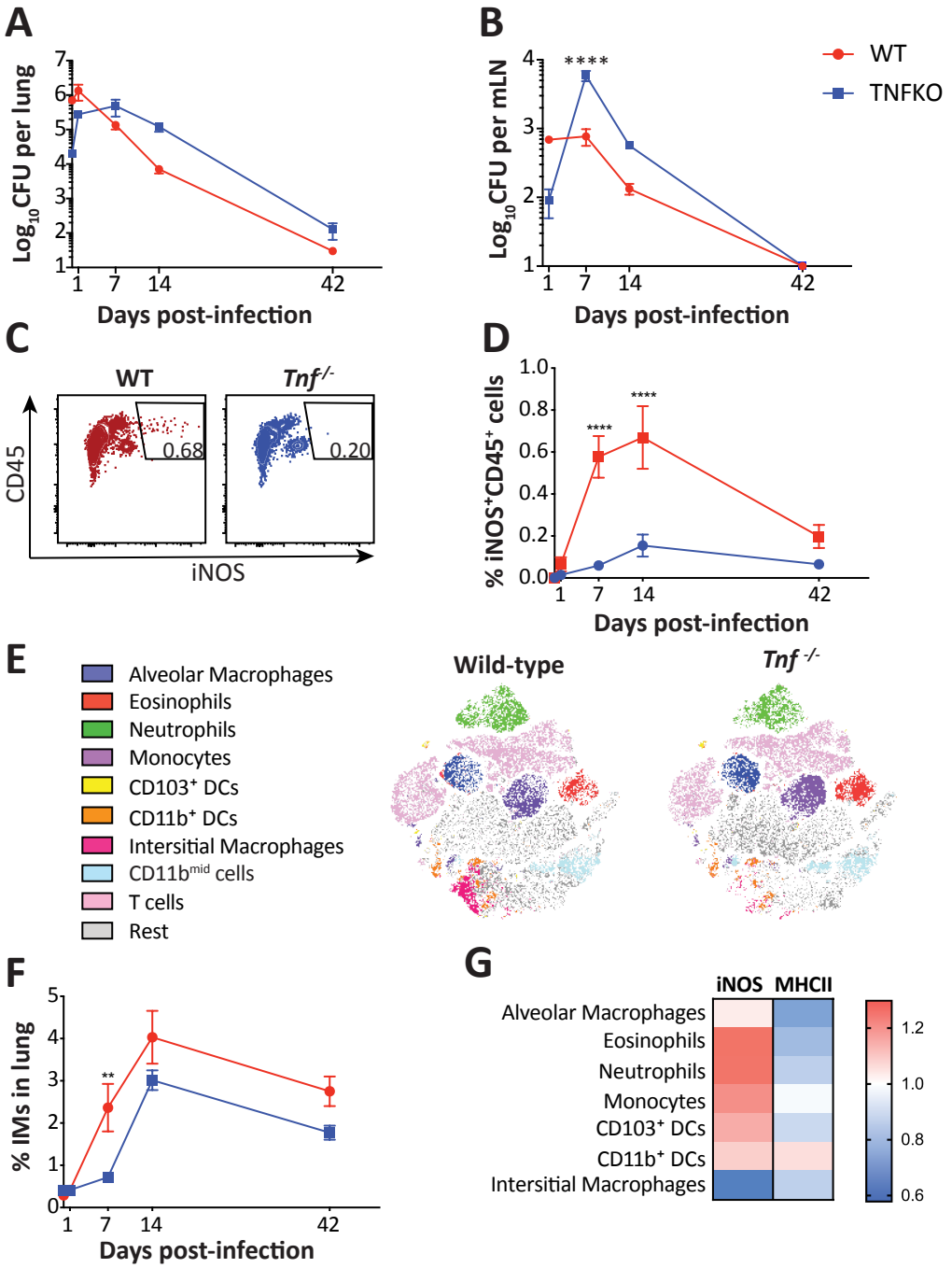

Figure 3.12. Role of TNF in innate immune responses to pulmonary *M. abscessus*. C57BL/6 (red) or tnf$^{-/-}$ (blue) mice were infected with 10^6 CFU *M. abscessus* MA07 by intranasal route and lungs and spleen were collected 6 hours, 1, 7, 14 or 42 days after infection to enumerate bacterial load and assess cell subsets by flow cytometry. Bacterial load following infection is shown in the lung **(A)** and spleen **(B)**. **(C)** Representative FACS plots and **(D)** Mean ± SEM Percentage of iNOS-producing cells in the lung following infection. **(E)** t-SNE representation of differences in cell subsets between infected WT (red) and tnf$^{-/-}$ (blue) mice at 14 dpi was generated using FlowJo software by clustering on phenotypic markers and subset identity was confirmed using the manual gating strategy outlined in Figure 2.2.**(F)** Proportions of interstitial macrophages in WT (red) and tnf$^{-/-}$ (blue) mice infected with *M. abscessus*. **(G)** Heat maps of geometric mean fluorescence intensity (MFI) expression of iNOS and MHCII for tnf$^{-/-}$ mice infected with *M. abscessus* MA07 at 14dpi, shown as fold change relative to WT mice. Mean values are representative of n=3-4 per group and represent two independent experiments. Significance of difference between groups for (A-D) was determined by two-way ANOVA (**P<0.01, ****P<0.0001).

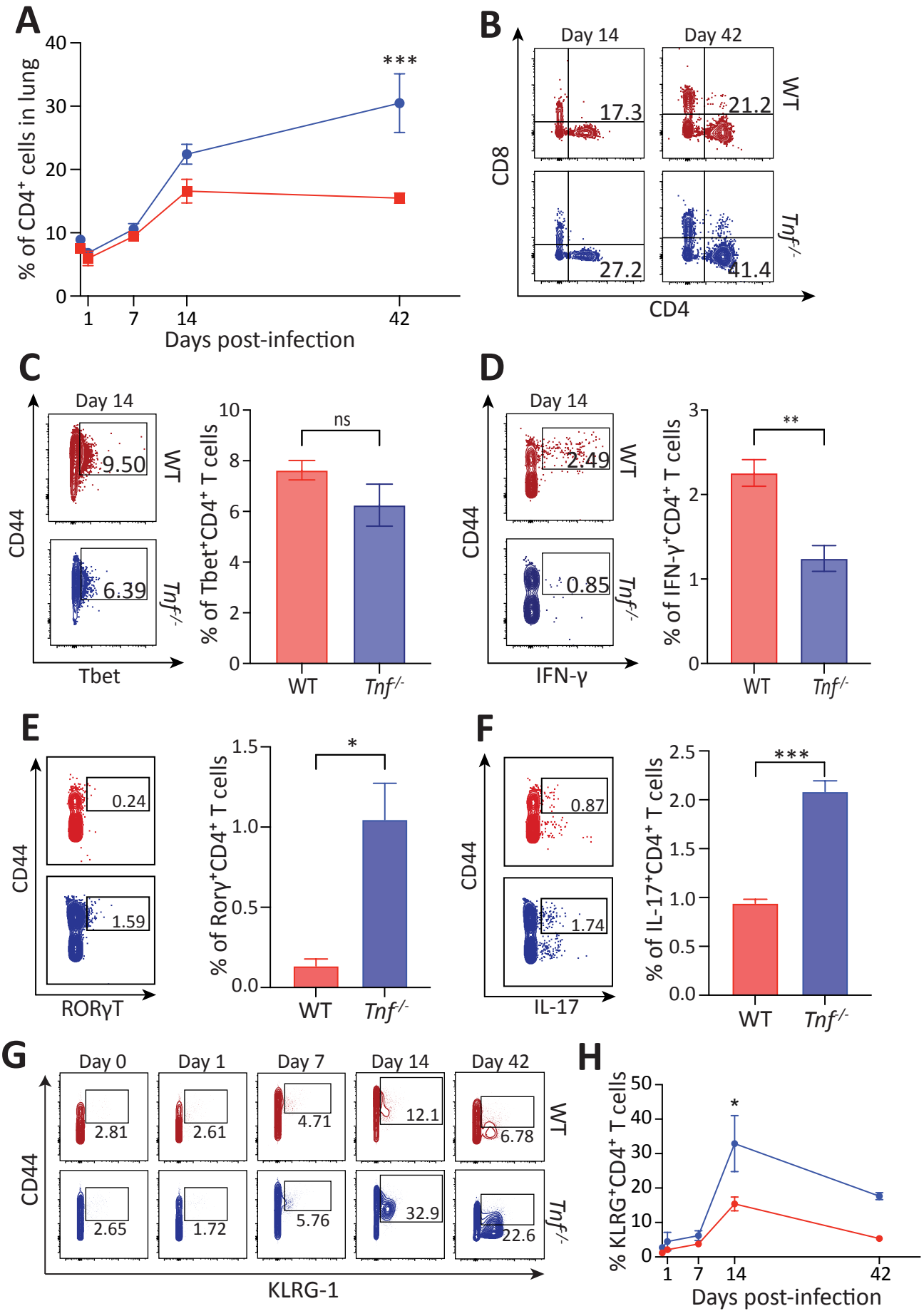
A
% of CD4+ cells in lung
***
Days post-infection
B
Day 14
Day 42
17.3
21.2
27.2
41.4
WT
Tnf-/-
CD8
CD4
C
Day 14
9.50
6.39
CD44
Tbet
% of Tbet+CD4+ T cells
ns
WT
Tnf-/-
D
Day 14
2.49
0.85
IFN-γ
% of IFN-γ+CD4+ T cells
**
E
0.24
1.59
RORγT
% of Rorγ+CD4+ T cells
*
F
0.87
1.74
IL-17
% of IL-17+CD4+ T cells
***
G
Day 0
Day 1
Day 7
Day 14
Day 42
2.81
2.61
4.71
12.1
6.78
2.65
1.72
5.76
32.9
22.6
KLRG-1
H
% KLRG+CD4+ T cells
Days post-infection

Figure 3.13. Role of TNF in adaptive immune response to intranasal *M. abscessus* challenge. C57BL/6 (red) or $tnf^{-/-}$ (blue) mice were infected with 10^6 CFU *M. abscessus* MA07 by intranasal route and lungs were collected 6 hours, 1, 7, 14 or 42 days after infection to assess T cell subsets by flow cytometry. **(A)** Percentage of $CD4^+$ T cells in the lungs of WT (red) or $tnf^{-/-}$ (blue) mice following *M. abscessus* infection. **(B)** Representative FACS plots of $CD4^+$ and $CD8^+$T cells lungs of WT (red) or $tnf^{-/-}$ mice 14 days following *M. abscessus* infection. **C-F** shows representative FACS plots and summary data of Tbet **(C)**, *M. abscessus*-specific IFN-γ **(D)**, RorγT **(E)**, and *M. abscessus*-specific IL-17 **(F)** expression in WT and $tnf^{-/-}$ mice 14 days following *M. abscessus* infection. **(G-H)** Representative FACS plots and summary data of KLRG-1 expression in the lungs of WT (red) or $tnf^{-/-}$ (blue) mice following *M. abscessus* infection. Mean values are representative of n=3-4 per group and represent two independent experiments. Significance of difference between groups was determined by one-way **(C-F)** or two-way **(B, H)** ANOVA (*P<0.05, **P<0.01, ***P<0.001).

Further, there was a noticeable reduction in Tbet expression between WT and *tnf*$^{-/-}$ groups, though this did not reach statistical significance (Figure 3.13C). Importantly, in the absence of TNF, IFN-γ production was significantly reduced at 14 days-post infection with *M. abscessus* (Figure 3.13D). Conversely, there was a compensatory increase in RORγT expression and IL-17 production by CD4$^+$ T cells in the absence of TNF (Figure 3.13E-F). Recent studies in our laboratory using *M. tuberculosis* vaccine design revealed that killer cell lectin-like receptor subfamily G member 1 (KLRG-1) expression correlates with T cell exhaustion and terminal differentiation. These cells also displayed a reduced capacity to protect against infection compared with KLRG-1-negative T cells (Reiley et al., 2010). Thus, KLRG-1 expression in CD4$^+$ T cells following *M. abscessus* infection was explored. A significantly higher proportion of CD4$^+$ T cells expressed KLRG-1 in the lungs of *M. abscessus*-infected mice when TNF was not present (Figure 3.13G-H). Taken together, these data suggest that during intranasal *M. abscessus* infection, TNF is required for the development of a 'Th1-like' immune response and may limit T cell exhaustion.

3.3. Discussion

M. abscessus has emerged in recent decades as a significant respiratory pathogen in susceptible individuals, such as CF patients and those with chronic obstructive pulmonary disease (COPD). However, despite the increasing concern in the medical community, little is known about the complex interplay between infection and the host immune response. This chapter therefore aimed to identify corelates of protection against *M. abscessus* infection, by identifying important immune cell subsets that could be used to develop host-directed immunotherapies and effective vaccine design.

The first aim of this chapter was to identify the ability of an *M. abscessus* clinical isolate to replicate and persist within the host, as well as generate a sufficient inflammatory response. Previous literature has described differences in the fate of S- and R-*M. abscessus* strains during infection due to the presence of glycopeptidolipids on the surface of bacilli (Daher et al., 2022; Roux et al., 2016). Results presented in this Chapter showed no noticeable pattern in the growth rates between S- and R-*M. abscessus* morphotypes in growth media; there was however a greater proportion of R variants that had high levels of phagocytosis and persistence in macrophages (Figure 3.1, 3.2). This suggests that these strains may have a greater propensity to disseminate and propagate in infected individuals (Bryant et al., 2016), or alternatively, that GPL are an immune evasive mechanism to prevent phagocytosis. Interestingly, previous studies have suggested that R morphotypes are unable to be phagocytosed due to their ability to replicate in large cords (Bernut et al., 2014). This is in contrast with our studies, which demonstrated that R morphotypes persisted to a greater magnitude in macrophages compared to S morphotypes. This difference may be due to the use of the *M. abscessus* ATCC 19977 type strain in the study of (Bernut et al., 2014), while this Chapter made use of a panel of strains of differing phenotypes, isolated directly from CF patients. The finding that R morphotypes elicited a greater cytokine response by macrophages (Figure 3.3) is in keeping with previous studies which identified that the high GPL content of S morphotypes can mask antigenic properties of the bacilli, and subsequently a reduction in macrophage activation (Roux et al., 2016). Similarly, the high levels of GM-CSF, TNF and IL-6 production by macrophages infected with R-*M. abscessus* strains (Figure 3.3) may suggest a propensity of these strains to induce inflammation in the lung to recruit components of the adaptive immune response. Production of these cytokines is also important to induce both adequate clearance of infection and memory cell formation to prevent subsequent infection (Chen, Li, et al., 2016).

While a number of studies have used infection models to characterise *M. abscessus* interaction with the host, most of these studies make use of the ATCC 19977 type strain, which may not fully recapture the infection observed with clinical isolates (Nicola et al., 2022). In this Chapter it was observed that *M. abscessus* MA07 strain persisted in mice up to 21 days after intranasal infection, with some dissemination of bacteria to the spleen (Figure 3.4). This is in contrast to a previous study in which C57BL/6 mice were inoculated with the ATCC 19977 strain via intratracheal route with *M. abscessus* fibrin plugs, which showed clearance by 14 days post-infection, with very minimal dissemination to the spleen (Caverly et al., 2015). Instead, the kinetics of infection in the present study are more in keeping with those in which a high dose aerosol (1000 CFU per mouse) model was used. Ordway and colleagues demonstrated that with this route, *M. abscessus* ATCC 19977 persists between days 0 and 15 and is subsequently cleared before day 30 of infection, with significant dissemination to the spleen (Ordway et al., 2008). Low-dose aerosol (100 CFU per mouse), on other hand, did not produce any recoverable CFU from lung or spleen at any time following infection. Thus, it appears that strain MA07 may persist in mouse lungs to a greater extent than the widely used ATCC19977; direct comparison between clinical isolates and the reference study would delineate this. We also investigated the use of CH3eB/FeJ – or “Kramnik” – mice as previous literature has suggested that *M. abscessus* persists up to 40 days following i.v. infection (Obregón-Henao et al., 2015). However, this was not replicated when administered via i.n. delivery in our study (Figure 3.5), suggesting that differences in persistence is dependent upon strain type in mice. Further, no observable difference in infection kinetics was observed after infection with different clinical isolates (Figure 3.4). This includes S (MA14) and R (MA07, MA11, and MA15) isolates, for which differences in infection dynamics have been previously reported in the literature (Bernut et al., 2014; Jönsson et al., 2013), as well as the worse clinical outcome for individuals infected with R strains (Hedin et al., 2023). This may be confounded by their differing origins, as each strain examined has been identified to originate from a different clade (Table 2.2). Bryant et al. (2016) demonstrated that different clades of *M. abscessus* possess varying degrees of virulence and can be correlated with worse clinical outcomes. Although we were unable to obtain S and R morphotypes of the same clinical isolates used in this study, it would be of interest to examine the infection kinetics of these strains in future, and where possible correlate this with clinical data.

The innate immune response to infection is crucial in early control of disease, as well as engaging the adaptive immune response for long term protection. Following infection of mice

with the *M. abscessus* type strain, there was significant neutrophil infiltration of the bronchoalveolar lavage fluid (BALF) at 3 and 14 days post-infection (Caverly et al., 2015). Further, neutrophils have been shown to be crucial in granuloma formation in the zebrafish model (Bernut et al., 2016). However, in this current study, while we observed an initial spike in neutrophil influx to the lung, proportions rapidly dropped over the course of infection (Figure 3.8). This was further supported by the initial peak and rapid reduction in CXCL1 and G-CSF (Figure 3.11), mediators important in the recruitment and function of neutrophils, in the lung immediately after infection (Drummond et al., 2019; Ramakrishna & Cantin, 2018). This may be explained by the finding that R-*M. abscessus* morphotypes, such as the MA07 isolate used here, are resistant to intracellular killing by neutrophils, and are able to inhibit neutrophil activation (Malcolm et al., 2013). Indeed, Malcom et al. (2013) reported that R *M. abscessus* infection of neutrophils can induce apoptosis, potentially explaining the relatively limited neutrophil response observed here compared to previous reports.

DCs are well known to be important antigen presenting cells (APCs) and are required to stimulate the adaptive immune system. When DCs are stimulated with *M. abscessus* antigens, the TLR4-MAPK signalling system drives DC maturation and strongly promotes a Th1 phenotype (Lee et al., 2014). In this study, we identified a biphasic infiltration of DCs; $CD11b^+$ DCs were present early during infection, and $CD103^+$ DCs were evident at later timepoints (Figure 3.7). In *M. tuberculosis* infection, $CD11b^+$ DCs have been shown to be important in controlling early infection by homing to the mediastinal lymph nodes (mLN) for $CD4^+$ T cell activation (Wolf et al., 2007). It is possible that the early $CD11b^+$ response in the current study reflects this early activation of $CD11b^+$ DCs for mediastinal lymph node (mLN) homing. On the other hand, $CD103^+$ DCs have been shown to be crucial in controlling bacterial infection. In an intranasal adoptive transfer experiment, transfer of $CD103^+$ DCs into the lung following *Chlamydia muridarum* infection induced a Th1 skewed phenotype (Shekhar et al., 2018). Indeed, $CD103^+$ DC transfer resulted in better control of infection compared to $CD11b^+$ DC transfer. In this chapter, the rise in $CD103^+$ DCs correlated with the peak of $CD4^+$ T cell recruitment to the lung. Thus, it could be postulated that following *M. abscessus* infection, high proportions of $CD103^+$ DCs are important for stimulating strong $CD4^+$ T cell responses and enhancing protective immunity. The DC stimulation of Th1 phenotype is known to be mediated by IL-12p40 (Khader et al., 2006; Lee et al., 2014); although we could not detect IL-12p40 levels in the lung following *M. abscessus* infection, defining the interplay between DCs and $CD4^+$ T cells during *M. abscessus* infection is an important area of future study.

It is well-known that macrophages are the principal cell subset involved in the control of mycobacterial infection, playing a key role in phagosome destruction of bacteria, adaptive cell recruitment, and can even serve as a niche in which mycobacteria can propagate (Awuh & Flo, 2017). In this chapter, IMs were the predominant subset identified in the lung following infection with *M. abscessus*. Historically, AMs have been deemed as the primary responders to mycobacterial infection; these cells reside in the alveolar air space and are largely anti-inflammatory in the steady state, responding to the constant exposure to airway pathogens (Guilliams et al., 2013). During active infection, AMs can upregulate their phagocytic capacity and self-renew (Ardain et al., 2020). AMs are highly permissible to *M. tuberculosis* infection, providing a nutrient-dense niche in which infection can propagate (Huang et al., 2018). Interestingly, AMs have been shown to be defective in diseases of chronic pulmonary inflammation – such as CF and COPD – and thus are unable to respond to infection (Allard et al., 2018). IMs, on the other hand, reside on the bronchial side of the alveoli and demonstrate high expression of monocyte lineage markers and are thought to be replenished from blood monocytes (Schyns et al., 2019). Similar to our findings that IMs were recruited during *M. abscessus* infection in mice, this is also true for *M. tuberculosis* (Srivastava et al., 2014). IMs are able to restrict bacterial growth, and in their absence, pulmonary bacterial burden dramatically rises (Huang et al., 2018). IMs have been shown to express high levels of MHCII (Schyns et al., 2019) and *in vitro* coculture experiments have demonstrated they have higher antigen presentation capacity than AMs, and (Chakarov et al., 2019). IMs also express high levels of IL-10 which dampens the immune response and prevents excessive immunopathology (Kawano et al., 2016). In this study, we observed IL-10 expression in the lungs at day 7 post infection (Figure 3.11). It is possible that the enhanced IL-10 expression could be a result of IMs accumulating in the lung. Defining the cell subset expression of IL-10 expression should be possible area of future investigation. While outside the scope of this study, defining the role of IMs in *M. abscessus* by selective cell subset depletion (Huang et al., 2018) would be useful in defining the true role of these cells in bacterial control.

This chapter demonstrates the highly novel finding that IMs are responsible for the majority of iNOS production after *M. abscessus* infection, which plays a role in bacterial clearance (Figure 3.9). iNOS expression allows for the production of NO, a potent antimicrobial molecule that is crucial for controlling infection (Ahn et al., 2021; Strijdom et al., 2009). In addition to possessing antimicrobial activity, NO is able to act as a secondary messenger, influencing expression of cytokines and chemokines to limit inflammation in the lung

following infection (Braverman & Stanley, 2017; Mishra et al., 2013). Previous studies have identified that iNOS expression is regulated by TNF and IFN-γ (Strijdom et al., 2009). Indeed, we confirmed in a *M. abscessus* infection model that iNOS production is abolished in the absence of TNF (Figure 3.12). Notably, the downregulation of iNOS expression was uniquely confined to the IM population, suggesting that TNF is crucial for the maintenance of this cell subset. There was also a lack of IM recruitment in TNF-deficient mice, significantly higher bacterial burden, and greater dissemination of infection to the spleen (Figure 3.12). This is concurrent with observations that patients on anti-TNF therapy have an increased susceptibility to NTM infections (Brode et al., 2015). Early during infection, TLR-4 stimulation by PAMPs results in NFκB signalling to produce TNF along with other cytokines (Wesemann & Benveniste, 2003). Among other functions, such as inducing antimicrobial mechanisms described above, TNF is a master regulator of cytokine and chemokine expression. TNF depletion results in reduced expression of CXCL9 and CXCL10, which are involved in macrophage chemoattraction (Algood et al., 2004). Further, TNF is also able to increase the proliferation and differentiation of macrophages (Guilbert et al., 1993; Witsell & Schook, 1992). The data presented in this Chapter shows that the recruitment, proliferation and differentiation in IMs is mediated by TNF in response to *M. abscessus* infection, corelating with previous literature. The observed increase in bacterial dissemination in TNF-deficient mice may be attributed to the role of TNF in granuloma formation, considering the known role that TNF plays in the formation of granulomas to prevent and restrict *M. abscessus* spreading within the host (Bernut et al., 2016; Jeon et al., 2009). However, it is important to note that bacterial clearance in the lungs began prior to the peak of iNOS expression following infection, and further investigation of other methods of bacterial clearance in *M. abscessus* infection will be important in further characterising the immune response to infection.

Following intranasal infection with *M. abscessus*, $CD4^+$ T cells were the predominant adaptive immune cell population recruited to the lungs, reaching maximal response 14 days after infection. The majority of $CD4^+$ T cells identified in the lung were of Th1 phenotype, characterised by expression of its master transcription factor Tbet (Johnson et al., 2018), and production of TNF and IFN-γ (Johansen et al., 2020). IFN-γ and TNF are crucial effector molecules produced by Th1 cells at the site of infection. $CD4^+$ T cells expressing IFN-γ, IL-2 and TNF are considered key correlates of protection against mycobacterial infection (Counoupas et al., 2017; Lindenstrøm et al., 2014). IFN-γ and TNF function synergistically

to activate macrophages and induce iNOS expression, enhancing bacterial control (Flynn & Chan, 2001). Further, Th1 cells have been implicated in the containment of mycobacterial infection to the lung by contributing to granuloma formation (Johansen et al., 2020). Clinically, patients with functionally impaired T cells infected with *M. abscessus* have worse clinical outcomes, which highlights the importance of Th1 cells in adequately controlling *M. abscessus* infection (Shu, Pan, et al., 2019). The critical role of Th1 cells was also evident in TNF-deficient mice. In the absence of TNF, infected mice had significantly higher *M. abscessus* burden, while $CD4^+$ T cells were elevated yet displayed lower Tbet expression and IFN-γ production (Figure 3.13). Indeed, infection of TNF-deficient mice with BCG results in low levels of IFN-γ production, which is restored when mice are infected with a recombinant BCG expressing TNF (Kaufmann et al., 2000). As discussed previously, TNF is required for the recruitment of macrophages to the infected tissue, and for the induction of iNOS expression and subsequent NO production for early infection control (Bekker et al., 2001; Kaufmann et al., 2000). It is possible that this high bacterial burden results in a TNF-independent inflammatory cascade in the lungs, which drives an influx of more $CD4^+$ T cells into the lungs in the absence of TNF. For example, in the absence of TNF receptor signalling, mice infected with *M. avium* demonstrate a hyperinflammatory response, with higher levels of IL-12 and IFN-γ (Kaufmann et al., 1999). Further, TNF depletion resulted in T-helper cell skewing to a Th17 phenotype (Figure 3.12). We observed a compensatory increase in RORγT expression and IL-17 production by $CD4^+$ T cells in the lung following *M.* abscessus in TNF-deficient animals. Thus, TNF is required for the recruitment of Th1 effector cells to the site of *M. abscessus* infection to adequately control infection and in its absence, $CD4^+$ T cells are functionally impaired. It is important to note however, that interpretations may be skewed by the effects of higher bacterial burdens which are difficult to uncouple, as antigenic load is thought to be a major contributor to T cell priming (Moguche et al., 2017).

In this chapter, an intranasal model of infection using *M. abscessus* clinical isolates was established. To our knowledge, these studies are the first to define in detail the pulmonary cell subsets responding to *M. abscessus* infection. My findings identified IMs as a crucial immune cell subset for controlling *M. abscessus* infection due to their potent iNOS production and role in mediating Th1 responses and bacterial clearance from the lung. TNF is required for the control of *M. abscessus* infection, by its stimulation of iNOS production, as well as recruitment of IMs. Further, TNF is required for the differentiation of functional Th1 cells to the lung following *M. abscessus* infection. Thus, this study highlights the complex interplay between TNF, IMs and iNOS and how they work together to mediate both

early innate responses as well as how they function to induce adaptive immunity. These findings are significant to aid future vaccine development, as they propose correlates of protection against *M. abscessus* infection. This is a major aim of the subsequent chapters in this thesis.

Chapter 4: Protective efficacy of BCG vaccination against pulmonary *M. abscessus* infection

This Chapter in part forms a manuscript submitted for publication to the Journal of Cystic Fibrosis:

Sherridan Warner, Anneliese Blaxland, Claudio Counoupas, Janine Verstraete, Mark Zampoli, Ben Marais, Dominic A. Fitzgerald, Paul D. Robinson, James A Triccas. (2023). Clinical and experimental determination of protection afforded by BCG vaccination against infection with non-tuberculous mycobacteria. (Submitted manuscript).

Author contributions: The majority of the total work presented here was undertaken by Sherridan Warner, including all animal experiments, data analysis, figure construction and writing. Epidemiological data was curated and analysed by Annelise Blaxland, Janine Verstraete, and Mark Zampoli. All authors have kindly approved inclusion of this data in this thesis. Other authors listed were involved in conceptualisation of the project, as well as review and editing of the manuscript.

I have obtained permission to include the published material from the corresponding author James A Triccas.

Signed:……

Sherridan Warner

As supervisor for the candidature upon which this thesis is based, I can confirm that the authorship attributions stated above are correct.

Signed:……

James A Triccas

4.1. Introduction

Mycobacterium abscessus is a respiratory pathogen of increasing concern, particularly in patients with underlying lung pathology such as Cystic Fibrosis (CF) and Chronic Obstructive Pulmonary Disease (COPD) (Martiniano et al., 2019). Currently, it is estimated that 20% of CF patients infected with non-tuberculous mycobacteria (NTM) are infected with *M. abscessus,* an incidence that is estimated to increase further over time (Martiniano et al., 2019). In these patients, *M. abscessus* in many cases causes a progressive decline in lung function and subsequently reduced quality of life (Griffith et al., 2007). In some more serious cases, it can even be fatal due to acute respiratory failure (Lee et al., 2015) with a 15-year cumulative mortality rate of 51% (Jhun et al., 2020).

The poor morbidity and mortality associated with *M. abscessus* infection, is in part driven by the limited treatments available and poor response to these treatments. Due to its extensive drug resistance profile, patients infected with *M. abscessus* are recommended to undergo up to eighteen months of treatment with a cocktail of multiple antibiotics (Degiacomi et al., 2019). Often, these treatment regimens result in significant adverse effects and toxicity (Choi et al., 2018). Further, these prolonged treatments are costly to both the individual and the health care system (Mirsaeidi et al., 2015). Given the difficulty in treating *M. abscessus* infection, prophylactic strategies to prevent infection are critical. Development of a vaccine to prevent *M. abscessus* infection is one such strategy that could significantly improve the quality of life of many CF patients as well as lower health care burden and cost.

Mycobacterium bovis Bacillus Calmette Guérin (BCG) is currently the only approved vaccine to prevent tuberculosis (TB) which, until the arrival of SARS-CoV-2, was responsible for the greatest annual number of deaths caused by a single infectious agent worldwide (WHO, 2021). As an attenuated strain of *M. bovis*, it has been safely used in humans since 1921 (Calmette & Plotz, 1929), is relatively cheap to manufacture and is globally available (Kilpeläinen et al., 2018). BCG vaccination induces potent neutrophil, macrophage and dendritic cell (DC) responses, which in turn elicit a strong Th1 response, evident by the production of high levels of IFN-γ by $CD4^+$ T cells in vaccinated individuals (Moliva et al., 2017). Whilst highly protective against disseminated and meningitis TB, its efficacy against pulmonary TB wanes over time and ranges from 0-80% in clinical trials. This may reflect a number a factors including BCG strain, population genetics and impact of previous exposure to environmental mycobacteria (Colditz et al., 1995). BCG is known to be cross protective

against other NTM infections: it is currently recommended to prevent transmission of *M. leprae*, the causative agent of leprosy (Schoenmakers et al., 2020). Epidemiological data suggests that protection against, or delayed onset of Buruli ulcer caused by *M. ulcerans* (Pittet et al., 2021), while BCG vaccination is associated with reduced rates of *M. avium* infection in some countries (Švandová, 1994). The possible cross-protective effects of BCG have been explored against *M. abscessus* in an *ex vivo* model using BCG-vaccinated patient peripheral mononuclear blood cells (PBMCs), which showed that BCG-specific T cells inhibited growth of *M. abscessus*, as well as inducing strong $IFN\gamma^{+}CD4^{+}$ T cell responses when stimulated with *M. abscessus ex vivo* (Abate et al., 2019). While this suggests cross-reactivity between BCG and *M. abscessus*, whether and how this translates to protection against *M. abscessus* infection has not been evaluated in either humans or preclinical models.

In addition to its efficacy against NTM, BCG is widely known to have unique cross-protective properties against other unrelated pathogens through its ability to induce trained immunity. Through epigenetic programming BCG vaccination drives monocytes, macrophages and NK cells to a more “vigilant” state where they possess non-specific protection against other infections (Covián et al., 2019). These cells have a higher capacity to produce pro-inflammatory cytokines, and PRRs are more responsive to PAMPs allowing for earlier detection and response to pathogens (Netea et al., 2011). This is evident in studies that have observed that BCG vaccination in some countries correlates with reduced childhood all-cause mortality, as well as against specific infections, which are reviewed here (Covián et al., 2019).

This study aimed to assess the protective efficacy of BCG vaccination against pulmonary *M. abscessus* infection by (i), using an animal model of pulmonary *M. abscessus* infection to describe the effect of BCG vaccination on infection characteristics and immunological pathways, in comparison to naturally acquired immunity, and (ii) examining observational data regarding NTM and *M. abscessus* infection rates in two tertiary CF clinics with and without routine BCG vaccination.

4.2 Results

4.2.1 *M. abscessus*-specific cytokine responses in murine PBMCs after BCG vaccination

The previous chapter identified Th1 cells to be crucial in the control of pulmonary *M. abscessus* infection. The first series of experiments in this chapter sought to determine if BCG was capable of inducing cross-reactive immunity against *M. abscessus* in the murine model. *In silico* analysis revealed BCG Pasteur shares approximately 60% genetic homology with the reference strain of *M. abscessus*, indicating the likelihood of shared antigenic components (Figure 4.1). This suggests a possible mechanism of BCG-induced protection using a murine model of *M. abscessus* infection.

To examine immunity, mice initially were either vaccinated subcutaneously (s.c.) with BCG or infected via the intranasal (i.n.) route with *M. abscessus* (MA07) (as a control for natural immunity acquired from prior exposure, hereafter referred to as convalescent) and the frequency of *M. abscessus*-specific T cells examined ten weeks after vaccination in the PBMCs of mice restimulated with 10^5 CFU *M. abscessus* MA07. BCG-vaccinated mice displayed significantly higher proportions of $CD4^+$ T cells secreting IFN-γ compared to naïve mice (Figure 4.2A). BCG vaccination also induced noticeably more IL-2^+ and TNF^+ circulating $CD4^+$ T cells, though this did not reach significance. When Boolean gating was performed to assess the presence of polyfunctional $CD4^+$ T cells, BCG-vaccinated mice demonstrated significantly higher levels of triple-positive (IFN-γ^+IL-2^+TNF^+), and double positive (IFN-γ^+IL-2^+; IL-2^+TNF^+) $CD4^+$ T cells. Convalescent mice also had notably increased proportions of IFNγ^+IL-2^+TNF^+ triple-positive $CD4^+$ T cells in the blood, though this did not reach significance (Figure 4.2B). Thus, BCG vaccination results in significant levels of circulating *M. abscessus*-specific polyfunctional $CD4^+$ T cells in mice.

4.2.2 Protection conferred by BCG vaccination against intranasal *M. abscessus* infection

To determine the impact of BCG-induced immunity on protective efficacy, vaccinated mice were challenged i.n. with MA07. Prior infection with *M. abscessus* resulted in significant reduction in bacterial load against subsequent *M. abscessus* infection in the lung (Figure 4.3A) and spleen (Figure 4.3B) compared to unvaccinated mice (~1 $\log_{10}$ CFU protection in lung, ~2 $\log_{10}$ CFU in spleen), indicating that protective immunity to *M. abscessus* can be

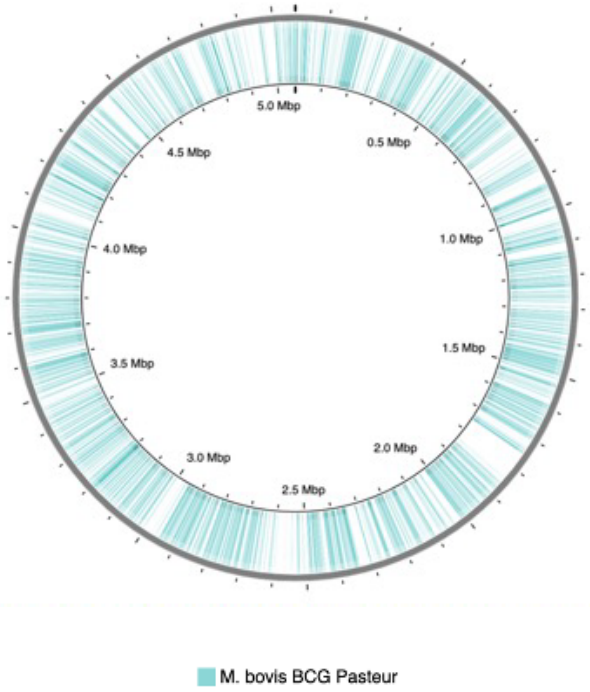

Figure 4.1. Gene homology between *M. abscessus* and M. bovis BCG Pasteur strain. Blast shows the sequence homology between *M. abscessus* ATCC 19977 (outer grey line) and *M. bovis* BCG Pasteur strain (turquoise). Genetic sequences were obtained from the National Centre for Biotechnology Information Nucleotide Database and homology assessed using its Basic Local Alignment Search Tool (BLAST) .

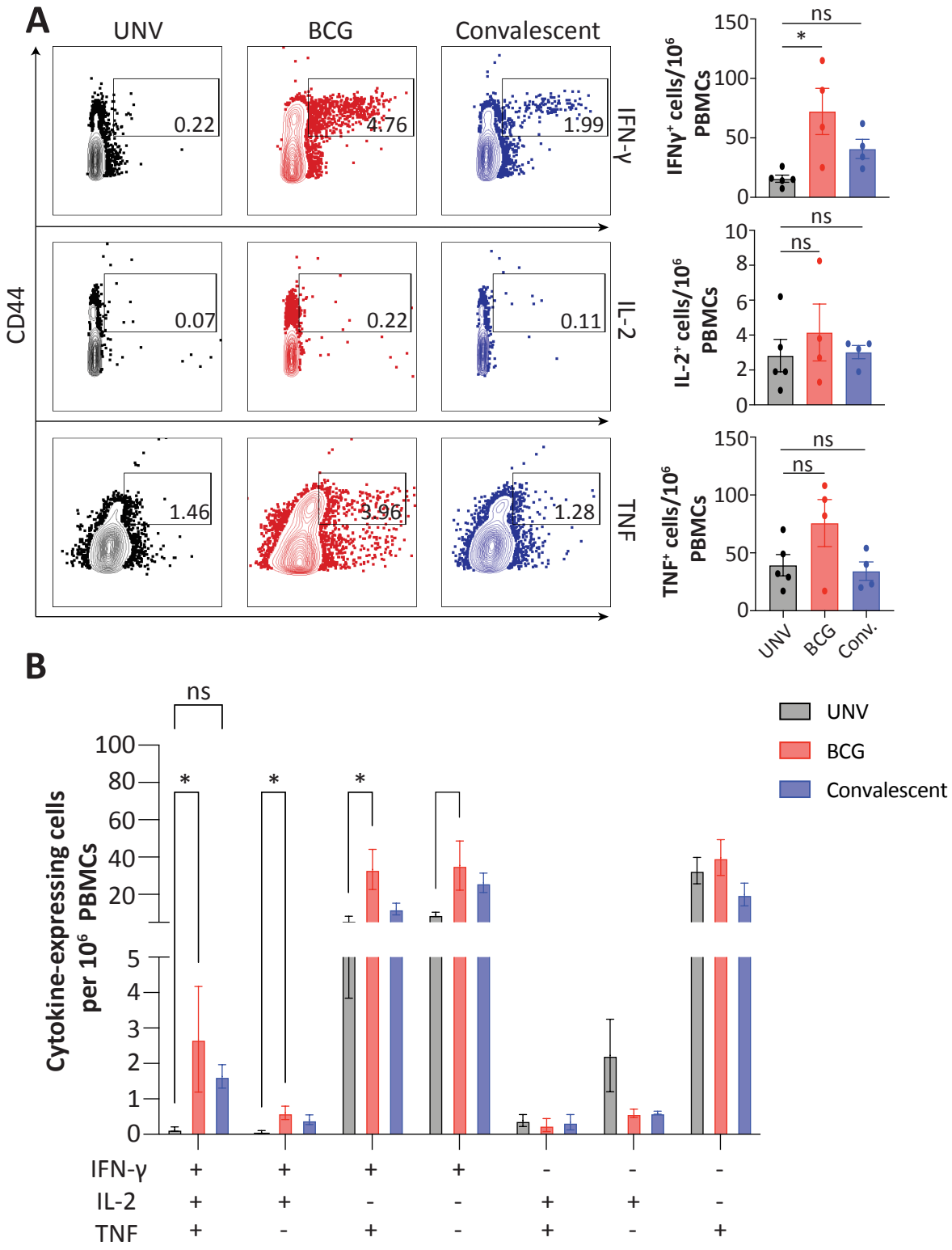

Figure 4.2. *M. abscessis*-specific cytokine production by circulating CD4⁺ T cells following BCG vaccination. C57BL/6 mice (n=4-6) were vaccinated s.c. with 10^6 CFU BCG, infected i.n. with 10^6 CFU *M. abscessus* MA07 or left untreated. Ten weeks after vaccination, PBMCs were isolated by tail vein bleed and restimulated *ex vivo* with $5x10^5$ CFU/mL *M. abscessus*. IFN-γ, IL-2 or TNF was assessed using flow cytometry. **(A)** Representative FACS plots of cytokine-expressing CD4⁺ T cells in the blood and corresponding summary graphs of cytokine expressing cells per 10^6 PBMCs. **(B)** Proportion of CD4⁺ T cells expressing single, double or triple positive combinations of cytokines was determined using Boolean gating. Data is representative of two independent experiments and is shown as mean ± SEM for n=4-6. Differences between BCG-vaccinated and previously-infected groups compared to unvaccinated controls was determined by two-way ANOVA (*p<0.05, **p<0.01).

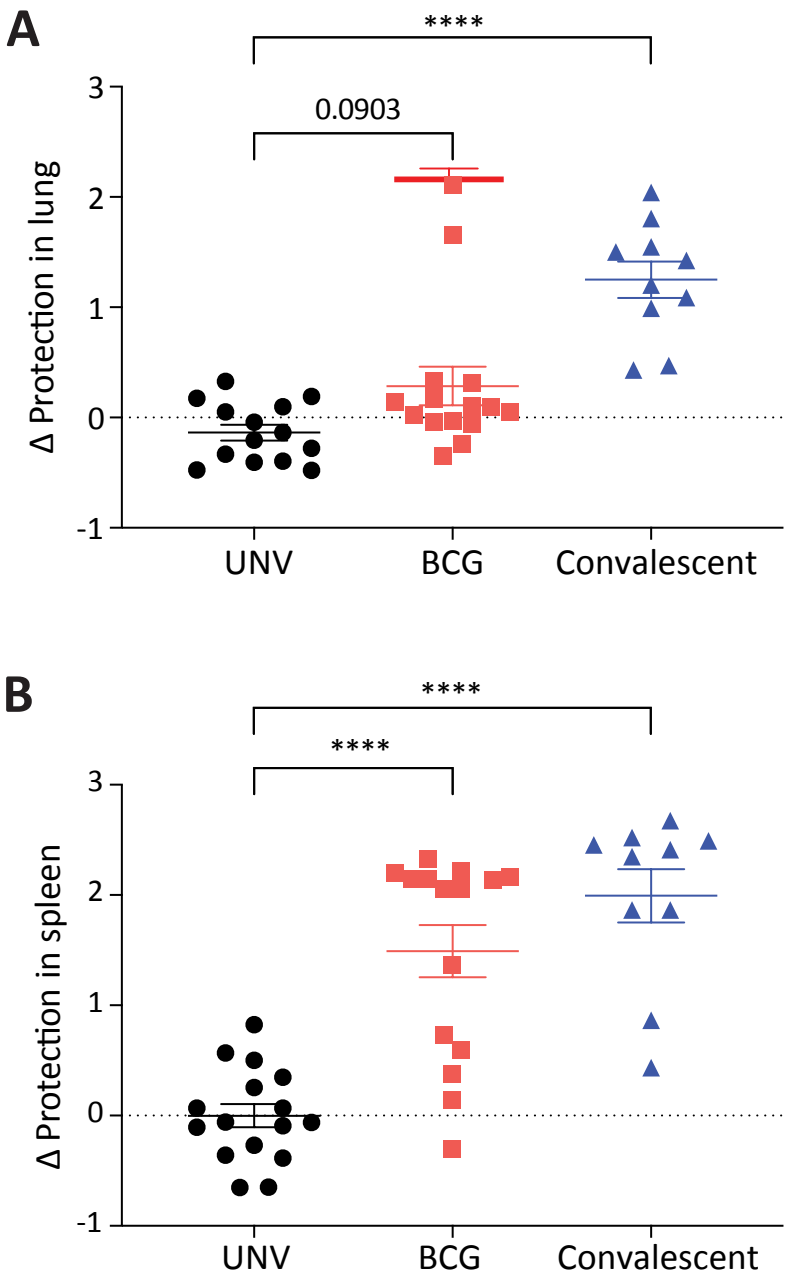

Figure 4.3. Meta-analysis of the degree of protection conferred by BCG against *M. abscessus*. C57BL/6 mice were vaccinated s.c. once with 10^6 CFU BCG, infected i.n. with 10^6 CFU M. abscessus or left unvaccinated. Twelve weeks after vaccination, mice were challenged intranasally with 10^6 CFU *M. abscessus*. Seven days post-infection, bacterial load in the **(A)** lungs and **(B)** spleen was enumerated. Data was pooled from two independent experiments and is represented as Log_{10} difference in CFU for individual mice compared to unvaccinated mice. Statistical significance was evaluated by one-way ANOVA (****p<0.0001).

achieved in this model. While there was some protection afforded by BCG vaccination in the lung (Mean 0.33 $\log_{10}$ CFU), this did not reach statistical significance, possibly due to wide variation between mice (p=.09; Range -0.30-2.32). However, BCG vaccination resulted in significant protection against *M. abscessus* in the spleen, with a reduction of ~1.5 $\log_{10}$ CFU compared to unvaccinated mice (Figure 4.3B). Thus, BCG could impart some level of protective immunity against *M. abscessus* in a murine model, which was most apparent in limiting dissemination of infection.

4.2.3 Analysis of innate and adaptive cellular response after BCG vaccination and *M. abscessus* challenge.

To determine if the recruitment, expansion and activation of immune cells subsets correlated with the protection observed in section 4.2.1, both the innate and adaptive cellular response was examined in vaccinated and *M. abscessus* challenged mice. Myeloid populations were assessed using the gating strategy outlined in Figure 2.2. When comparing the myeloid response to *M. abscessus* following vaccination, there were no significant differences between innate immune cell populations between BCG-vaccinated and naïve mice (Figure 4.4A). On the other hand, convalescent mice displayed an increase in IMs in the lung following re-infection when compared to naïve mice (Figure 4.4A). This population was not evident in BCG-vaccinated mice. Further, the accumulation of IMs in re-infected mice correlated with a significant increase in production of iNOS in the lungs, which was absent in BCG-vaccinated or naïve groups (Figure 4.4B&C). The correlation between reduced bacterial load, IM accumulation and iNOS production in convalescent mice indicates a protective role for these cells. The failure of s.c.-administered BCG vaccination to induce this immune profile may provide one explanation for its limited protective efficacy against *M. abscessus* challenge.

Analysis of $CD4^+$ T cells in the lung revealed that overall numbers following *M. abscessus* challenge did not differ between BCG-vaccinated mice compared to convalescent mice (Figure 4.5A-C). However, there were enhanced $CD4^+$ T cell numbers in re-infected mice compared to BCG-vaccinated or unvaccinated animals in the lung (Figure 4.5B). There were no significant differences in $CD8^+$ T cell numbers in either BCG-vaccinated or re-infected mice compared to naïve controls. Interestingly, there were higher levels of B cells in the lungs of BCG-vaccinated mice, which was not observed in mice previously infected with *M. abscessus* (Figure 4.5B).

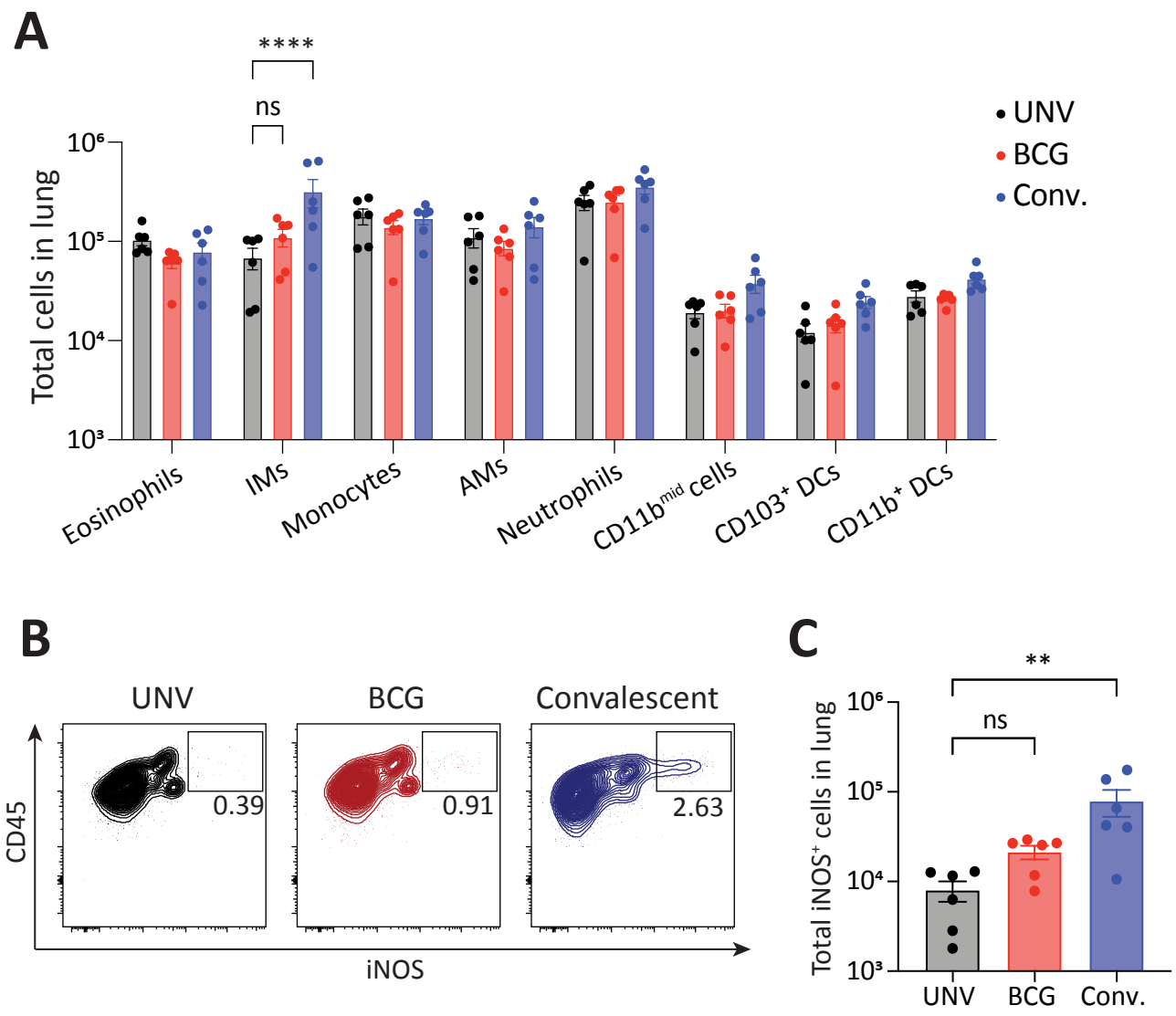

Figure 4.4. Myeloid cell recruitment and iNOS production in the lung following *M. abscessus* challenge in BCG-vaccinated mice. C57BL/6 mice were vaccinated once with 10^6 CFU BCG s.c., infected with 10^6 CFU *M. abscessus* i.n. or left unvaccinated. Twelve weeks after vaccination, mice were challenged intranasally with 10^6 CFU *M. abscessus*. Seven days post-infection, cells were isolated from the lung and analysed using flow cytometry according to the gating strategy outlined in Figure 2.2. **(A)** Total numbers of myeloid cell populations in the lung 7dpi. **(B)** Representative FACS plots of iNOS expression in CD45$^+$ cells in the lung 7dpi. **(C)** Mean ± SEM of iNOS$^+$ CD45$^+$ cells in the lung 7dpi. Data is representative of two independent experiments (n=4-6). Statistical significance was determined using two-way **(A)** or one-way **(C)** ANOVA (**p<0.01, ****p<0.0001).

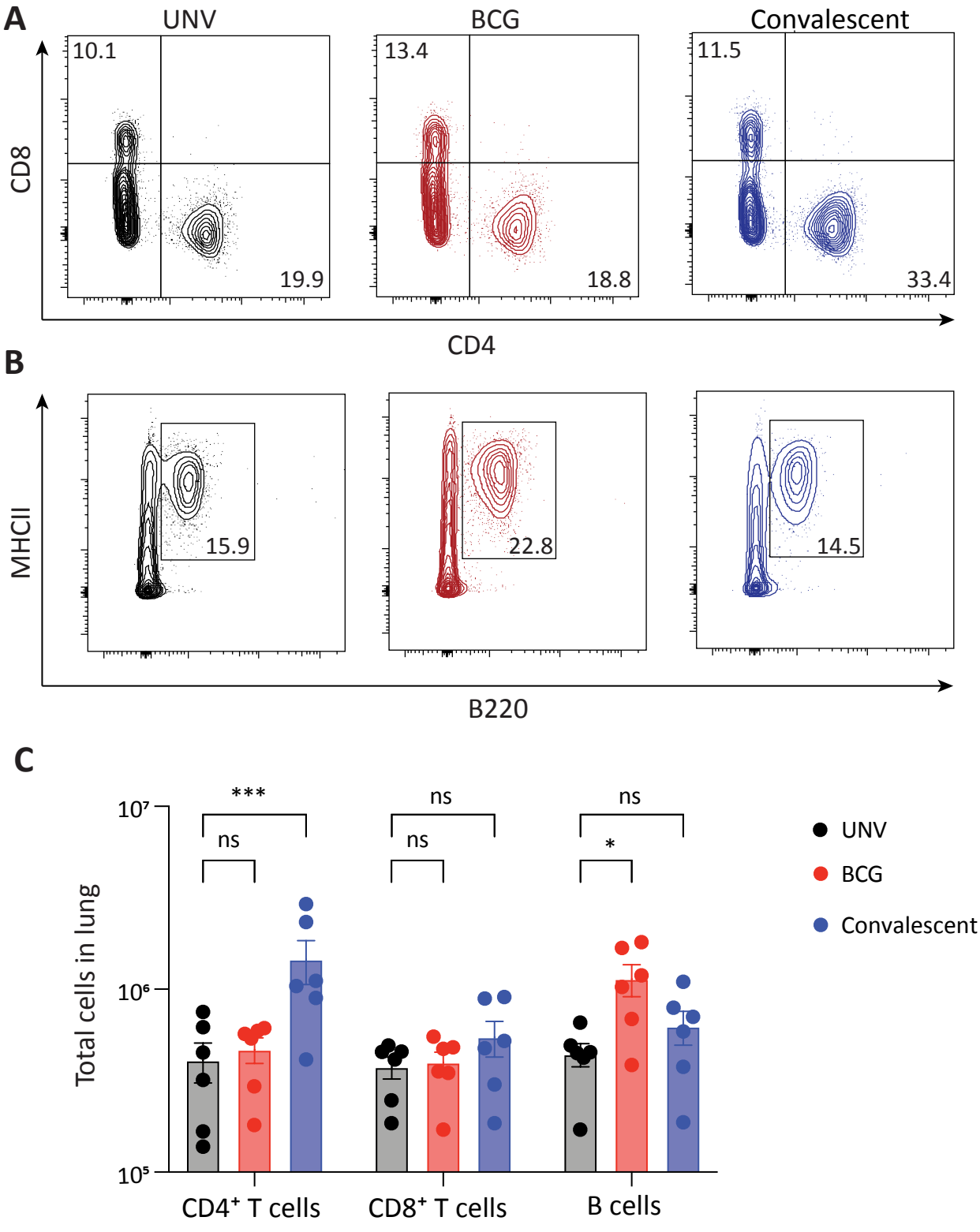

Figure 4.5. Adaptive immune cell distribution in the lungs of BCG-vaccinated mice challenged with *M. abscessus*. C57BL/6 mice were vaccinated and challenged as described in Figure 4.4. Seven days post-infection, mice cells were isolated from the lung and analysed using flow cytometry following the gating strategy outlined in Figure 2.3. **(A)** Representative FACS plots of the proportion of $CD4^+$ and $CD8^+$ T cells in the lung 7dpi. **(B)** Representative FACS plots of proportion of B cells in the lungs 7dpi. **(C)** Mean ± SEM total $CD4^+$, $CD8^+$ and B cells in the lung following vaccination. Data is representative of two independent experiments (n=4-6) and statistical differences were evaluated using two-way ANOVA (*p<0.05, ***<0.001).

When the expression of master regulators of T cell differentiation of $CD4^+$ T cells in the lung following *M. abscessus* challenge were assessed, both vaccinated groups showed enhanced T-bet expression (Figure 4.6A, 4.6B). There was no significant difference in RorγT expression between groups (Figure 4.6A, 4.6C), nor was there any significant IL-17 production (data not shown). When Th1 effector cytokine production was examined, there was increased IFN-γ, IL-2 and TNF production in $CD4^+$ T cells of convalescent re-infected mice (Figure 4D-4H). In contrast, $CD4^+$ T cells from BCG-vaccinated mice elicited intermediate levels of IFN-γ, IL-2 and TNF, which did not differ significantly to the levels observed in unvaccinated mice. Thus, BCG vaccination in this model induced Th1-like responses within the lung of immunised animals, however the response was noticeably smaller in magnitude compared with mice previously exposed to *M. abscessus*. Convalescent mice also displayed significantly increased proportions of IFN-γ^+TNF$^+$ double positive $CD4^+$ T cells in the lung.

The presence of memory-like $CD4^+$ T cells in the lungs of vaccinated mice was also assessed. Effector memory cells ($CD44^{hi}$ $CD62L^{lo}$) circulate in the peripheral tissues, whereas central memory cells ($CD44^{hi}$ $CD62L^{hi}$) home to lymphoid organs (Mousset et al., 2019). Following *M. abscessus* challenge, both BCG-vaccinated and previously infected groups showed higher levels of effector memory-like $CD4^+$ T cells in the lungs (Figure 4.7A, 4.7B). Central memory-like (CM) populations were not detected in appreciable numbers in any of the groups at the examined timepoint. Thus, these data suggest that BCG-vaccination and previous *M. abscessus* exposure induces substantial effector memory-like populations in the lung.

4.2.4 Comparison of *M. abscessus* infection across two CF clinics

Given the findings that BCG offers some protection against disseminated *M. abscessus*, and invokes some cross-reactive immune responses, we next sought to determine whether this effect correlated with epidemiological data. The medical records of all patients attending CF clinics at the Children's Hospital Westmead (CHW, Sydney, Australia) where BCG vaccination is not routine, and Red Cross War Memorial Children's Hospital (RCWMCH, Cape Town, South Africa), where children are routinely BCG-vaccinated, were examined. In total, 91 and 231 children attended across a three year period at RCWMCH and CHW, respectively. Characteristics of those children attending both clinics are summarised in Table 4.1. Comparing the cohorts, CHW children were taller (0.06 vs -0.57 peak height z

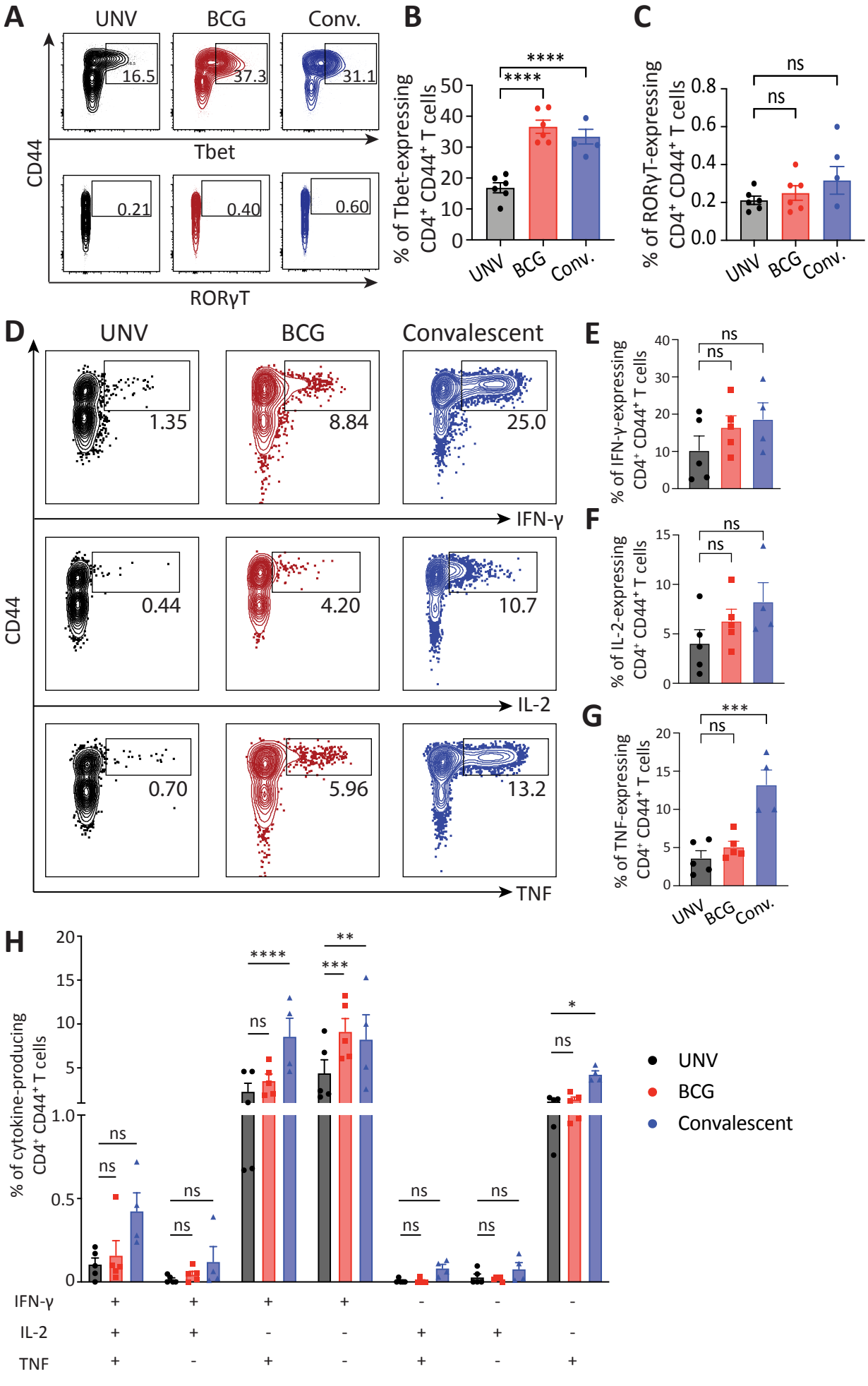
A
UNV
BCG
Conv.
16.5
37.3
31.1
Tbet
CD44
0.21
0.40
0.60
RORγT
B
% of Tbet-expressing CD4+ CD44+ T cells
****
****
UNV
BCG
Conv.
C
% of RORγT-expressing CD4+ CD44+ T cells
ns
ns
D
UNV
BCG
Convalescent
1.35
8.84
25.0
IFN-γ
CD44
0.44
4.20
10.7
IL-2
0.70
5.96
13.2
TNF
E
% of IFN-γ-expressing CD4+ CD44+ T cells
F
% of IL-2-expressing CD4+ CD44+ T cells
G
% of TNF-expressing CD4+ CD44+ T cells
***
H
% of cytokine-producing CD4+ CD44+ T cells
IFN-γ
IL-2
TNF
UNV
BCG
Convalescent

Figure 4.6. Transcription factor and cytokine production by CD4+ T cells in the lungs of BCG-vaccinated mice after *M. abscessus* challenge. C57BL/6 mice were vaccinated and challenged as in Figure 4.4 and 7 days post-infection cells were isolated from the lung and analysed using flow cytometry. **(A)** Representative FACS plots of the proportion of $CD4^+$ T cells expressing Tbet and RORγT. **(B-C)** Mean ± SEM $CD4^+$ T cells expressing Tbet and RORγT respectively. **(D)** Representative FACS plots of cytokine-producing $CD4^+$ T cells following ex vivo stimulation with 10^5 *M. abscessus*. **(E-G)** Mean ± SEM $CD4^+$ T cells producing IFN-γ, IL-2, or TNF respectively, 7dpi. (H) Mean ± SEM $CD4^+$ T cells production multiple cytokines as determined using Boolean gating. Data is representative of two independent experiments (n=5-6) and statistical differences were evaluated using two-way ANOVA (*p<0.05, ***<0.001).

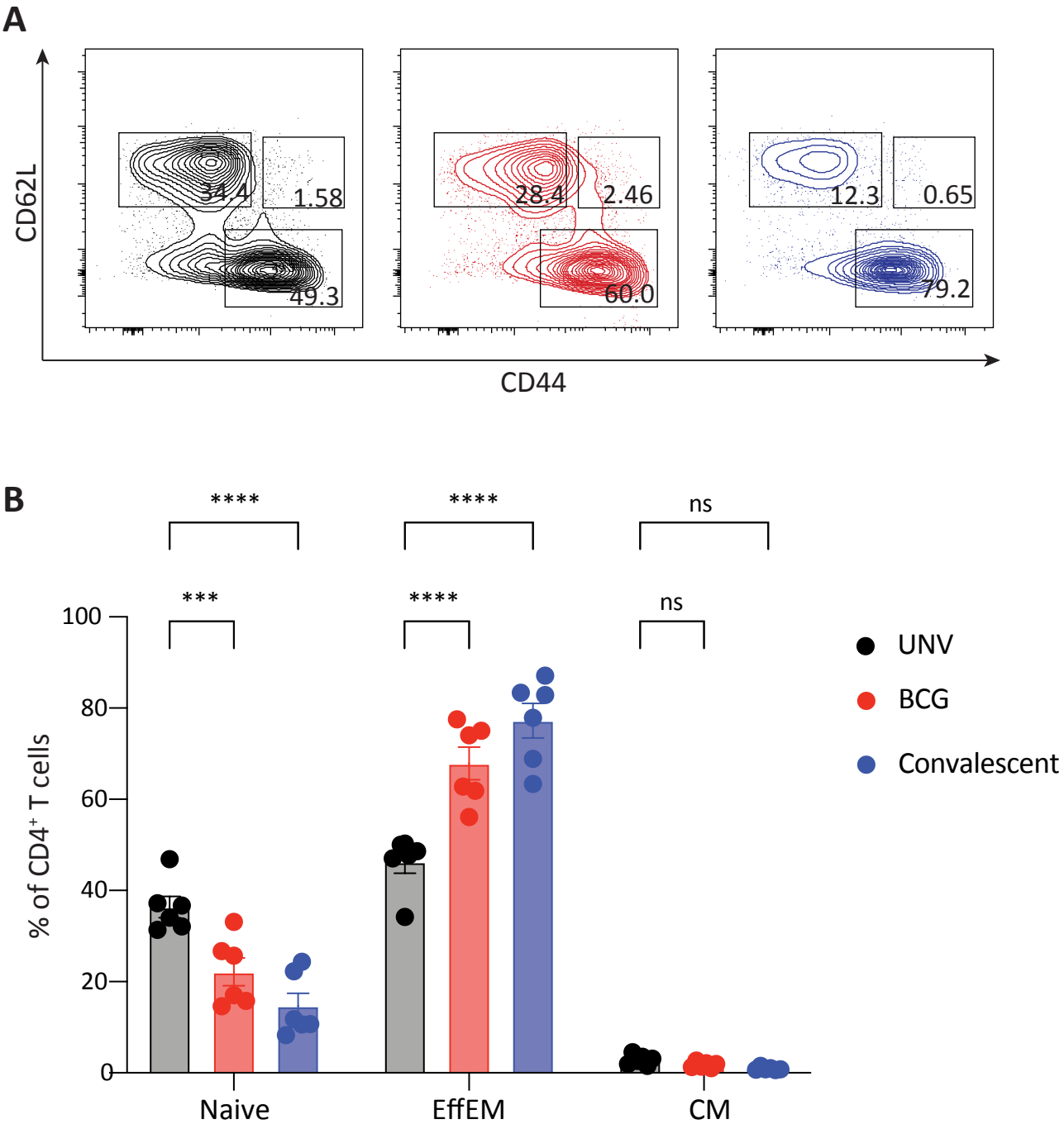

Figure 4.7: Memory CD4⁺ T cell subsets in the lungs of BCG-vaccinated mice following *M. abscessus* challenge. C57BL/6 mice were vaccinated and challenged as in Figure 4.5 and 7 days post-infection cells were isolated from the lung and analysed using flow cytometry. **(A)** Representative FACS plots of the proportion of naïve (CD62L⁺CD44-), central memory (CM, CD62L⁺CD44⁺), and effector memory (EffEM, CD62L-CD44⁺) CD4⁺ T cells **(B)** Mean ± SEM of memory cell subsets as a percentage of total CD4⁺ T cells. Data is representative of two independent experiments (n=4-6) and statistical differences were evaluated using two-way ANOVA (*p<0.05, ***<0.001, ****<0.0001).

Table 4.1. Characteristics of children attending the two Cystic Fibrosis clinics over the 3-year period of the study (2017-2019).

		CHW, AUSTRALIA*				RCWMCH, SOUTH AFRICA*			
		Year 1	**Year 2**	**Year 3**	**Overall**	**Year 1**	**Year 2**	**Year 3**	**Overall**
No. patients		71	80	82	91	208	208	213	231
% males		51	49	50	49	51	51	52	52
Age (years)		8.8	8.9	9.7	9.4	9.1	9.4	9.7	9.8
Peak FEV_1 (% predicted)		88.0	86.3	85.4	91.3	95.6	96.5	94.7	98.7
Peak Height (z score)		-0.91	-0.89	-0.86	-0.57	-0.08	-0.13	-0.09	0.06
Peak Weight (z score)		-0.78	-0.74	-0.72	-0.45	-0.01	-0.03	-0.03	0.18
Peak BMI mean (z score)		-0.22	-0.26	-0.27	0.04	0.06	0.06	0.11	0.27
Number tested for NTM (% sampled)		43 (61)	41 (51)	55 (67)	77 (85)	129 (62)	139 (67)	131 (62)	193 (84)
Any NTM	isolated (%)	2.33	4.88	1.82	7.77	4.65	5.04	6.11	5.19
	colonised (%)	0	0	0	6.74	3.88	5.76	6.11	0
	isolated or colonised (%)	2.33	4.88	1.82	11.92	8.53	10.79	12.21	5.19
M. abscessus	isolated (%)	2.33	0	0	2.59	0.78	0	3.05	1.30
	colonised (%)	0	0	0	5.70	3.10	5.04	6.11	0
	isolated or colonised (%)	2.33	0	0	7.25	3.88	5.04	9.16	1.30
M. avium	isolated (%)	2.33	2.44	1.82	4.66	3.88	3.60	3.05	3.90
	colonised (%)	0	0	0	1.55	1.55	1.44	0	0
	isolated or colonised (%)	2.33	2.44	1.82	5.70	5.43	5.04	3.05	3.90
M. intracellulare	isolated (%)	0	4.88	1.82	1.55	0	1.44	0.76	3.90
	colonised (%)	0	0	0	0	0	0	0	0
	isolated or colonised (%)	0	4.88	1.82	1.55	0	1.44	0.76	3.90
Number tested for other bacteria (% sampled)		71 (100)	80 (100)	82 (100)	91 (100)	208 (100)	208 (100)	213 (100)	231 (100)
Pseudomonas aeruginosa	isolated (%)	28.17	18.75	29.27	45.05	19.71	14.90	15.49	35.50
	colonised (%)	16.90	18.75	14.63	28.57	13.94	12.02	9.39	19.05
Staphylococcus aureus	isolated (%)	64.79	66.25	67.70	84.62	74.04	78.85	80.75	90.48
Haemophilus spp.	isolated (%)	12.68	15.00	12.20	27.47	16.83	10.58	11.74	28.14

Aspergillus spp.	isolated (%)	25.35	21.25	20.73	32.97	22.60	25.48	23.00	37.66

*Data is shown as mean unless otherwise indicated. The overall value is calculated from the mean result of data from the entire 3 year period. As such the overall % of subjects tested for NTM reflects the % of children screened over the entire 3 year period and is therefore higher than the individual year on year values.

Table 4.2: Isolation, colonisation and isolation or colonisation rates of NTM and subspecies

	Isolated			**Colonised**			**Isolated or colonised**		
	SA (%)	AUS (%)	p	SA (%)	AUS (%)	p	SA (%)	AUS (%)	p
NTM (overall)	5.2	7.8	0.45	0.0	6.7	0.02	5.2	11.9	0.10
M. abscessus	1.3	2.6	0.52	0.0	5.7	0.03	1.3	7.3	0.05
M. avium	3.9	4.7	0.78	0.0	1.6	0.27	3.9	5.7	0.55
M. intracellulare	3.9	1.6	0.24	0.0	0.0	-	3.9	1.6	0.24

score, p<0.001) with higher BMIs (0.27 vs 0.04 peak BMI z score, p=0.26), yet had similar lung function (98.7 vs 91.3 peak FEV1 %predicted, p=0.20).

The overall rates of NTM sampling during the three year period were equivalent between the RCWMCH and CHW cohort: 85% vs 84%, p=0.87. Table 1 details the rates of NTM isolation, colonisation, and isolation and/or colonisation between the cohorts, as well as other common bacterial pathogens. Overall rates of NTM isolation, colonisation, and isolation and/or colonisation were all numerically lower in the RCWMCH cohort vs CHW cohort (Table 2) and reached statistical significance for rates of NTM colonisation (0.0 vs 6.7%, p=0.02), *M. abscessus* colonisation (0.0 vs. 5.7%, p=0.03), and either isolation or colonisation of *M. abscessus* (1.3% vs 7.3%, p=0.05). There was no significant difference for overall rates of isolation for other common CF pathogens (Table 4.2). Thus BCG vaccination appears to play a role in reducing colonisation/isolation of NTM in these cohorts, particularly *M. abscessus*, however further correlation analysis may be required to further elucidate this finding.

4.3 Discussion

The major aim of this chapter was to assess the utility of BCG vaccination in providing protection against *M. abscessus* infection and to determine a role for BCG in a clinical context where *M. abscessus* infection is problematic. BCG vaccination did confer significant protection against dissemination of *M. abscessus* to the spleen, however unlike prior *M. abscessus* infection, minimal protection was afforded by BCG in the lung (Figure 4.3). BCG is a live-attenuated vaccine delivered parenterally that is known to be protective against disseminated TB (Dockrell & Smith, 2017). BCG seeds to the spleen to induce localised immunity, preventing significant dissemination upon subsequent intranasal mycobacterial challenge (Darrah et al., 2020). Indeed, BCG induced the greatest level of circulating, cytokine-expressing *M. abscessus*-specific $CD4^+$ T cells in the blood (Figure 4.2), yet was a relatively poor inducer of T cell responses in the lung (Figure 4.5). While both BCG and prior *M. abscessus* infection elicited Th1 responses and multifunctional $CD4^+$ T cells in the lung, convalescent mice had higher responses which correlated with the protective efficacy observed. The role of multifunctional $CD4^+$ T cells in *M. abscessus* infection has been studied recently in a large cohort study, where triple-positive $CD4^+$ T cells correlated with better disease control (Shu, Wu, et al., 2019). The functional capacity of triple-positive $CD4^+$ T cells has also been studied in other mycobacterial models, though the evidence is less well-defined. In *M. tuberculosis* infection, polyfunctional $CD4^+$ T cells appear to have higher proliferative capacity and are correlated with better disease control (Day et al., 2011). However, in a Phase IIb randomised control trial of the TB vaccine candidate MVA85A, polyfunctional T cells did not correlate with protection against *M. tuberculosis* (Tameris et al., 2013).

Both BCG vaccination and prior *M. abscessus* exposure resulted in significant levels of effector memory-like $CD4^+$ T cells in the lung following intranasal challenge. The presence of effector memory-like cells are crucial in the context of vaccine development as these cells are able to rapidly acquire effector functions, enabling inflammatory cytokine production to recruit other effector cells for early bacterial control (Kaech et al., 2002). The extensive influx of these cells into the lung following intranasal *M. abscessus* challenge in previously BCG-vaccinated or *M. abscessus*-exposed mice suggests their importance in the early control of *M. abscessus* infection. BCG vaccination was also associated with elevated levels of B cells in the lung following *M. abscessus* challenge, which was not seen after prior *M. abscessus* exposure. The role of B cells in the context of BCG vaccination against *M. abscessus* has

been explored previously. Following BCG vaccination, B cell-deficient mice have overwhelming neutrophilia, which hinders the capacity for DC migration to the mLN in order to prime $CD4^+$ T cells to induce a potent Th1 response (Kozakiewicz et al., 2013). Several studies have demonstrated a significant level of antigen-specific IgM and IgG production in the context of BCG vaccination (Tanner et al., 2019). BCG-specific antibodies have been shown to enhance Th1 responses in *M. tuberculosis* infection (Chen, Blanc, et al., 2016; de Vallière et al., 2005). Thus, while there is some evidence suggesting a role for B cells in enhancing anti-mycobacterial protective immunity, the data presented here suggests that expansion of BCG-specific B cells does not appear to play a major role in protection against pulmonary *M. abscesses* infection in mice.

The next aim of this chapter was to determine whether epidemiological data shows any evidence of BCG conferring a protective effect against *M. abscessus* infection in humans. In paediatric CF patients in South Africa, where BCG is part of the routine immunisation schedule, lower rates of NTM and *M. abscessus* colonisation were found, as well as lower rates of isolation or colonisation of *M. abscessus* compared to those in a CF centre in Australia, where patients have not been vaccinated with BCG. Lower rate of infection in countries with routine BCG vaccination is also supported by a recent report of incidence in a Turkish CF centre where only 2.1% had at least one NTM positive culture from respiratory samples between 2012-20 (Ademhan Tural et al., 2021). While epidemiological observations such as this correlate with the notion of the cross-reactivity of BCG and NTM, it is important to consider some confounding factors that may skew the interpretation of these data. The overwhelming prevalence of *M. tuberculosis*, as well as a higher prevalence of ubiquitous mycobacteria in South Africa may contribute to the cross-protective immunity observed (Davenne & McShane, 2016). This theory is supported by evidence that prior sensitisation to NTMs can adversely affect protection afforded by BCG against pulmonary TB (Mangtani et al., 2014). Alternatively, differences in baseline prevalence of *M. abscessus* infection in South African versus Australian populations may contribute to differences seen. In a worldwide study of NTM prevalence by the NTM Network European Trials framework (NTM-NET), *M. abscessus* accounted for 0-2% of all NTM isolates in South Africa, compared with >8% of isolates in Australia (Hoefsloot et al., 2013). Given that the prevalence of pulmonary *M. abscessus* infections in Australia appears higher, this may have skewed the results of our study as the higher rates of infections in Australia could be due to the absence of BCG vaccination. While beyond the scope of this study, these confounders

could be addressed using a randomised control trial of BCG vaccination to prevent *M. abscessus* infection across multiple centres with differing rates of *M. abscessus* infection.

It is important to note that the route of administration may play a role in the efficacy of BCG vaccination against *M. abscessus* infection when compared to convalescent infection. It is well-documented that mucosal and parenteral BCG vaccination confer differing levels of protection against mycobacteria. For example, intranasal BCG vaccination has been shown to induce antigen-specific tissue-resident memory T cells (Wu et al., 2021). This has been shown to be associated with better protection when compared directly with subcutaneous vaccination (Chen et al., 2004). As such, the role of pulmonary BCG vaccination in *M. abscessus* infection would be an interesting area of future research.

In conclusion, this chapter has explored the potential of BCG vaccination to protect against *M. abscessus* infection. While vaccination induced strong IFN-γ-producing antigen-specific $CD4^+$ T cells in the blood, it was not protective against pulmonary *M. abscessus* infection. However, the vaccine was protective against dissemination of bacteria to the spleen. BCG vaccination induced some level of Th1 effector responses, significant levels of EffEM populations in the lung, and strong B cell responses/recruitment. Although these responses were not sufficient to significantly protect against murine, pulmonary *M. abscessus* infection. None-the-less, the results of this chapter provide a platform for future evaluation of BCG as a tool for enhancing protection against *M. abscessus*. Further, this chapter has defined possible immune correlates of protection against *M. abscessus*. Prior-*M. abscessus* infection imparted strong protective immunity that correlated with correlated with iNOS-producing IMs in the lung, as well as the expansion of IFN-γ^+- and TNF^+-secreting $CD4^+$ T cells. Together, these provide an excellent foundation for identifying novel vaccine candidates to protect against *M. abscessus* infection, which will be further explored in Chapter 5 of this thesis.

Chapter 5: Assessment of novel inactivated vaccines to combat pulmonary *M. abscessus* infection

5.1. Introduction

Mycobacterium abscessus is a non-tuberculous mycobacterium (NTM) pathogen of increasing concern, due to rapidly increasing incidence of infection in people living with Cystic Fibrosis (CF) and other chronic respiratory pathologies (Martiniano et al., 2019). In this cohort, *M. abscessus* infection can cause progressive pulmonary function decline, diminish quality of life and even cause acute respiratory failure, which can be fatal (Lee et al., 2015). The extensive intrinsic and acquired drug resistance profile of *M. abscessus* renders it an onerous and costly ordeal to treat with antimicrobials for both the individual and the healthcare system (Degiacomi et al., 2019). Indeed in some cases, antimicrobials fail to eliminate *M. abscessus* colonisation from the lung (Choi et al., 2018). Preventative strategies such as vaccination are required to reduce the need for antimicrobials and limit the prevalence of *M. abscessus* infections in the CF community.

At the time of writing, very little literature exists in the field of vaccine design for *M. abscessus* infection. Reverse vaccinology has been used to produce a *M. abscessus* Phospholipase C (PLC) DNA vaccine, which elicited a strong IgG response in a mouse model of CF (Le Moigne et al., 2015). Interestingly, this effect was diminished in wildtype (WT) mice. In another study by the same group, immunisation with virulence factor MtgC DNA also induced protection against *M. abscessus* infection and antibody titres in CF mice (Le Moigne, Belon, et al., 2016). Vaccination of CF mice with TLR2 enriched fraction (TLR2eF), a *M. abscessus* cell wall component known to be a potent stimulator of TLR2-mediated inflammation, did not provide significant protection against aerosol *M. abscessus* challenge, but conferred some protection against intravenous *M. abscessus* challenge (Le Moigne, Roux, et al., 2020). Importantly, none of these studies reported on the role of cellular-mediated immunity in protection against *M. abscessus* infection. This is an obvious limitation of previous studies, as the role of cell mediated immunity in the control of mycobacterial infection is well established (Han et al., 2020; Mauch et al., 2020). Lee et. al (2016) described D-alanyl-D-alanine dipeptidase as a potential vaccine candidate, due to its potent role in dendritic cell (DC) activation and Th1 cell polarisation, however assessment of vaccine efficacy has not been performed. More recently, *in silico* analysis of the *M. abscessus* genome has identified core proteins as potential subunit vaccine candidates (Dar et al., 2021). Computational analysis of protein structures and receptor binding revealed their potential in TLR2 stimulation and lymphocyte activation (Dar et al., 2021). However, translation of this data into an animal model is required to assess protective efficacy.

Most candidates proposed to combat *M. abscessus* infections have been DNA or protein subunit vaccines. Whole-cell vaccines (WCV) are a strategy that has been used to engineer vaccines against many other diseases, such as influenza, polio and rabies. WCV are an attractive approach for vaccine design in that they contain a more diverse antigenic profile than subunit vaccines (Schrager et al., 2020). In whole cell mycobacterial vaccine candidates, the presence of lipids, glycolipids and other metabolites on the mycobacterial cell wall is thought to recruit diverse components of the immune system, thus contributing to a more robust response and stronger induction of protective immune responses (Busch et al., 2016; Spencer et al., 2008; Van Rhijn & Moody, 2015). For inactivated WCVs, heat or chemical inactivation are common methods that have been used for vaccine development. However, some studies suggest that heat and chemical treatments can alter the structure of surface antigens, rendering them less immunogenic (Fertey et al., 2016; Sabbaghi et al., 2019). Gamma-irradiation is an alternative inactivation treatment which targets nucleic acids while preserving antigenic epitopes on the cell surface, therefore maintaining immunogenic potential (Babb et al., 2016). Intranasal immunisation with γ-irradiated *Streptococcus pneumoniae* induced potent antibody responses and conferred significant protection when compared to heat-killed or formalin-inactivated *S. pneumoniae* (Jwa et al., 2018).

This Chapter aimed to assess the protective efficacy of three WCVs engineered by γ-irradiation, heat treatment or paraformaldehyde inactivation of *M. abscessus*. Both subcutaneous and intranasal vaccine delivery was explored. The intranasal pulmonary infection model from Chapter 3 was used here to examine the immunogenicity and protective efficacy afforded by each vaccine type. Further, addition of a delta inulin polysaccharide adjuvant, Advax^{CpG}, was used in combination with γ-irradiated *M. abscessus* to develop combination vaccines with enhanced immunogenicity.

5.2. Results

5.2.1 Inactivation of *M. abscessus* MA07 to produce novel vaccine candidates

The first aim of this Chapter was to create three vaccine candidates from different inactivation methods described in the literature: γ-irradiated (γ-*Mabs)*, heat-killed (HK-*Mabs*) or paraformaldehyde (PFA)-inactivated (PFA-*Mabs*), using the procedures detailed in Chapter 2.2.3. To verify these, single cell culture of *M. abscessus* MA07 were inactivated using the three methods, and viability was assessed by measuring growth on solid agar. All inactivation methods resulted in strains with no growth on media after four weeks of incubation (Figure 5.1). Given that γ-irradiation damages nucleic acids while preserving protein structure and function, it is believed that irradiated material should remain somewhat metabolically active, while DNA replication is arrested (Jwa et al., 2018). Metabolic activity was measured using the resazurin assay, which is a colorimetric assay that measures the reduction of resazurin to resorufin by NAD in actively metabolizing cells (Präbst et al., 2017). γ-*Mabs* showed metabolic activity comparable to live *M. abscessus* controls, while HK-*Mabs* or PFA-*Mabs* showed no activity (Figure 5.1). Thus, γ-*Mabs* maintains some metabolic activity while remaining non-viable and unable to replicate, while other inactivation techniques do not preserve metabolic function.

The differential metabolic activity of the different inactivated vaccines suggests that they have different capacities to activate host cells. To assess this ability, the three WCV candidates were incubated with RAW264.7 cells *in vitro* and chemokine/cytokine production was determined in the cell culture supernatants. Overall, the strongest chemokine responses were seen with γ-*Mabs* or live *M. abscessus*-stimulated cells. γ-*Mabs* produced significant levels of CCL3 (MIP-1α) compared to unstimulated or other vaccine groups (Figure 5.2A). CCL22 production was significantly increased in all inactivated vaccine groups compared to unstimulated cells, but not in the live bacteria group (Figure 5.2B). CCL5 levels were similar across all vaccinated groups with greatest responses observed in γ-*Mabs* vaccination (Figure 5.2C). There was no significant difference in CCL2 (MCP-1) production by any of the vaccinated groups compared to unstimulated cells (Figure 5.2D). When cytokine production was assessed, only live *M. abscessus* resulted in significantly higher levels of GM-CSF and IL-1β compared to unstimulated cells (Figure 5.2E,F). Similarly, γ-*Mabs* was the only vaccine capable of stimulating significant release of IL-6 (Figure 5.2G). TNF production was highest in live-stimulated and HK-stimulated cells, but

A

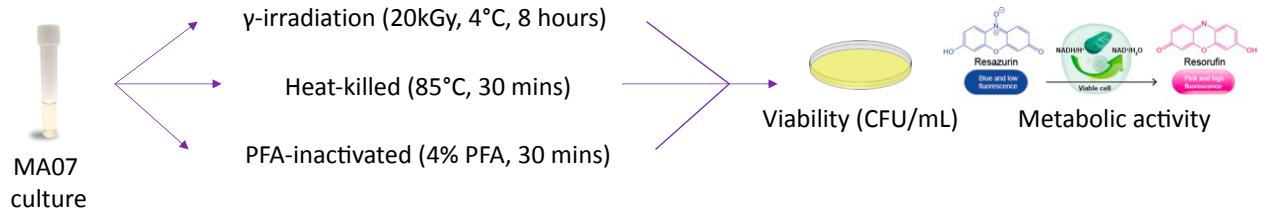

B

	Metabolic activity (Mean ± SD)	Viability (CFU/mL)
Live MA07	100	$3.62x10^8$
γ-*Mabs*	97.76 (±4.98)	<10
HK-*Mabs*	1.73 (±1.02)	<10
PFA-*Mabs*	10.56 (±5.34)	<10

C

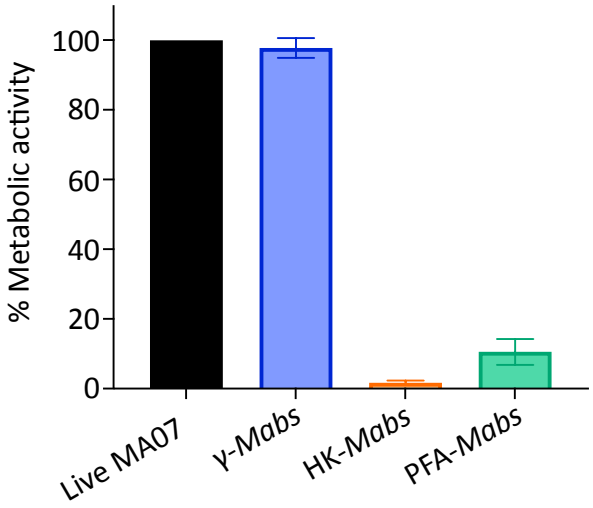

Figure 5.1. Viability and metabolic activity of inactivated *M. abscessus* vaccine candidates. *M. abscessus* MA07 vaccines were prepared as described in 2.2.3. **(A)** Representative flow diagram of how viability and metabolic activity was assessed. **(B)** Summary table of viability and metabolic activity of *M. abscessus* vaccine candidates compared to live MA07 culture. **(C)** Percentage of metabolic activity of *M. abscessus* vaccine candidates relative to live MA07 culture.

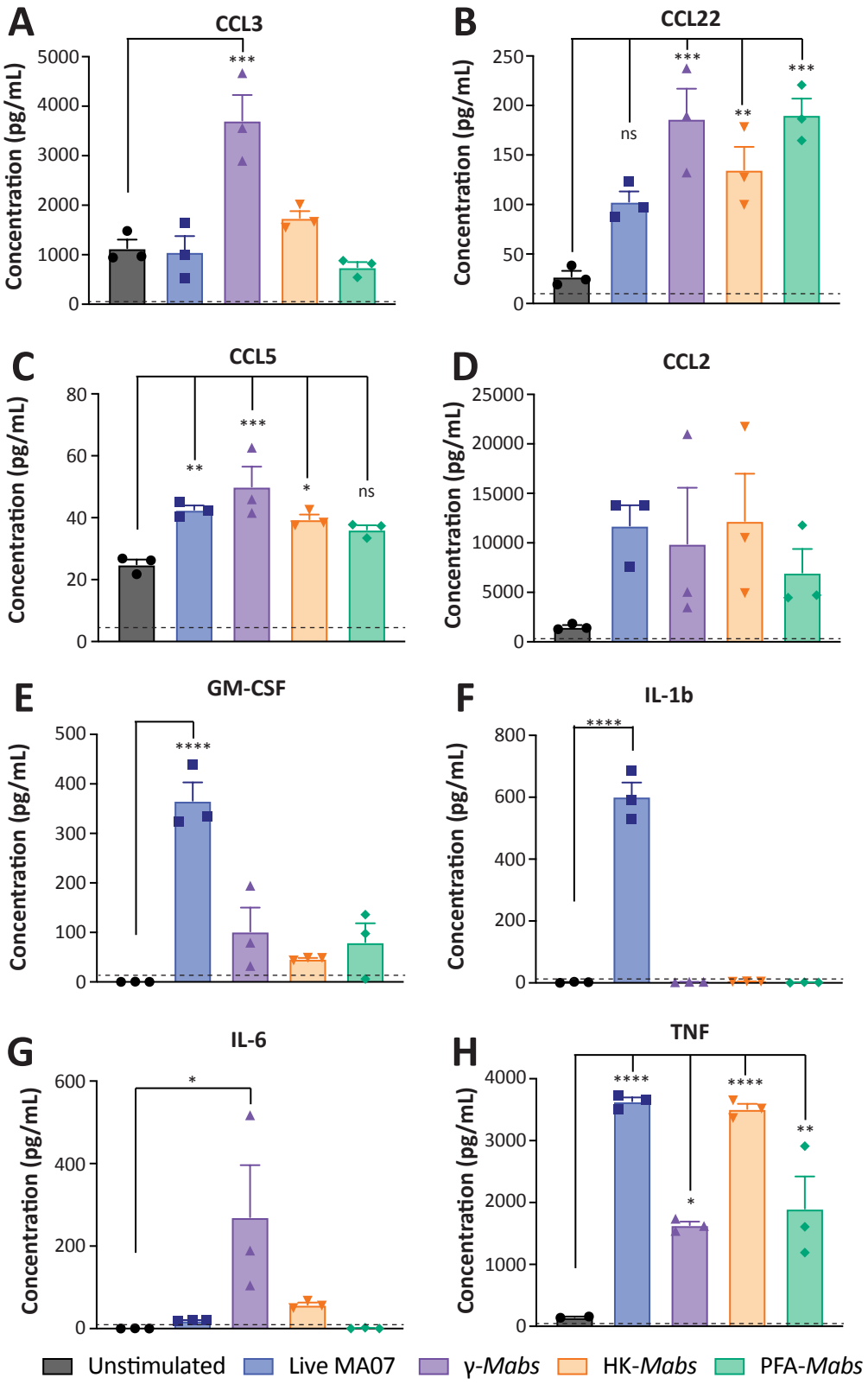

Figure 5.2. *In vitro* cytokine and chemokine production by RAW 264.7 cells following stimulation with *M. abscessus* vaccine candidates. RAW264.7 cells were stimulated with live *M. abscessus*, or γ-irradiated (γ-*Mabs*), heat-killed (HK-*Mabs*) or paraformaldehyde-inactivated *M. abscessus* (PFA-*Mabs*) at a MOI of 10:1 for 2 hours. The supernatant was analysed for cytokine and chemokine production by cytokine bead array as per manufacturer's instructions. **(A-H)** Mean concentration of cytokine/chemokine ± SEM (n=3). Data shown is representative of one experiment. Statistical analysis was conducted using two-way ANOVA compared to unstimulated samples (*P<0.05), **P<0.01, ***P<0.001, ****P<0.001; ns=not significant). Dashed line = limit of detection.

was also significantly increased in cells stimulated with γ-irradiated and PFA-inactivated vaccines (Figure 5.2H). Thus while all inactivated vaccine strains could stimulate release of chemokine/cytokine by RAW macrophage cells, the most diverse response was observed with γ-*Mabs.*

5.2.2 Protection against *M. abscessus* challenge by inactivated vaccines

The next series of experiments examined the protective efficacy of inactivated *M. abscessus* vaccines and determined if any particular immune signatures correlated with protection against pulmonary *M. abscessus* challenge. Mice were vaccinated via subcutaneous (s.c.) route with γ-*Mabs*, HK-*Mabs* and PFA-*Mabs* vaccines three times, two weeks apart. Given that mucosal vaccination has also been shown to be effective in murine models of pulmonary *M. tuberculosis* infection (Counoupas et al., 2020), the protective efficacy of intranasal (i.n.) γ-*Mabs* was also examined. Preliminary studies showed that γ-*Mabs* was the most immunogenic formulation, and so it was selected as the i.n. test group. After vaccination mice were rested for seven weeks and then challenged with i.n. *M. abscessus*. Lungs and spleen were harvested for enumeration of bacterial load and flow cytometric assessment of immune cell phenotype at 7 days post-infection (Figure 5.3A).

After vaccination, and prior to pulmonary challenge, mice were bled to assess the presence of vaccine-specific T cells, by *ex vivo* stimulation of peripheral blood mononuclear cells (PBMCs) with 10^5 CFU *M. abscessus* culture. No significant difference in the proportions of circulating $CD4^+$ or $CD8^+$ T cells was observed (Figure 5.3B-C). Given that a Th1 $CD4^+$ T response has been previously identified to correlate with the control of *M. abscessus* infection (Chapter 3), Tbet production was examined, the transcription factor driving Th1. Vaccination with s.c. γ-*Mabs* or HK-*Mabs* induced significantly higher levels of Tbet-expressing $CD4^+$ T cells compared to naïve, i.n. γ-irradiated or PFA-inactivated vaccination groups (Figure 5.3D-E; $P<0.001$, $P<0.05$, respectively). Indeed, γ-*Mabs* vaccination induced the highest Tbet expression. Further, s.c. γ-*Mabs* vaccination induced greater levels of IFN-γ- and TNF-producing $CD4^+$ T cells compared to unvaccinated mice (Figure 5.3F-G, J-K; $P<0.05$, $P<0.01$, respectively). IL-2 production by $CD4^+$ T cells was not significantly different across any of the vaccinated groups when compared to unvaccinated mice (Figure 5.3H-I). Therefore, vaccination with γ-*Mabs* induced a higher number of circulating vaccine-specific Th1 $CD4^+$ T cells compared with other vaccine types. Intranasal γ-*Mabs* vaccination did not result in any difference in circulating $CD4^+$ T cells.

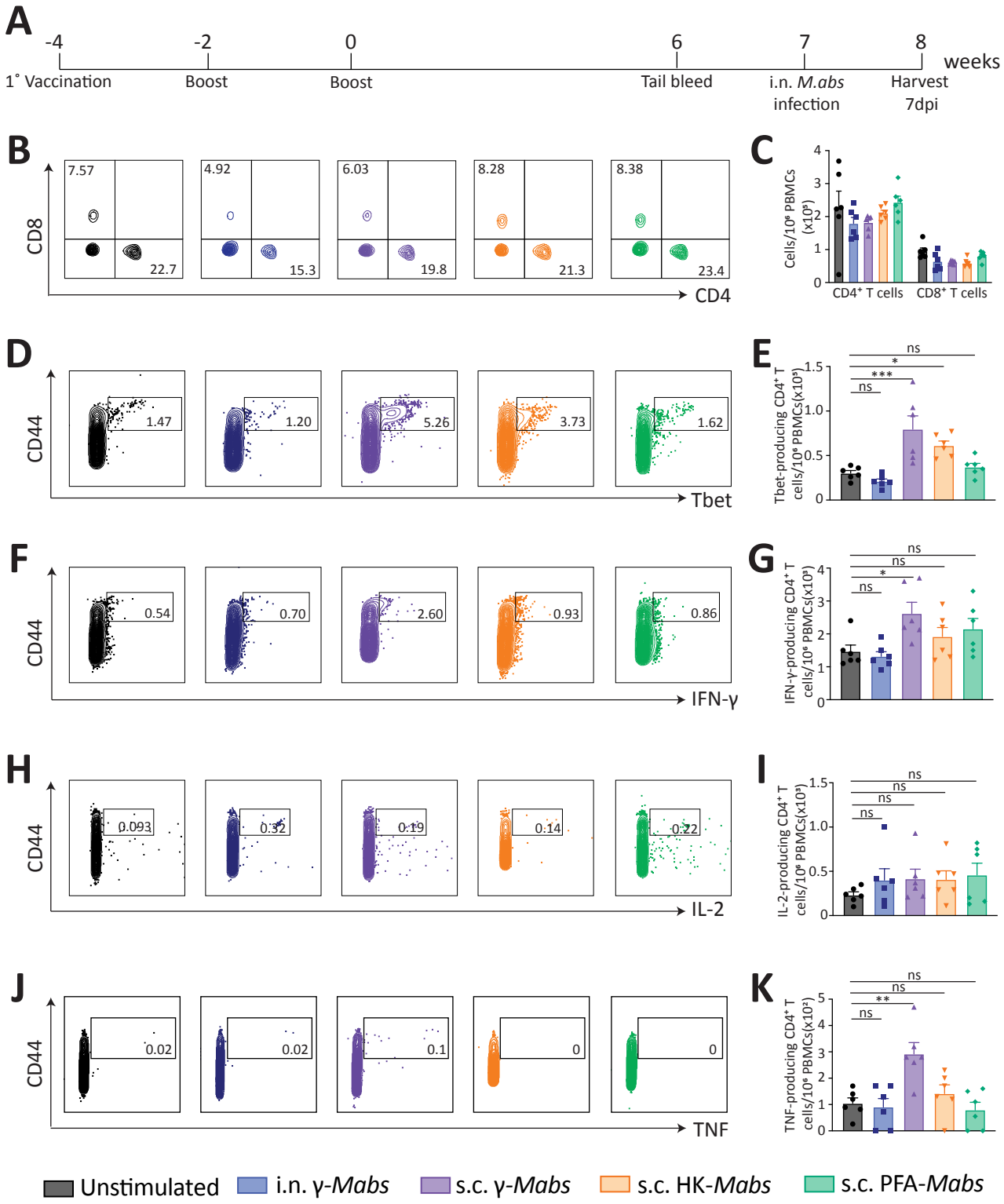

Figure 5.3. Vaccine-mediated induction of circulating cytokine-producing CD4⁺ T cells. C57BL/6 mice (n=6) were vaccinated three times, two weeks apart intranasally (i.n.) with 10^6 CFU γ-Mabs, or subcutaneously (s.c.) with 10^6 CFU γ-*Mabs*, HK-*Mabs* or PFA-*Mabs*. Four weeks after the last vaccination, mice were bled to isolate PBMCs **(A)**. Cells were restimulated *ex vivo* with *M. abscessus* and CD4⁺ and CD8⁺ T cell proportions **(B-C)**, and expression of Tbet **(D-E)**, IFN-γ **(F-G)**, IL-2 **(H-I)** or TNF **(J-K)** CD4⁺ T cells were assessed by flow cytometry. Data is represented as mean number of cells producing transcription factor or cytokine per 10^6 PBMCs ± SEM. Data shown is representative of one experiment. Statistical significance was determined by ANOVA (*P<0.05, **P<0.01, ***P<0.001; ns=not significant).

Protection conferred by the vaccine candidates was assessed by challenging the mice with i.n. *M. abscessus* and enumerating the CFU in the lungs and spleen 7 days post-challenge. In the lungs, γ-*Mabs* and HK-*Mabs* vaccination conferred significant protection, resulting in approximately 1.5-log reduction in bacterial load compared to unvaccinated mice (Figure 5.4A, $P<0.05$). Intranasal γ-irradiated and PFA-inactivated *M. abscessus* vaccination did not confer any significant difference in pulmonary bacterial load compared to unvaccinated groups (Figure 5.4A). To examine whether the vaccine candidates provided any protection against disseminated infection, bacterial load in the spleen was assessed. None of the vaccination types resulted in significant different in bacterial load in the spleen when compared to unvaccinated mice (Figure 5.4B). Therefore, WCV candidates γ-*Mabs* and HK-*Mabs* induce circulating Th1 cells and protect mice from pulmonary *M. abscessus* infection.

5.2.3 Protective *M. abscessus* vaccines induce strong innate immune cell responses, including a marked interstitial macrophage recruitment

Flow cytometry was used to assess the immune cell phenotype in the lungs 7 days after *M. abscessus* challenge in vaccinated and unvaccinated mice. Overall, there was a marked increase in total $CD45^+$ cells in the lungs of s.c. γ-*Mabs* and HK-*Mabs*-vaccinated groups compared to unvaccinated mice (Figure 5.5; $P<0.0001$, $P<0.001$, respectively). The composition of the innate immune response was assessed by applying the myeloid gating strategy outlined in Figure 2.2. Representative FACS plots of the proportions of each innate immune cell subset examined in each vaccination group is shown in Figure 5.6.

The total number of alveolar macrophages (AMs) were not significantly different between groups, however there were noticeably higher numbers of AMs in intranasally-vaccinated mice (Figure 5.7A). Monocytes in the lungs were only altered in s.c. γ-*Mabs* vaccinated mice compared to unvaccinated mice, with a significant drop in cell number (Figure 5.7B; $P<0.05$, $P<0.01$, respectively). Strikingly, the most protective vaccines (s.c. γ-*Mabs* and HK-*Mabs*) induced significant increases in numbers of interstitial macrophages (IMs) and $CD11b^{mid}$ cells, which was not observed with other vaccinated groups (Figure 5.7C,D). Subcutaneous delivery of γ-*Mabs*, HK-*Mabs* or PFA-*Mabs* induced a significant neutrophil response following pulmonary *M. abscessus* challenge (Figure 5.7E; $P<0.01$, $P<0.05$, $P<0.05$, respectively). Examination of DC recruitment to the lungs after *M. abscessus* challenge revealed no significant difference in $CD11b^+$ DC populations (Figure 5.7F). However there

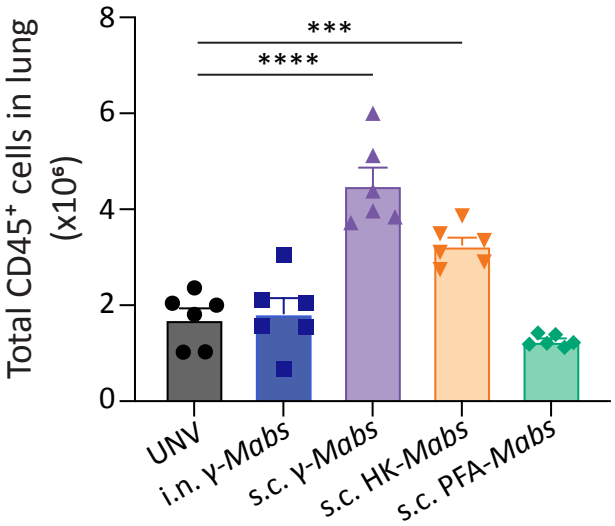

Figure 5.5. Immune cell recruitment to the lungs in vaccinated mice following pulmonary *M. abscessus* challenge. C57BL/6 mice (n=6) were vaccinated and challenged as described in Figure 5.4. 7 days post-challenge, lungs were processed into single cell suspensions and cell number determined by flow cytometry. Data mean total $CD45^+$ cells in the lung±SEM 7 days post-infection. Data representative of one independent experiment for i.n. γ-irradiated vaccination and two independent experiments for s.c. vaccinations. Statistical significance was determined by ANOVA (***P<0.001, ****P<0.001; ns=no significance).

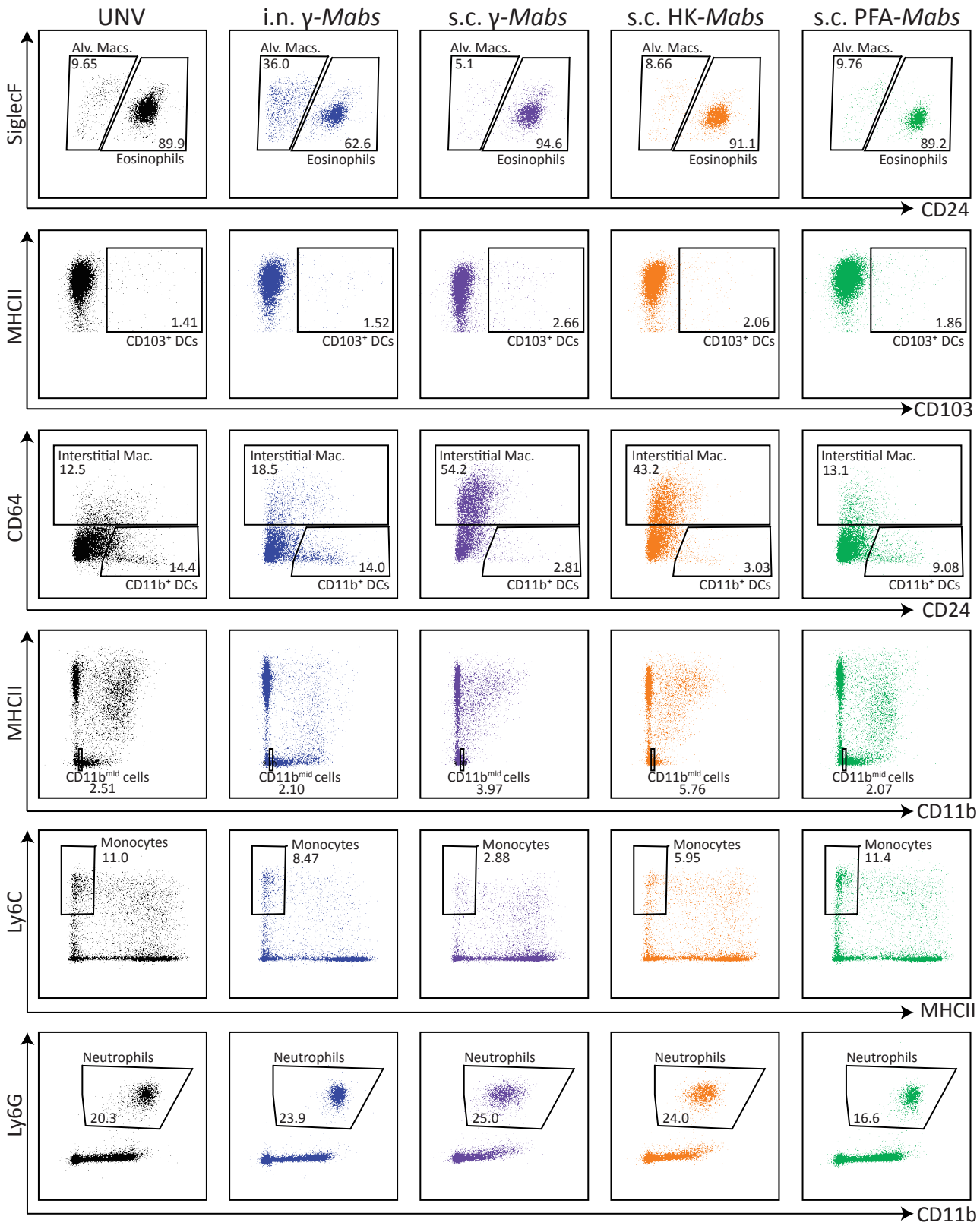

Figure 5.6. Proportions of myeloid cells in the lungs of vaccinated mice following pulmonary *M. abscessus* challenge. C57BL/6 mice (n=6) were vaccinated and challenged as in Figure 5.4. 7 days post-challenge, lungs were processed into single cell suspensions and stained for myeloid cell surface markers. Data shows representative FACS plots for myeloid populations assessed by flow cytometry and is representative of one independent experiment for i.n. γ-*Mabs* vaccination and two independent experiments for s.c. vaccinations.

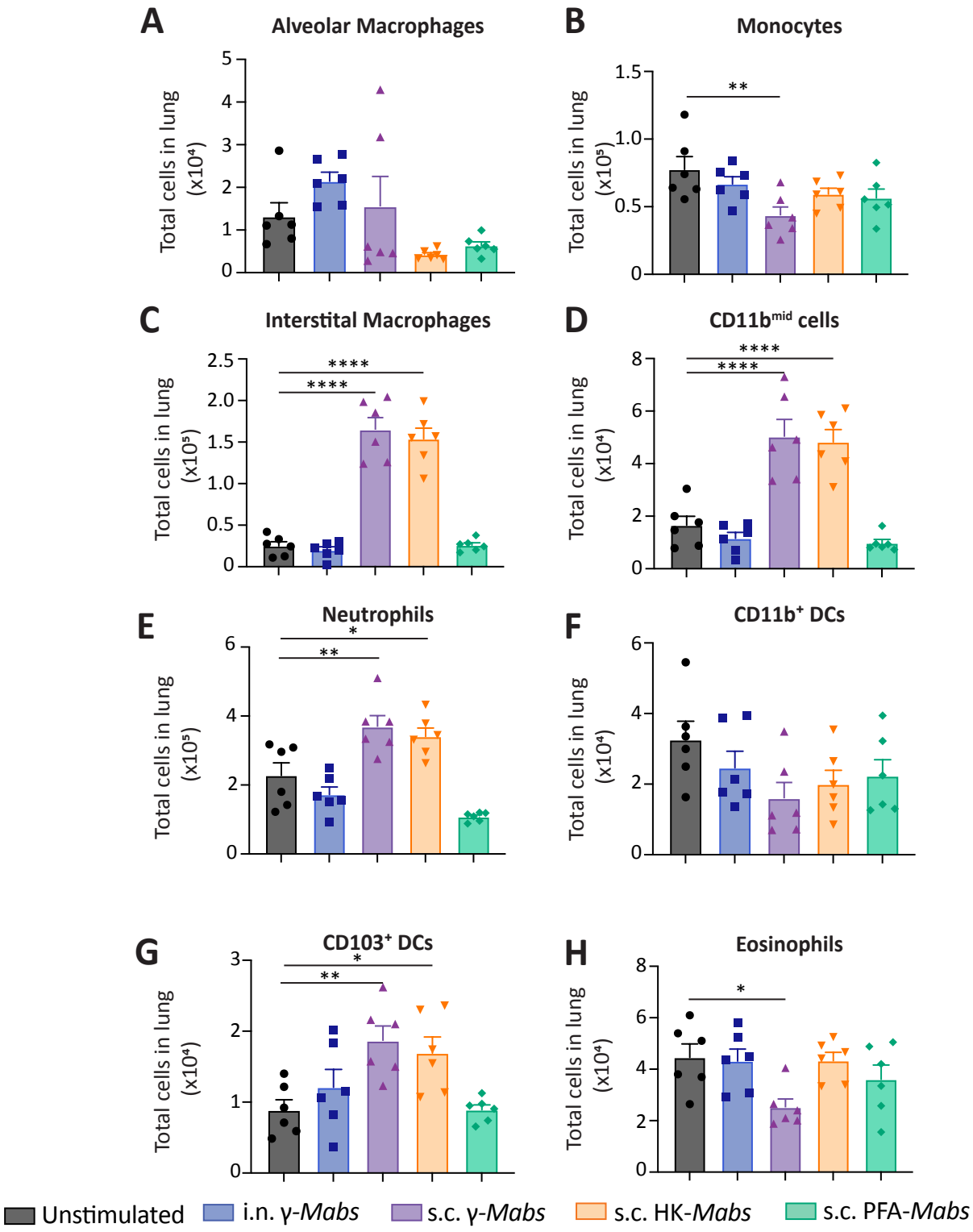

Figure 5.7. Myeloid cell recruitment to the lungs of vaccinated mice following pulmonary *M. abscessus* challenge. C57BL/6 mice (n=6) were vaccinated and challenged as in Figure 5.4. 7 days post-challenge, lungs were processed into single cell suspensions and stained for myeloid cell surface markers. Numbers of alveolar macrophages **(A)**, monocytes **(B)**, interstitial macrophages **(C)**, NK cells **(D)**, neutrophils **(E)**, CD11b⁺ DCs **(F)**, CD103⁺ DCs **(DCs; G)**, or eosinphils **(H)** were determined by flow cytometry using the gating strategy detailed in Figure 2.2. Data shows mean cell number ± SEM in lungs 7 days post-challenge. Data representative of one independent experiment for i.n. γ-irradiated vaccination and two independent experiments for s.c. vaccinations. Statistical significance was determined by ANOVA (*P<0.05, **P<0.01, ***P<0.001, ****P<0.001; ns=no significance).

were significantly higher numbers of CD103$^+$ DCs in s.c. γ-*Mabs* and HK-*Mabs* vaccinated groups compared to unvaccinated mice (Figure 5.7G; P<0.01, P<0.05, respectively). There was no significant difference in eosinophils between vaccinated and unvaccinated groups (Figure 5.7H).

To define a possible mechanism for the link between elevated innate immune cells populations and protective efficacy, iNOS production in vaccinated groups was examined (Chapter 3). γ-*Mabs* vaccination resulted in the greatest number of iNOS$^+$ CD45$^+$ cells in the lungs 7 days following *M. abscessus* challenge (Figure 5.8A,B; P<0.001). Mice vaccinated with s.c. HK *M. abscessus* also had significantly higher iNOS production in the lungs compared to unvaccinated mice (Figure 5.8A,B; P<0.05). When examining the distribution of iNOS production, it was evident that IMs were responsible for almost all observed iNOS production in s.c. γ-*Mabs* and HK-*Mabs* vaccinated mice. Whereas iNOS production for i.n. γ-*Mabs* or PFA-*Mabs* vaccinated groups was distributed more evenly between AMs and IMs (Figure 5.8C). Thus γ-*Mabs* and HK-*Mabs* vaccines, delivered subcutaneously, drive a potent lung localised IM response characterised by iNOS production.

5.2.4 Subcutaneous γ-irradiated and heat-killed *M. abscessus* vaccines induce strong Th1 CD4$^+$ T cell responses in the lungs following pulmonary *M. abscessus* challenge

Next, the adaptive immune response following vaccination and pulmonary *M. abscessus* challenge was examined. There was no significant difference in the number of CD8$^+$ T cells in the lungs of vaccinated mice when compared to unvaccinated mice (Figure 5.9A, B). However, there were enhanced numbers of CD4$^+$ T cells in the lungs of mice previously vaccinated with s.c. γ-*Mabs* or HK-*Mabs* (Figure 5.9A-B, P<0.0001). There were significantly more Tbet-producing CD4$^+$ T cells in the lungs of mice vaccinated with s.c. γ-*Mabs* or HK-*Mabs*, suggestive of a Th1 phenotype (Figure 5.9C,D; P<0.0001). Given that mucosal vaccinations have been shown to induce Th17 CD4$^+$ T cell responses, RORγT expression was also examined as the transcription factor driving Th17 polarisation (Counoupas et al., 2020). There was no appreciable RORγT expression observed across unvaccinated and vaccinated groups (data not shown).

Finally, the memory cell phenotype induced after pulmonary *M. abscessus* challenge was assessed. Mice previously vaccinated with s.c. γ-*Mabs* or HK-*Mabs* showed increased

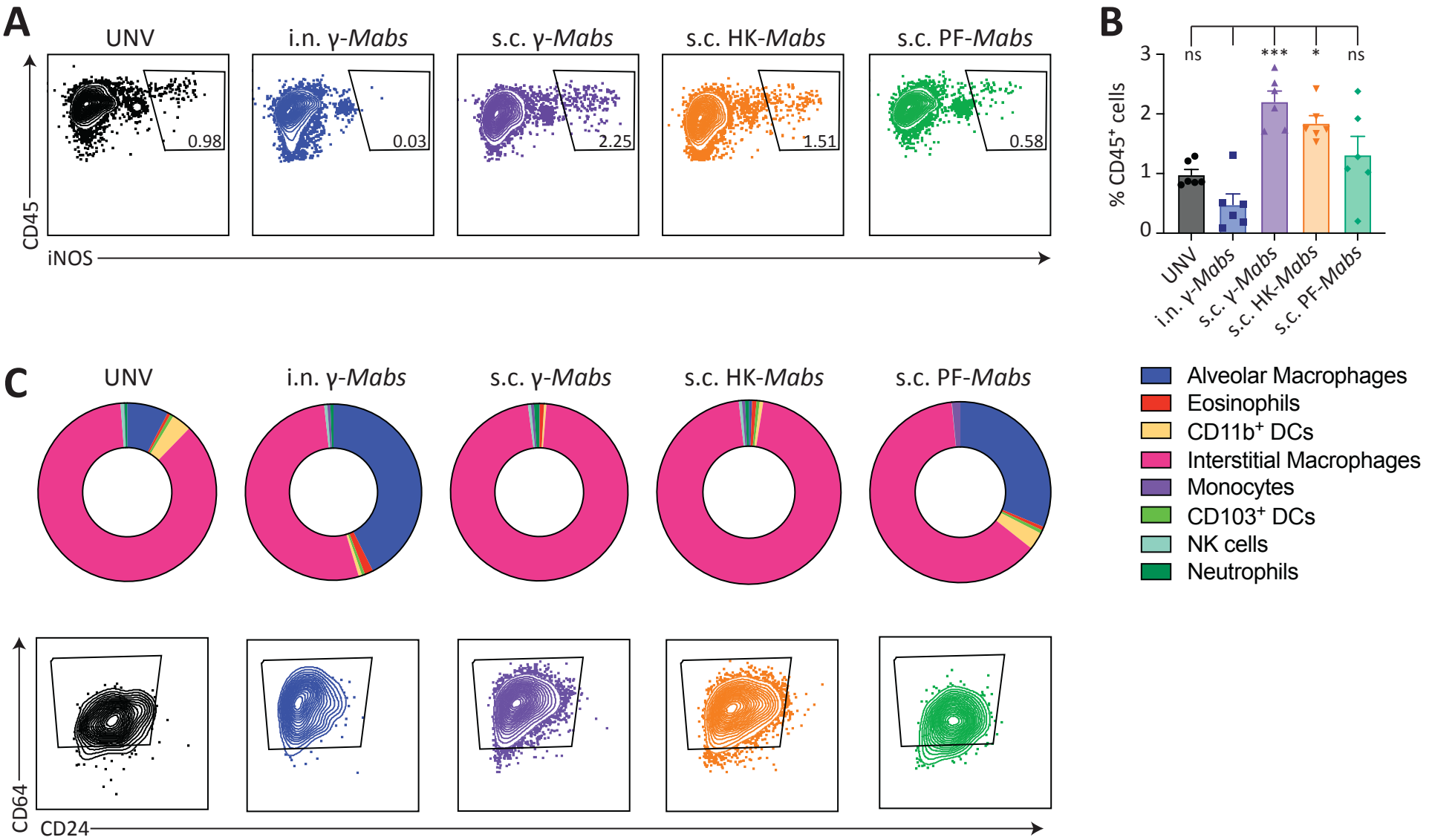
A
UNV
i.n. γ-Mabs
s.c. γ-Mabs
s.c. HK-Mabs
s.c. PF-Mabs
0.98
0.03
2.25
1.51
0.58
CD45
iNOS
B
% CD45+ cells
ns
***
*
ns
UNV
i.n. γ-Mabs
s.c. γ-Mabs
s.c. HK-Mabs
s.c. PF-Mabs
C
Alveolar Macrophages
Eosinophils
CD11b+ DCs
Interstitial Macrophages
Monocytes
CD103+ DCs
NK cells
Neutrophils
CD64
CD24

Figure 5.8. iNOS production in the lungs of vaccinated mice following pulmonary *M. abscessus* challenge. C57BL/6 mice (n=6) were vaccinated and challenged as described in Figure 5.4. 7 days post-challenge, lungs were processed into single cell suspensions and stained for myeloid cell surface markers and intracellular iNOS expression. **(A)** Representative FACS plots of iNOS production by $CD45^+$ cells in the lung. **(B)** Mean percentage of $iNOS^+$ $CD45^+$ cells in the lung ± SEM. **(C)** Distribution of iNOS production amongst myeloid cells in the lungs 7 days post-challenge. **(D)** Representative FACS plots of $iNOS^+$ IMs. Data representative of one independent experiment for i.n. γ-irradiated vaccination and two independent experiments for s.c. vaccinations. Statistical significance was determined by ANOVA (*P<0.05, ***P<0.001; ns=no significance).

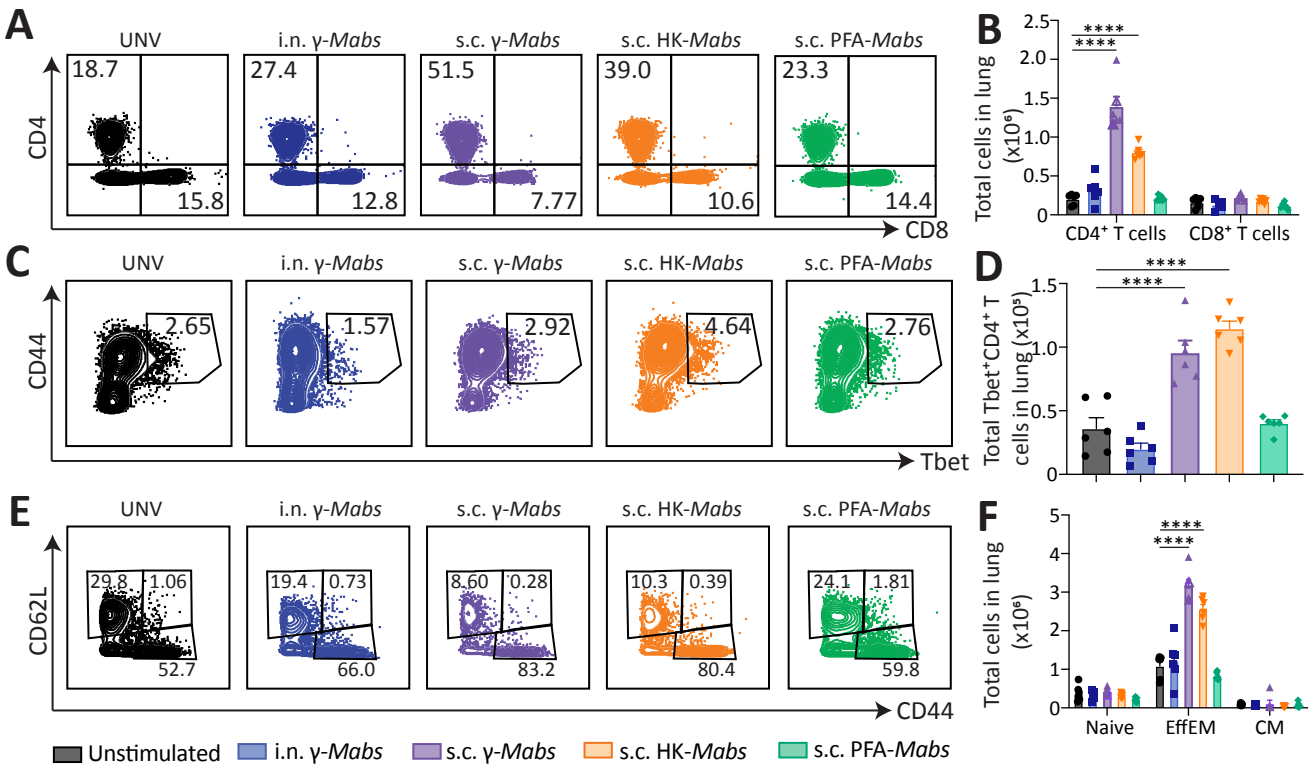

Figure 5.9. T cell recruitment and phenotype in the lungs of vaccinated mice following pulmonary *M. abscessus* challenge. C57BL/6 mice (n=6) were vaccinated and challenged as described in Figure 5.4. 7 days post-challenge, lungs were processed into single cell suspensions and stained for T cell surface markers and transcription factor expression. **(A-B)** Numbers of $CD4^+$ and $CD8^+$ T cells in the lung following *M. abscessus challenge*. **(C-D)** Tbet-expressing $CD4^+$ T cells in the lung following *M. abscessus* infection. **(E-F)** Memory $CD4^+$ T cell populations were determined by flow cytometry; Naive ($CD44^{lo}CD62L^{hi}$), Effector-like (EffEM, $CD44^{hi}CD62L^{lo}$), and Central Memory (CM, $CD44^{hi}CD62L^{lo}$). Data shown is representative FACS plots and mean cells±SEM in the lung 7 days post-challenge. Data representative of one independent experiment for i.n. γ-irradiated vaccination and two independent experiments for s.c. vaccinations. Statistical significance was determined by ANOVA (*P<0.05, **P<0.01, ***P<0.001, ****P<0.001; ns=no significance).

numbers of effector-type ($CD44^+CD62L^-$) $CD4^+$ T cells in the lungs (Figure 5.9 E-F; $P<0.0001$). There was no difference observed in $CD4^+$ T cells displaying a naïve phenotype ($CD44^-CD62L^+$) or central memory phenotype ($CD44^+CD62L^+$) across all vaccinated groups when compared with unvaccinated mice (Figure 5.9E-F).

5.2.5 Mucosal delivery of γ-irradiated *M. abscessus* vaccine induces a stronger B-cell response than subcutaneous vaccination

While i.n. γ-*Mabs* did not display a markedly different $CD4^+$ T cell phenotype, B cells were significantly increased in mice previously vaccinated with i.n. γ-*Mabs* following pulmonary challenge with *M. abscessus* in the lungs (Figure 5.10A). When expressed as total number of B cells in the lungs, there were significantly more B cells in i.n. γ-*Mabs*, s.c. γ-*Mabs* and HK-*Mabs* vaccinated mice (Figure 5.10B; $P<0.05$, $P<0.0001$, $P<0.001$, respectively). This correlated with a noticeably higher titre of *M. abscessus*-specific IgG antibodies in the lungs in mice vaccinated with i.n. γ-*Mabs* following infection, however this did not reach statistical significance (Figure 5.10C). Therefore, mucosal vaccination induced a potent B cell response in the lungs following *M. abscessus* challenge, which correlated with stronger antibody production.

5.2.6 Impact of Advax^{CpG} adjuvant on immunogenicity and protective efficacy of γ-irradiated *M. abscessus*

Given the vaccine potential of γ-*Mabs*, we aimed to enhance its protective efficacy with the addition of an adjuvant. Advax^{CpG} has been shown to afford significant protection against other mycobacterial pathogens, when combined with immunogenic antigens (Counoupas et al., 2020; Counoupas et al., 2017; Quan et al., 2021). To examine the impact of Advax^{CpG} on vaccine efficacy, mice were vaccinated s.c. three times, two weeks apart with γ-*Mabs* alone or in combination with Advax^{CpG} (γ-*Mabs*-Advax^{CpG}), then rested for six weeks before pulmonary *M. abscessus* challenge. Seven days after challenge, the cellular composition and bacterial load in lungs and mediastinal lymph nodes (mLN) was determined. Three out of six mice vaccinated with γ-*Mabs*+Advax^{CpG} developed ulceration at the site of vaccination, and were euthanased before the end of the experiment due to ethical reasons.

Mice vaccinated with γ-*Mabs* alone or γ-*Mabs*+Advax^{CpG} demonstrated a significant increase in total cells in the lungs following pulmonary *M. abscessus* infection (Figure 5.11A; $P<0.05$,

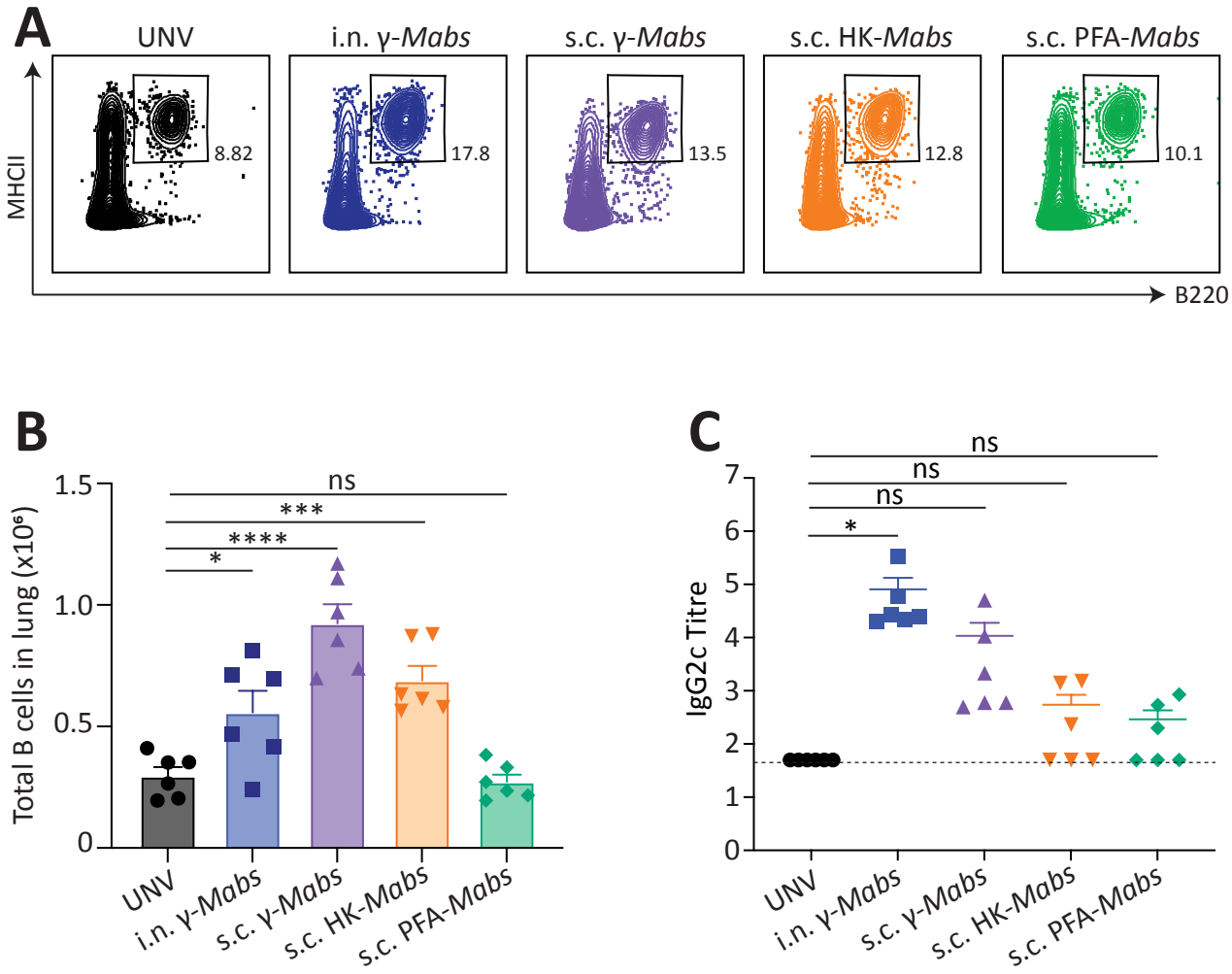

Figure 5.10. Humoral responses in vaccinated mice following *M. abscessus* challenge. C57BL/6 mice (n=6) were vaccinated and challenged as described in Figure 5.4. 7 days post-challenge, lungs were harvested and processed into single cell suspension for flow cytometry or homogenised and the supernatant collected for ELISA. **(A-B)** Representative FACS plots and mean ± SEM B cells in the lungs 7dpi. **(C)** Titres of IgG2c in lung homogenates as calculated by ELISA. Data representative of one independent experiment. Statistical significance compared to unvaccinated mice was determined by ANOVA (*P<0.05, ***P<0.001, ****P<0.001; ns=no significance).

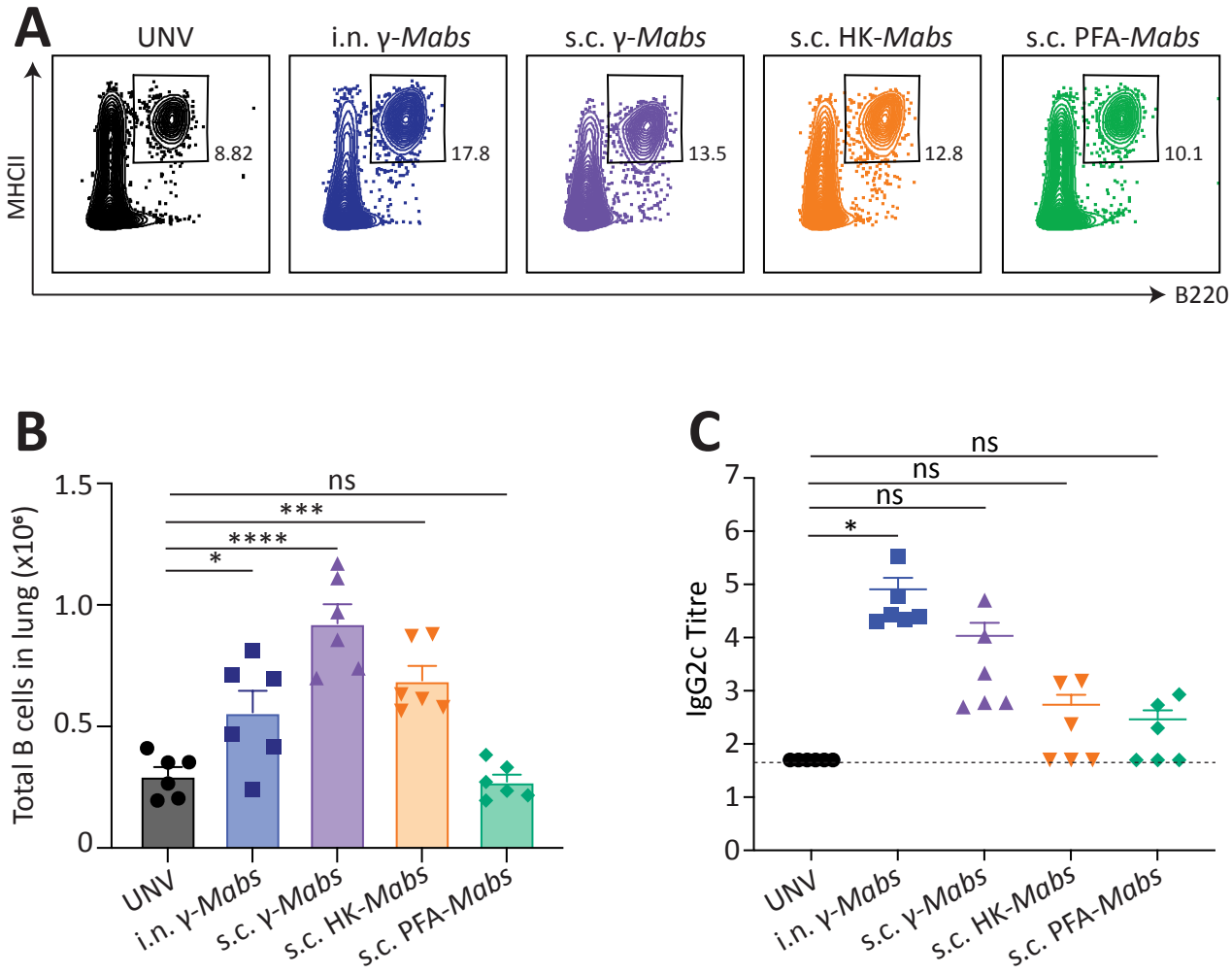

Figure 5.10. Humoral responses in vaccinated mice following *M. abscessus* challenge. C57BL/6 mice (n=6) were vaccinated and challenged as described in Figure 5.4. 7 days post-challenge, lungs were harvested and processed into single cell suspension for flow cytometry or homogenised and the supernatant collected for ELISA. **(A-B)** Representative FACS plots and mean ± SEM B cells in the lungs 7dpi. **(C)** Titres of IgG2c in lung homogenates as calculated by ELISA. Data representative of one independent experiment. Statistical significance compared to unvaccinated mice was determined by ANOVA (*P<0.05, ***P<0.001, ****P<0.001; ns=no significance).

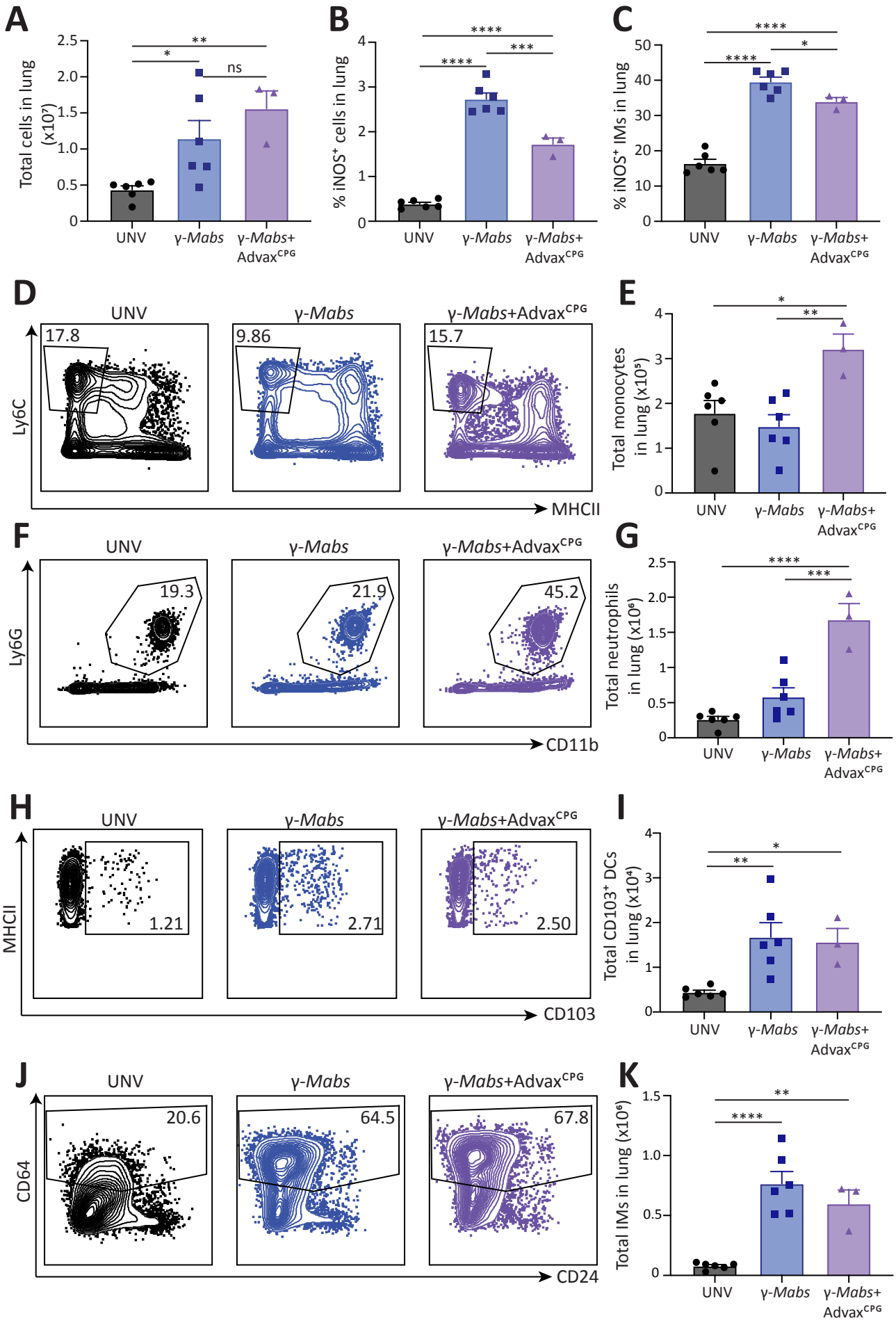
A
Total cells in lung (x10⁷)
2.5
2.0
1.5
1.0
0.5
0
**
*
ns
UNV
γ-Mabs
γ-Mabs+ Advax^CPG
B
% iNOS⁺ cells in lung
4
3
2
1
0
****
***
****
UNV
γ-Mabs
γ-Mabs+ Advax^CPG
C
% iNOS⁺ IMs in lung
50
40
30
20
10
0
****
*
****
UNV
γ-Mabs
γ-Mabs+ Advax^CPG
D
UNV
γ-Mabs
γ-Mabs+Advax^CPG
17.8
9.86
15.7
Ly6C
MHCII
E
Total monocytes in lung (x10⁵)
4
3
2
1
0
*
**
UNV
γ-Mabs
γ-Mabs+ Advax^CPG
F
UNV
γ-Mabs
γ-Mabs+Advax^CPG
19.3
21.9
45.2
Ly6G
CD11b
G
Total neutrophils in lung (x10⁶)
2.5
2.0
1.5
1
0.5
0
****
***
UNV
γ-Mabs
γ-Mabs+ Advax^CPG
H
UNV
γ-Mabs
γ-Mabs+Advax^CPG
1.21
2.71
2.50
MHCII
CD103
I
Total CD103⁺ DCs in lung (x10⁴)
4
3
2
1
0
*
**
UNV
γ-Mabs
γ-Mabs+ Advax^CPG
J
UNV
γ-Mabs
γ-Mabs+Advax^CPG
20.6
64.5
67.8
CD64
CD24
K
Total IMs in lung (x10⁶)
1.5
1.0
0.5
0
**
****
UNV
γ-Mabs
γ-Mabs+ Advax^CPG

Figure 5.11: Innate immune cell recruitment and iNOS production in the lungs of mice vaccinated with γ-irradiated vaccine alone or with adjuvant following pulmonary *M. abscessus* challenge. Vaccination and *M. abscessus* challenge was performed as described in Figure 5.11. Lungs were processed into single cell suspension and stained for myeloid surface markers and iNOS expression. Flow cytometry was performed as detailed in Figure 2.2 and total cell number **(A)**, total iNOS expression **(B)**, and iNOS-producing interstitial macrophages **(IMs; C)** as well as the total numbers of monocytes, **(D-E)**, neutrophils**(F-G)**, $CD103^+$ DCs**(H-I)** and IMs **(J-K)** were determined. Data is expressed as representative FACS plots as well as mean cell number or percentage in the lung±SEM. Statistical significance was determined by ANOVA (*P<0.05, **P<0.01, ***P<0.001, ****P<0.001; ns=no significance).

P<0.01). However, the γ-*Mabs*+Advax^{CpG} group had greater numbers of monocytes and neutrophils in the lungs compared to vaccination with γ-*Mabs* alone (Figure 5.D-G).

While both vaccine groups induced significant CD103$^+$ DC recruitment to the lungs following *M. abscessus* infection, the addition of Advax^{CpG} did not alter the total number of CD103$^+$ DCs (Figure 5.11H-I). Interestingly, the addition of Advax^{CpG} resulted in significantly less total iNOS-producing CD45$^+$ cells in the lungs following *M. abscessus* infection compared to γ-*Mabs* alone (Figure 5.11B, P<0.001). However, both γ-*Mabs* alone or γ-*Mabs*+Advax^{CpG} resulted in significantly higher numbers of iNOS-producing CD45$^+$ cells in the lungs when compared to unvaccinated mice (Figure 5.11B, P<0.0001). Indeed, this same trend was observed in the total number of IMs as well as the proportion of iNOS-producing IMs; while both groups had significantly more total IMs and iNOS-producing IMs compared to unvaccinated mice, the addition of Advax^{CpG} appeared to dampen the response (Figure 5.11C, J-K). These data demonstrate that adjuvanted γ-*Mabs* results in a less dramatic iNOS and IM response to *M. abscessus* infection, and a more dominant neutrophil response.

Addition of Advax^{CpG} to γ-irradiated *M. abscessus* vaccination results in significantly higher numbers of CD4$^+$ T cells in the lungs following pulmonary *M. abscessus* challenge, and no difference in CD8$^+$ T cell numbers (Figure 5.12A-C). Both vaccine groups demonstrated significantly higher proportions of Tbet-expressing CD4$^+$ T cells in the lungs compared to unvaccinated mice, indicating a strong Th1 response; however, there was no significant difference in IFN-γ production between vaccinated and unvaccinated groups (Figure 5.12D-F). Advax^{CpG} has been shown in previous studies to induce a Th17 response in the lungs, which is characterised by expression of the transcription factor RORγT, as well as expression of the classical Th17 cytokine, IL-17 (Counoupas et al., 2020). Indeed, the addition of Advax^{CpG} resulted in higher proportions of CD4$^+$ T cells expressing RORγT and IL-17 in response to pulmonary *M. abscessus* infection (Figure 5.12G-I). Analysis of overall cytokine responses in the mLN showed that only γ-*Mabs*+Advax^{CpG}-vaccinated mice demonstrated significantly higher proportions of IFN-γ, IL-2, IL-17 and TNF cytokine expressing CD4$^+$ T cells compared to unvaccinated mice (Figure 5.13A-B; P<0.05, P<0.001, P<0.05, P<0.001, respectively). In addition, mice vaccinated with γ-*Mabs*+Advax^{CpG} showed significantly higher proportions of all polyfunctional T cell subsets in mLN compared to mice vaccinated with γ-*Mabs* alone (Figure 5.13C-F).

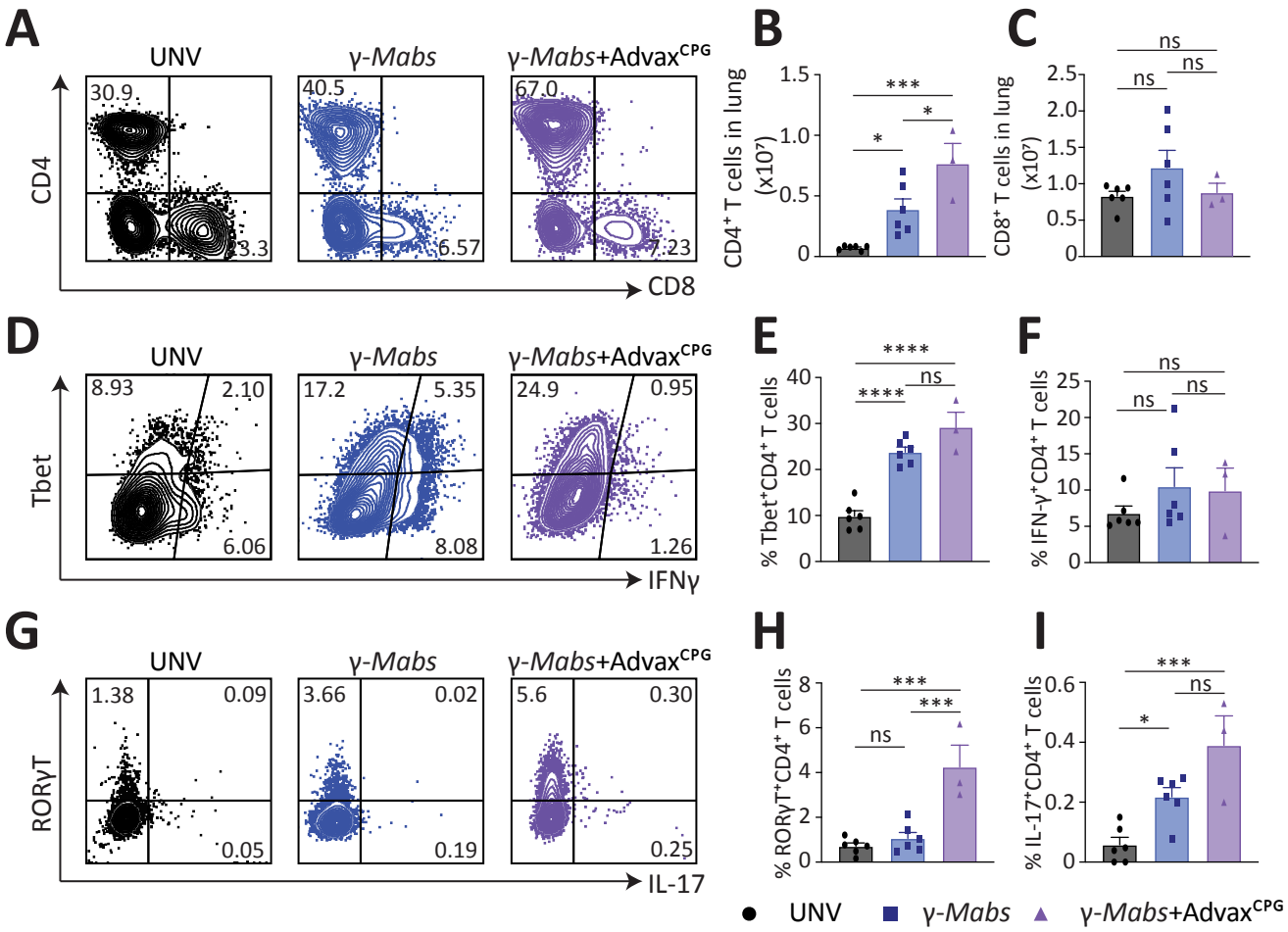

Figure 5.12. T cell recruitment and phenotype in the lungs of mice vaccinated with γ-irradiated vaccine alone or with adjuvant following pulmonary *M. abscessus* challenge. Vaccination and *M. abscessus* challenge was performed as described in Figure 5.11. Lungs were processed into single cell suspension and restimulated *ex vivo* with 10^5 CFU *M. abscessus*. Cells were stained for $CD4^+$ and $CD8^+$ T cells **(A-C)**, as well as transcription factors Tbet- **(D-E)** and RORγT-expressing $CD4^+$ T cells **(G-H)** and IFN-γ **(D, F)** and IL-17-producing $CD4^+$ T cells **(G, I)**. Data is expressed as representative FACS plots as well as mean cell number or percentage in the lung SEM. Statistical significance was determined by ANOVA (*P<0.05, **P<0.01, ***P<0.001, ****P<0.001; ns=no significance).

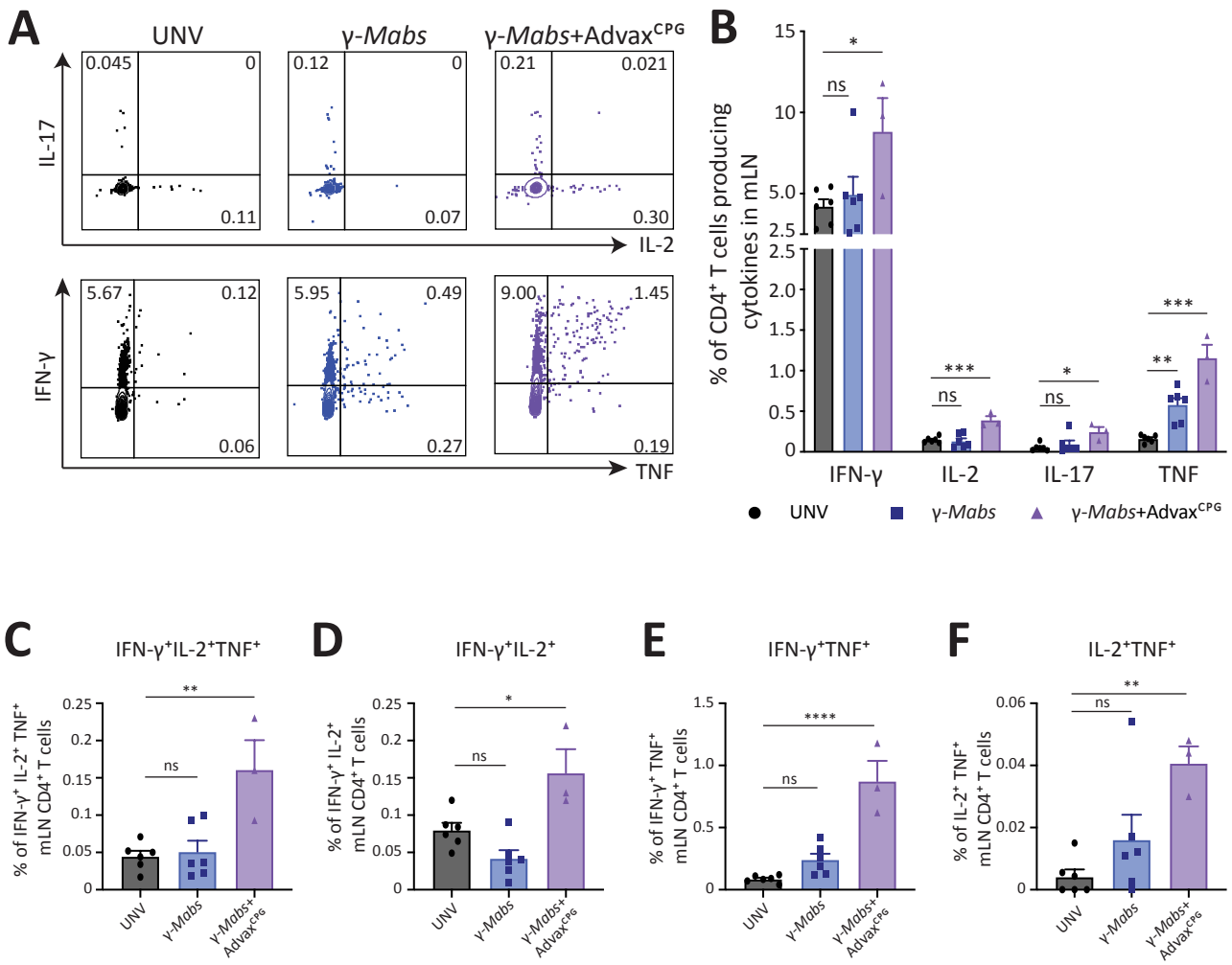

Figure 5.13. T cell recruitment and phenotype in the mediastinal lymph nodes of mice vaccinated with γ-irradiated vaccine alone or with adjuvant following pulmonary *M. abscessus* challenge. Vaccination and *M. abscessus* challenge was performed as described in Figure 5.11. Mediastinal lymph nodes were processed into single cell suspension and restimulated *ex vivo* with *M. abscessus*. **(A-B)** Representative FACS plots and mean proportion ± SEM of cytokine producing $CD4^+$ T cells in the mLN. **(C)** Percentage of polyfunctional CD4+ T cells in the mLN. Statistical significance was determined by ANOVA (*P<0.05, **P<0.01, ***P<0.001, ****P<0.001; ns=no significance).

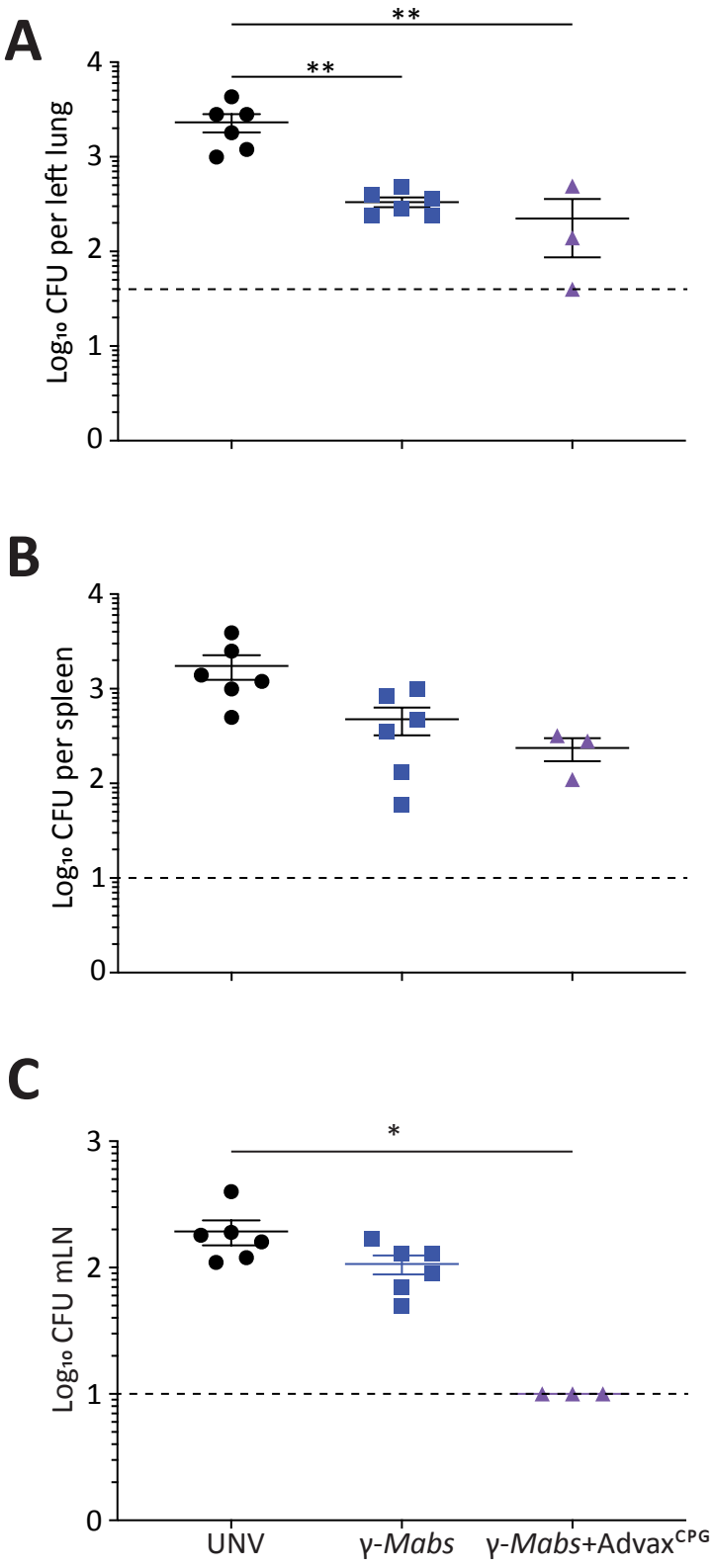

Figure 5.14: Protection conferred by γ-irradiated vaccination alone or with adjuvant following pulmonary *M. abscessus challenge*. C57BL/6 mice (n=6) were vaccinated and challenged as described in Figure 5.11. Mice were euthanased 7 days post-challenge and bacterial load was assessed in the lungs **(A)**, spleen **(B)** and mediastinal lymph nodes **(mLN; C)**. Data is presented as log_{10} CFU±SEM and statistical significance was determined by ANOVA (*P<0.05, **P<0.01). Dashed line = limit of detection.

To determine if the increased immunogenicity of γ-*Mabs*+Advax^{CpG} resulted in greater protection against infection, the bacterial load in lungs, spleen and mLN was examined. Both γ-*Mabs* alone or γ-*Mabs*+Advax^{CpG} vaccinated groups showed a significant reduction inbacterial load in the lungs compared to unvaccinated mice (Figure 5.14A; $P<0.01$). Addition of Advax^{CpG} did not significantly enhance protection conferred by the irradiated vaccine. In the spleen, mice vaccinated with γ-*Mabs*- Advax^{CpG} had a lower CFU burden, however this did not reach statistical significance (Figure 5.14B). In the mLN, there was no significant protection conferred by γ-*Mabs* vaccination alone (Figure 5.14C). However, γ-*Mabs*- Advax^{CpG} resulted in significantly less bacterial load in the mLN compared to unvaccinated mice (Figure 5.14C; $P<0.05$). Thus, this data suggests that the addition of Advax^{CpG} to γ-*Mabs* vaccination might confer a level of protection against disseminated *M. abscessus* infection.

5.3. Discussion

At the time of writing, no vaccines are currently licensed for the prevention of *M. abscessus* infection. This study aimed to evaluate three whole-cell inactivated vaccines (WCVs) created from the same *M. abscessus* clinical isolate to determine if the method of inactivation impacts the development of protective immunity. All vaccine approaches tested; γ-irradiation, heat killing (HK) or paraformaldehyde (PFA) treatment, were successful at rendering the bacteria non-viable (Figure 5.1). This is an important consideration for vaccine development, given that *M. abscessus* often infects those with underlying immune or respiratory conditions (Ademhan Tural et al., 2021), making live vaccine strategies problematic for targeting at risk populations (something like that). In addition, the γ-irradiated candidate was the only vaccine that retained metabolic activity at rates comparable to live cultures. Gamma irradiation affects DNA and RNA, but leaves the rest of the cell to function (Babb et al., 2016). This is in contrast to HK and PFA-inactivating techniques, where proteins, as well as nucleic acids, are damaged (Fertey et al., 2016; Sabbaghi et al., 2019). Indeed, a study comparing γ-irradiated *Brucella abortus* – an intracellular pathogen – to HK *B. abortus* showed an association between the preserved metabolic activity and the immunogenicity of these vaccines (Sanakkayala et al., 2005). This was reflected in *in vitro* studies of the immunogenicity of *M. abscessus* vaccine candidates. Gamma-irradiation was consistently more inflammatory than other inactivation types, resulting in significantly higher CCL3, CCL5, CCL22, and IL-6 production (Figure 5.2). These chemokines and cytokines function to enhance migration, activation and proliferation of monocytes, macrophages, neutrophils and T-helper lymphocytes, all of which were consistent with *in vivo* findings (Baba & Mukaida, 2014; Culley et al., 2006; Rapp et al., 2019).

Subcutaneous γ-irradiated vaccination induced significantly more circulating Th1-type $CD4^+$ T cells; that is, more Tbet-expressing, as well as IFN-γ- and TNF-producing $CD4^+$ T cells (Figure 5.3). HK vaccination also induced significant numbers of Tbet-expressing $CD4^+$ T cells, without impacting cytokine production. The production of vaccine-specific circulating Th1 cells has previously been shown to be critical in protection against mycobacterial infection (Counoupas et al., 2020; Counoupas et al., 2017; Lindenstrøm et al., 2009). More recently, the role of circulating multifunctional Th1 cells were shown to correlate with *M. abscessus* disease control in a large cohort study (Shu, Wu, et al., 2019). Post-infection assessment of the adaptive immune response to *M. abscessus* vaccination showed that γ-

irradiated and HK vaccines induces a greater magnitude of $CD4^+$ T cell influx into the lung as well as potent Th1 responses, which correlates with reduction in bacterial load (Figure 5.9). Th1-type cells have been well-characterised in the context of mycobacterial vaccination and their role in protection against mycobacterial challenge. The production of IFN-γ by Th1 cells significantly enhances innate immune responses to infection, through activation and recruitment of macrophages, enhanced antigen presentation and potent stimulation of iNOS production (Thirunavukkarasu et al., 2017). Indeed, this is reflected in the current study; the more potent Th1 response observed in mice vaccinated with γ-irradiated and HK vaccines correlates with greater IM, neutrophil and $CD103^+$ DC recruitment, as well as significantly more iNOS production. Further, the more rapid accumulation of effector-type $CD4^+$ cells ($CD44^+CD62L^-$) in the lungs following mycobacterial challenge has been correlated with more effective clearance of bacterial load (Jung et al., 2005). While a greater magnitude of the effector response was observed in this Chapter, it would be interesting to investigate whether vaccination with γ-*Mabs* or HK-*Mabs* improves the kinetics of effector Th1 cell recruitment to the lungs following pulmonary challenge.

Gamma-irradiated and HK vaccines induced significant protection in the lungs upon pulmonary *M. abscessus* challenge, whereas PFA-*Mabs* vaccination did not (Figure 5.4). These findings can be correlated with the innate and adaptive immune responses in the lungs following infection. It has been shown previously in this thesis that there is a unique innate immune response to *M. abscessus* in the lungs following infection; that is, iNOS-producing IMs appear to be the most important myeloid cell subset in clearing *M. abscessus* (Chapter 3). Indeed, both γ-*Mabs* and HK-*Mabs*-vaccinated mice had significantly increased numbers of IMs in the lungs following *M. abscessus* infection (Figure 5.7). Further, iNOS production appeared to be specifically produced by IMs in these groups, a cell type that has a major role in bacterial clearance (Bogdanovski et al., 2020; MacMicking et al., 1997). Here, we confirm the findings in Chapter 3 that iNOS-producing IMs are crucial in controlling *M. abscessus* infection, and the proportion of these cells directly correlates with pulmonary bacterial burden. It is also possible that the protection associated with IMs seen in this Chapter may be due to the ability of IMs to traffic to the mediastinal draining lymph nodes (mLN) and enhance antigen presentation to T cells. This has been demonstrated in the literature, as IMs have been shown to express high levels of MHCII for antigen presentation (Chakarov et al., 2019). This could validated by assessing the antigen presenting function of IMs after exposure to *M. abscessus* by using methodology previously developed to assess these functions (Hou et al., 2021).

Vaccination with γ-*Mabs* and subsequent pulmonary *M. abscessus* challenge also induced significantly lower numbers of monocytes in the lungs when compared to unvaccinated mice (Figure 5.7). IMs appear to be derived from monocytes, as evident by expression of Ly6C, CX3CR1 and CD11b (Huang et al., 2018). It is possible that γ-*Mabs* vaccination results in rapid migration and differentiation of monocytes into IMs in the lungs upon *M. abscessus* challenge, resulting in the observed reduction in monocyte populations. It would be interesting to investigate this further using fluorescent reporter mice that can track monocyte migration and differentiation. Conversely, vaccination with γ-*Mabs* and HK-*Mabs* resulted in significant influx of neutrophils, $CD11b^{mid}$ cells and $CD103^{+}$ DCs (Figure 5.7) after pulmonary challenge. Neutrophil accumulation is associated with granuloma formation and containment of *M. abscessus* infection (Bernut et al., 2016). NK cells have been shown to play an important role in *M. fortuitum* infection. Antibody depletion of NK cells, as well as infection of NK-deficient beige mice resulted in significantly increased susceptibility to infection (Tomioka et al., 2004). It has been proposed that NK cells mediate their effect on mycobacterial clearance by enhancing intracellular killing of mycobacteria, or by enhancing production of inflammatory cytokines such as IFN-γ and TNF, which potentiate the microbicidal activity of macrophages in the infection microenvironment (Bermudez et al., 1995; Brill et al., 2001). $CD103^{+}$ DCs are known to play a role in transport of mycobacteria to the mLN following infection and early activation of T cells, in the context of *M. tuberculosis* infection (V. H. Q. Koh et al., 2017). It is possible that this holds true for *M. abscessus* infection as well. Further, the increased activity of IMs, neutrophils, and NK cells in the lung may also explain the reduction in the number of AMs seen in mice vaccinated with γ-irradiated *M. abscessus*. Given that AMs are the primary host of *M. abscessus* infection, combined with the magnitude of IM, neutrophil and $CD11b^{mid}$ cell influx into in the lungs of vaccinated mice, γ-*Mabs* vaccination may induce more significant killing of *M. abscessus*-infected AMs (Johansen et al., 2020). Further characterisation of $CD11b^{mid}$ cells as NK cells would be required to delineate these notions.

Mucosal delivery of vaccines has been increasingly recognised as an attractive strategy to induce more localised immunity and enhance rapid elimination upon pulmonary bacterial challenge (Bull et al., 2019; Moliva et al., 2019). Thus, intranasal delivery of γ-irradiated *M. abscessus* was assessed in this Chapter. However, while subcutaneous γ-*Mabs* vaccination induced a myriad of immune responses that correlated with protection, the same was not observed with intranasal administration of *M. abscessus.* Importantly, the lack of protection

conferred by i.n. γ-*Mabs* vaccination also correlated with reduced numbers of IM and limited iNOS expression (Figure 5.7 & 5.8). Intranasal vaccination also induced a higher proportion of iNOS-expressing AMs compared to the s.c. route. This may be reflective of a more localised response to infection, rather than systemic recruitment of IMs as observed with s.c. vaccination (Huang et al., 2018). Future studies may seek to define the inflammatory response in the lung parenchyma after i.n. vaccination before *M. abscessus* challenge, to more discretely identify the local immune response to vaccination, such as the presence of tissue-resident memory T cells (TRMs). TRMs have been shown to be a key mediator in mucosal vaccination, as they rapidly respond to secondary antigen challenge in the absence of circulating memory cells to afford enhanced protection (Darrah et al., 2020; Perdomo et al., 2016).

Mucosal vaccination with γ-irradiated *M. abscessus* induced a significant humoral response in the lungs to *M. abscessus* challenge (Figure 5.10). Indeed, mucosal delivery of a γ-irradiated streptococcal vaccine induced potent humoral responses which correlated with protection against subsequent streptococcal challenge (Babb et al., 2016). However, the role of B cells in mycobacterial infection is more contentious, and does not always correlate with protection (Rottman et al., 2007). It is possible that the presence of B cells and antibodies is reflective of inducible bronchus-associated lymphoid tissue (iBALT) formation in the lungs; a niche similar to secondary lymphoid tissue that has been shown to promote the survival of TRMs (Schreiner & King, 2018). Further imaging studies would be required to assess the localisation of B cells in the lungs following *M. abscessus* challenge in i.n. vaccinated mice.

The addition of adjuvants to vaccines have been shown to enhance the initial innate immune response, consequently mediating an increased engagement of the adaptive immune response (Awate et al., 2013; Reed et al., 2013). Advax^{CpG} is one such adjuvant that is currently being evaluated in many vaccine studies. Advax is a delta-inulin polysaccharide adjuvant which has been formulated with CpG, a TLR9 agonist which has been shown to induce strong Th1 polarisation when combined with protein subunit vaccination (Counoupas et al., 2017). While addition of Advax^{CpG} to γ-*Mabs* vaccination did not significantly enhance clearance of *M. abscessus* from the lungs compared to γ-*Mabs* alone, there was marked a reduction in bacterial load in the mLN (Figure 5.11). This correlated with enhanced cytokine expressing CD4$^+$ T cells in the mLN, that may serve to limit bacterial replication at that site (Figure 5.14). Interestingly, Advax^{CpG} significantly increased proportions of 'multifunctional'

$CD4^+$ T cells that have been shown to mediate rapid effector functions following infection, resulting in earlier bacterial clearance (Seder et al., 2008). Further, the greater proportion of $CD4^+TNF^+IL\text{-}2^+$ T cells seen here have been previously identified to have a higher proliferative capacity, which has been correlated with protective efficacy in murine models of *M. tuberculosis* infection (Lindenstrøm et al., 2009). Coformulation of $Advax^{CpG}$ with γ-*Mabs* did not increase Th1 cell responses in the lung of vaccinated mice; this may explain why there was no significant difference in pulmonary bacterial load between these groups. However, significant Th17 responses were observed in γ-*Mabs*+ $Advax^{CpG}$ vaccinated mice. It has been postulated that Th17 responses to mycobacterial infection trigger chemokine responses, which lead to the recruitment of T cells to the lungs (Kay et al., 2018). Previous studies within our laboratory have demonstrated that mucosal vaccination with $Advax^{CpG}$ stimulates the production of tissue-resident Th17 responses following *M. tuberculosis* infection. Additionally, these cells were shown correlate with recruitment of neutrophils and macrophages to the lungs following *M. tuberculosis* infection (Counoupas et al., 2020). Thus in this study, it is possible that the addition of $Advax^{CpG}$ to γ-*Mabs* vaccination induced more Th17 responses, thereby mediating the inflammatory milieu in the lungs following *M. abscessus* infection. Indeed, addition of $Advax^{CPG}$ to γ-*Mabs* vaccine enhanced the magnitude of innate immune cell responses, including monocytes and neutrophils numbers in the lung following *M. abscessus* challenge (Figure 5.12). $Advax^{CpG}$ is known to induce significant neutrophil and monocyte recruitment through potent chemoattractant and cytokine production (Counoupas et al., 2017; Ferrell et al., 2021).

While the addition of $Advax^{CpG}$ to γ-*Mabs* vaccination shows promise, caution must be taken when evaluating it as a potential vaccine candidate. Three of six mice showed extensive ulceration at the site of vaccination that was not seen with γ-*Mabs* vaccination. It is known that IL-17-mediated inflammation can be detrimental to the host, and a delicate balance must be struck between protection and pathology (Das & Khader, 2017). Thus the combination of γ-irradiated *M. abscessus* with $Advax^{CpG}$ may be too inflammatory for human use. One potential strategy to dampen the deleterious excessive inflammation while preserving immunogenicity of the vaccine is through delipidation of *M. abscessus* before undergoing the γ-irradiation process. Delipidation removes pro-inflammatory lipids present in the mycobacterial cell wall, while maintaining the antigenicity of proteins (Tran et al., 2016). Indeed, delipidation of BCG has been shown to reduce immunopathology while maintaining protective efficacy against *M. tuberculosis* (Moliva et al., 2019).

In conclusion, this study has identified γ-irradiated *M. abscessus* as a novel vaccine against *M. abscessus* infection. The vaccine would be safer to use in immunocompromised hosts compared to live-attenuated vaccines, while the conservation of metabolic activity may permit the prolonged secretion of metabolites and antigens, creating a 'self-adjuvanting vaccine'. Systemic vaccination with γ-irradiated *M. abscessus* affords significant protection against subsequent pulmonary *M. abscessus* challenge, which correlated with the induction of iNOS-producing IMs and the recruitment of Th1 $CD4^+$ T cells to the lungs. This study thus identified a vaccine strategy that induced an immune profile which correlated with the immune control of *M. abscessus* infection identified in Chapter 3. This was further confirmed by the use of vaccine approaches that were unable to afford significant protective efficacy and were poor stimulators of iNOS-producing IMs and Th1 cell recruitment. This Chapter also demonstrated that while addition of adjuvants can enhance the immunity imparted by γ-irradiated *M. abscessus,* enhanced inflammation in the lungs and the site of vaccination may be detrimental, highlighting the need to balance vaccine efficacy with safety.

Chapter 6: General Discussion

Mycobacterium abscessus is a pathogen of increasing concern within susceptible populations such as those with Cystic Fibrosis (CF) and Chronic Obstructive Pulmonary Disease (COPD) (Johansen et al., 2020). Both intrinsic and acquired antibiotic resistance genes have rendered *M. abscessus* an extremely difficult pathogen to treat (Daley et al., 2020). Given that the prevalence of *M. abscessus* infections in CF patients is rising, combined with evidence of patient-to-patient transmission and the difficulty in treating it, development of a vaccine to prevent the initial acquisition of *M. abscessus* infection and/or limit disease severity is desperately needed (Martiniano et al., 2022). However little progress has been made in this area. Some cross-reactivity between BCG – the only currently licensed TB vaccine – and *M. abscessus* has been proposed, yet cross-protection in animal models or humans has not been demonstrated (Abate et al., 2019). DNA and subunit vaccine candidates have been identified, yet at the time of writing none have progressed to clinical development (Le Moigne, Belon, et al., 2016; Le Moigne, Gaillard, et al., 2016; Le Moigne, Roux, et al., 2020).

In order to develop a vaccine, a robust animal model in which to evaluate novel candidates is required, in particular to allow precise definition of immune cell subsets important for infection. Despite the growing need for a vaccine, as well as new antimicrobials to combat infection, the literature regarding animal models is heterogenous. Murine models are the most suitable for preclinical assessment of vaccine candidates, however there are large variations in mouse or *M. abscessus* strains used, infection route and dose (Nicola et al., 2022). Further, limited literature exists regarding the immune correlates of protection for pulmonary *M. abscessus* infection. Therefore the overarching aims of this thesis were to firstly determine if a pulmonary murine infection model of *M. abscessus* could be used to identify the immune cell subsets that are important in clearance of infection. Subsequently, the possibility of repurposing the BCG vaccine for *M. abscessus* control was investigated, as well as the vaccine potential of three whole-cell inactivated *M. abscessus* candidates.

6.1. Infection models for assessment of *M. abscessus* host-pathogen interactions and preclinical evaluation of vaccine efficacy

A wide heterogeneity exists in the literature regarding animal models used for preclinical evaluation of therapeutics and vaccine candidates against pulmonary *M. abscessus*

infection. Immunodeficient mouse models are commonly used for preclinical assessment of novel therapeutics, however lack of defined immune components may hinder their use for determining vaccine effectiveness and defining immune correlates of protection. In this thesis, an intranasal, pulmonary infection model using immunocompetent C57BL/6 mice was employed, utilising an immunogenic clinical *M. abscessus* isolate that was selected from a library of strains (Chapter 3). This model allowed immune cell subsets to be identified that were clearly pertinent in the clearance of pulmonary *M. abscessus* infection. Le Moigne and colleagues (2020) used C3HeB/FeJ mice to examine the efficacy of a bedaquiline-imipenem treatment combination, as C3HeB/FeJ mice have a higher susceptibility to mycobacterial infection due to their lack of intracellular pathogen resistance 1 (*Ipr1*) (Kramnik et al., 2000). However, in this thesis persistent *M. abscessus* infection in C3HeB/FeJ mice was not observed; this difference may be due to the intravenous route used in the Le Moigne study, which may allow greater bacterial colonisation and persistence, but is not representative of the natural *M. abscessus* infection in humans. As such, the intranasal route used here is less labour intensive and more reproducible than other models used, such as aerosol delivery or intratracheal delivery of *M. abscessus*-coated agar beads (Ordway et al., 2008; Riva et al., 2020). Thus this thesis described a simple and effective murine model in which to study *M. abscessus* infection and host-pathogen interactions (Chapter 3), assess vaccine efficacy (Chapters 4,5) and potentially test novel antimicrobials.

It is important to note that almost all previous studies in the literature have utilised a single reference strain of *M. abscessus*, ATCC19977, also known as CIP104536^{T} (Gupta et al., 2018). This strain is a clinical isolate of unknown origin that was first described in 1992 (Kusunoki & Ezaki, 1992). The variation in virulence between different *M. abscessus* strains may explain the differential growth pattern observed between the isolates used in this thesis, and the previous studies using similar animal models (Boeck et al., 2022; Nicola et al., 2022). Indeed in the current study, rough *M. abscessus* strains displayed higher rates of phagocytosis and persistence in macrophages *in vitro* and elicited higher cytokine responses (Chapter 3). This is in keeping with previous findings that the lack of glycopeptidolipids (GPLs) on rough phenotypes exposes TLR2 agonists, leading to high levels of TNF expression and inflammation (Davidson et al., 2011). Interestingly, there was no appreciable difference in pulmonary bacterial load between smooth and rough strains *in vivo*, despite well-documented differences between smooth and rough phenotypes existing in the literature (Bernut et al., 2014; Jönsson et al., 2013). This may relate to strains differences overriding any morphotype-specific effects; matched S and R strains from each

isolate would account for this and is a future avenue of investigation. Previous studies suggest that infection with rough phenotypes drive a Th1 response in the host, while the presence of GPLs on smooth variants drive a more humoral-mediated response (Kam et al., 2022). While an appreciable difference in $CD4^+$ T cell infiltration into the lungs was observed between rough and smooth phenotypes (Chapter 3), more detailed analysis of humoral responses is required to further delineate the complex dichotomy between smooth and rough *M. abscessus* variants. Understanding this could allow more targeted pathogen-and host-directed therapies to combat *M. abscessus* infection, such as phage or immunomodulatory therapies (Nick et al., 2022). Further, while we did not have access to data on the clinical progression of infected individuals for the strains used in this thesis, such information would be useful to correlate strain characteristics with clinical outcome. A recent study has shown that rough *M. abscessus* isolates are associated with radiological evidence of cavitary lesions and have a significantly lower odds ratio of clinical cure when compared to smooth isolates (Hedin et al., 2023). Being able to predict clinical outcome based on morphology and genotyping of the strain would be useful to determine the best course of action for treatment and prioritise lung transplantation.

6.2. The interplay between interstitial macrophages and $CD4^+$ T cells for protective immunity to pulmonary *M. abscessus* infection.

This thesis provides a detailed framework for the interaction of immune cell subsets and mediators in response to pulmonary *M. abscessus* infection and the immune correlates of protection against infection. A visual summary of the mechanisms of protection against pulmonary *M. abscessus* challenge can be found in Figure 6.1. It is likely that alveolar macrophages (AMs) are the primary infection source of *M. abscessus,* as seen with other pathogenic mycobacteria (Cohen et al., 2018). Early production of pro-inflammatory cytokines (e.g. G-CSF, CXCL1, IL-6 and TNF) correlates with neutrophil accumulation in the lung (Chapter 3); G-CSF promotes recruitment, proliferation, differentiation and maturation of neutrophils at the site of infection, and CXCL1 is also essential in neutrophil trafficking to the lung (Cai et al., 2010; Roberts, 2005). The early production of IL-6 may also reflect its role in differentiation of monocytes into macrophages by potentiating M-CSF expression, as well as migration and activation of interstitial macrophages (IMs) (Velazquez-Salinas et al., 2019). In addition, IMs are recruited to the lung from the blood via CCL2 chemokine gradient

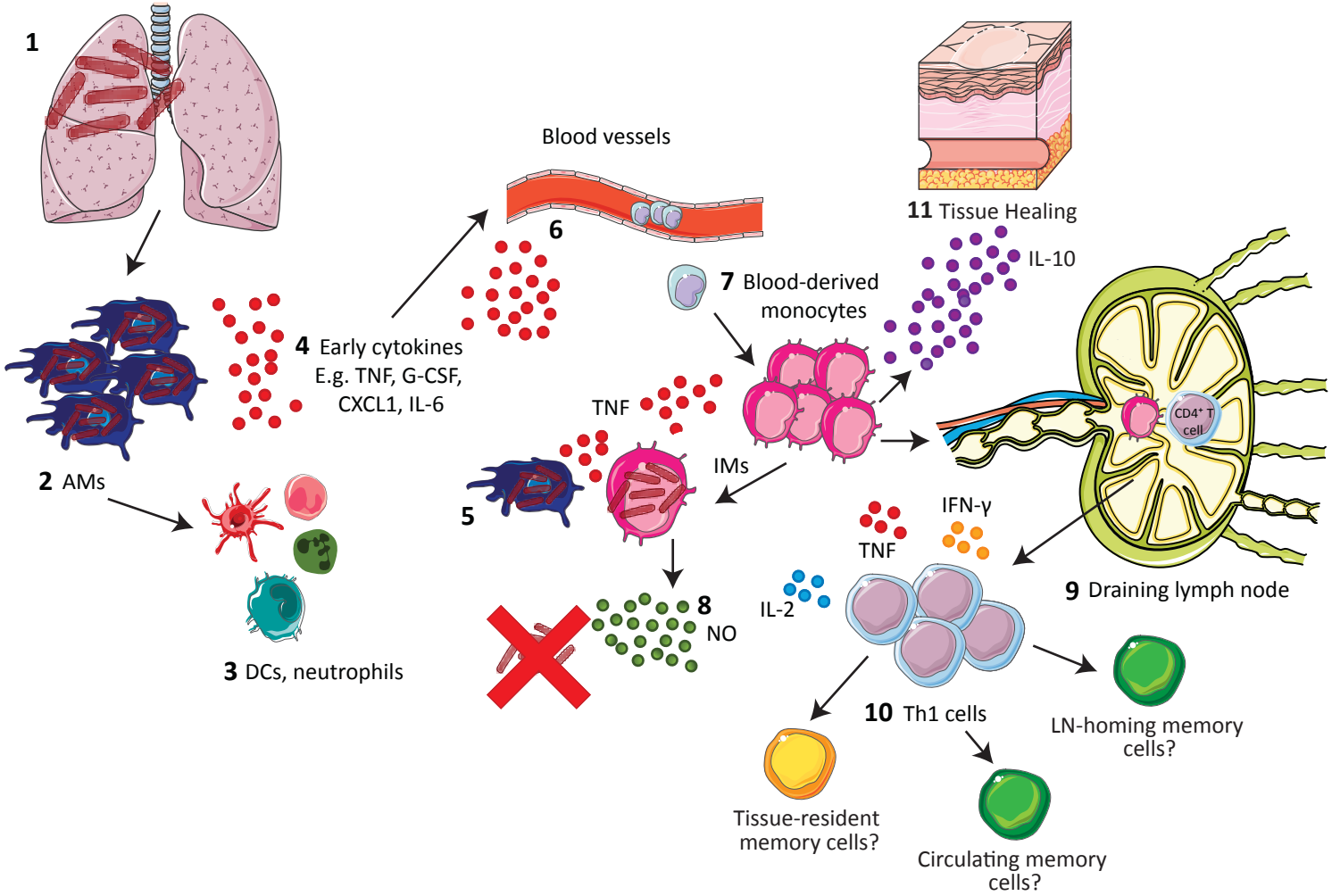

Figure 6.1: Immune response to pulmonary *M. abscessus* infection proposed in this thesis. (1) Intranasal *M. abscessus* infection results in **(2)** engulfment of bacilli into alveolar macrophages (AMs) on the bronchial side of lung tissue, leading to local inflammation including cytokine release and **(3)** recruitment of neutrophils and dendritic cells (DCs). **(4)** TNF and early cytokines, as well as **(5)** AM migration into the lung parenchyma, leads to activation of interstitial macrophages (IMs). Chemoattraction results in **(6)** recruitment of monocytes from the blood and **(7)** differentiation into IMs, amplifying the IM response. **(8)** IMs expression large amounts of iNOS which leads to NO-mediated killing of *M. abscessus*. **(9)** IMs also migrate to draining lymph nodes, expressing MHCII to recruit CD4+ T cells. **(10)** Th1 cells migrate to the lung and further enhance clearance of *M. abscessus*. Later in infection, **(11)** IMs produce IL-10, to dampen inflammation and promote tissue repair.

(Liegeois et al., 2018) and this thesis identified two major roles for this subset: direct antimicrobial effect by induction of iNOS expression, together with expansion of $CD4^+$ T cells to drive Th1 polarization and recruitment (Chapter 3). IMs have been shown to have a significantly increased rate of killing of *M. tuberculosis* when compared to AMs and neutrophils, and clodronate depletion of IM populations leads to significant increases in bacterial load (Huang et al., 2018). IM recruitment is dependent on TNF (Chapter 3); this may be explained by TNF's capacity to induce expression of chemokines and chemoattractants required for macrophage recruitment to the site of infection, as well as proliferation and differentiation of macrophages within the lung tissue (Algood et al., 2004; Guilbert et al., 1993; Witsell & Schook, 1992). The majority of inducible nitric oxide synthase (iNOS) production in the lungs following *M. abscessus* challenge comes from IMs, which was also TNF dependant (Chapter 3). Expression of iNOS leads to the production of nitric oxide (NO), which is essential for intracellular killing of *M. abscessus* (Lee et al., 2017) and can also act as a second messenger, driving IL-12R expression, IFN-γ production and subsequently, Th1 polarization (Niedbala et al., 2002). IMs induced after *M. abscessus* infection also displayed significant MHCII expression, which may implicate a role for antigen presentation to T cells and subsequent recruitment of the adaptive immune system.

These findings not only provide insight into the role of IMs, $CD4^+$ T cells, TNF and iNOS in clearance of *M. abscessus* infection, but also provide targets for therapies. In a disease where antimicrobials are often futile, host-directed therapies are an attractive alternative, as the emergence of resistance is significantly reduced. The role of iNOS and NO identified in this thesis provides further support for the emerging development of NO therapies for multi-drug resistant strains of *M. abscessus*. Indeed, inhaled NO therapies are currently in Phase II clinical trials for CF patients with pulmonary *M. abscessus* disease, where they have been shown to reduce bacterial load in the sputum, and improve lung function (Bentur et al., 2020; Quang & Jang, 2021; Yaacoby-Bianu et al., 2018). Aerosolised IFN-γ therapy has been evaluated in the context of drug-resistant *M. tuberculosis* infection; studies have shown reduced time to sputum conversion, and when used as an adjunct to antimicrobial therapy, facilitation of lung repair (Dawson et al., 2009; Gao et al., 2011). More recently, macrophage and monocyte microRNA has declared itself as an exciting host-directed therapy which may be able to target and modulate macrophage functions, to enhance host-mediated defences against TB (Sampath et al., 2021). Finally, the emergence of immunometabolism and its differential effect on macrophage phenotypes also provides an area of future research (Sheedy & Divangahi, 2021). Understanding the role of IMs in regulating inflammation and

role in infection and immunity may reveal targets to potentiate this effect with immunometabolic stimuli.

The vaccine studies in this these provide additional insights into the requirements for protection against *M. abscessus* infection. In Chapter 4, we demonstrate that BCG is not strongly protective against *M. abscessus* challenge in our model; however, in Chapter 5, subcutaneous vaccination with whole-cell inactivated (WCI) *M. abscessus* – namely γ-*Mabs* and HK-*Mabs* – are protective. Assessment of the immune cells present in the lungs of these different vaccination groups provide crucial insight into the correlates of protection. Most importantly, γ-*Mabs* and HK-*Mabs* induce significant IM responses in the lungs and subsequent iNOS production, whereas BCG does not. To our knowledge, this is the first study to directly correlate IMs with protection against *M. abscessus* infection. Most *M. abscessus* vaccination studies have focused primarily on the humoral response, despite cellular immunity being well-established as the more predominant mediator of mycobacterial immunity (Le Moigne, Gaillard, et al., 2016). While both BCG and WCI vaccines induced strong Th1 cell infiltrates in the lungs, WCI vaccination (specifically γ-*Mabs*) were able to induce more polyfunctional $CD4^+$ T cells. Previous studies have detailed the inability of peripheral BCG vaccination to induce strong pulmonary T cell responses, and this observation has been postulated to at least partially explain the mixed data regarding BCG vaccination and only partial protection against TB (Horvath et al., 2012). The role of polyfunctional Th1 cells has emerged as a more accurate correlate of protection in mycobacterial infection. In *M. tuberculosis* infection, polyfunctional $CD4^+$ T cells display increased proliferative capacity which is associated with better disease control (Day et al., 2011). More recently, polyfunctional $CD4^+$ T cells isolated from CF patients with NTM disease also correlated with improved control of disease (Shu, Pan, et al., 2019). In summary, these findings provide a platform for future evaluation of *M. abscessus* vaccine candidate, and may be applicable to assessment of candidates for other mycobacterial pathogens.

6.3. Repurposing old vaccines and identifying new candidates for control of *M. abscessus* infection

While BCG vaccination did not succeed in conferring protection against *M. abscessus* challenge, the findings in this thesis provide a platform for future development. BCG vaccination induced significant circulating *M. abscessus*-specific multifunctional $CD4^+$ T

cells, and significantly prevented dissemination of *M. abscessus* infection to the spleen. It is possible that some of the cross-reactivity and protection immunity observed here may be non-specific and is trained immunity. Trained immunity is the concept of an innate immune system-mediated response to secondary infection with either the same or different pathogen, that results in an enhanced immune response, independent of T and B-lymphocytes (Netea et al., 2011). In healthy volunteers, BCG vaccination resulted in high levels of IL-1β and IL-6 production in NK cells when stimulated with *M. tuberculosis, S. aureus* and *C. albicans* (Kleinnijenhuis et al., 2014). BCG vaccination also triggers metabolic reprogramming which has an effect on the function of innate immune cells (Arts et al., 2016; Covián et al., 2019). Not only is the production of these memory-like innate immune cells important for early control of infection, inducing trained immunity within the bone marrow would lead to the generation of immune cell populations with a greater capacity to respond to pathogens, and subsequently elicit stronger engagements with the adaptive immune system, leading to the generation of stronger and longer lasting memory T and B cell populations (Covián et al., 2019). Delineating whether the partial protection afforded by BCG in this model is due to shared antigenicity or some aspect of trained immunity is an interesting avenue for future research.

BCG also serves as an excellent vector for a recombinant vaccine. It is safe, and relatively easy and inexpensive for mass production (Kilpeläinen et al., 2018). Indeed, recombinant BCG (rBCG) has been explored as a TB vaccine candidate. VPM1002 is a rBCG vaccine candidate expressing listeriolysin (LLO), a toxin isolated from *Listeria monocytogenes*, currently in Phase III clinical trials. VPM1002 has shown promise in clinical evaluation through its broad and strong T cell response to TB, by enhancing inflammasome activation (Grode et al., 2013; Loxton et al., 2017). rBCG vaccines have also been designed for other pathogens. Recently, rBCG expressing the nucleoprotein of respiratory syncytial virus (RSV) has been evaluated in Phase I clinical trial, which showed strong neutralising antibody production and significantly increased IFN-γ and IL-2 production by T cells (Abarca et al., 2020). Thus, protective effect of BCG could be improved by either using modified rBCG strains such as VPM1002 with enhanced immunomodulatory activity, or the development of BG strains expressing immunogenic components of *M. abscessus* that are absent from the vaccine.

Given that *M. abscessus* primarily infects individuals with a partially compromised immune system, WCI methods are an attractive vaccine design strategy compared to live-attenuated

vaccines such as BCG. While eliminating the potential for reversion to virulence, WCI vaccines preserve the full antigenic spectrum of the cell, which is thought to invoke a more robust immune response and immunological memory (Van Rhijn & Moody, 2015). Further, WCI vaccines tend to be more stable than live vaccines, rendering them a more practical vaccine (Vetter et al., 2018). However, the inactivation processes such as heat or chemical inactivation are harsh on the cells, and have been shown to denature membrane proteins which affects the immunogenicity of antigens. Gamma-irradiation was highlighted in this thesis as a promising tool in the future of vaccine design. Gamma-irradiation disrupts the nucleic acids within cells while leaving proteins unaffected, thereby preserving antigenic epitopes and their immunologic potential (Babb et al., 2016). In this thesis, γ-*Mabs* showed superior vaccine potential when compared to other inactivation types (Chapter 5). These findings support current γ-irradiation vaccines targeting other pathogens. Of note, an intranasal irradiated pneumococcal vaccine has been developed which confers significantly more protection, greater pneumococcal-specific antibody responses within the respiratory tract, significantly more DC maturation and recruitment of follicular T helper cell populations when compared to its heat- or chemically-inactivated counterparts (Ko et al., 2021). In January 2023, this vaccine has progressed to Phase I clinical trial (Clinical Trials Identifier NCT05667740). This provides an important framework for the clinical testing of other irradiated vaccines that progress through preclinical development, such as γ-*Mabs.*

6.4. Relevance of findings to control of lung disease

While this thesis provides strong evidence for the protective role of the immune cell types and vaccine candidates, care must be taken in applying these findings to the human situation, in particular individuals with CF. Most studies of IMs have been performed in animal models, however some studies have compared and contrasted the macrophage landscape of murine and human tissues. In these studies, similarities have been identified, with respect to phenotypic markers and phagocytic capacity (Bharat et al., 2016). Further, given the complex and dynamic environment of human lungs, with constant exposure to the external environment, more heterogeneity may exist within human IM cells, rendering it difficult to study these populations (Schyns et al., 2018). Further research into the role of IMs in humans during infection may be required to fully understand their function in the context of protective immune responses.

Due to both intrinsic and extrinsic factors described in the literature, such as the type of CFTR mutation and colonisation of other microbes, the lungs of CF patients are highly inflammatory (Bruscia & Bonfield, 2016). The term “CF macrophage” has been coined to describe this phenomenon; that is, overactivated inflammatory macrophages are present in large numbers in the lungs which perpetuate neutrophilic inflammation, subsequently accelerating pulmonary demise (Öz et al., 2022). While this may in part explain why people with CF are susceptible to *M. abscessus* infections, care must be taken in developing vaccines that may potentiate the pro-inflammatory state of macrophages in the lung. Delineation of the duplicity of the IM population, that is, pro- and anti-inflammatory effects, will be important in harnessing the true therapeutic potential of this cell subset. Analysis of histopathology of the lung parenchyma following vaccination, as well as lung function tests would be also be useful in assessing any immunopathology of IM involvement in clearance of *M. abscessus* infection (Quan et al., 2022). Further, determining if these findings are replicated in a *cftr*-deficient murine model (Bacci et al., 2021; Grubb & Livraghi-Butrico, 2022) may help evaluate the safety of these vaccine candidates for this population.

In conclusion, the results presented in this thesis significantly advance the field of *M. abscessus* vaccine research and provides important information on the role of specific immune mediators in control of bacterial infection. The murine pulmonary model of *M. abscessus* infection used, as well as the identification of keys mediators of protective immunity, delivers key insights into host immunity and will aid future vaccine development/testing. The vaccine γ-*Mabs* was identified as a highly promising candidate for future development. Overall, this work provides a myriad of possibilities for future vaccine and drug development, in the hope to combat the debilitating effects of rising incidence of *M. abscessus* infection.

References

Abarca, K., Rey-Jurado, E., Muñoz-Durango, N., Vázquez, Y., Soto, J. A., Gálvez, N. M. S., Valdés-Ferrada, J., Iturriaga, C., Urzúa, M., Borzutzky, A., Cerda, J., Villarroel, L., Madrid, V., González, P. A., González-Aramundiz, J. V., Bueno, S. M., & Kalergis, A. M. (2020). Safety and immunogenicity evaluation of recombinant BCG vaccine against respiratory syncytial virus in a randomized, double-blind, placebo-controlled phase I clinical trial. *EClinicalMedicine*, *27*, 100517. https://doi.org/10.1016/j.eclinm.2020.100517

Abate, G., Hamzabegovic, F., Eickhoff, C. S., & Hoft, D. F. (2019). BCG Vaccination Induces M. avium and M. abscessus Cross-Protective Immunity. *Front Immunol*, *10*, 234. https://doi.org/10.3389/fimmu.2019.00234

Ademhan Tural, D., Emiralioglu, N., Ozsezen, B., Saribas, Z., Ozcan, N., Alp, A., Sunman, B., Hizal, M., Eryilmaz Polat, S., Yalcin, E., Dogru, D., Ozcelik, U., & Kiper, N. (2021). The frequency and related factors of non-tuberculosis mycobacteria infections among patients with cystic fibrosis. *Pediatr Int*, *63*(11), 1369-1375. https://doi.org/10.1111/ped.14688

Adjemian, J., Olivier, K. N., & Prevots, D. R. (2018). Epidemiology of Pulmonary Nontuberculous Mycobacterial Sputum Positivity in Patients with Cystic Fibrosis in the United States, 2010-2014. *Ann Am Thorac Soc*, *15*(7), 817-826. https://doi.org/10.1513/AnnalsATS.201709-727OC

Ahn, J.-H., Park, J.-Y., Kim, D.-Y., Lee, T.-S., Jung, D.-H., Kim, Y.-J., Lee, Y.-J., Lee, Y.-J., Seo, I.-S., Song, E.-J., Jang, A.-R., Yang, S.-J., Shin, S. J., & Park, J.-H. (2021). Type I Interferons Are Involved in the Intracellular Growth Control of Mycobacterium abscessus by Mediating NOD2-Induced Production of Nitric Oxide in Macrophages [Original Research]. *Front Immunol*, *12*. https://doi.org/10.3389/fimmu.2021.738070

Albanesi, C., Cavani, A., & Girolomoni, G. (1999). IL-17 is produced by nickel-specific T lymphocytes and regulates ICAM-1 expression and chemokine production in human keratinocytes: synergistic or antagonist effects with IFN-gamma and TNF-alpha. *J Immunol*, *162*(1), 494-502.

Algood, H. M., Lin, P. L., Yankura, D., Jones, A., Chan, J., & Flynn, J. L. (2004). TNF influences chemokine expression of macrophages in vitro and that of CD11b+ cells in vivo during Mycobacterium tuberculosis infection. *J Immunol*, *172*(11), 6846-6857.

Alix, E., & Blanc-Potard, A. B. (2007). MgtC: a key player in intramacrophage survival. *Trends Microbiol*, *15*(6), 252-256. https://doi.org/10.1016/j.tim.2007.03.007

Allard, B., Panariti, A., & Martin, J. G. (2018). Alveolar Macrophages in the Resolution of Inflammation, Tissue Repair, and Tolerance to Infection. *Front Immunol*, *9*, 1777. https://doi.org/10.3389/fimmu.2018.01777

Andrew, E. C., Connell, T., Robinson, P., Curtis, N., Massie, J., Robertson, C., Harrison, J., Shanthikumar, S., Bryant, P. A., Starr, M., Steer, A., Ranganathan, S., & Gwee, A. (2019). Pulmonary Mycobacterium abscessus complex in children with cystic fibrosis: A practical management guideline. *J Paediatr Child Health*, *55*(5), 502-511. https://doi.org/https://doi.org/10.1111/jpc.14427

Arbues, A., Aguilo, J. I., Gonzalo-Asensio, J., Marinova, D., Uranga, S., Puentes, E., Fernandez, C., Parra, A., Cardona, P. J., & Vilaplana, C. (2013). Construction, characterization and preclinical evaluation of MTBVAC, the first live-attenuated M. tuberculosis-based vaccine to enter clinical trials. *Vaccine*, *31*(42), 4867-4873.

Ardain, A., Marakalala, M. J., & Leslie, A. (2020). Tissue-resident innate immunity in the lung. *Immunology*, *159*(3), 245-256. https://doi.org/10.1111/imm.13143

Arts, R. J., Novakovic, B., Ter Horst, R., Carvalho, A., Bekkering, S., Lachmandas, E., Rodrigues, F., Silvestre, R., Cheng, S. C., Wang, S. Y., Habibi, E., Gonçalves, L. G., Mesquita, I., Cunha, C., van Laarhoven, A., van de Veerdonk, F. L., Williams, D. L., van der Meer, J. W., Logie, C., . . . Netea, M. G. (2016). Glutaminolysis and Fumarate Accumulation Integrate Immunometabolic and Epigenetic Programs in Trained Immunity. *Cell Metab*, *24*(6), 807-819. https://doi.org/10.1016/j.cmet.2016.10.008

Australian Cystic Fibrosis Data Registry. (2021). Australian Cystic Fibrosis Data Registry Annual Report 2020. In. Melbourne, Victoria: Monash University.

Awate, S., Babiuk, L. A., & Mutwiri, G. (2013). Mechanisms of action of adjuvants. *Front Immunol*, *4*, 114. https://doi.org/10.3389/fimmu.2013.00114

Awuh, J. A., & Flo, T. H. (2017). Molecular basis of mycobacterial survival in macrophages. *Cell Mol Life Sci*, *74*(9), 1625-1648. https://doi.org/10.1007/s00018-016-2422-8

Baba, T., & Mukaida, N. (2014). Role of macrophage inflammatory protein (MIP)-1α/CCL3 in leukemogenesis. *Mol Cell Oncol*, *1*(1), e29899. https://doi.org/10.4161/mco.29899

Babb, R., Chen, A., Hirst, T. R., Kara, E. E., McColl, S. R., Ogunniyi, A. D., Paton, J. C., & Alsharifi, M. (2016). Intranasal vaccination with γ-irradiated Streptococcus pneumoniae whole-cell vaccine provides serotype-independent protection mediated by B-cells and innate IL-17 responses. *Clin Sci (Lond)*, *130*(9), 697-710. https://doi.org/10.1042/cs20150699

Bacci, G., Rossi, A., Armanini, F., Cangioli, L., De Fino, I., Segata, N., Mengoni, A., Bragonzi, A., & Bevivino, A. (2021). Lung and Gut Microbiota changes associated with Pseudomonas aeruginosa infection in Mouse models of cystic fibrosis. *Int J Mol Sci*, *22*(22), 12169.

Bailey, J. D., Diotallevi, M., Nicol, T., McNeill, E., Shaw, A., Chuaiphichai, S., Hale, A., Starr, A., Nandi, M., Stylianou, E., McShane, H., Davis, S., Fischer, R., Kessler, B. M., McCullagh, J., Channon, K. M., & Crabtree, M. J. (2019). Nitric Oxide Modulates Metabolic Remodeling in Inflammatory Macrophages through TCA Cycle Regulation and Itaconate Accumulation. *Cell Rep*, *28*(1), 218-230.e217. https://doi.org/10.1016/j.celrep.2019.06.018

Bedoret, D., Wallemacq, H., Marichal, T., Desmet, C., Calvo, F. Q., Henry, E., Closset, R., Dewals, B., Thielen, C., & Gustin, P. (2009). Lung interstitial macrophages alter dendritic cell functions to prevent airway allergy in mice. *J Clin Invest*, *119*(12), 3723-3738.

Bekker, L. G., Freeman, S., Murray, P. J., Ryffel, B., & Kaplan, G. (2001). TNF-alpha controls intracellular mycobacterial growth by both inducible nitric oxide synthase-dependent and inducible nitric oxide synthase-independent pathways. *J Immunol*, *166*(11), 6728-6734. https://doi.org/10.4049/jimmunol.166.11.6728

Belon, C., Soscia, C., Bernut, A., Laubier, A., Bleves, S., & Blanc-Potard, A. B. (2015). A Macrophage Subversion Factor Is Shared by Intracellular and Extracellular Pathogens. *PLoS Pathog*, *11*(6), e1004969. https://doi.org/10.1371/journal.ppat.1004969

Bentur, L., Gur, M., Ashkenazi, M., Livnat-Levanon, G., Mizrahi, M., Tal, A., Ghaffari, A., Geffen, Y., Aviram, M., & Efrati, O. (2020). Pilot study to test inhaled nitric oxide in cystic fibrosis patients with refractory Mycobacterium abscessus lung infection. *J Cyst Fibros*, *19*(2), 225-231. https://doi.org/10.1016/j.jcf.2019.05.002

Benwill, J. L., & Wallace, R. J., Jr. (2014). Mycobacterium abscessus: challenges in diagnosis and treatment. *Curr Opin Infect Dis*, *27*(6), 506-510. https://doi.org/10.1097/qco.0000000000000104

Bermudez, L. E., Wu, M., & Young, L. S. (1995). Interleukin-12-stimulated natural killer cells can activate human macrophages to inhibit growth of Mycobacterium avium. *Infect Immun*, *63*(10), 4099-4104.

Bernut, A., Dupont, C., Ogryzko, N. V., Neyret, A., Herrmann, J. L., Floto, R. A., Renshaw, S. A., & Kremer, L. (2019). CFTR Protects against Mycobacterium abscessus Infection by Fine-Tuning Host Oxidative Defenses. *Cell Rep*, *26*(7), 1828-1840.e1824. https://doi.org/10.1016/j.celrep.2019.01.071

Bernut, A., Dupont, C., Sahuquet, A., Herrmann, J. L., Lutfalla, G., & Kremer, L. (2015). Deciphering and Imaging Pathogenesis and Cording of Mycobacterium abscessus in Zebrafish Embryos. *J Vis Exp*(103). https://doi.org/10.3791/53130

Bernut, A., Herrmann, J. L., Kissa, K., Dubremetz, J. F., Gaillard, J. L., Lutfalla, G., & Kremer, L. (2014). Mycobacterium abscessus cording prevents phagocytosis and promotes abscess formation. *Proc Natl Acad Sci U S A*, *111*(10), E943-952. https://doi.org/10.1073/pnas.1321390111

Bernut, A., Herrmann, J. L., Ordway, D., & Kremer, L. (2017). The Diverse Cellular and Animal Models to Decipher the Physiopathological Traits of Mycobacterium abscessus Infection. *Front Cell Infect Microbiol*, *7*, 100. https://doi.org/10.3389/fcimb.2017.00100

Bernut, A., Nguyen-Chi, M., Halloum, I., Herrmann, J. L., Lutfalla, G., & Kremer, L. (2016). Mycobacterium abscessus-Induced Granuloma Formation Is Strictly Dependent on TNF

Signaling and Neutrophil Trafficking. *PLoS Pathog*, *12*(11), e1005986. https://doi.org/10.1371/journal.ppat.1005986

Bharat, A., Bhorade, S. M., Morales-Nebreda, L., McQuattie-Pimentel, A. C., Soberanes, S., Ridge, K., DeCamp, M. M., Mestan, K. K., Perlman, H., & Budinger, G. S. (2016). Flow cytometry reveals similarities between lung macrophages in humans and mice. *Am J Respir Cell Mol Biol*, *54*(1), 147-149.

Blomgran, R., & Ernst, J. D. (2011). Lung neutrophils facilitate activation of naive antigen-specific CD4+ T cells during Mycobacterium tuberculosis infection. *J Immunol*, *186*(12), 7110-7119.

Boeck, L., Burbaud, S., Skwark, M., Pearson, W. H., Sangen, J., Wuest, A. W., Marshall, E. K. P., Weimann, A., Everall, I., Bryant, J. M., Malhotra, S., Bannerman, B. P., Kierdorf, K., Blundell, T. L., Dionne, M. S., Parkhill, J., & Andres Floto, R. (2022). Mycobacterium abscessus pathogenesis identified by phenogenomic analyses. *Nat Microbiol*, *7*(9), 1431-1441. https://doi.org/10.1038/s41564-022-01204-x

Bogdanovski, K., Chau, T., Robinson, C. J., MacDonald, S. D., Peterson, A. M., Mashek, C. M., Wallin, W. A., Rimkus, M., Montgomery, F., Lucas da Silva, J., Gupta, S., Ghaffari, A., Zelazny, A. M., & Olivier, K. N. (2020). Antibacterial activity of high-dose nitric oxide against pulmonary Mycobacterium abscessus disease. *Access Microbiol*, *2*(9), acmi000154. https://doi.org/10.1099/acmi.0.000154

Bourinbaiar, A. S., Batbold, U., Efremenko, Y., Sanjagdorj, M., Butov, D., Damdinpurev, N., Grinishina, E., Mijiddorj, O., Kovolev, M., Baasanjav, K., Butova, T., Prihoda, N., Batbold, O., Yurchenko, L., Tseveendorj, A., Arzhanova, O., Chunt, E., Stepanenko, H., Sokolenko, N., . . . Stanford, J. (2020). Phase III, placebo-controlled, randomized, double-blind trial of tableted, therapeutic TB vaccine (V7) containing heat-killed M. vaccae administered daily for one month. *J Clin Tuberc Other Mycobact Dis*, *18*, 100141. https://doi.org/10.1016/j.jctube.2019.100141

Bouzeyen, R., & Javid, B. (2022). Therapeutic Vaccines for Tuberculosis: An Overview [Mini Review]. *Front Immunol*, *13*. https://doi.org/10.3389/fimmu.2022.878471

Braverman, J., & Stanley, S. A. (2017). Nitric Oxide Modulates Macrophage Responses to Mycobacterium tuberculosis Infection through Activation of HIF-1α and Repression of NF-κB. *J Immunol*, *199*(5), 1805-1816. https://doi.org/10.4049/jimmunol.1700515

Brennan, P. J., & Nikaido, H. (1995). The envelope of mycobacteria. *Annu Rev Biochem*, *64*(1), 29-63.

Brill, K. J., Li, Q., Larkin, R., Canaday, D. H., Kaplan, D. R., Boom, W. H., & Silver, R. F. (2001). Human natural killer cells mediate killing of intracellular Mycobacterium tuberculosis H37Rv via granule-independent mechanisms. *Infect Immu*, *69*(3), 1755-1765.

Brode, S. K., Jamieson, F. B., Ng, R., Campitelli, M. A., Kwong, J. C., Paterson, J. M., Li, P., Marchand-Austin, A., Bombardier, C., & Marras, T. K. (2015). Increased risk of mycobacterial infections associated with anti-rheumatic medications. *Thorax*, *70*(7), 677-682. https://doi.org/10.1136/thoraxjnl-2014-206470

Bruscia, E. M., & Bonfield, T. L. (2016). Cystic Fibrosis Lung Immunity: The Role of the Macrophage. *J Innate Immun*, *8*(6), 550-563. https://doi.org/10.1159/000446825

Bruxvoort, K. J., Luo, Y., Ackerson, B., Tanenbaum, H. C., Sy, L. S., Gandhi, A., & Tseng, H. F. (2019). Comparison of vaccine effectiveness against influenza hospitalization of cell-based and egg-based influenza vaccines, 2017-2018. *Vaccine*, *37*(39), 5807-5811. https://doi.org/10.1016/j.vaccine.2019.08.024

Bryant, J. M., Brown, K. P., Burbaud, S., Everall, I., Belardinelli, J. M., Rodriguez-Rincon, D., Grogono, D. M., Peterson, C. M., Verma, D., Evans, I. E., Ruis, C., Weimann, A., Arora, D., Malhotra, S., Bannerman, B., Passemar, C., Templeton, K., MacGregor, G., Jiwa, K., . . . Floto, R. A. (2021). Stepwise pathogenic evolution of Mycobacterium abscessus. *Science*, *372*(6541). https://doi.org/10.1126/science.abb8699

Bryant, J. M., Grogono, D. M., Greaves, D., Foweraker, J., Roddick, I., Inns, T., Reacher, M., Haworth, C. S., Curran, M. D., & Harris, S. R. (2013). Whole-genome sequencing to identify transmission of Mycobacterium abscessus between patients with cystic fibrosis: a retrospective cohort study. *Lancet*, *381*(9877), 1551-1560.

Bryant, J. M., Grogono, D. M., Rodriguez-Rincon, D., Everall, I., Brown, K. P., Moreno, P., Verma, D., Hill, E., Drijkoningen, J., & Gilligan, P. (2016). Emergence and spread of a human-

transmissible multidrug-resistant nontuberculous mycobacterium. *Science*, *354*(6313), 751-757.

Bull, N. C., Stylianou, E., Kaveh, D. A., Pinpathomrat, N., Pasricha, J., Harrington-Kandt, R., Garcia-Pelayo, M. C., Hogarth, P. J., & McShane, H. (2019). Enhanced protection conferred by mucosal BCG vaccination associates with presence of antigen-specific lung tissue-resident PD-1+ KLRG1− CD4+ T cells. *Mucosal Immunol*, *12*(2), 555-564. https://doi.org/10.1038/s41385-018-0109-1

Busch, M., Herzmann, C., Kallert, S., Zimmermann, A., Höfer, C., Mayer, D., Zenk, S. F., Muche, R., Lange, C., Bloom, B. R., Modlin, R. L., & Stenger, S. (2016). Lipoarabinomannan-Responsive Polycytotoxic T Cells Are Associated with Protection in Human Tuberculosis. *Am J Respir Crit Care Med*, *194*(3), 345-355. https://doi.org/10.1164/rccm.201509-1746OC

Cai, R. T., Yu, F. X., Tao, Z., Qian, X. Q., Chen, J., & Lu, H. Z. (2017). Routinely detected indicators in plasma have a predictive effect on the identification of HIV-infected patients with non-tuberculous mycobacterial and tuberculous infections. *Infect Dis Poverty*, *6*(1), 132. https://doi.org/10.1186/s40249-017-0347-6

Cai, S., Batra, S., Lira, S. A., Kolls, J. K., & Jeyaseelan, S. (2010). CXCL1 Regulates Pulmonary Host Defense to Klebsiella Infection via CXCL2, CXCL5, NF-κB, and MAPKs. *J Immunol*, *185*(10), 6214-6225. https://doi.org/10.4049/jimmunol.0903843

Calmette, A., & Plotz, H. (1929). Protective inoculation against tuberculosis with BCG. *Am Rev Tuberc*, *19*, 567-572.

Cantin, A. M., Hartl, D., Konstan, M. W., & Chmiel, J. F. (2015). Inflammation in cystic fibrosis lung disease: Pathogenesis and therapy. *J Cyst Fibros*, *14*(4), 419-430. https://doi.org/10.1016/j.jcf.2015.03.003

Caruso, A. M., Serbina, N., Klein, E., Triebold, K., Bloom, B. R., & Flynn, J. L. (1999). Mice deficient in CD4 T cells have only transiently diminished levels of IFN-γ, yet succumb to tuberculosis. *J Immunol*, *162*(9), 5407-5416.

Casanova, J. L., & Abel, L. (2002). Genetic dissection of immunity to mycobacteria: the human model. *Annu Rev Immunol*, *20*, 581-620. https://doi.org/10.1146/annurev.immunol.20.081501.125851

Catherinot, E., Roux, A. L., Vibet, M. A., Bellis, G., Ravilly, S., Lemonnier, L., Le Roux, E., Bernède-Bauduin, C., Le Bourgeois, M., Herrmann, J. L., Guillemot, D., & Gaillard, J. L. (2013). Mycobacterium avium and Mycobacterium abscessus complex target distinct cystic fibrosis patient subpopulations. *J Cyst Fibros*, *12*(1), 74-80. https://doi.org/10.1016/j.jcf.2012.06.009

Caverly, L. J., Caceres, S. M., Fratelli, C., Happoldt, C., Kidwell, K. M., Malcolm, K. C., Nick, J. A., & Nichols, D. P. (2015). Mycobacterium abscessus Morphotype Comparison in a Murine Model. *PloS one*, *10*(2), e0117657. https://doi.org/10.1371/journal.pone.0117657

Chadha, R., Grover, M., Sharma, A., Lakshmy, A., Deb, M., Kumar, A., & Mehta, G. (1998). An outbreak of post-surgical wound infections due to Mycobacterium abscessus. *Pediatr Surg Int*, *13*(5-6), 406-410. https://doi.org/10.1007/s003830050350

Chakarov, S., Lim, H. Y., Tan, L., Lim, S. Y., See, P., Lum, J., Zhang, X. M., Foo, S., Nakamizo, S., Duan, K., Kong, W. T., Gentek, R., Balachander, A., Carbajo, D., Bleriot, C., Malleret, B., Tam, J. K. C., Baig, S., Shabeer, M., . . . Ginhoux, F. (2019). Two distinct interstitial macrophage populations coexist across tissues in specific subtissular niches. *Science*, *363*(6432). https://doi.org/10.1126/science.aau0964

Chan, J., Mehta, S., Bharrhan, S., Chen, Y., Achkar, J. M., Casadevall, A., & Flynn, J. (2014). The role of B cells and humoral immunity in Mycobacterium tuberculosis infection. *Semin Immunol*, *26*(6), 588-600. https://doi.org/10.1016/j.smim.2014.10.005

Chandrashekaran, S., Escalante, P., & Kennedy, C. C. (2017). Mycobacterium abscessus disease in lung transplant recipients: Diagnosis and management. *J Clin Tuberc Other Mycobact Dis*, *9*, 10-18. https://doi.org/10.1016/j.jctube.2017.08.002

Chen, L., Wang, J., Zganiacz, A., & Xing, Z. (2004). Single intranasal mucosal Mycobacterium bovis BCG vaccination confers improved protection compared to subcutaneous vaccination against pulmonary tuberculosis. *Infection and immunity*, *72*(1), 238-246.

Chen, T., Blanc, C., Eder, A. Z., Prados-Rosales, R., Souza, A. C., Kim, R. S., Glatman-Freedman, A., Joe, M., Bai, Y., Lowary, T. L., Tanner, R., Brennan, M. J., Fletcher, H. A., McShane, H., Casadevall, A., & Achkar, J. M. (2016). Association of Human Antibodies to Arabinomannan

With Enhanced Mycobacterial Opsonophagocytosis and Intracellular Growth Reduction. *J Infect Dis*, *214*(2), 300-310. https://doi.org/10.1093/infdis/jiw141

Chen, T., Li, Z., Yu, L., Li, H., Lin, J., Guo, H., Wang, W., Chen, L., Zhang, X., Wang, Y., Chen, Y., Liao, Q., Tan, Y., Shu, Y., Huang, W., Cai, C., Zhou, Z., Yu, M., Li, G., . . . Zhou, J. (2016). Profiling the human immune response to Mycobacterium tuberculosis by human cytokine array. *Tuberculosis (Edinb)*, *97*, 108-117. https://doi.org/10.1016/j.tube.2015.12.007

Choi, H., Jhun, B. W., Kim, S. Y., Kim, D. H., Lee, H., Jeon, K., Kwon, O. J., Huh, H. J., Ki, C. S., Lee, N. Y., Shin, S. J., Daley, C. L., & Koh, W. J. (2018). Treatment outcomes of macrolide-susceptible Mycobacterium abscessus lung disease. *Diagn Microbiol Infect Dis*, *90*(4), 293-295. https://doi.org/10.1016/j.diagmicrobio.2017.12.008

Claeys, T. A., Rosas Mejia, O., Marshall, S., Jarzembowski, J. A., Hayes, D., Hull, N. M., Liyanage, N. P. M., Chun, R. H., Sulman, C. G., Huppler, A. R., & Robinson, R. T. (2019). Attenuation of Helper T Cell Capacity for TH1 and TH17 Differentiation in Children With Nontuberculous Mycobacterial Infection. *J Infect Dis*, *220*(11), 1843-1847. https://doi.org/10.1093/infdis/jiz371

Cohen, S. B., Gern, B. H., Delahaye, J. L., Adams, K. N., Plumlee, C. R., Winkler, J. K., Sherman, D. R., Gerner, M. Y., & Urdahl, K. B. (2018). Alveolar macrophages provide an early Mycobacterium tuberculosis niche and initiate dissemination. *Cell Host Microbe*, *24*(3), 439-446. e434.

Colditz, G. A., Berkey, C. S., Mosteller, F., Brewer, T. F., Wilson, M. E., Burdick, E., & Fineberg, H. V. (1995). The efficacy of bacillus Calmette-Guerin vaccination of newborns and infants in the prevention of tuberculosis: meta-analyses of the published literature. *Pediatrics*, *96*(1), 29-35.

Costello, A. M., Kumar, A., Narayan, V., Akbar, M. S., Ahmed, S., Abou-Zeid, C., Rook, G. A., Stanford, J., & Moreno, C. (1992). Does antibody to mycobacterial antigens, including lipoarabinomannan, limit dissemination in childhood tuberculosis? *Trans R Soc Trop Med Hyg*, *86*(6), 686-692. https://doi.org/10.1016/0035-9203(92)90192-f

Coulston, J., & Balaratnam, N. (2005). Irreversible sensorineural hearing loss due to clarithromycin. *Postgrad Med J*, *81*(951), 58-59. https://doi.org/10.1136/pgmj.2004.020412

Counoupas, C., Ferrell, K. C., Ashhurst, A., Bhattacharyya, N. D., Nagalingam, G., Stewart, E. L., Feng, C. G., Petrovsky, N., Britton, W. J., & Triccas, J. A. (2020). Mucosal delivery of a multistage subunit vaccine promotes development of lung-resident memory T cells and affords interleukin-17-dependent protection against pulmonary tuberculosis. *NPJ Vaccines*, *5*(1), 105. https://doi.org/10.1038/s41541-020-00255-7

Counoupas, C., Pinto, R., Nagalingam, G., Britton, W. J., Petrovsky, N., & Triccas, J. A. (2017). Delta inulin-based adjuvants promote the generation of polyfunctional CD4+ T cell responses and protection against Mycobacterium tuberculosis infection. *Sci Rep*, *7*(1), 1-11.

Covián, C., Fernández-Fierro, A., Retamal-Díaz, A., Díaz, F. E., Vasquez, A. E., Lay, M. K., Riedel, C. A., González, P. A., Bueno, S. M., & Kalergis, A. M. (2019). BCG-Induced Cross-Protection and Development of Trained Immunity: Implication for Vaccine Design [Review]. *Front Immunol*, *10*(2806). https://doi.org/10.3389/fimmu.2019.02806

Culley, F. J., Pennycook, A. M., Tregoning, J. S., Dodd, J. S., Walzl, G., Wells, T. N., Hussell, T., & Openshaw, P. J. (2006). Role of CCL5 (RANTES) in viral lung disease. *J Virol*, *80*(16), 8151-8157. https://doi.org/10.1128/jvi.00496-06

Daher, W., Leclercq, L. D., Johansen, M. D., Hamela, C., Karam, J., Trivelli, X., Nigou, J., Guérardel, Y., & Kremer, L. (2022). Glycopeptidolipid glycosylation controls surface properties and pathogenicity in Mycobacterium abscessus. *Cell Chem Biol*, *29*(5), 910-924.e917. https://doi.org/10.1016/j.chembiol.2022.03.008

Dahl, V. N., Mølhave, M., Fløe, A., van Ingen, J., Schön, T., Lillebaek, T., Andersen, A. B., & Wejse, C. (2022). Global trends of pulmonary infections with nontuberculous mycobacteria: a systematic review. *Int J Infect Dis*, *125*, 120-131. https://doi.org/https://doi.org/10.1016/j.ijid.2022.10.013

Daley, C. L., Iaccarino, J. M., Lange, C., Cambau, E., Wallace, R. J., Andrejak, C., Böttger, E. C., Brozek, J., Griffith, D. E., Guglielmetti, L., Huitt, G. A., Knight, S. L., Leitman, P., Marras, T. K., Olivier, K. N., Santin, M., Stout, J. E., Tortoli, E., van Ingen, J., . . . Winthrop, K. L. (2020). Treatment of nontuberculous mycobacterial pulmonary disease: an official

ATS/ERS/ESCMID/IDSA clinical practice guideline. *Eur Respir J*, *56*(1), 2000535. https://doi.org/10.1183/13993003.00535-2020

Dar, H. A., Ismail, S., Waheed, Y., Ahmad, S., Jamil, Z., Aziz, H., Hetta, H. F., & Muhammad, K. (2021). Designing a multi-epitope vaccine against Mycobacteroides abscessus by pangenome-reverse vaccinology. *Sci Rep*, *11*(1), 11197. https://doi.org/10.1038/s41598-021-90868-2

Darrah, P. A., Zeppa, J. J., Maiello, P., Hackney, J. A., Wadsworth, M. H., 2nd, Hughes, T. K., Pokkali, S., Swanson, P. A., 2nd, Grant, N. L., Rodgers, M. A., Kamath, M., Causgrove, C. M., Laddy, D. J., Bonavia, A., Casimiro, D., Lin, P. L., Klein, E., White, A. G., Scanga, C. A., . . . Seder, R. A. (2020). Prevention of tuberculosis in macaques after intravenous BCG immunization. *Nature*, *577*(7788), 95-102. https://doi.org/10.1038/s41586-019-1817-8

Das, S., & Khader, S. (2017). Yin and yang of interleukin-17 in host immunity to infection. *F1000Research*, *6*.

Davenne, T., & McShane, H. (2016). Why don't we have an effective tuberculosis vaccine yet? *Expert Rev Vaccines*, *15*(8), 1009-1013. https://doi.org/10.1586/14760584.2016.1170599

Davidson, L. B., Nessar, R., Kempaiah, P., Perkins, D. J., & Byrd, T. F. (2011). Mycobacterium abscessus glycopeptidolipid prevents respiratory epithelial TLR2 signaling as measured by HbetaD2 gene expression and IL-8 release. *PloS one*, *6*(12), e29148. https://doi.org/10.1371/journal.pone.0029148

Davis, J. M., Clay, H., Lewis, J. L., Ghori, N., Herbomel, P., & Ramakrishnan, L. (2002). Real-time visualization of mycobacterium-macrophage interactions leading to initiation of granuloma formation in zebrafish embryos. *Immunity*, *17*(6), 693-702.

Dawson, R., Condos, R., Tse, D., Huie, M. L., Ress, S., Tseng, C.-H., Brauns, C., Weiden, M., Hoshino, Y., & Bateman, E. (2009). Immunomodulation with recombinant interferon-γ1b in pulmonary tuberculosis. *PloS one*, *4*(9), e6984.

Day, C. L., Abrahams, D. A., Lerumo, L., Janse van Rensburg, E., Stone, L., O'Rie, T., Pienaar, B., de Kock, M., Kaplan, G., Mahomed, H., Dheda, K., & Hanekom, W. A. (2011). Functional capacity of Mycobacterium tuberculosis-specific T cell responses in humans is associated with mycobacterial load. *J Immunol*, *187*(5), 2222-2232. https://doi.org/10.4049/jimmunol.1101122

De Groote, M. A., Pace, N. R., Fulton, K., & Falkinham, J. O., 3rd. (2006). Relationships between Mycobacterium isolates from patients with pulmonary mycobacterial infection and potting soils. *Appl Environ Microbiol*, *72*(12), 7602-7606. https://doi.org/10.1128/aem.00930-06

de Vallière, S., Abate, G., Blazevic, A., Heuertz, R. M., & Hoft, D. F. (2005). Enhancement of innate and cell-mediated immunity by antimycobacterial antibodies. *Infect Immun*, *73*(10), 6711-6720. https://doi.org/10.1128/iai.73.10.6711-6720.2005

Dedrick, R. M., Guerrero-Bustamante, C. A., Garlena, R. A., Russell, D. A., Ford, K., Harris, K., Gilmour, K. C., Soothill, J., Jacobs-Sera, D., Schooley, R. T., Hatfull, G. F., & Spencer, H. (2019). Engineered bacteriophages for treatment of a patient with a disseminated drug-resistant Mycobacterium abscessus. *Nat Med*, *25*(5), 730-733. https://doi.org/10.1038/s41591-019-0437-z

Dedrick, R. M., Smith, B. E., Cristinziano, M., Freeman, K. G., Jacobs-Sera, D., Belessis, Y., Whitney Brown, A., Cohen, K. A., Davidson, R. M., van Duin, D., Gainey, A., Garcia, C. B., Robert George, C. R., Haidar, G., Ip, W., Iredell, J., Khatami, A., Little, J. S., Malmivaara, K., . . . Hatfull, G. F. (2022). Phage Therapy of Mycobacterium Infections: Compassionate Use of Phages in 20 Patients With Drug-Resistant Mycobacterial Disease. *Clin Infect Dis*, *76*(1), 103-112. https://doi.org/10.1093/cid/ciac453

Degiacomi, G., Sammartino, J. C., Chiarelli, L. R., Riabova, O., Makarov, V., & Pasca, M. R. (2019). Mycobacterium abscessus, an Emerging and Worrisome Pathogen among Cystic Fibrosis Patients. *Int J Mol Sci*, *20*(23). https://doi.org/10.3390/ijms20235868

Dockrell, H. M., & Smith, S. G. (2017). What Have We Learnt about BCG Vaccination in the Last 20 Years? *Front Immunol*, *8*, 1134. https://doi.org/10.3389/fimmu.2017.01134

Dorman, S. E., & Holland, S. M. (2000). Interferon-gamma and interleukin-12 pathway defects and human disease. *Cytokine Growth Factor Rev*, *11*(4), 321-333. https://doi.org/10.1016/s1359-6101(00)00010-1

Driver, E. R., Ryan, G. J., Hoff, D. R., Irwin, S. M., Basaraba, R. J., Kramnik, I., & Lenaerts, A. J. (2012). Evaluation of a mouse model of necrotic granuloma formation using C3HeB/FeJ mice for testing of drugs against Mycobacterium tuberculosis. *Antimicrob Agents Chemother*, *56*(6), 3181-3195.

Drummond, R. A., Swamydas, M., Oikonomou, V., Zhai, B., Dambuza, I. M., Schaefer, B. C., Bohrer, A. C., Mayer-Barber, K. D., Lira, S. A., Iwakura, Y., Filler, S. G., Brown, G. D., Hube, B., Naglik, J. R., Hohl, T. M., & Lionakis, M. S. (2019). CARD9(+) microglia promote antifungal immunity via IL-1β- and CXCL1-mediated neutrophil recruitment. *Nat Immunol*, *20*(5), 559-570. https://doi.org/10.1038/s41590-019-0377-2

Dubin, P. J., McAllister, F., & Kolls, J. K. (2007). Is cystic fibrosis a TH17 disease? *Inflamm Res*, *56*(6), 221-227. https://doi.org/10.1007/s00011-007-6187-2

Ehlers, S., & Schaible, U. E. (2012). The granuloma in tuberculosis: dynamics of a host-pathogen collusion. *Front Immunol*, *3*, 411. https://doi.org/10.3389/fimmu.2012.00411

El Helou, G., Viola, G. M., Hachem, R., Han, X. Y., & Raad, II. (2013). Rapidly growing mycobacterial bloodstream infections. *Lancet Infect Dis*, *13*(2), 166-174. https://doi.org/10.1016/s1473-3099(12)70316-x

Elborn, J. S. (2016). Cystic fibrosis. *Lancet*, *388*(10059), 2519-2531. https://doi.org/10.1016/s0140-6736(16)00576-6

Esteban, J., & García-Coca, M. (2017). Mycobacterium Biofilms. *Front Microbiol*, *8*, 2651. https://doi.org/10.3389/fmicb.2017.02651

Falkinham, J. O., 3rd. (2011). Nontuberculous mycobacteria from household plumbing of patients with nontuberculous mycobacteria disease. *Emerg Infect Dis*, *17*(3), 419-424. https://doi.org/10.3201/eid1703.101510

Fan, Y. C., Chiu, H. C., Chen, L. K., Chang, G. J., & Chiou, S. S. (2015). Formalin Inactivation of Japanese Encephalitis Virus Vaccine Alters the Antigenicity and Immunogenicity of a Neutralization Epitope in Envelope Protein Domain III. *PLOS Negl Trop Dis*, *9*(10), e0004167. https://doi.org/10.1371/journal.pntd.0004167

Feazel, L. M., Baumgartner, L. K., Peterson, K. L., Frank, D. N., Harris, J. K., & Pace, N. R. (2009). Opportunistic pathogens enriched in showerhead biofilms. *Proc Natl Acad Sci U S A*, *106*(38), 16393-16399. https://doi.org/10.1073/pnas.0908446106

Feng, C. G., & Britton, W. J. (2000). CD4+ and CD8+ T cells mediate adoptive immunity to aerosol infection of Mycobacterium bovis bacillus Calmette-Guerin. *J Infect Dis*, *181*(5), 1846-1849.

Ferrell, K. C., Johansen, M. D., Triccas, J. A., & Counoupas, C. (2022). Virulence mechanisms of Mycobacterium abscessus: Current knowledge and implications for vaccine design. *Frontiers in Microbiology*, *13*.

Ferrell, K. C., Stewart, E. L., Counoupas, C., Ashhurst, T. M., Britton, W. J., Petrovsky, N., & Triccas, J. A. (2021). Intrapulmonary vaccination with delta-inulin adjuvant stimulates non-polarised chemotactic signalling and diverse cellular interaction. *Mucosal Immunol*, *14*(3), 762-773. https://doi.org/10.1038/s41385-021-00379-6

Fertey, J., Bayer, L., Grunwald, T., Pohl, A., Beckmann, J., Gotzmann, G., Casado, J. P., Schönfelder, J., Rögner, F. H., Wetzel, C., Thoma, M., Bailer, S. M., Hiller, E., Rupp, S., & Ulbert, S. (2016). Pathogens Inactivated by Low-Energy-Electron Irradiation Maintain Antigenic Properties and Induce Protective Immune Responses. *Viruses*, *8*(11). https://doi.org/10.3390/v8110319

Floto, R. A., Olivier, K. N., Saiman, L., Daley, C. L., Herrmann, J.-L., Nick, J. A., Noone, P. G., Bilton, D., Corris, P., & Gibson, R. L. (2016). US Cystic Fibrosis Foundation and European Cystic Fibrosis Society consensus recommendations for the management of non-tuberculous mycobacteria in individuals with cystic fibrosis. *Thorax*, *71*(Suppl 1), i1-i22.

Flynn, J. L., & Chan, J. (2001). Immunology of tuberculosis. *Annu Rev Immunol*, *19*, 93-129. https://doi.org/10.1146/annurev.immunol.19.1.93

Flynn, J. L., Chan, J., & Lin, P. L. (2011). Macrophages and control of granulomatous inflammation in tuberculosis. *Mucosal Immunol*, *4*(3), 271-278. https://doi.org/10.1038/mi.2011.14

Gagliani, N., & Huber, S. (2017). Basic Aspects of T Helper Cell Differentiation. *Methods Mol Biol*, *1514*, 19-30. https://doi.org/10.1007/978-1-4939-6548-9_2

Gao, X.-F., Yang, Z.-W., & Li, J. (2011). Adjunctive therapy with interferon-gamma for the treatment of pulmonary tuberculosis: a systematic review. *Int J Infect Dis*, *15*(9), e594-e600.

Gibbings, S. L., & Jakubzick, C. V. (2018). A Consistent Method to Identify and Isolate Mononuclear Phagocytes from Human Lung and Lymph Nodes. *Methods Mol Biol*, *1799*, 381-395. https://doi.org/10.1007/978-1-4939-7896-0_28

Gibbings, S. L., Thomas, S. M., Atif, S. M., McCubbrey, A. L., Desch, A. N., Danhorn, T., Leach, S. M., Bratton, D. L., Henson, P. M., & Janssen, W. J. (2017). Three unique interstitial macrophages in the murine lung at steady state. *Am J Respir Cell Mol Biol*, *57*(1), 66-76.

Gonzalez-Perez, M., Sanchez-Tarjuelo, R., Shor, B., Nistal-Villan, E., & Ochando, J. (2021). The BCG Vaccine for COVID-19: First Verdict and Future Directions [Mini Review]. *Front Immunol*, *12*(579). https://doi.org/10.3389/fimmu.2021.632478

Gonzalo-Asensio, J., Marinova, D., Martin, C., & Aguilo, N. (2017). MTBVAC: Attenuating the Human Pathogen of Tuberculosis (TB) Toward a Promising Vaccine against the TB Epidemic [Mini Review]. *Front Immunol*, *8*(1803). https://doi.org/10.3389/fimmu.2017.01803

Griffith, D. E. (2019). Mycobacterium abscessus and Antibiotic Resistance: Same As It Ever Was. In *Clin Infect Dis* (Vol. 69, pp. 1687-1689). https://doi.org/10.1093/cid/ciz071

Griffith, D. E., Aksamit, T., Brown-Elliott, B. A., Catanzaro, A., Daley, C., Gordin, F., Holland, S. M., Horsburgh, R., Huitt, G., Iademarco, M. F., Iseman, M., Olivier, K., Ruoss, S., von Reyn, C. F., Wallace, R. J., Jr., & Winthrop, K. (2007). An official ATS/IDSA statement: diagnosis, treatment, and prevention of nontuberculous mycobacterial diseases. *Am J Respir Crit Care Med*, *175*(4), 367-416. https://doi.org/10.1164/rccm.200604-571ST

Grode, L., Ganoza, C. A., Brohm, C., Weiner, J., 3rd, Eisele, B., & Kaufmann, S. H. (2013). Safety and immunogenicity of the recombinant BCG vaccine VPM1002 in a phase 1 open-label randomized clinical trial. *Vaccine*, *31*(9), 1340-1348. https://doi.org/10.1016/j.vaccine.2012.12.053

Grubb, B. R., & Livraghi-Butrico, A. (2022). Animal models of cystic fibrosis in the era of highly effective modulator therapies. *Curr Opin Pharm*, *64*, 102235.

Guilbert, L. J., Winkler-Lowen, B., Smith, A., Branch, D. R., & Garcia-Lloret, M. (1993). Analysis of the synergistic stimulation of mouse macrophage proliferation by macrophage colony-stimulating factor (CSF-1) and tumor necrosis factor alpha (TNF-alpha). *J Leukoc Biol*, *54*(1), 65-72. https://doi.org/10.1002/jlb.54.1.65

Guilliams, M., Lambrecht, B. N., & Hammad, H. (2013). Division of labor between lung dendritic cells and macrophages in the defense against pulmonary infections. *Mucosal Immunol*, *6*(3), 464-473. https://doi.org/10.1038/mi.2013.14

Guo, J., Garratt, A., & Hill, A. (2022). Worldwide rates of diagnosis and effective treatment for cystic fibrosis. *J Cyst Fibros*, *21*(3), 456-462.

Gupta, R. S., Lo, B., & Son, J. (2018). Phylogenomics and Comparative Genomic Studies Robustly Support Division of the Genus Mycobacterium into an Emended Genus Mycobacterium and Four Novel Genera. *Front Microbiol*, *9*, 67. https://doi.org/10.3389/fmicb.2018.00067

Gutiérrez, A. V., Viljoen, A., Ghigo, E., Herrmann, J. L., & Kremer, L. (2018). Glycopeptidolipids, a Double-Edged Sword of the Mycobacterium abscessus Complex. *Front Microbiol*, *9*, 1145. https://doi.org/10.3389/fmicb.2018.01145

Hamilton, J. A. (2020). GM-CSF in inflammation. *J Exp Med*, *217*(1). https://doi.org/10.1084/jem.20190945

Han, S. A., Ko, Y., Shin, S. J., & Jhun, B. W. (2020). Characteristics of Circulating CD4(+) T Cell Subsets in Patients with Mycobacterium avium Complex Pulmonary Disease. *J Clin Med*, *9*(5). https://doi.org/10.3390/jcm9051331

Hedin, W., Fröberg, G., Fredman, K., Chryssanthou, E., Selmeryd, I., Gillman, A., Orsini, L., Runold, M., Jönsson, B., Schön, T., & Davies Forsman, L. (2023). A rough colony morphology of Mycobacterium abscessus is associated with cavitary pulmonary disease and poor clinical outcome. *J Infect Dis*. https://doi.org/10.1093/infdis/jiad007

Heffernan, C. B., McKeon, M. G., Molony, S., Kawai, K., Stiles, D. J., Lachenauer, C. S., Kenna, M. A., & Watters, K. (2018). Does Clarithromycin Cause Hearing Loss? A 12-Year Review of Clarithromycin Therapy for Nontuberculous Mycobacterial Lymphadenitis in Children. *Annals of Otology, Rhinology & Laryngology*, *127*(10), 687-693. https://doi.org/10.1177/0003489418788112

Herrmann, J. L., & Lagrange, P. H. (2005). Dendritic cells and Mycobacterium tuberculosis: which is the Trojan horse? *Pathol Biol (Paris)*, *53*(1), 35-40. https://doi.org/10.1016/j.patbio.2004.01.004

Higgins, S. C., & Mills, K. H. (2010). TLR, NLR Agonists, and Other Immune Modulators as Infectious Disease Vaccine Adjuvants. *Curr Infect Dis Rep*, *12*(1), 4-12. https://doi.org/10.1007/s11908-009-0080-9

Hoefsloot, W., van Ingen, J., Andrejak, C., Angeby, K., Bauriaud, R., Bemer, P., Beylis, N., Boeree, M. J., Cacho, J., Chihota, V., Chimara, E., Churchyard, G., Cias, R., Daza, R., Daley, C. L., Dekhuijzen, P. N., Domingo, D., Drobniewski, F., Esteban, J., . . . Wagner, D. (2013). The geographic diversity of nontuberculous mycobacteria isolated from pulmonary samples: an NTM-NET collaborative study. *Eur Respir J*, *42*(6), 1604-1613. https://doi.org/10.1183/09031936.00149212

Honda, J. R., Virdi, R., & Chan, E. D. (2018). Global Environmental Nontuberculous Mycobacteria and Their Contemporaneous Man-Made and Natural Niches. *Front Microbiol*, *9*, 2029. https://doi.org/10.3389/fmicb.2018.02029

Hoppstädter, J., Diesel, B., Zarbock, R., Breinig, T., Monz, D., Koch, M., Meyerhans, A., Gortner, L., Lehr, C. M., Huwer, H., & Kiemer, A. K. (2010). Differential cell reaction upon Toll-like receptor 4 and 9 activation in human alveolar and lung interstitial macrophages. *Respir Res*, *11*(1), 124. https://doi.org/10.1186/1465-9921-11-124

Horsburgh, C. R., Jr., Hanson, D. L., Jones, J. L., & Thompson, S. E., III. (1996). Protection from Mycobacterium avium Complex Disease in Human Immunodeficiency Virus-Infected Persons with a History of Tuberculosis. *J Infect Dis*, *174*(6), 1212-1217. https://doi.org/10.1093/infdis/174.6.1212

Horvath, C., Shaler, C., Jeyanathan, M., Zganiacz, A., & Xing, Z. (2012). Mechanisms of delayed anti-tuberculosis protection in the lung of parenteral BCG-vaccinated hosts: a critical role of airway luminal T cells. *Mucosal Immunol*, *5*(4), 420-431.

Hou, F., Xiao, K., Tang, L., & Xie, L. (2021). Diversity of Macrophages in Lung Homeostasis and Diseases [Review]. *Front Immunol*, *12*. https://doi.org/10.3389/fimmu.2021.753940

Howard, S. T., Rhoades, E., Recht, J., Pang, X., Alsup, A., Kolter, R., Lyons, C. R., & Byrd, T. F. (2006). Spontaneous reversion of Mycobacterium abscessus from a smooth to a rough morphotype is associated with reduced expression of glycopeptidolipid and reacquisition of an invasive phenotype. *Microbiology (Reading)*, *152*(Pt 6), 1581-1590. https://doi.org/10.1099/mic.0.28625-0

Huang, L., Nazarova, E. V., Tan, S., Liu, Y., & Russell, D. G. (2018). Growth of Mycobacterium tuberculosis in vivo segregates with host macrophage metabolism and ontogeny. *J Exp Med*, *215*(4), 1135-1152. https://doi.org/10.1084/jem.20172020

Jarand, J., Levin, A., Zhang, L., Huitt, G., Mitchell, J. D., & Daley, C. L. (2011). Clinical and microbiologic outcomes in patients receiving treatment for Mycobacterium abscessus pulmonary disease. *Clin Infect Dis*, *52*(5), 565-571. https://doi.org/10.1093/cid/ciq237

Jeon, B.-Y., Kwak, J., Lee, S.-S., Cho, S., Won, C. J., Kim, J. M., & Shin, S. J. (2009). Comparative analysis of immune responses to Mycobacterium abscessus infection and its antigens in two murine models. *J Microbiol*, *47*(5), 633-640.

Jhun, B. W., Moon, S. M., Jeon, K., Kwon, O. J., Yoo, H., Carriere, K. C., Huh, H. J., Lee, N. Y., Shin, S. J., Daley, C. L., & Koh, W.-J. (2020). Prognostic factors associated with long-term mortality in 1445 patients with nontuberculous mycobacterial pulmonary disease: a 15-year follow-up study. *Eur Respir J*, *55*(1), 1900798. https://doi.org/10.1183/13993003.00798-2019

Johanneke Kleinnijenhuis and Jessica Quintin and Frank Preijers and Leo, A. B. J. a. C. J. a. R. J. X. a. J. W. M. a. R. a. M. G. (2014). BCG-induced trained immunity in NK cells: Role for non-specific protection to infection. *Clin Immunol*, *155*(2), 213-219. https://doi.org/https://doi.org/10.1016/j.clim.2014.10.005

Johansen, M. D., Herrmann, J. L., & Kremer, L. (2020). Non-tuberculous mycobacteria and the rise of Mycobacterium abscessus. *Nat Rev Microbiol*, *18*(7), 392-407. https://doi.org/10.1038/s41579-020-0331-1

Johnson, M. M., & Odell, J. A. (2014). Nontuberculous mycobacterial pulmonary infections. *J Thorac Dis*, *6*(3), 210-220. https://doi.org/10.3978/j.issn.2072-1439.2013.12.24

Johnson, M. O., Wolf, M. M., Madden, M. Z., Andrejeva, G., Sugiura, A., Contreras, D. C., Maseda, D., Liberti, M. V., Paz, K., Kishton, R. J., Johnson, M. E., de Cubas, A. A., Wu, P., Li, G., Zhang, Y., Newcomb, D. C., Wells, A. D., Restifo, N. P., Rathmell, W. K., . . . Rathmell, J. C. (2018). Distinct Regulation of Th17 and Th1 Cell Differentiation by Glutaminase-Dependent Metabolism. *Cell*, *175*(7), 1780-1795.e1719. https://doi.org/10.1016/j.cell.2018.10.001

Jönsson, B., Ridell, M., & Wold, A. E. (2013). Phagocytosis and cytokine response to rough and smooth colony variants of Mycobacterium abscessus by human peripheral blood mononuclear cells. *Apmis*, *121*(1), 45-55. https://doi.org/10.1111/j.1600-0463.2012.02932.x

Jönsson, B. E., Gilljam, M., Lindblad, A., Ridell, M., Wold, A. E., & Welinder-Olsson, C. (2007). Molecular epidemiology of Mycobacterium abscessus, with focus on cystic fibrosis. *J Clin Microbiol*, *45*(5), 1497-1504. https://doi.org/10.1128/jcm.02592-06

Jung, Y.-J., Ryan, L., LaCourse, R., & North, R. J. (2005). Properties and protective value of the secondary versus primary T helper type 1 response to airborne Mycobacterium tuberculosis infection in mice. *J Exp Med*, *201*(12), 1915-1924.

Jwa, M. Y., Jeong, S., Ko, E. B., Kim, A. R., Kim, H. Y., Kim, S. K., Seo, H. S., Yun, C. H., & Han, S. H. (2018). Gamma-irradiation of Streptococcus pneumoniae for the use as an immunogenic whole cell vaccine. *J Microbiol*, *56*(8), 579-585. https://doi.org/10.1007/s12275-018-8347-1

Kaech, S. M., Wherry, E. J., & Ahmed, R. (2002). Effector and memory T-cell differentiation: implications for vaccine development. *Nat Rev Immunol*, *2*(4), 251-262. https://doi.org/10.1038/nri778

Kam, J. Y., Hortle, E., Krogman, E., Warner, S. E., Wright, K., Luo, K., Cheng, T., Manuneedhi Cholan, P., Kikuchi, K., & Triccas, J. A. (2022). Rough and smooth variants of Mycobacterium abscessus are differentially controlled by host immunity during chronic infection of adult zebrafish. *Nat Commun*, *13*(1), 1-11.

Kaufmann, S. H. (2013). Tuberculosis vaccines: time to think about the next generation. *Semin Immunol*, *25*(2), 172-181. https://doi.org/10.1016/j.smim.2013.04.006

Kaufmann, S. H. E. (2020). Vaccination Against Tuberculosis: Revamping BCG by Molecular Genetics Guided by Immunology. *Front Immunol*, *11*, 316. https://doi.org/10.3389/fimmu.2020.00316

Kaufmann, S. H. E., Bekker, L.-G., Moreira, A. L., Bergtold, A., Freeman, S., Ryffel, B., & Kaplan, G. (2000). Immunopathologic Effects of Tumor Necrosis Factor Alpha in Murine Mycobacterial Infection Are Dose Dependent. *Infect Immun*, *68*(12), 6954-6961. https://doi.org/doi:10.1128/IAI.68.12.6954-6961.2000

Kaufmann, S. H. E., Ehlers, S., Benini, J., Kutsch, S., Endres, R., Rietschel, E. T., & Pfeffer, K. (1999). Fatal Granuloma Necrosis without Exacerbated Mycobacterial Growth in Tumor Necrosis Factor Receptor p55 Gene-Deficient Mice Intravenously Infected with Mycobacterium avium. *Infect Immun*, *67*(7), 3571-3579. https://doi.org/doi:10.1128/IAI.67.7.3571-3579.1999

Kawano, H., Kayama, H., Nakama, T., Hashimoto, T., Umemoto, E., & Takeda, K. (2016). IL-10-producing lung interstitial macrophages prevent neutrophilic asthma. *Int Immunol*, *28*(10), 489-501. https://doi.org/10.1093/intimm/dxw012

Kay, E. S., Rice, W. S., Crockett, K. B., Atkins, G. C., Batey, D. S., & Turan, B. (2018). Experienced HIV-Related Stigma in Health Care and Community Settings: Mediated Associations With Psychosocial and Health Outcomes. *J Acquir Immune Defic Syndr*, *77*(3), 257-263. https://doi.org/10.1097/qai.0000000000001590

Khadangi, F., Forgues, A. S., Tremblay-Pitre, S., Dufour-Mailhot, A., Henry, C., Boucher, M., Beaulieu, M. J., Morissette, M., Fereydoonzad, L., Brunet, D., Robichaud, A., & Bossé, Y. (2021). Intranasal versus intratracheal exposure to lipopolysaccharides in a murine model of acute respiratory distress syndrome. *Sci Rep*, *11*(1), 7777. https://doi.org/10.1038/s41598-021-87462-x

Khader, S. A., Partida-Sanchez, S., Bell, G., Jelley-Gibbs, D. M., Swain, S., Pearl, J. E., Ghilardi, N., Lund, F. E., & Cooper, A. M. (2006). Interleukin 12p40 is required for dendritic cell migration and T cell priming after Mycobacterium tuberculosis infection. *J Exp Med*, *203*(7), 1805-1815.

Kilpeläinen, A., Maya-Hoyos, M., Saubí, N., Soto, C. Y., & Joseph Munne, J. (2018). Advances and challenges in recombinant Mycobacterium bovis BCG-based HIV vaccine development:

lessons learned. *Expert Rev Vaccines*, *17*(11), 1005-1020. https://doi.org/10.1080/14760584.2018.1534588

Kim, C. J., Kim, N. H., Song, K. H., Choe, P. G., Kim, E. S., Park, S. W., Kim, H. B., Kim, N. J., Kim, E. C., Park, W. B., & Oh, M. D. (2013). Differentiating rapid- and slow-growing mycobacteria by difference in time to growth detection in liquid media. *Diagn Microbiol Infect Dis*, *75*(1), 73-76. https://doi.org/10.1016/j.diagmicrobio.2012.09.019

Kim, J. S., Kang, M. J., Kim, W. S., Han, S. J., Kim, H. M., Kim, H. W., Kwon, K. W., Kim, S. J., Cha, S. B., Eum, S. Y., Koh, W. J., Cho, S. N., Park, J. H., & Shin, S. J. (2015). Essential engagement of Toll-like receptor 2 in initiation of early protective Th1 response against rough variants of Mycobacterium abscessus. *Infect Immun*, *83*(4), 1556-1567. https://doi.org/10.1128/iai.02853-14

Kim, S. W., Subhadra, B., Whang, J., Back, Y. W., Bae, H. S., Kim, H. J., & Choi, C. H. (2017). Clinical Mycobacterium abscessus strain inhibits autophagy flux and promotes its growth in murine macrophages. *Pathog Dis*, *75*(8). https://doi.org/10.1093/femspd/ftx107

Kleinnijenhuis, J., Quintin, J., Preijers, F., Joosten, L. A., Jacobs, C., Xavier, R. J., van der Meer, J. W., van Crevel, R., & Netea, M. G. (2014). BCG-induced trained immunity in NK cells: Role for non-specific protection to infection. *Clin Immunol*, *155*(2), 213-219. https://doi.org/10.1016/j.clim.2014.10.005

Ko, E., Jeong, S., Jwa, M. Y., Kim, A. R., Ha, Y. E., Kim, S. K., Jeong, S., Ahn, K. B., Seo, H. S., Yun, C. H., & Han, S. H. (2021). Immune Responses to Irradiated Pneumococcal Whole Cell Vaccine. *Vaccines (Basel)*, *9*(4). https://doi.org/10.3390/vaccines9040405

Koh, V. H. Q., Ng, S. L., Ang, M. L. T., Lin, W., Ruedl, C., & Alonso, S. (2017). Role and contribution of pulmonary CD103+ dendritic cells in the adaptive immune response to Mycobacterium tuberculosis. *Tuberculosis*, *102*, 34-46. https://doi.org/https://doi.org/10.1016/j.tube.2016.12.003

Koh, W. J., Jeong, B. H., Kim, S. Y., Jeon, K., Park, K. U., Jhun, B. W., Lee, H., Park, H. Y., Kim, D. H., Huh, H. J., Ki, C. S., Lee, N. Y., Kim, H. K., Choi, Y. S., Kim, J., Lee, S. H., Kim, C. K., Shin, S. J., Daley, C. L., . . . Kwon, O. J. (2017). Mycobacterial Characteristics and Treatment Outcomes in Mycobacterium abscessus Lung Disease. *Clin Infect Dis*, *64*(3), 309-316. https://doi.org/10.1093/cid/ciw724

Kothavade, R. J., Dhurat, R. S., Mishra, S. N., & Kothavade, U. R. (2013). Clinical and laboratory aspects of the diagnosis and management of cutaneous and subcutaneous infections caused by rapidly growing mycobacteria. *Eur J Clin Microbiol Infect Dis*, *32*(2), 161-188. https://doi.org/10.1007/s10096-012-1766-8

Kozakiewicz, L., Chen, Y., Xu, J., Wang, Y., Dunussi-Joannopoulos, K., Ou, Q., Flynn, J. L., Porcelli, S. A., Jacobs, W. R., Jr., & Chan, J. (2013). B cells regulate neutrophilia during Mycobacterium tuberculosis infection and BCG vaccination by modulating the interleukin-17 response. *PLoS Pathog*, *9*(7), e1003472. https://doi.org/10.1371/journal.ppat.1003472

Kramnik, I., Dietrich, W. F., Demant, P., & Bloom, B. R. (2000). Genetic control of resistance to experimental infection with virulent Mycobacterium tuberculosis. *Proc Natl Acad Sci U S A*, *97*(15), 8560-8565. https://doi.org/10.1073/pnas.150227197

Kusunoki, S., & Ezaki, T. (1992). Proposal of Mycobacterium peregrinum sp. nov., nom. rev., and elevation of Mycobacterium chelonae subsp. abscessus (Kubica et al.) to species status: Mycobacterium abscessus comb. nov. *Int J Syst Bacteriol*, *42*(2), 240-245. https://doi.org/10.1099/00207713-42-2-240

Kwak, N., Dalcolmo, M. P., Daley, C. L., Eather, G., Gayoso, R., Hasegawa, N., Jhun, B. W., Koh, W. J., Namkoong, H., Park, J., Thomson, R., van Ingen, J., Zweijpfenning, S. M. H., & Yim, J. J. (2019). M ycobacterium abscessus pulmonary disease: individual patient data meta-analysis. *Eur Respir J*, *54*(1). https://doi.org/10.1183/13993003.01991-2018

Le Moigne, V., Belon, C., Goulard, C., Accard, G., Bernut, A., Pitard, B., Gaillard, J. L., Kremer, L., Herrmann, J. L., & Blanc-Potard, A. B. (2016). MgtC as a Host-Induced Factor and Vaccine Candidate against Mycobacterium abscessus Infection. *Infect Immun*, *84*(10), 2895-2903. https://doi.org/10.1128/iai.00359-16

Le Moigne, V., Gaillard, J. L., & Herrmann, J. L. (2016). Vaccine strategies against bacterial pathogens in cystic fibrosis patients. *Med Mal Infect*, *46*(1), 4-9. https://doi.org/10.1016/j.medmal.2015.11.013

Le Moigne, V., Raynaud, C., Moreau, F., Dupont, C., Nigou, J., Neyrolles, O., Kremer, L., & Herrmann, J. L. (2020). Efficacy of Bedaquiline, Alone or in Combination with Imipenem, against Mycobacterium abscessus in C3HeB/FeJ Mice. *Antimicrob Agents Chemother*, *64*(6). https://doi.org/10.1128/aac.00114-20

Le Moigne, V., Rottman, M., Goulard, C., Barteau, B., Poncin, I., Soismier, N., Canaan, S., Pitard, B., Gaillard, J.-L., & Herrmann, J.-L. (2015). Bacterial phospholipases C as vaccine candidate antigens against cystic fibrosis respiratory pathogens: the Mycobacterium abscessus model. *Vaccine*, *33*(18), 2118-2124.

Le Moigne, V., Roux, A. L., Jobart-Malfait, A., Blanc, L., Chaoui, K., Burlet-Schiltz, O., Gaillard, J. L., Canaan, S., Nigou, J., & Herrmann, J. L. (2020). A TLR2-Activating Fraction From Mycobacterium abscessus Rough Variant Demonstrates Vaccine and Diagnostic Potential. *Front Cell Infect Microbiol*, *10*, 432. https://doi.org/10.3389/fcimb.2020.00432

Lee, H. M., Yuk, J. M., Kim, K. H., Jang, J., Kang, G., Park, J. B., Son, J. W., & Jo, E. K. (2012). Mycobacterium abscessus activates the NLRP3 inflammasome via Dectin-1-Syk and p62/SQSTM1. *Immunol Cell Biol*, *90*(6), 601-610. https://doi.org/10.1038/icb.2011.72

Lee, J. Y., Lee, M. S., Kim, D. J., Yang, S. J., Lee, S. J., Noh, E. J., Shin, S. J., & Park, J. H. (2017). Nucleotide-Binding Oligomerization Domain 2 Contributes to Limiting Growth of Mycobacterium abscessus in the Lung of Mice by Regulating Cytokines and Nitric Oxide Production. *Front Immunol*, *8*, 1477. https://doi.org/10.3389/fimmu.2017.01477

Lee, M. R., Cheng, A., Lee, Y. C., Yang, C. Y., Lai, C. C., Huang, Y. T., Ho, C. C., Wang, H. C., Yu, C. J., & Hsueh, P. R. (2012). CNS infections caused by Mycobacterium abscessus complex: clinical features and antimicrobial susceptibilities of isolates. *J Antimicrob Chemother*, *67*(1), 222-225. https://doi.org/10.1093/jac/dkr420

Lee, M. R., Sheng, W. H., Hung, C. C., Yu, C. J., Lee, L. N., & Hsueh, P. R. (2015). Mycobacterium abscessus Complex Infections in Humans. *Emerg Infect Dis*, *21*(9), 1638-1646. https://doi.org/10.3201/2109.141634

Lee, S. J., Jang, J. H., Yoon, G. Y., Kang, D. R., Park, H. J., Shin, S. J., Han, H. D., Kang, T. H., Park, W. S., Yoon, Y. K., Soh, B. Y., Jung, I. D., & Park, Y. M. (2016). Mycobacterium abscessus D-alanyl-D-alanine dipeptidase induces the maturation of dendritic cells and promotes Th1-biased immunity. *BMB Rep*, *49*(10), 554-559. https://doi.org/10.5483/bmbrep.2016.49.10.080

Lee, S. J., Shin, S. J., Lee, M. H., Kang, T. H., Noh, K. T., Shin, Y. K., Kim, H. W., Yun, C. H., Jung, I. D., & Park, Y. M. (2014). Mycobacterium abscessus MAB2560 induces maturation of dendritic cells via Toll-like receptor 4 and drives Th1 immune response. *BMB Rep*, *47*(9), 512-517. https://doi.org/10.5483/bmbrep.2014.47.9.001

Liegeois, M., Legrand, C., Desmet, C. J., Marichal, T., & Bureau, F. (2018). The interstitial macrophage: A long-neglected piece in the puzzle of lung immunity. *Cell Immunol*, *330*, 91-96. https://doi.org/10.1016/j.cellimm.2018.02.001

Lim, A., Allison, C., Price, P., & Waterer, G. (2010). Susceptibility to pulmonary disease due to Mycobacterium avium-intracellulare complex may reflect low IL-17 and high IL-10 responses rather than Th1 deficiency. *Clin Immunol*, *137*(2), 296-302. https://doi.org/10.1016/j.clim.2010.07.011

Lindenstrøm, T., Aagaard, C., Christensen, D., Agger, E. M., & Andersen, P. (2014). High-frequency vaccine-induced CD8+ T cells specific for an epitope naturally processed during infection with Mycobacterium tuberculosis do not confer protection. *Eur J Immunol*, *44*(6), 1699-1709.

Lindenstrøm, T., Agger, E. M., Korsholm, K. S., Darrah, P. A., Aagaard, C., Seder, R. A., Rosenkrands, I., & Andersen, P. (2009). Tuberculosis Subunit Vaccination Provides Long-Term Protective Immunity Characterized by Multifunctional CD4 Memory T Cells. *J Immunol*, *182*(12), 8047-8055. https://doi.org/10.4049/jimmunol.0801592

Lopeman, R. C., Harrison, J., Desai, M., & Cox, J. A. G. (2019). Mycobacterium abscessus: Environmental Bacterium Turned Clinical Nightmare. *Microorganisms*, *7*(3). https://doi.org/10.3390/microorganisms7030090

Loxton, A. G., Knaul, J. K., Grode, L., Gutschmidt, A., Meller, C., Eisele, B., Johnstone, H., van der Spuy, G., Maertzdorf, J., Kaufmann, S. H. E., Hesseling, A. C., Walzl, G., & Cotton, M. F. (2017). Safety and Immunogenicity of the Recombinant Mycobacterium bovis BCG Vaccine

VPM1002 in HIV-Unexposed Newborn Infants in South Africa. *Clin Vaccine Immunol*, *24*(2). https://doi.org/10.1128/cvi.00439-16

MacMicking, J. D., North, R. J., LaCourse, R., Mudgett, J. S., Shah, S. K., & Nathan, C. F. (1997). Identification of nitric oxide synthase as a protective locus against tuberculosis. *Proc Natl Acad Sci U S A*, *94*(10), 5243-5248. https://doi.org/10.1073/pnas.94.10.5243

Maglione, P. J., Xu, J., & Chan, J. (2007). B cells moderate inflammatory progression and enhance bacterial containment upon pulmonary challenge with Mycobacterium tuberculosis. *J Immunol*, *178*(11), 7222-7234. https://doi.org/10.4049/jimmunol.178.11.7222

Malcolm, K. C., Caceres, S. M., Pohl, K., Poch, K. R., Bernut, A., Kremer, L., Bratton, D. L., Herrmann, J. L., & Nick, J. A. (2018). Neutrophil killing of Mycobacterium abscessus by intra- and extracellular mechanisms. *PloS one*, *13*(4), e0196120. https://doi.org/10.1371/journal.pone.0196120

Malcolm, K. C., Nichols, E. M., Caceres, S. M., Kret, J. E., Martiniano, S. L., Sagel, S. D., Chan, E. D., Caverly, L., Solomon, G. M., Reynolds, P., Bratton, D. L., Taylor-Cousar, J. L., Nichols, D. P., Saavedra, M. T., & Nick, J. A. (2013). Mycobacterium abscessus Induces a Limited Pattern of Neutrophil Activation That Promotes Pathogen Survival. *PloS one*, *8*(2), e57402. https://doi.org/10.1371/journal.pone.0057402

Maloney, K. E., & Valvano, M. A. (2006). The mgtC gene of Burkholderia cenocepacia is required for growth under magnesium limitation conditions and intracellular survival in macrophages. *Infect Immun*, *74*(10), 5477-5486. https://doi.org/10.1128/iai.00798-06

Mangtani, P., Abubakar, I., Ariti, C., Beynon, R., Pimpin, L., Fine, P. E., Rodrigues, L. C., Smith, P. G., Lipman, M., & Whiting, P. F. (2014). Protection by BCG vaccine against tuberculosis: a systematic review of randomized controlled trials. *Clin Infect Dis*, *58*(4), 470-480.

Martiniano, S. L., Nick, J. A., & Daley, C. L. (2019). Nontuberculous Mycobacterial Infections in Cystic Fibrosis. *Thorac Surg Clin*, *29*(1), 95-108. https://doi.org/10.1016/j.thorsurg.2018.09.008

Martiniano, S. L., Nick, J. A., & Daley, C. L. (2022). Nontuberculous Mycobacterial Infections in Cystic Fibrosis. *Clin Chest Med*, *43*(4), 697-716. https://doi.org/10.1016/j.ccm.2022.06.010

Mata, E., Tarancon, R., Guerrero, C., Moreo, E., Moreau, F., Uranga, S., Gomez, A. B., Marinova, D., Domenech, M., & Gonzalez-Camacho, F. (2021). Pulmonary BCG induces lung-resident macrophage activation and confers long-term protection against tuberculosis. *Sci Immunol*, *6*(63), eabc2934.

Mathee, K., Narasimhan, G., Valdes, C., Qiu, X., Matewish, J. M., Koehrsen, M., Rokas, A., Yandava, C. N., Engels, R., Zeng, E., Olavarietta, R., Doud, M., Smith, R. S., Montgomery, P., White, J. R., Godfrey, P. A., Kodira, C., Birren, B., Galagan, J. E., & Lory, S. (2008). Dynamics of Pseudomonas aeruginosa genome evolution. *Proc Natl Acad Sci U S A*, *105*(8), 3100-3105. https://doi.org/10.1073/pnas.0711982105

Mauch, R. M., Alves, P. C. M., Levy, C. E., Ribeiro, J. D., Ribeiro, A. F., Høiby, N., & Nolasco da Silva, M. T. (2020). Lymphocyte responses to Mycobacterium tuberculosis and Mycobacterium bovis are similar between BCG-vaccinated patients with cystic fibrosis and healthy controls. *J Cyst Fibros*, *19*(4), 575-579. https://doi.org/10.1016/j.jcf.2020.01.013

Maurer, F. P., Bruderer, V. L., Ritter, C., Castelberg, C., Bloemberg, G. V., & Böttger, E. C. (2014). Lack of antimicrobial bactericidal activity in Mycobacterium abscessus. *Antimicrob Agents Chemother*, *58*(7), 3828-3836. https://doi.org/10.1128/aac.02448-14

Medjahed, H., & Reyrat, J.-M. (2009). Construction of Mycobacterium abscessus defined glycopeptidolipid mutants: comparison of genetic tools. *Appl Environ Microbiol*, *75*(5), 1331-1338.

Mehta, A. K., Gracias, D. T., & Croft, M. (2018). TNF activity and T cells. *Cytokine*, *101*, 14-18. https://doi.org/10.1016/j.cyto.2016.08.003

Meir, M., & Barkan, D. (2020). Alternative and Experimental Therapies of Mycobacterium abscessus Infections. *Int J Mol Sci*, *21*(18). https://doi.org/10.3390/ijms21186793

Mirsaeidi, M., Allen, M. B., Ebrahimi, G., & Schraufnagel, D. (2015). Hospital costs in the US for pulmonary mycobacterial diseases. *Int J Mycobacteriol*, *4*(3), 217-221. https://doi.org/10.1016/j.ijmyco.2015.05.003

Misharin, A. V., Morales-Nebreda, L., Mutlu, G. M., Budinger, G. R., & Perlman, H. (2013). Flow cytometric analysis of macrophages and dendritic cell subsets in the mouse lung. *Am J Respir Cell Mol Biol*, *49*(4), 503-510. https://doi.org/10.1165/rcmb.2013-0086MA

Mishra, B. B., Rathinam, V. A., Martens, G. W., Martinot, A. J., Kornfeld, H., Fitzgerald, K. A., & Sassetti, C. M. (2013). Nitric oxide controls the immunopathology of tuberculosis by inhibiting NLRP3 inflammasome-dependent processing of IL-1β. *Nat Immunol*, *14*(1), 52-60. https://doi.org/10.1038/ni.2474

Moguche, A. O., Musvosvi, M., Penn-Nicholson, A., Plumlee, C. R., Mearns, H., Geldenhuys, H., Smit, E., Abrahams, D., Rozot, V., Dintwe, O., Hoff, S. T., Kromann, I., Ruhwald, M., Bang, P., Larson, R. P., Shafiani, S., Ma, S., Sherman, D. R., Sette, A., . . . Urdahl, K. B. (2017). Antigen Availability Shapes T Cell Differentiation and Function during Tuberculosis. *Cell Host Microbe*, *21*(6), 695-706.e695. https://doi.org/10.1016/j.chom.2017.05.012

Moliva, J. I., Hossfeld, A. P., Sidiki, S., Canan, C. H., Dwivedi, V., Beamer, G., Turner, J., & Torrelles, J. B. (2019). Selective delipidation of Mycobacterium bovis BCG enables direct pulmonary vaccination and enhances protection against Mycobacterium tuberculosis. *Mucosal Immunol*, *12*(3), 805-815. https://doi.org/10.1038/s41385-019-0148-2

Moliva, J. I., Turner, J., & Torrelles, J. B. (2017). Immune Responses to Bacillus Calmette–Guérin Vaccination: Why Do They Fail to Protect against Mycobacterium tuberculosis? [Review]. *Front Immunol*, *8*(407). https://doi.org/10.3389/fimmu.2017.00407

Moore, M., & Frerichs, J. B. (1953). An unusual acid-fast infection of the knee with subcutaneous, abscess-like lesions of the gluteal region; report of a case with a study of the organism, Mycobacterium abscessus, n. sp. *J Invest Dermatol*, *20*(2), 133-169. https://doi.org/10.1038/jid.1953.18

Moorthy, R. S., Valluri, S., & Rao, N. A. (2012). Nontuberculous mycobacterial ocular and adnexal infections. *Surv Ophthalmol*, *57*(3), 202-235. https://doi.org/10.1016/j.survophthal.2011.10.006

Mougari, F., Guglielmetti, L., Raskine, L., Sermet-Gaudelus, I., Veziris, N., & Cambau, E. (2016). Infections caused by Mycobacterium abscessus: epidemiology, diagnostic tools and treatment. *Expert Rev Anti Infect Ther*, *14*(12), 1139-1154. https://doi.org/10.1080/14787210.2016.1238304

Mousset, C. M., Hobo, W., Woestenenk, R., Preijers, F., Dolstra, H., & van der Waart, A. B. (2019). Comprehensive Phenotyping of T Cells Using Flow Cytometry. *Cytometry A*, *95*(6), 647-654. https://doi.org/10.1002/cyto.a.23724

Mueller, D., Tascher, G., Damm, G., Nüssler, A. K., Heinzle, E., & Noor, F. (2013). Real-time in situ viability assessment in a 3D bioreactor with liver cells using resazurin assay. *Cytotechnology*, *65*(2), 297-305. https://doi.org/10.1007/s10616-012-9486-6

Mullbacher, A., Pardo, J., & Furuya, Y. (2020). SARS-CoV-2 Vaccines: Inactivation by Gamma Irradiation for T and B Cell Immunity. *Pathogens*, *9*(11). https://doi.org/10.3390/pathogens9110928

Nava, A., Hahn, A. C., Wu, T. H., & Byrd, T. F. (2022). Mice with lung airway ciliopathy develop persistent Mycobacterium abscessus lung infection and have a proinflammatory lung phenotype associated with decreased T regulatory cells. *Front Immunol*, *13*, 1017540. https://doi.org/10.3389/fimmu.2022.1017540

Nessar, R., Cambau, E., Reyrat, J. M., Murray, A., & Gicquel, B. (2012). Mycobacterium abscessus: a new antibiotic nightmare. *J Antimicrob Chemother*, dkr578.

Nessar, R., Reyrat, J. M., Davidson, L. B., & Byrd, T. F. (2011). Deletion of the mmpL4b gene in the Mycobacterium abscessus glycopeptidolipid biosynthetic pathway results in loss of surface colonization capability, but enhanced ability to replicate in human macrophages and stimulate their innate immune response. *Microbiology (Reading)*, *157*(Pt 4), 1187-1195. https://doi.org/10.1099/mic.0.046557-0

Netea, M. G., Quintin, J., & van der Meer, J. W. (2011). Trained immunity: a memory for innate host defense. *Cell Host Microbe*, *9*(5), 355-361. https://doi.org/10.1016/j.chom.2011.04.006

Nguyen, L., & Thompson, C. J. (2006). Foundations of antibiotic resistance in bacterial physiology: the mycobacterial paradigm. *Trends Microbiol*, *14*(7), 304-312.

Nick, J. A., Dedrick, R. M., Gray, A. L., Vladar, E. K., Smith, B. E., Freeman, K. G., Malcolm, K. C., Epperson, L. E., Hasan, N. A., Hendrix, J., Callahan, K., Walton, K., Vestal, B., Wheeler, E.,

Rysavy, N. M., Poch, K., Caceres, S., Lovell, V. K., Hisert, K. B., . . . Davidson, R. M. (2022). Host and pathogen response to bacteriophage engineered against Mycobacterium abscessus lung infection. *Cell*, *185*(11), 1860-1874.e1812. https://doi.org/10.1016/j.cell.2022.04.024

Nicola, F., Cirillo, D. M., & Lorè, N. I. (2022). Preclinical murine models to study lung infection with Mycobacterium abscessus complex. *Tuberculosis (Edinb)*, *138*, 102301. https://doi.org/10.1016/j.tube.2022.102301

Niedbala, W., Wei, X.-q., Campbell, C., Thomson, D., Komai-Koma, M., & Liew, F. Y. (2002). Nitric oxide preferentially induces type 1 T cell differentiation by selectively up-regulating IL-12 receptor β2 expression via cGMP. *Proc Natl Acad Sci U S A*, *99*(25), 16186-16191.

Novoa, B., & Figueras, A. (2012). Zebrafish: model for the study of inflammation and the innate immune response to infectious diseases. In *Current topics in innate immunity II* (pp. 253-275). Springer.

Novosad, S. A., Beekmann, S. E., Polgreen, P. M., Mackey, K., & Winthrop, K. L. (2016). Treatment of Mycobacterium abscessus Infection. In (Vol. 22, pp. 511-514): *Emerging Infectious Diseases*.

Oberley-Deegan, R. E., Rebits, B. W., Weaver, M. R., Tollefson, A. K., Bai, X., McGibney, M., Ovrutsky, A. R., Chan, E. D., & Crapo, J. D. (2010). An oxidative environment promotes growth of Mycobacterium abscessus. *Free radical biology & medicine*, *49*(11), 1666-1673. https://doi.org/https://doi.org/10.1016/j.freeradbiomed.2010.08.026

Obregón-Henao, A., Arnett, K. A., Henao-Tamayo, M., Massoudi, L., Creissen, E., Andries, K., Lenaerts, A. J., & Ordway, D. J. (2015). Susceptibility of Mycobacterium abscessus to antimycobacterial drugs in preclinical models. *Antimicrob Agents Chemother*, *59*(11), 6904-6912. https://doi.org/10.1128/aac.00459-15

Oddo, M., Renno, T., Attinger, A., Bakker, T., MacDonald, H. R., & Meylan, P. R. (1998). Fas ligand-induced apoptosis of infected human macrophages reduces the viability of intracellular Mycobacterium tuberculosis. *J Immunol*, *160*(11), 5448-5454.

Okayasu, H., Sein, C., Hamidi, A., Bakker, W. A., & Sutter, R. W. (2016). Development of inactivated poliovirus vaccine from Sabin strains: A progress report. *Biologicals*, *44*(6), 581-587. https://doi.org/10.1016/j.biologicals.2016.08.005

Ordway, D., Henao-Tamayo, M., Smith, E., Shanley, C., Harton, M., Troudt, J., Bai, X., Basaraba, R. J., Orme, I. M., & Chan, E. D. (2008). Animal model of Mycobacterium abscessus lung infection. *J Leukoc Biol*, *83*(6), 1502.

Ouyang, W., Kolls, J. K., & Zheng, Y. (2008). The biological functions of T helper 17 cell effector cytokines in inflammation. *Immunity*, *28*(4), 454-467.

Öz, H. H., Cheng, E.-C., Di Pietro, C., Tebaldi, T., Biancon, G., Zeiss, C., Zhang, P.-X., Huang, P. H., Esquibies, S. S., Britto, C. J., Schupp, J. C., Murray, T. S., Halene, S., Krause, D. S., Egan, M. E., & Bruscia, E. M. (2022). Recruited monocytes/macrophages drive pulmonary neutrophilic inflammation and irreversible lung tissue remodeling in cystic fibrosis. *Cell reports*, *41*(11), 111797. https://doi.org/https://doi.org/10.1016/j.celrep.2022.111797

Parameswaran, N., & Patial, S. (2010). Tumor necrosis factor-α signaling in macrophages. *Crit Rev Eukaryot Gene Expr*, *20*(2), 87-103. https://doi.org/10.1615/critreveukargeneexpr.v20.i2.10

Perdomo, C., Zedler, U., Kühl, A. A., Lozza, L., Saikali, P., Sander, L. E., Vogelzang, A., Kaufmann, S. H., & Kupz, A. (2016). Mucosal BCG vaccination induces protective lung-resident memory T cell populations against tuberculosis. *MBio*, *7*(6), e01686-01616.

Pérez, I., Uranga, S., Sayes, F., Frigui, W., Samper, S., Arbués, A., Aguiló, N., Brosch, R., Martín, C., & Gonzalo-Asensio, J. (2020). Live attenuated TB vaccines representing the three modern Mycobacterium tuberculosis lineages reveal that the Euro-American genetic background confers optimal vaccine potential. *EBioMedicine*, *55*, 102761. https://doi.org/10.1016/j.ebiom.2020.102761

Phuah, J., Wong, E. A., Gideon, H. P., Maiello, P., Coleman, M. T., Hendricks, M. R., Ruden, R., Cirrincione, L. R., Chan, J., & Lin, P. L. (2016). Effects of B cell depletion on early Mycobacterium tuberculosis infection in cynomolgus macaques. *Infect Immun*, *84*(5), 1301-1311.

Pittet, L. F., Tebruegge, M., Dutta, B., Donath, S., Messina, N., Casalaz, D., Hanekom, W. A., Britton, W. J., Robins-Browne, R., Curtis, N., & Ritz, N. (2021). Mycobacterium ulcerans-specific

immune response after immunisation with bacillus Calmette-Guérin (BCG) vaccine. *Vaccine*, *39*(4), 652-657. https://doi.org/10.1016/j.vaccine.2020.11.045

Pohl, K., Grimm, X. A., Caceres, S. M., Poch, K. R., Rysavy, N., Saavedra, M., Nick, J. A., & Malcolm, K. C. (2020). Mycobacterium abscessus Clearance by Neutrophils Is Independent of Autophagy. *Infect Immun*, *88*(8). https://doi.org/10.1128/iai.00024-20

Präbst, K., Engelhardt, H., Ringgeler, S., & Hübner, H. (2017). Basic colorimetric proliferation assays: MTT, WST, and resazurin. In *Cell viability assays* (pp. 1-17). Springer.

Quan, D. H., Counoupas, C., Nagalingam, G., Pinto, R., Petrovsky, N., Britton, W. J., & Triccas, J. A. (2021). Advax adjuvant formulations promote protective immunity against aerosol Mycobacterium tuberculosis in the absence of deleterious inflammation and reactogenicity. *Vaccine*, *39*(14), 1990-1996. https://doi.org/10.1016/j.vaccine.2021.02.041

Quan, D. H., Kwong, A. J., Hansbro, P. M., & Britton, W. J. (2022). No smoke without fire: the impact of cigarette smoking on the immune control of tuberculosis. *Eur Respir Rev*, *31*(164), 210252. https://doi.org/10.1183/16000617.0252-2021

Quang, N. T., & Jang, J. (2021). Current Molecular Therapeutic Agents and Drug Candidates for Mycobacterium abscessus [Review]. *Front Pharmacol*, *12*. https://doi.org/10.3389/fphar.2021.724725

Ramakrishna, C., & Cantin, E. M. (2018). IFNγ inhibits G-CSF induced neutrophil expansion and invasion of the CNS to prevent viral encephalitis. *PLoS Pathog*, *14*(1), e1006822. https://doi.org/10.1371/journal.ppat.1006822

Rapp, M., Wintergerst, M. W. M., Kunz, W. G., Vetter, V. K., Knott, M. M. L., Lisowski, D., Haubner, S., Moder, S., Thaler, R., Eiber, S., Meyer, B., Röhrle, N., Piseddu, I., Grassmann, S., Layritz, P., Kühnemuth, B., Stutte, S., Bourquin, C., von Andrian, U. H., . . . Anz, D. (2019). CCL22 controls immunity by promoting regulatory T cell communication with dendritic cells in lymph nodes. *J Exp Med*, *216*(5), 1170-1181. https://doi.org/10.1084/jem.20170277

Rathore, J. S., & Wang, Y. (2016). Protective role of Th17 cells in pulmonary infection. *Vaccine*, *34*(13), 1504-1514. https://doi.org/10.1016/j.vaccine.2016.02.021

Reed, S. G., Orr, M. T., & Fox, C. B. (2013). Key roles of adjuvants in modern vaccines. *Nat Med*, *19*(12), 1597-1608.

Reiley, W. W., Shafiani, S., Wittmer, S. T., Tucker-Heard, G., Moon, J. J., Jenkins, M. K., Urdahl, K. B., Winslow, G. M., & Woodland, D. L. (2010). Distinct functions of antigen-specific CD4 T cells during murine Mycobacterium tuberculosis infection. *Proc Natl Acad Sci U S A*, *107*(45), 19408-19413. https://doi.org/10.1073/pnas.1006298107

Riol-Blanco, L., Sánchez-Sánchez, N., Torres, A., Tejedor, A., Narumiya, S., Corbí, A. L., Sánchez-Mateos, P., & Rodríguez-Fernández, J. L. (2005). The chemokine receptor CCR7 activates in dendritic cells two signaling modules that independently regulate chemotaxis and migratory speed. *J Immunol*, *174*(7), 4070-4080. https://doi.org/10.4049/jimmunol.174.7.4070

Riordan, J. R., Rommens, J. M., Kerem, B., Alon, N., Rozmahel, R., Grzelczak, Z., Zielenski, J., Lok, S., Plavsic, N., Chou, J. L., & et al. (1989). Identification of the cystic fibrosis gene: cloning and characterization of complementary DNA. *Science*, *245*(4922), 1066-1073. https://doi.org/10.1126/science.2475911

Ripoll, F., Pasek, S., Schenowitz, C., Dossat, C., Barbe, V., Rottman, M., Macheras, E., Heym, B., Herrmann, J.-L., & Daffé, M. (2009). Non mycobacterial virulence genes in the genome of the emerging pathogen Mycobacterium abscessus. *PloS one*, *4*(6), e5660.

Riva, C., Tortoli, E., Cugnata, F., Sanvito, F., Esposito, A., Rossi, M., Colarieti, A., Canu, T., Cigana, C., Bragonzi, A., Loré, N. I., Miotto, P., & Cirillo, D. M. (2020). A New Model of Chronic Mycobacterium abscessus Lung Infection in Immunocompetent Mice. *Int J Mol Sci*, *21*(18), 6590. https://www.mdpi.com/1422-0067/21/18/6590

Roach, D. R., Briscoe, H., Saunders, B., France, M. P., Riminton, S., & Britton, W. J. (2001). Secreted lymphotoxin-α is essential for the control of an intracellular bacterial infection. *J Exp Med*, *193*(2), 239-246.

Roberts, A. W. (2005). G-CSF: A key regulator of neutrophil production, but that's not all! *Growth Factors*, *23*(1), 33-41. https://doi.org/10.1080/08977190500055836

Rottman, M., Catherinot, E., Hochedez, P., Emile, J.-F., Casanova, J.-L., Gaillard, J.-L., & Soudais, C. (2007). Importance of T cells, gamma interferon, and tumor necrosis factor in immune

control of the rapid grower Mycobacterium abscessus in C57BL/6 mice. *Infect Immun*, *75*(12), 5898-5907.

Roux, A.-L., Catherinot, E., Ripoll, F., Soismier, N., Macheras, E., Ravilly, S., Bellis, G., Vibet, M.-A., Le Roux, E., & Lemonnier, L. (2009). Multicenter study of prevalence of nontuberculous mycobacteria in patients with cystic fibrosis in France. *J Clin Microbiol*, *47*(12), 4124-4128.

Roux, A. L., Viljoen, A., Bah, A., Simeone, R., Bernut, A., Laencina, L., Deramaudt, T., Rottman, M., Gaillard, J. L., Majlessi, L., Brosch, R., Girard-Misguich, F., Vergne, I., de Chastellier, C., Kremer, L., & Herrmann, J. L. (2016). The distinct fate of smooth and rough Mycobacterium abscessus variants inside macrophages. *Open Biol*, *6*(11). https://doi.org/10.1098/rsob.160185

Ruangkiattikul, N., Rys, D., Abdissa, K., Rohde, M., Semmler, T., Tegtmeyer, P. K., Kalinke, U., Schwarz, C., Lewin, A., & Goethe, R. (2019). Type I interferon induced by TLR2-TLR4-MyD88-TRIF-IRF3 controls Mycobacterium abscessus subsp. abscessus persistence in murine macrophages via nitric oxide. *Int J Med Microbiol*, *309*(5), 307-318. https://doi.org/10.1016/j.ijmm.2019.05.007

Rubio, M., March, F., Garrigo, M., Moreno, C., Espanol, M., & Coll, P. (2015). Inducible and Acquired Clarithromycin Resistance in the Mycobacterium abscessus Complex. *PloS one*, *10*(10), e0140166. https://doi.org/10.1371/journal.pone.0140166

Ruis, C., Bryant, J. M., Bell, S. C., Thomson, R., Davidson, R. M., Hasan, N. A., van Ingen, J., Strong, M., Floto, R. A., & Parkhill, J. (2021). Dissemination of Mycobacterium abscessus via global transmission networks. *Nat Microbiol*, *6*(10), 1279-1288. https://doi.org/10.1038/s41564-021-00963-3

Sabbaghi, A., Miri, S. M., Keshavarz, M., Zargar, M., & Ghaemi, A. (2019). Inactivation methods for whole influenza vaccine production. *Rev Med Virol*, *29*(6), e2074. https://doi.org/10.1002/rmv.2074

Sabin, A. P., Ferrieri, P., & Kline, S. (2017). Mycobacterium abscessus Complex Infections in Children: A Review. *Curr Infect Dis Rep*, *19*(11), 46. https://doi.org/10.1007/s11908-017-0597-2

Sampath, P., Periyasamy, K. M., Ranganathan, U. D., & Bethunaickan, R. (2021). Monocyte and Macrophage miRNA: Potent Biomarker and Target for Host-Directed Therapy for Tuberculosis [Mini Review]. *Front Immunol*, *12*. https://doi.org/10.3389/fimmu.2021.667206

Sanakkayala, N., Sokolovska, A., Gulani, J., HogenEsch, H., Sriranganathan, N., Boyle, S. M., Schurig, G. G., & Vemulapalli, R. (2005). Induction of Antigen-Specific Th1-Type Immune Responses by Gamma-Irradiated Recombinant Brucella abortus RB51. *Clinical and Vaccine Immunology*, *12*(12), 1429-1436. https://doi.org/doi:10.1128/CDLI.12.12.1429-1436.2005

Sassi, M., & Drancourt, M. (2014). Genome analysis reveals three genomospecies in Mycobacterium abscessus. *BMC Genomics*, *15*(1), 359. https://doi.org/10.1186/1471-2164-15-359

Saunders, B. M., Briscoe, H., & Britton, W. J. (2004). T cell-derived tumour necrosis factor is essential, but not sufficient, for protection against Mycobacterium tuberculosis infection. *Clin Exp Immunol*, *137*(2), 279-287. https://doi.org/10.1111/j.1365-2249.2004.02518.x

Schoenmakers, A., Mieras, L., Budiawan, T., & van Brakel, W. H. (2020). The State of Affairs in Post-Exposure Leprosy Prevention: A Descriptive Meta-Analysis on Immuno- and Chemo-Prophylaxis. *Res Rep Trop Med*, *11*, 97-117. https://doi.org/10.2147/rrtm.s190300

Schrager, L. K., Vekemens, J., Drager, N., Lewinsohn, D. M., & Olesen, O. F. (2020). The status of tuberculosis vaccine development. *Lancet Infect Dis*, *20*(3), e28-e37. https://doi.org/10.1016/s1473-3099(19)30625-5

Schreiner, D., & King, C. G. (2018). CD4+ Memory T Cells at Home in the Tissue: Mechanisms for Health and Disease. *Front Immunol*, *9*, 2394. https://doi.org/10.3389/fimmu.2018.02394

Schyns, J., Bai, Q., Ruscitti, C., Radermecker, C., De Schepper, S., Chakarov, S., Farnir, F., Pirottin, D., Ginhoux, F., Boeckxstaens, G., Bureau, F., & Marichal, T. (2019). Non-classical tissue monocytes and two functionally distinct populations of interstitial macrophages populate the mouse lung. *Nat Commun*, *10*(1), 3964. https://doi.org/10.1038/s41467-019-11843-0

Schyns, J., Bureau, F., & Marichal, T. (2018). Lung Interstitial Macrophages: Past, Present, and Future. *J Immunol Res*, *2018*, 5160794. https://doi.org/10.1155/2018/5160794

Seder, R. A., Darrah, P. A., & Roederer, M. (2008). T-cell quality in memory and protection: implications for vaccine design. *Nat Rev Immunol*, *8*(4), 247-258. https://doi.org/10.1038/nri2274

Seo, H. S. (2015). Application of radiation technology in vaccines development. *Clin Exp Vaccine Res*, *4*(2), 145-158. https://doi.org/10.7774/cevr.2015.4.2.145

Shanmugham, B., & Pan, A. (2013). Identification and characterization of potential therapeutic candidates in emerging human pathogen Mycobacterium abscessus: a novel hierarchical in silico approach. *PloS one*, *8*(3), e59126. https://doi.org/10.1371/journal.pone.0059126

Sheedy, F. J., & Divangahi, M. (2021). Targeting immunometabolism in host defence against Mycobacterium tuberculosis. *Immunology*, *162*(2), 145-159. https://doi.org/https://doi.org/10.1111/imm.13276

Shekhar, S., Peng, Y., Wang, S., & Yang, X. (2018). CD103+ lung dendritic cells (LDCs) induce stronger Th1/Th17 immunity to a bacterial lung infection than CD11b(hi) LDCs. *Cell Mol Immunol*, *15*(4), 377-387. https://doi.org/10.1038/cmi.2016.68

Shin, D. M., Yang, C. S., Yuk, J. M., Lee, J. Y., Kim, K. H., Shin, S. J., Takahara, K., Lee, S. J., & Jo, E. K. (2008). Mycobacterium abscessus activates the macrophage innate immune response via a physical and functional interaction between TLR2 and dectin-1. *Cell Microbiol*, *10*(8), 1608-1621. https://doi.org/10.1111/j.1462-5822.2008.01151.x

Shu, C. C., Pan, S. W., Feng, J. Y., Wang, J. Y., Chan, Y. J., Yu, C. J., & Su, W. J. (2019). The Clinical Significance of Programmed Death-1, Regulatory T Cells and Myeloid Derived Suppressor Cells in Patients with Nontuberculous Mycobacteria-Lung Disease. *J Clin Med*, *8*(5). https://doi.org/10.3390/jcm8050736

Shu, C. C., Wu, L. S., Wu, M. F., Lai, H. C., Wang, P. H., Cheng, S. L., Wang, J. Y., & Yu, C. J. (2019). Mono- and poly-functional T cells in nontuberculous mycobacteria lung disease patients: Implications in analyzing risk of disease progression. *Cytokine*, *120*, 176-185. https://doi.org/10.1016/j.cyto.2019.05.001

Sissoko, M. S., Healy, S. A., Katile, A., Zaidi, I., Hu, Z., Kamate, B., Samake, Y., Sissoko, K., Mwakingwe-Omari, A., & Lane, J. (2022). Safety and efficacy of a three-dose regimen of Plasmodium falciparum sporozoite vaccine in adults during an intense malaria transmission season in Mali: a randomised, controlled phase 1 trial. *Lancet Infect Dis*, *22*(3), 377-389.

Sommers, C. H., & Rajkowski, K. T. (2011). Radiation inactivation of foodborne pathogens on frozen seafood products. *J Food Prot*, *74*(4), 641-644. https://doi.org/10.4315/0362-028x.jfp-10-419

Spencer, C. T., Abate, G., Blazevic, A., & Hoft, D. F. (2008). Only a subset of phosphoantigen-responsive gamma9delta2 T cells mediate protective tuberculosis immunity. *J Immunol*, *181*(7), 4471-4484. https://doi.org/10.4049/jimmunol.181.7.4471

Srivastava, S., Ernst, J. D., & Desvignes, L. (2014). Beyond macrophages: the diversity of mononuclear cells in tuberculosis. *Immunol Rev*, *262*(1), 179-192. https://doi.org/10.1111/imr.12217

Strijdom, H., Chamane, N., & Lochner, A. (2009). Nitric oxide in the cardiovascular system: a simple molecule with complex actions. *Cardiovascular journal of Africa*, *20*(5), 303.

Švandová, L. T. a. D. D. a. E. (1994). Six years' experience with the discontinuation of BCG vaccination: 4. Protective effect of BCG vaccination against the Mycobacterium avium intracellulare complex. *Tubercle and Lung Disease*, *75*(5), 348-352. https://doi.org/https://doi.org/10.1016/0962-8479(94)90080-9

Tailleux, L., Schwartz, O., Herrmann, J.-L., Pivert, E., Jackson, M., Amara, A., Legres, L., Dreher, D., Nicod, L. P., & Gluckman, J. C. (2003). DC-SIGN is the major Mycobacterium tuberculosis receptor on human dendritic cells. *J Exp Med*, *197*(1), 121-127.

Tameris, M. D., Hatherill, M., Landry, B. S., Scriba, T. J., Snowden, M. A., Lockhart, S., Shea, J. E., McClain, J. B., Hussey, G. D., Hanekom, W. A., Mahomed, H., & McShane, H. (2013). Safety and efficacy of MVA85A, a new tuberculosis vaccine, in infants previously vaccinated with BCG: a randomised, placebo-controlled phase 2b trial. *Lancet*, *381*(9871), 1021-1028. https://doi.org/10.1016/s0140-6736(13)60177-4

Tanaka, T., Narazaki, M., & Kishimoto, T. (2014). IL-6 in inflammation, immunity, and disease. *Cold Spring Harb Perspect Biol*, *6*(10), a016295. https://doi.org/10.1101/cshperspect.a016295

Tanner, R., Villarreal-Ramos, B., Vordermeier, H. M., & McShane, H. (2019). The Humoral Immune Response to BCG Vaccination. *Front Immunol*, *10*, 1317. https://doi.org/10.3389/fimmu.2019.01317

Thirunavukkarasu, S., Plain, K. M., Purdie, A. C., Whittington, R. J., & de Silva, K. (2017). IFN-γ fails to overcome inhibition of selected macrophage activation events in response to pathogenic mycobacteria. *PloS one*, *12*(5), e0176400. https://doi.org/10.1371/journal.pone.0176400

Thomson, R., Tolson, C., Carter, R., Coulter, C., Huygens, F., & Hargreaves, M. (2013). Isolation of nontuberculous mycobacteria (NTM) from household water and shower aerosols in patients with pulmonary disease caused by NTM. *J Clin Microbiol*, *51*(9), 3006-3011. https://doi.org/10.1128/jcm.00899-13

Tomioka, H., Shimizu, T., Sato, K., Sano, C., Kamei, T., Emori, M., & Saito, H. (2004). Comparative roles of macrophages and NK cells in the host innate resistance of mice to Mycobacterium fortuitum infection. *J Infect*, *48*(1), 74-80. https://doi.org/https://doi.org/10.1016/S0163-4453(03)00133-6

Tortoli, E., Kohl, T. A., Brown-Elliott, B. A., Trovato, A., Leão, S. C., Garcia, M. J., Vasireddy, S., Turenne, C. Y., Griffith, D. E., Philley, J. V., Baldan, R., Campana, S., Cariani, L., Colombo, C., Taccetti, G., Teri, A., Niemann, S., Wallace, R. J., Jr., & Cirillo, D. M. (2016). Emended description of Mycobacterium abscessus, Mycobacterium abscessus subsp. abscessus and Mycobacteriumabscessus subsp. bolletii and designation of Mycobacteriumabscessus subsp. massiliense comb. nov. *Int J Syst Evol Microbiol*, *66*(11), 4471-4479. https://doi.org/10.1099/ijsem.0.001376

Tran, V., Ahn, S. K., Ng, M., Li, M., & Liu, J. (2016). Loss of Lipid Virulence Factors Reduces the Efficacy of the BCG Vaccine. *Sci Rep*, *6*(1), 29076. https://doi.org/10.1038/srep29076

Tsikas, D. (2007). Analysis of nitrite and nitrate in biological fluids by assays based on the Griess reaction: appraisal of the Griess reaction in the L-arginine/nitric oxide area of research. *J Chromatogr B Analyt Technol Biomed Life Sci*, *851*(1-2), 51-70. https://doi.org/10.1016/j.jchromb.2006.07.054

Turner, J., Frank, A. A., Brooks, J. V., Gonzalez-Juarrero, M., & Orme, I. M. (2001). The progression of chronic tuberculosis in the mouse does not require the participation of B lymphocytes or interleukin-4. *Exp Gerontol*, *36*(3), 537-545. https://doi.org/10.1016/s0531-5565(00)00257-6

Van Rhijn, I., & Moody, D. B. (2015). CD1 and mycobacterial lipids activate human T cells. *Immunol Rev*, *264*(1), 138-153. https://doi.org/10.1111/imr.12253

Velazquez-Salinas, L., Verdugo-Rodriguez, A., Rodriguez, L. L., & Borca, M. V. (2019). The Role of Interleukin 6 During Viral Infections. *Front Microbiol*, *10*, 1057. https://doi.org/10.3389/fmicb.2019.01057

Verma, D., Stapleton, M., Gadwa, J., Vongtongsalee, K., Schenkel, A. R., Chan, E. D., & Ordway, D. (2019). Mycobacterium avium Infection in a C3HeB/FeJ Mouse Model. *Front Microbiol*, *10*, 693. https://doi.org/10.3389/fmicb.2019.00693

Vetter, V., Denizer, G., Friedland, L. R., Krishnan, J., & Shapiro, M. (2018). Understanding modern-day vaccines: what you need to know. *Ann Med*, *50*(2), 110-120. https://doi.org/10.1080/07853890.2017.1407035

Victoria, L., Gupta, A., Gómez, J. L., & Robledo, J. (2021). Mycobacterium abscessus complex: A Review of Recent Developments in an Emerging Pathogen. *Front Cell Infect Microbiol*, *11*, 659997. https://doi.org/10.3389/fcimb.2021.659997

Viviani, L., Harrison, M. J., Zolin, A., Haworth, C. S., & Floto, R. A. (2016). Epidemiology of nontuberculous mycobacteria (NTM) amongst individuals with cystic fibrosis (CF). *J Cyst Fibros*, *15*(5), 619-623. https://doi.org/10.1016/j.jcf.2016.03.002

Wang, X., Chen, S., Ren, H., Chen, J., Li, J., Wang, Y., Hua, Y., & Huang, N. (2019). HMGN2 regulates non-tuberculous mycobacteria survival via modulation of M1 macrophage polarization. *J Cell Mol Med*, *23*(12), 7985-7998. https://doi.org/10.1111/jcmm.14599

Waters, V., Stanojevic, S., & Ratjen, F. (2016). Special considerations for the treatment of pulmonary exacerbations in children with cystic fibrosis. *Expert Rev Respir Med*, *10*(11), 1221-1228.

Wesemann, D. R., & Benveniste, E. N. (2003). STAT-1 alpha and IFN-gamma as modulators of TNF-alpha signaling in macrophages: regulation and functional implications of the TNF receptor 1:STAT-1 alpha complex. *J Immunol*, *171*(10), 5313-5319. https://doi.org/10.4049/jimmunol.171.10.5313

White, A. D., Sibley, L., Sarfas, C., Morrison, A., Gullick, J., Clark, S., Gleeson, F., McIntyre, A., Arlehamn, C. L., Sette, A., Salguero, F. J., Rayner, E., Rodriguez, E., Puentes, E., Laddy, D., Williams, A., Dennis, M., Martin, C., & Sharpe, S. (2021). MTBVAC vaccination protects rhesus macaques against aerosol challenge with M. tuberculosis and induces immune signatures analogous to those observed in clinical studies. *NPJ Vaccines*, *6*(1), 4. https://doi.org/10.1038/s41541-020-00262-8

WHO. (2021). Impact of the COVID-19 pandemic on TB detection and mortality. In. Geneva: World Health Organisation.

Witsell, A. L., & Schook, L. B. (1992). Tumor necrosis factor alpha is an autocrine growth regulator during macrophage differentiation. *Proc Natl Acad Sci U S A*, *89*(10), 4754-4758. https://doi.org/10.1073/pnas.89.10.4754

Wolf, A. J., Linas, B., Trevejo-Nuñez, G. J., Kincaid, E., Tamura, T., Takatsu, K., & Ernst, J. D. (2007). Mycobacterium tuberculosis infects dendritic cells with high frequency and impairs their function in vivo. *J Immunol*, *179*(4), 2509-2519.

Wu, Q., Kang, S., Huang, J., Wan, S., Yang, B., & Wu, C. (2021). Antigen-specific tissue-resident memory T cells in the respiratory system were generated following intranasal vaccination of mice with BCG. *Journal of Immunology Research*, *2021*, 1-15.

Wu, U. I., Olivier, K. N., Kuhns, D. B., Fink, D. L., Sampaio, E. P., Zelazny, A. M., Shallom, S. J., Marciano, B. E., Lionakis, M. S., & Holland, S. M. (2019). Patients with Idiopathic Pulmonary Nontuberculous Mycobacterial Disease Have Normal Th1/Th2 Cytokine Responses but Diminished Th17 Cytokine and Enhanced Granulocyte-Macrophage Colony-Stimulating Factor Production. *Open Forum Infect Dis*, *6*(12), ofz484. https://doi.org/10.1093/ofid/ofz484

Yaacoby-Bianu, K., Gur, M., Toukan, Y., Nir, V., Hakim, F., Geffen, Y., & Bentur, L. (2018). Compassionate nitric oxide adjuvant treatment of persistent Mycobacterium infection in cystic fibrosis patients. *Pediatr Infect Dis J*, *37*(4), 336-338.